Recent Progress in Observational Studies of Electric Fields and Currents in the Polar Ionosphere: A Review

Yohsuke KAMIDE*

極域電場・電流の最近の観測的研究

上 出 洋 介*

要旨. 最近の新しいロケット, 人工衛星, レーダーなどの技術発達により, 極域電場・電流, および極光・極光粒子分布・変動に関する理解が一段と深まった. 本論文は, これら広範な分野のここ数年間の研究の主な結果をまとめることを目的とし, 極磁気嵐時の電離層内諸量の変動を, 鉛直電流との関係において議論する. さらに, 極光分布, 磁気圏・電離圏の電場, 磁場, 電流分布の複雑な観測結果を統一的に理解しようとする最近の傾向にも触れる.

Abstract: The recent development of several new observational techniques has contributed significantly to our understanding of the characteristics of electric fields and currents in the high-latitude ionosphere as well as those of auroral particle precipitation and the auroral distribution. This paper attempts to review the main results of several years of research in these diverse fields in order to construct a plausible working model that is consistent with the basic physical requirements. Various ionospheric processes including substorm variations are discussed with special emphasis on field-aligned currents. It also contains sections of recent efforts in synthesizing the vast amount of the observations of large-scale auroras, electric and magnetic fields, and currents in the ionosphere and magnetosphere, and it concludes with a list of several questions to which satisfactory agreements have not been reached.

Contents

* 京都産業大学理学部. Kyoto Sangyo University, Kamigamo, Kita-ku, Kyoto 603.

1. Introduction

The purpose of this paper is to examine (1) what are believed to be agreeable and (2) what are still matters of serious controversy and thus need future clarification for some important topics in studies of magnetospheric and ionospheric processes For this purpose we attempt to sum up the main observational results

of the electric fields and currents in the polar ionosphere obtained during the period from 1973 to the present. The choice of the year 1973 as the starting time for this topical review is made based on the author's view that efforts in deducing some consistent interpretations from accumulated data of various rocket- and satellite-borne and ground-based measurements have begun around 1973, and that during the last several years (1973 to the present), a significant advance has been made on the electrodynamics of the polar ionosphere owing to the development of new techniques, such as the ISIS, DMSP and TRIAD satellites, and incoherent scatter radars in auroral latitudes. It was also in 1973 that the National Institute of Polar Research, Tokyo was established as the center of polar research programs in Japan. While many new measurements relevant to the high-latitude phenomena have been accumulated in the course of observational studies during the last several years, quite a few important problems remain unanswered.

Undoubtedly, the International Magnetospheric Study (IMS) is a most exciting period for the studies of the electrodynamic phenomena in the polar ionosphere, since many coordinated spacecraft and ground-based observations in progress and under contemplation will provide crucial data sets which should unveil the basic ionospheric and magnetospheric processes. We believe that it is quite timely to

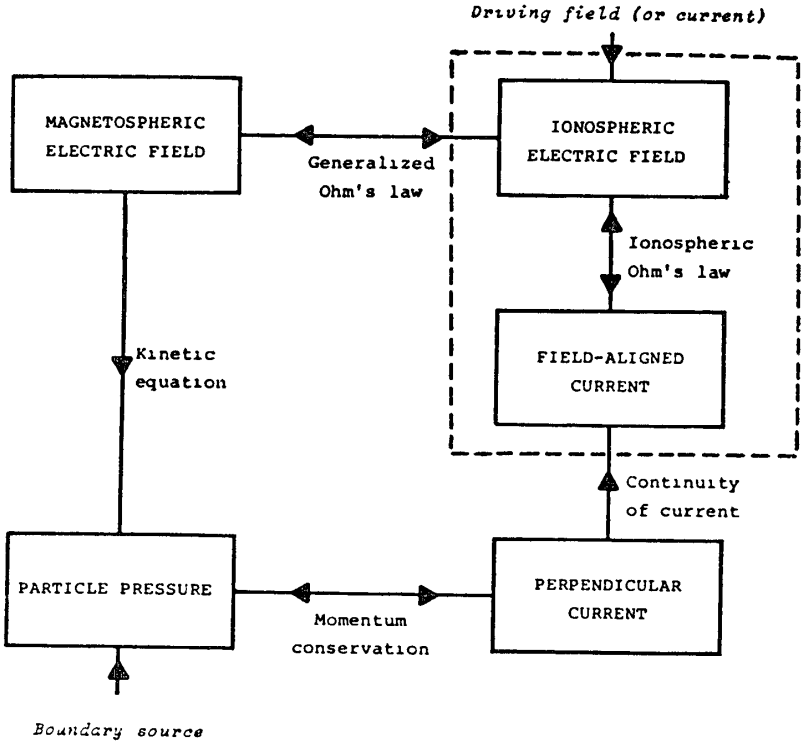

Fig. 1a. Outline of the self-consistent calculation of magnetospheric convection (after VASYLIUNAS, 1970).

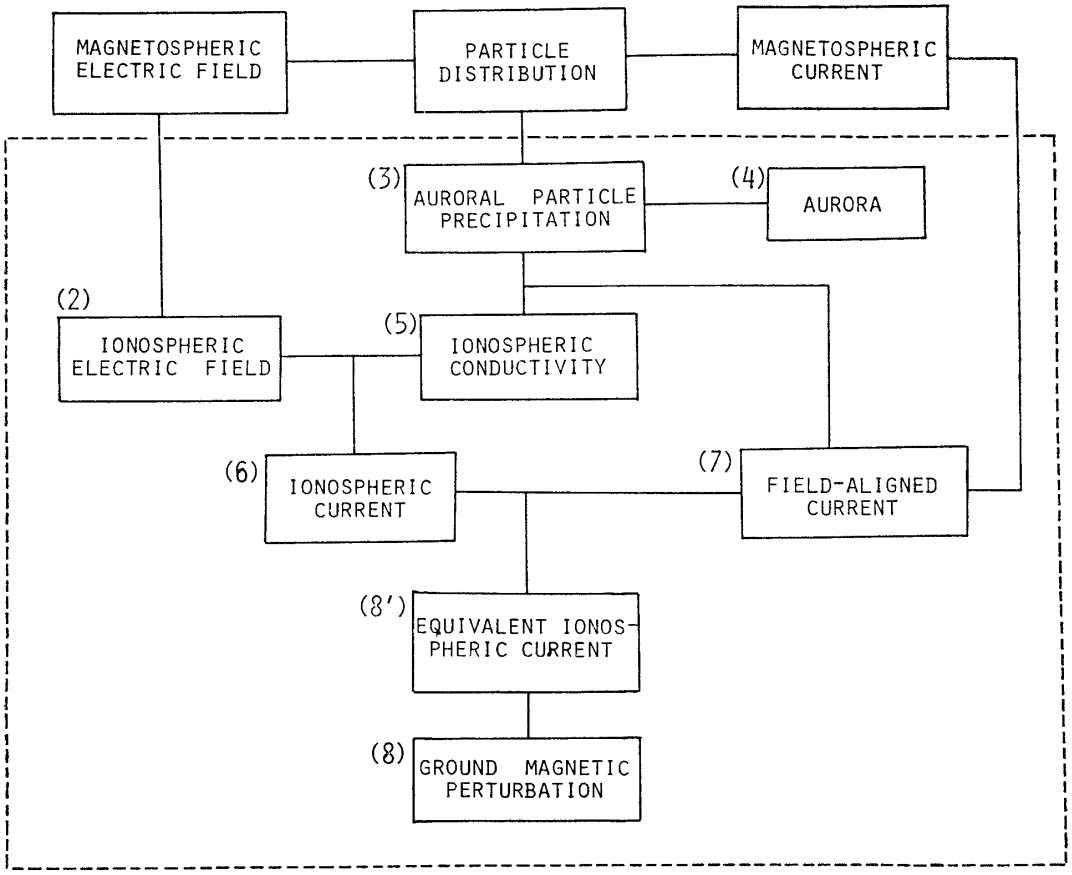

Fig 1b Flow chart of electromagnetic processes occurring in the polar ionosphere

make clear the present status of our observational understanding of the electric fields and currents in the polar ionosphere, in terms of considerable progress during the last years and future problems. There is no doubt that this task of reviewing such diverse subjects is extremely difficult for one author to cover the whole topics which are to be combined into a single consistent description, and also that such an attempt itself is subject to bias of the author. It is the present author's hope that the contents which follow will contribute to an improved understanding of various pieces of observational evidence of the high-latitude electric fields and currents, as well as serve as a reference source for the scientific community of related subjects It should be noted that there are several areas on important aspects of polar phenomena which are not intentionally covered in this paper. They are, for example, observations of geomagnetic pulsations and parallel electric fields, that are reviewed extensively in this conference by KOKUBUN (1979) and TERASAWA (1979), respectively. Thermospheric and ionospheric disturbances caused by particle bombardment, electric fields and currents during polar substorms are also excluded from this review. Readers are encouraged to consult

REES (1975), WICKWAR *et al.* (1975), ROBLE and REES (1977), and BREKKE (1977) for these topics.

In Fig. 1a, we show a logic diagram of electromagnetic processes occurring in the magnetosphere and ionosphere system in a way it is outlined by VASYLIUNAS (1970). The same 'loop' of the large-scale coupling between the magnetosphere and the ionosphere has been utilized by WOLF (1975) to discuss a self-consistent calculation of the convection electric field in the equatorial plane of the magnetosphere. Although it is extremely complicated to obtain a solution of the complete chain even with drastic simplifications, it is possible to break the 'closed' loop into individual links.

The link which is dealt with in this review paper is marked with a dashed box in Fig. 1a, and it is further decomposed into several boxes from a physical viewpoint in Fig. 1b. The number alongside each box expresses section number of this paper in which the corresponding topic is discussed.

2. Electric Field

The large-scale electric field plays a key role in the electrical coupling between the ionosphere and the magnetosphere. The motion of charged particles and the resultant pressure distribution in the magnetosphere are determined primarily by the electric field. A history of the observational study of the electric field is relatively new, compared with observations of the distribution of trapped particles and the magnetic field. During the 1973–1978 period, general reviews concerning the electric fields in the ionosphere and the magnetosphere have been published, including the work of MOZER (1973a), PUDOVKIN (1974), KANE (1976), GUREVICH *et al.* (1976), PFOTZER (1976), ROEDERER (1977) and STERN (1977).

2.1. Double probe observations

Experimental methods by which the electric field in the vicinity of the earth could be, directly or indirectly, determined are described in detail by STERN (1977). Satellites in polar orbit equipped with electric double probe, such as OGO 6 and INJUN 5, have determined the existence of a roughly circular region around the magnetic pole, called the polar cap, where the dawn-to-dusk electric field exists almost always. The measurements are in agreement with models in which the plasma convection across the polar cap is adequately described by a two-cell pattern, corresponding to the original idea of the magnetospheric convection by AXFORD and HINES (1961). The electric field has usually a total potential drop of the order of 20–100 kV across the entire region. The first global survey of the con-

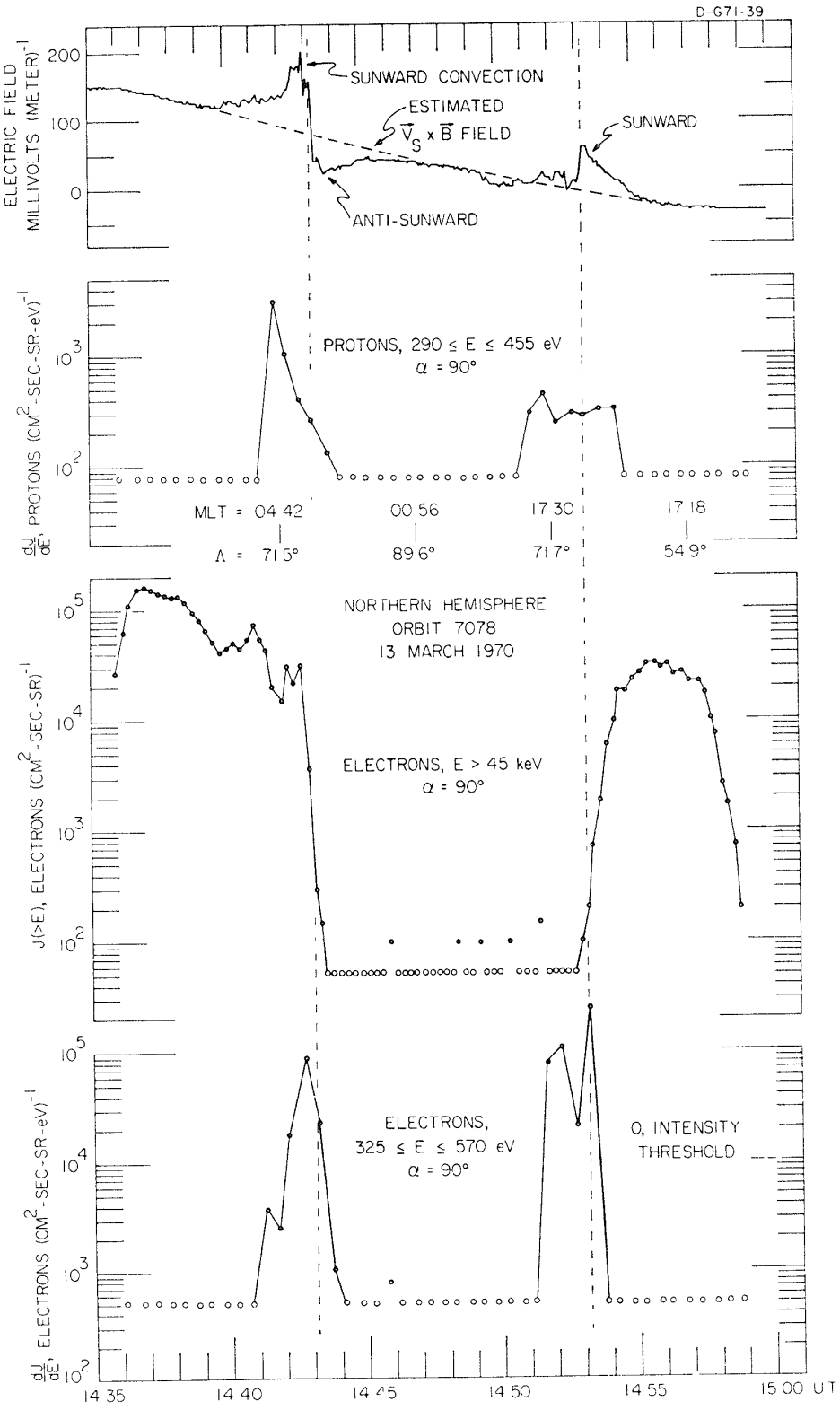

Fig 2. Simultaneous electric field and charged particle measurements showing the correspondence between the electric field reversals at 1443 and 1453 UT and the electron E>45 keV trapping boundary (after GURNETT, *1972b)*

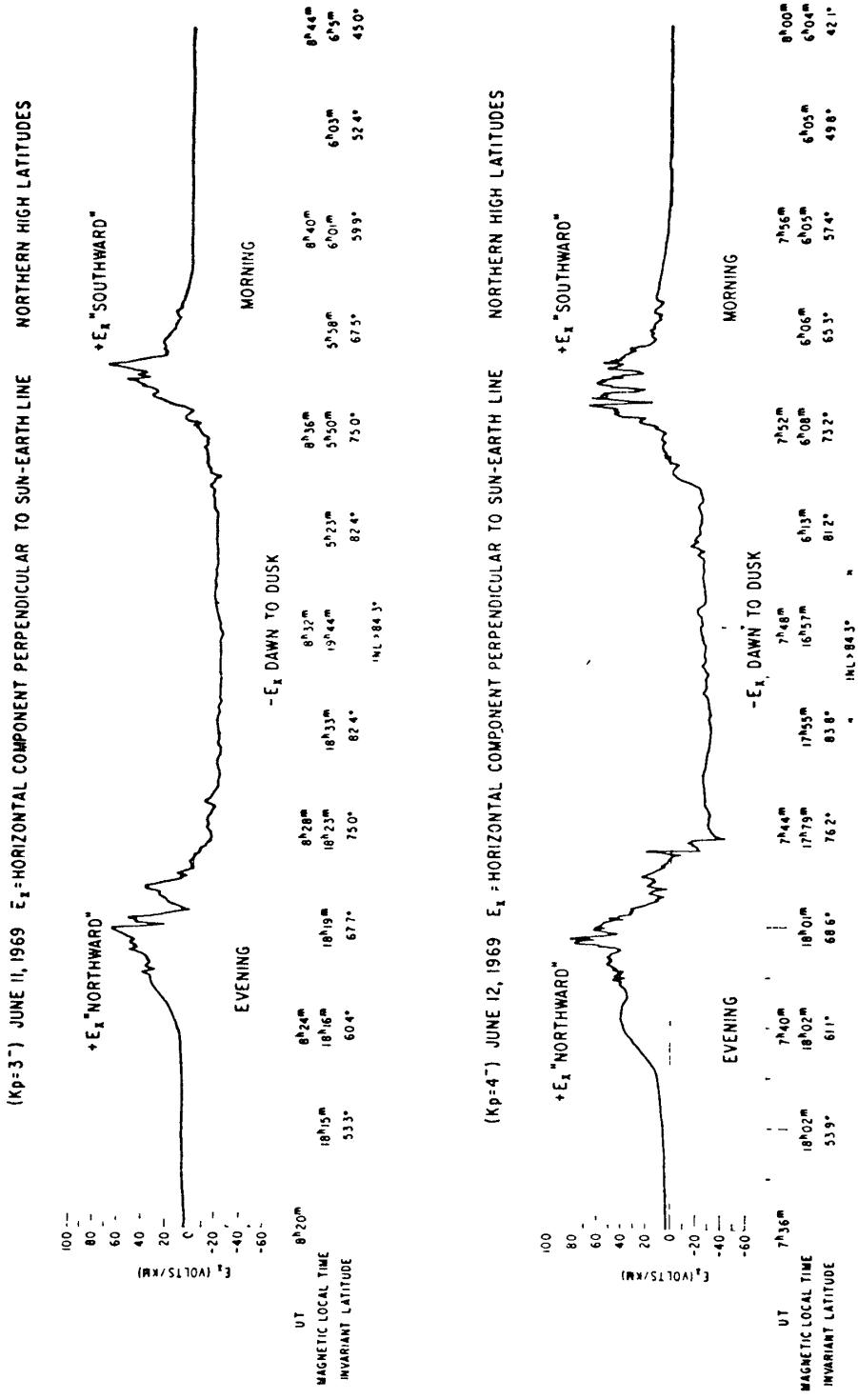

Fig. 3. Variations of the dawn-dusk component of the electric field observed by OGO 6 (after HEPPNER, *1972a).*

vection electric field was obtained from the double-probe experiment on the low-altitude (677 to 2528 km) satellite INJUN 5 (CAUFFMAN and GURNETT, 1971, 1972; GURNETT, 1972a, b). The most prominent feature of the INJUN 5 electric field data is the persistent occurrence of abrupt reversals in the electric field (and

thus in the convection velocity) at about 70° to 80° invariant latitude, with the occurrence of generally anti-sunward convection poleward of the reversal in the polar cap and sunward convection equatorward of it. These reversals are evident in Fig. 2 which is reproduced from GURNETT (1972b). FRANK and GURNETT (1971) found that the so-called trapping boundary for electrons with energies $E>45$ keV is located essentially coincident with the electric field reversal. This feature is clearly seen in Fig. 2 in which the times when the high-latitude termination of $E>45$ keV electron intensities is traversed by the satellite are shown by the vertical dashed lines at 1443 and 1453 UT. Since open magnetic field lines cannot sustain trapped energetic electron intensities, the observed correspondence between the electron trapping boundary and the electric field reversal provides evidence that the electric field reversal corresponds to the boundary between open and closed field lines (GURNETT, 1972b). A double-probe electric field experiment was also carried out by the OGO 6 satellite (HEPPNER, 1972a, b, c) Fig. 3 shows a relatively typical traverse across the polar region in the northern hemisphere. Although large fluctuations exist in the profile of the anti-sunward flow over the polar region observed by these satellites, the gross pattern shows a close similarity between the INJUN 5 and OGO 6 measurements in the dawn-dusk meridional plane, including the magnitude of the total potential difference across the entire polar cap The most important point to be noted is that the electric field pattern under very quiet conditions is basically the same as that observed under disturbed conditions (HEPPNER, 1972a). HEPPNER (1972a) thus concluded that electric field changes on a global scale cannot be invoked as a direct cause of magnetospheric substorms.

A quantitative disagreement between the observations with the INJUN 5 and OGO 6, however, seems to exist concerning the relative occurrence of the different types of convection profiles The INJUN 5 data showed that cases of uniform anti-sunward convection over the polar cap were relatively uncommon, as seen in Fig. 4a, while HEPPNER (1972a) showed that the convection pattern was nearly uniform over the polar cap region, as in Fig 4b The dased line in Fig. 4, separating the two regions of the sunward and anti-sunward flow, is the average location of the electric field reversal. It is, at present, unclear whether or not these two different flow patterns incorporate each other, and more practically, a question remains unsettled concerning under what condition each of the flow patterns occurs.

Dawn-dusk asymmetry of the magnitude of the dawn-dusk component of the electric field across the polar cap, occurs correlated systematically with the B_y component of the interplanetary magnetic field (HEPPNER, 1972b) An important

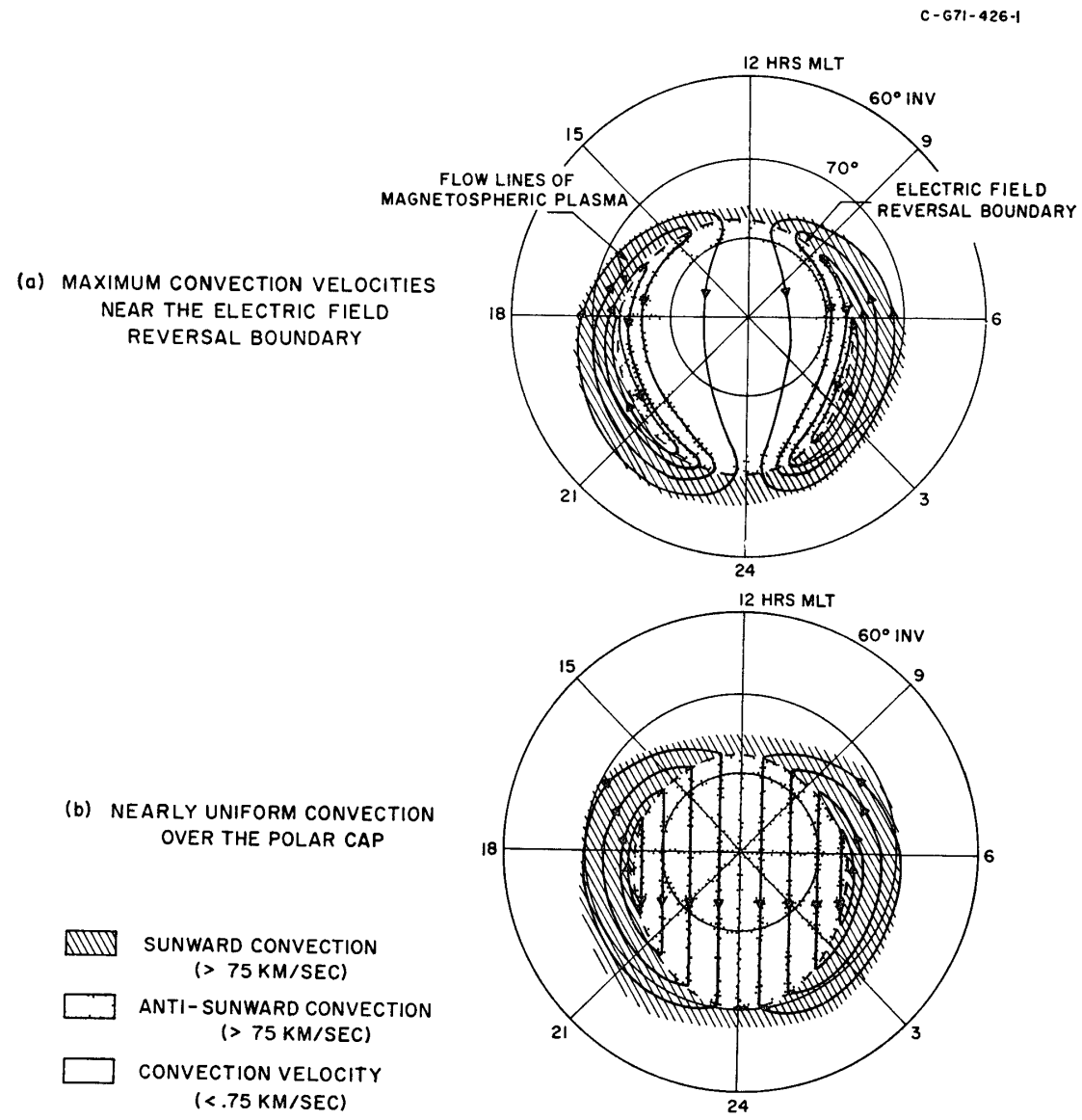

Fig. 4. Schematic diagram showing "average" convection patterns observed by INJUN 5 and OGO 6, ranging from (a) distinctly non-uniform and often asymmetrical anti-sunward flow over the polar region to (b) essentially uniform anti-sunward flow over the entire polar cap (after GURNETT, *1972b).*

feature is that the electric field distribution is strongly skewed toward either the morning or evening hours, depending on the azimuthal angle, ϕ, of the interplanetary magnetic field (see also HEPPNER, 1973). That is, the electric field tends to be stronger in the side of the polar cap on which the azimuthal component of the IMF and the projection of the earth's magnetic field into the equatorial plane point in the same direction; away from the sun's field, causing an enhancement on the dawnside of the northern hemisphere and the reverse is true for a sunward-pointing interplanetary magnetic field. RUSSELL and ATKINSON (1973) have

pointed out that the basic dawn-dusk shift of the convection field can be explained as an effect of the merging of magnetic field lines at the nose of the magnetosphere.

However, it should be pointed out that plasma flow patterns corresponding to away and toward sectors of the interplanetary magnetic field are not simple mirror images in the noon-midnight plane (HEPPNER, 1972b), suggesting that an additional effect which squeezes the antisunward flow toward the dawnside of the polar cap still remains. ATKINSON and HUTCHISON (1978) and KAMIDE and MATSUSHITA (1978b, c) have shown that an ionospheric conductivity gradient decreasing toward the nightside in the polar cap can produce such an effect.

Based on OGO 6 data, HEPPNER (1977) presented most recently empirical model convection (electric field) patterns corresponding to the two possible direction of B_y of the interplanetary magnetic field. These patterns are further modified on the nightside to represent the observed slant of the Harang discontinuity (MAYNARD, 1974a), as reproduced here in Fig. 5. Both types of models have a total potential difference of 76 kV. It was noted that these 'observed' field distributions at and near the polar cap boundary do not resemble the distributions frequently used in theoretical studies in that the maximum field intensities occur actually within the auroral belt and not at its polar cap boundary as depicted in theoretical models.

SWIFT and GURNETT (1973) studied the electric field behavior in the vicinity of auroral forms for both quiet and substorm times, using the INJUN 5 data. It was found that in the region of substantial electric field, a diffuse auroral arc was observed during the magnetically quiet pass, and auroral patches were observed during the substorm pass. In the substorm case, the electric field reversal tended to occur very near a discrete auroral arc at the poleward side of the diffuse arcs and patches. It was further noted, by comparing the quiet and substorm cases, that the convection electric field penetrates deeper into the magnetosphere during a magnetospheric substorm. Fig. 6 shows one substorm event when an anomalously large potential drop (~240 kV) was observed across the polar cap under the typical substorm circumstance (GURNETT and AKASOFU, 1974). They also found for the event that the electric fields across the polar cap immediately before the substorm onset and during the maximum phase of the substorm were essentially unchanged, indicating that an enhancement in the ionospheric conductivity rather than the electric field must be responsible for the large increase in the auroral electrojet current during the substorm.

It should be noted that the results from the INJUN 5 and OGO 6 data need not completely match. Some differences in detector sensitivity and data resolution

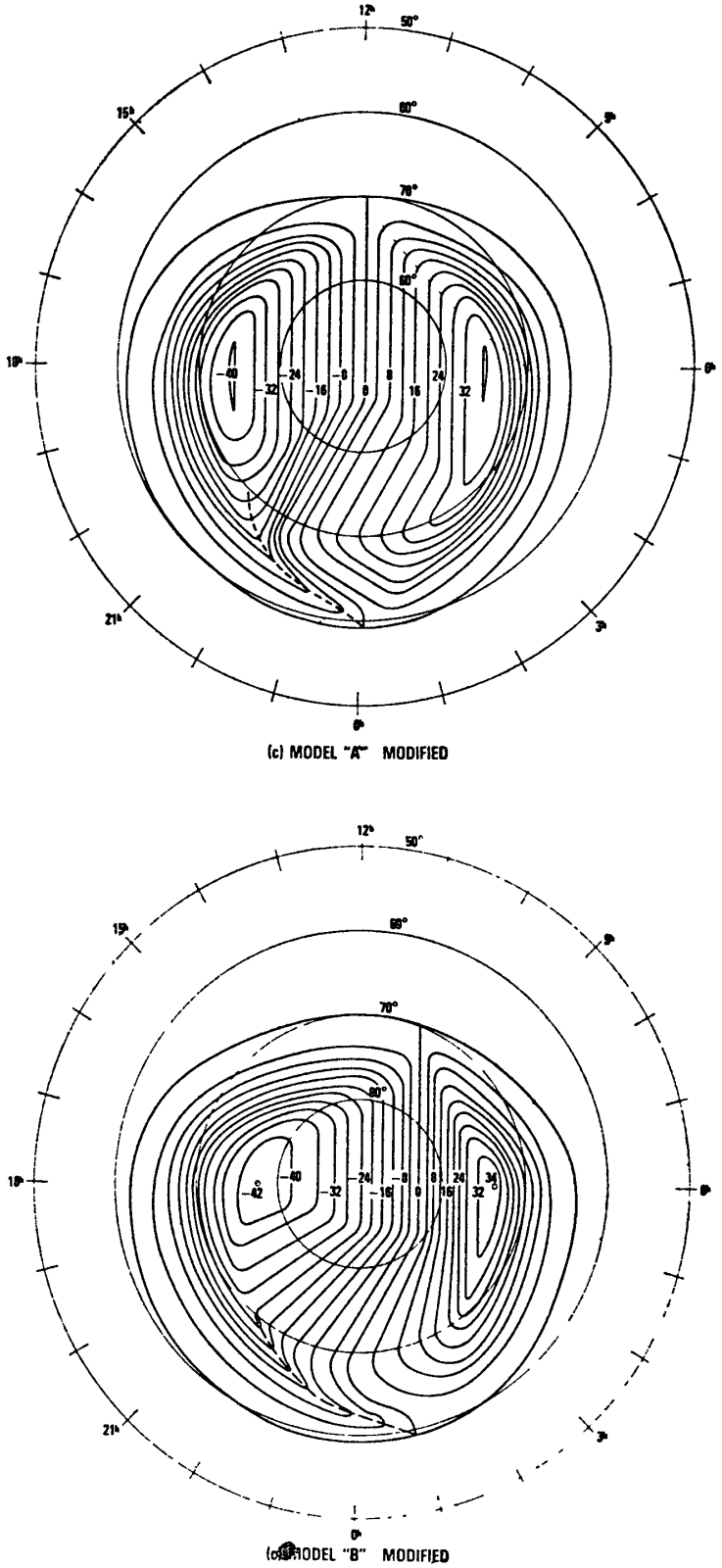

Fig. 5. Electric potential patterns corresponding to the positive and negative B_y of the interplanetary magnetic field (after HEPPNER, *1977).*

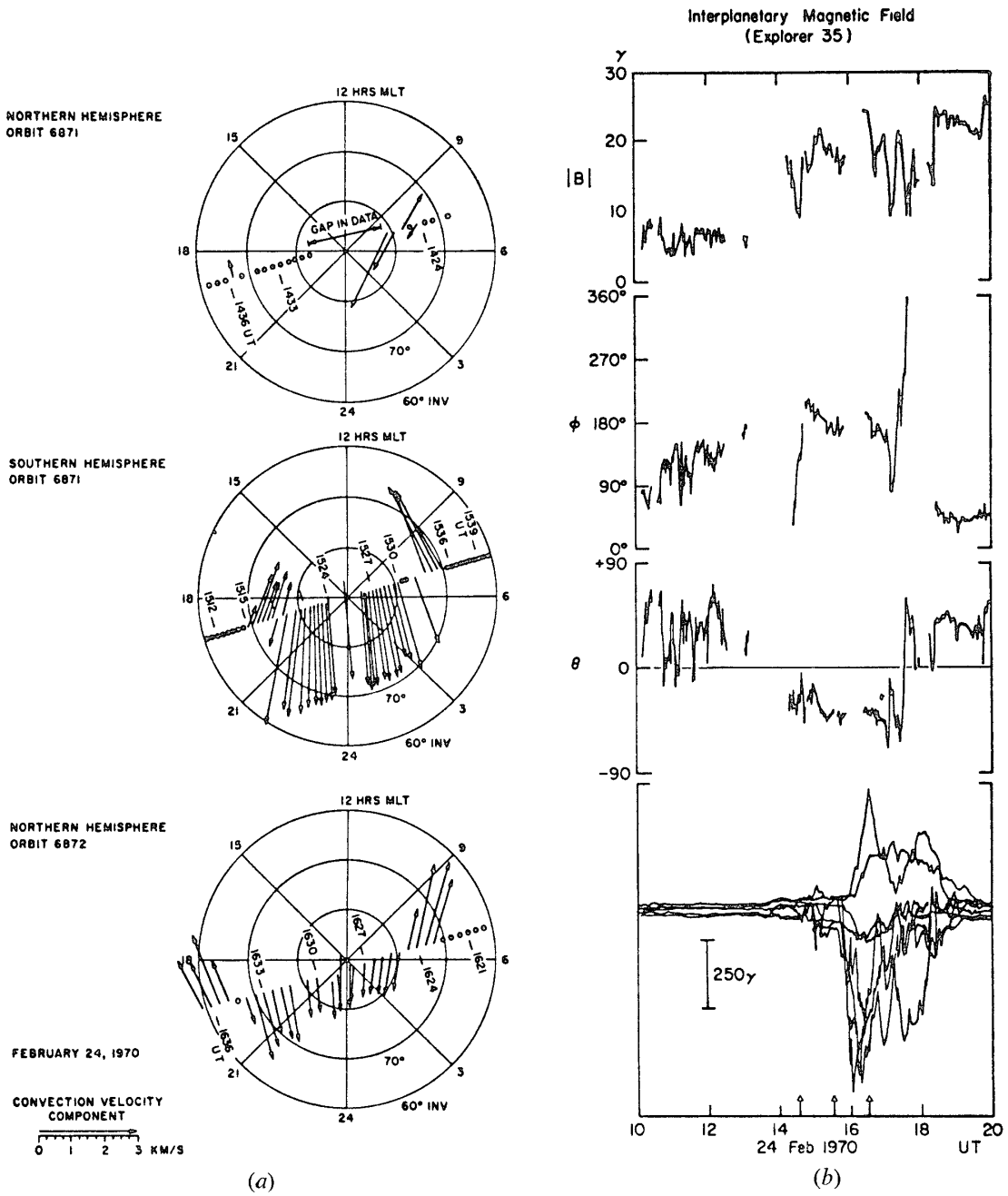

Fig 6. (a) Sudden enhancement of the polar cap electric field and (b) the associated IMF and geomagnetic field changes (after GURNETT and AKASOFU, 1974)

between the two satellites have been noted by GURNETT (1972b). The discrepancy may also be attributed either to the difference in the altitudes at which the satellite observations were made (PUDOVKIN, 1974) or to the fact that the both experiments used only a single pair of antennas and therefore were able to observe only one component of the electric field depending on the probe direction (STERN, 1977), or both.

The similar double probe is carried by various sounding rockets which are orbited into active auroral forms (MAYNARD and JOHNSTONE, 1974; WHALEN *et al.*, 1974, 1975; KELLEY *et al.*, 1975; CARLSON and KELLEY, 1977; MAYNARD *et al.*, 1977; EVANS *et al.*, 1977). It is one of the advantages of the rocket measurements that various conditions for auroral forms and substorm activity can be chosen for the particular rocket flights, thus allowing one to study in detail the small-scale field configuration in the auroras, whereas the orbital period (~100 min) of the polar-orbiting satellites is too long to follow individual auroral displays. Some results of the vector electric field associated with auroral arcs are discussed later together with the results based on other methods.

We discuss the results of measurements of horizontal electric field by means of balloon-borne double probes in the upper atmosphere (MOZER, 1973a). Although this method resembles those of satellite- and rocket-borne probes, it observes the field strength in the neutral atmosphere (~30 km altitude), not in the ionosphere or above it; see MOZER (1973b) and OGAWA (1973, 1976) for the reliability of this technique. PARK (1976) and BERING *et al.* (1977) have drawn attention to the problem of electrical coupling between the ionosphere and the lower atmosphere and indicated that the horizontal electric fields in the ionosphere map down to nearly 10 km with little attenuation. Fig. 7a shows hourly averages of electric field components as a function of local time which were measured in a nonrotating frame obtained from 32 balloon flights in the auroral zone (MOZER and LUCHT, 1974). These average values mapped in the equatorial plane of the magnetosphere (shown in Fig. 7b) fit well into the general picture of the sunward

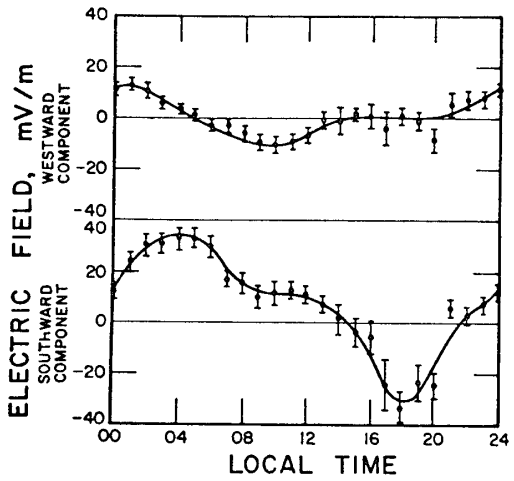

Fig. 7a. Hourly averages of electric field components measured in a nonrotating frame of reference on 32 balloons flown in the auroral zone (after MOZER and LUCHT, 1974).

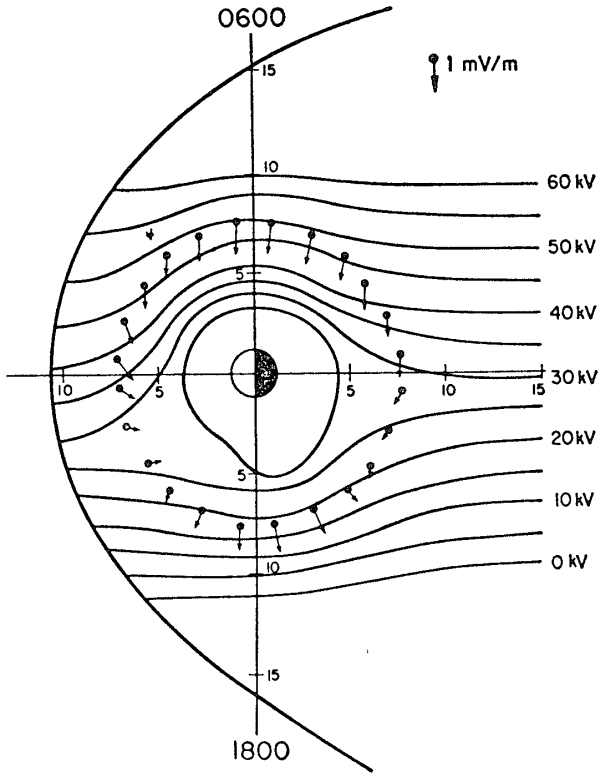

Fig. 7b. Hourly averaged electric field vectors plotted on the equatorial plane of a nonrotating frame of reference, as viewed from above the north pole (after MOZER *and* LUCHT, *1974).*

streaming plasma.

Electric field behavior obtained from individual balloon flights was also compared with other simultaneous observed parameters, such as the interplanetary magnetic field and the auroral distribution (MOZER, 1973c; MOZER *et al.*, 1974; KELLEY and MOZER, 1975; MADSEN *et al.*, 1976).

TANAKA *et al.* (1977a, b) have recently reported the results of measurements of vector electric fields made with balloons launched at Syowa Station, Antarctica, and obtained the convection pattern that has been normally observed in the auroral belt. It was also found that enhancements of the electric field were generally observed during polar substorms, but shorter period variations were shown not to correspond to those in ground magnetic fluctuations, indicating the importance of the great variability of the ionospheric conductivity.

HOLZWORTH *et al.* (1977) reported the results of four days of simultaneous auroral zone electric field measurements on balloons flown from six sites spanning approximately 180° of magnetic longitude. It was shown that if the observed configuration of the electric fields is mapped to the equatorial plane, the instantaneous

field does not generally exhibit a steady global dawn-dusk component, although there is a dawn-dusk component on the average at most local times. This indicates that at any given time the electric field can be quite variable. Their electric field data obtained during quiet periods also exhibit some characteristic differences from balloon data of electric field obtained for more active periods by MOZER and LUCHT (1974), in that the region of relatively large electric field during quiet times is more confined near midnight than that for more active times.

2.2. Barium cloud releases

This method of measuring the electric field involves releases of barium vapor into the atmosphere, as discussed by HAERENDEL *et al.* (1967) and DAVIS and WALLIS (1972). The experiment is usually carried out when the sun is below the horizon of the earth's surface but it still illuminates the released cloud, which can be visible and be partially ionized. Many releases provided interesting results, including a confirmation of the large-scale electric field pattern deduced from other measurements (WESCOTT *et al.*, 1969, 1970).

Recently, by the method of barium shaped charges injection it has become possible to follow plasma on magnetic field lines to great distances (WESCOTT *et al.*, 1974) and to test whether the assumption that the field lines are equipotentials is correct. Such shaped-charge injections of barium clouds were used to examine substorm features of the electric field, in particular, the parallel field (WESCOTT *et al.*, 1975), and the electric field structure in the vicinity of the dayside cusp (JEFFRIES *et al.*, 1975; WESCOTT *et al.*, 1978).

2.3. Rocket and satellite observations of ion drifts

It may also be possible to estimate the electric field by observing from spacecraft the bulk velocity of ambient plasmas. This method has been most extensively utilized in near-earth spacecraft, the AE-C satellite (HANSON *et al.*, 1973; HANSON and HEELIS, 1975; HEELIS *et al.*, 1976). BURCH *et al.* (1976) have studied the characteristics of pairs of oppositely directed spikes in ionospheric convection velocities and found that these phenomena tend to occur near the large-scale reversal from sunward to antisunward convection on the nightside of the earth, where inverted V-type electron precipitation is observed. This relationship between the electron precipitation and the electric field spikes is consistent with an upward-flowing current that is fed by Pedersen currents. They also have shown a case in which the step-like electric fields were pointing away from the region in between, where a sharp electron flux dropout was seen. This may be an indication of counterparts to inverted V-structure existing in regions of downward field-aligned

currents.

A determination of the convective electric fields from rocket measurements of the ionospheric bulk flow of thermal ions was made recently by MORGAN and ARNOLDY (1978).

2.4. Incoherent scatter radar

Doppler shifts of radar waves scattered incoherently from the ionosphere can give the bulk velocity in the ionosphere at altitude up to approximately 500 km (LEADABRAND *et al.*, 1972; DOUPNIK *et al.*, 1972; BANKS *et al.*, 1973; BREKKE *et al.*, 1973, 1974; HORWITZ *et al.*, 1978a) At altitudes above 160 km, ion velocities are almost entirely due to $E \times B$ drifts, thus from velocity measurements by the radars at these altitudes, the electric field impressed in the ionosphere can be obtained directly This field is mapped down to E-region altitudes (ECKLUND *et al*, 1977), where ion motion is influenced by ion-neutral collisions as well. This method provides an important tool for deriving the electric field, since it can monitor the field variation continuously for a comparatively long period and it provides simultaneously some other ionospheric quantities, such as currents, conductivity and neutral wind (*e.g*, PERREAULT *et al.*, 1977). The only facility of this kind presently operationing on a satisfactory basis in high latitudes is that at Chatanika, Alaska, which conducts many useful observations of the electric field near and in the auroral region during quiet and substorm times; see the review paper by BANKS and DOUPNIK (1975). A second facility of the incoherent scatter radar is the EISCAT system in Scandinavia, scheduled to begin the operation in 1978 (BOSTRÖM, 1975b; BREKKE, 1978, personal communication).

2.5. Some recent topics

In this subsection, some relevant topics of the high-latitude electric fields are briefly highlighted.

2 5.1. Electric field associated with auroras

It is reasonable to expect that the large-scale electric field and current are modified locally in and near auroral arcs, since an arc is a region of enhanced conductivity. However, the problem of the electric field and current inside an auroral arc associated with energetic electron precipitation is not well settled Accordingly, the following two important problems remain unsolved· (1) What are the main charge carriers responsible for field-aligned currents and where do these particles originate? (2) How are the field-aligned currents connected to ionosphere currents in and near auroral arcs? In order to examine observationally these questions, it may be necessary to conduct simultaneous measurements of, at least, the

electric field and the auroral location.

As discussed by ROSTOKER (1977), there appear two conflicting measurements of the electric field associated with auroral arcs where an intense electron precipitation exists. AGGSON (1969), POTTER (1970) and WESCOTT *et al.* (1969) indicated a decrease of the electric field within auroral form, whereas MOZER and FAHLESON (1970), GURNETT and FRANK (1973), and SWIFT and GURNETT (1973) observed an increase in the southward electric field inside auroral arcs. Most recently, MAYNARD *et al.* (1977) have shown by the use of a rocket measurement that electron precipitation is anticorrelated with electric field intensity (both in the north-south and east-west components) inside the arc, in agreement with the earlier report of MAYNARD *et al.* (1973). EVANS *et al.* (1977) have suggested for this particular observation that a polarization electric field is built within the arc such that current continuity is held at the arc boundary.

On the other hand, CARLSON and KELLEY (1977) have found based on ion flow data of a rocket double-probe that within a substorm-activated auroral arc, the electric field and energetic electron flux are correlated. EDWARDS *et al.* (1976) have reported that there was no simple relationship between the intensities of the electric field and precipitating electron flux.

In most of these conflicting observations, it was not conclusive enough to derive a definite understanding concerning the field and current around auroral arcs, because only a few ionospheric parameters were measured. As pointed out by BANKS and DOUPNIK (1975), however, the incoherent scatter radar can determine most of the electromagnetic properties. DE LA BEAUJARDIERE *et al.* (1977) have recently presented a set of comprehensive observations made with the Chatanika radar. These measurements are made with a relatively simple technique in which the radar antenna was pointed stationarily to the magnetic west, but discrete auroral arcs moved in the north-south direction so that one could observe the spatial variation of the physical parameters of interest assuming no temporal variation occurred during the observation interval. They have noted that the electric field data are interpreted by separating into two parts; an ambient field that is the large-scale electric field and an arc-associated electric field within the arc form. It is essential to stress this point in discussing the electric field intensity in relation to auroral arcs, since, as seen in the diurnal change of the electric field shown in Fig. 7, the large-scale electric field in the auroral latitudes is directed primarily northward in the evening sector while southward in the morning sector. According to DE LA BEAUJARDIERE *et al.* (1977), evening sector arcs yield a reduced northward electric field in the region where the enhanced electron density is present,

indicating that the reduced northward field is due to an added southward field associated with the auroral arc. For morning sector arcs, the southward field is stronger inside the arcs compared with outside. These features are clearly demonstrated in Figs. 8a and 8b, which are reproduced from Figs. 5 and 13, respectively, of DE LA BEAUJARDIERE *et al.* (1977).

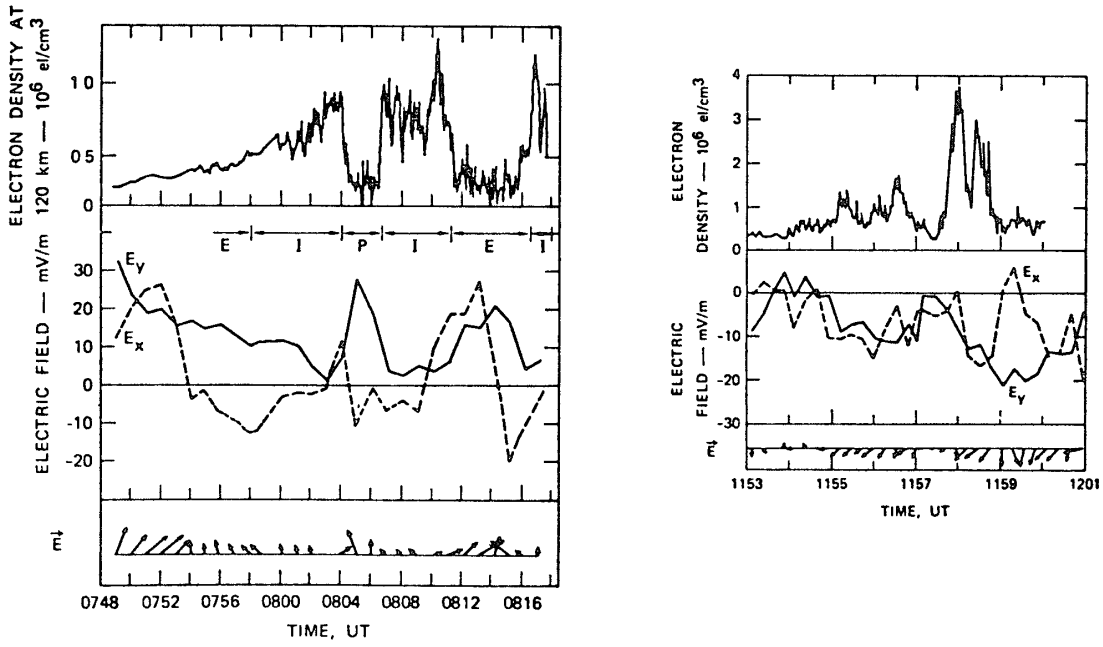

(*a*) (*b*)

Fig. 8. (*a*) *Electron density and electric field variations associated with the discrete evening arc. In the middle panel the solid line is the meridional field, positive northward, and the dashed line is the zonal field, positive eastward.* (*b*) *Same as* (*a*) *but for the intense morning arc* (*after* DE LA BEAUJARDIERE *et al*, *1977*).

It is noted in this connection that the results of DE LA BEAUJARDIERE *et al* (1977) may explain the opposite conclusions reached by several workers regarding correlations of the electric field intensity with energetic electron fluxes and electron density inside auroral arcs. It is interesting to point out that the observations by MAYNARD *et al.* (1977) were indeed made when the ambient electric field was directed northward, while those of CARLSON and KELLEY (1977) were obtained when the southward electric field was present in the vicinity of the substorm-associated arc. It is noted, however, that HORWITZ *et al* (1978a) have recently compared the electric fields probed at several latitudes by the Chatanika radar with optical auroral data from DMSP and all-sky photographs, and obtained that in the morning sector, sharp reductions of the southward electric field strength were seen in regions of bright, active auroras, with large electric fields often appearing immediately poleward of the high-latitude borders of these auroral re-

gions. Note also that MAHON *et al.* (1977) have recently observed a southward electric field with 35–40 mV/m intensity in the region of 2 kR diffuse aurora.

2.5.2. Electric field near the Harang discontinuity

Various phenomena reverse or change significantly their characteristics across

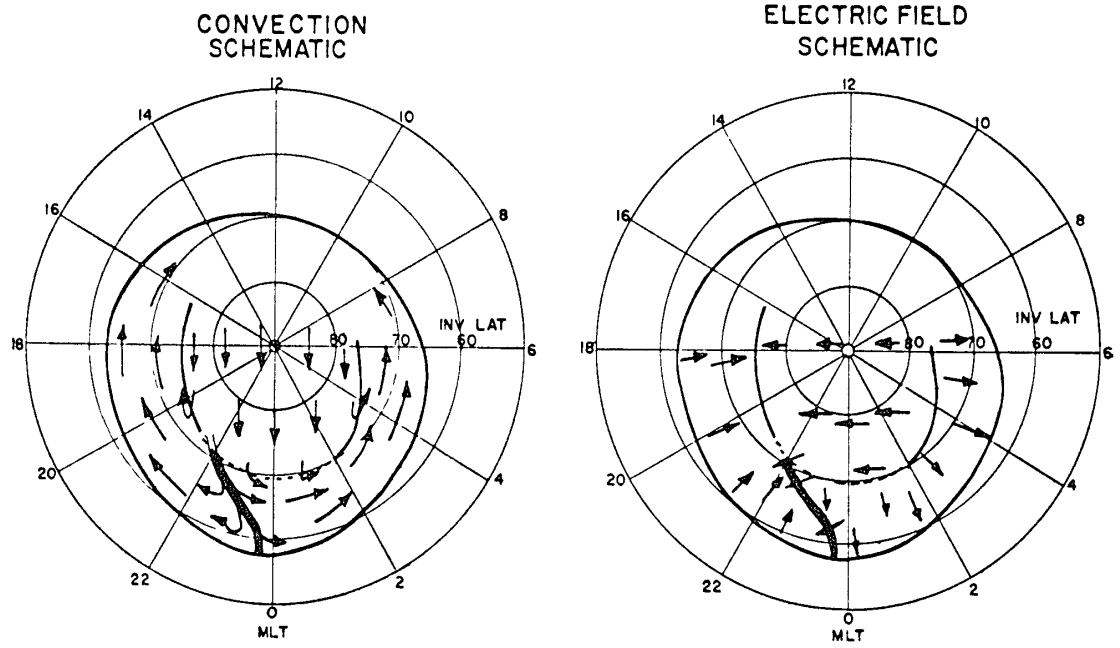

Fig. 9a. Schematic diagram of the convective flow and electric field distributions in the polar region (after MAYNARD, 1974a).

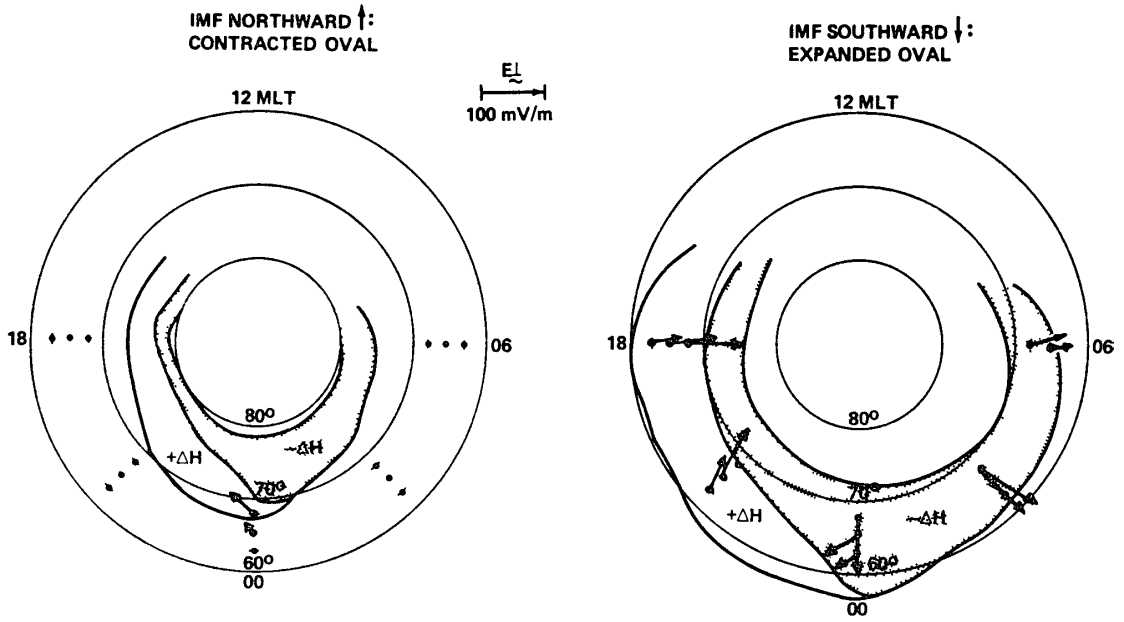

Fig. 9b. Schematic diagram showing the different geomagnetic ΔH and electric field patterns observed for northward and southward directions of the interplanetary magnetic field (after HORWITZ et al., 1978b).

the 'Harang discontinuity', denoted by HEPPNER (1972d). One of the phenomena that are used to identify the discontinuity is the direction change of the electric field. That is the locus separating the northward and southward electric fields. Fig 9 shows a schematic illustration of typical convective flow and the corresponding electric field directions in the polar region (MAYNARD, 1974a), where the Harang discontinuity can be seen which occurs in higher latitudes at earlier local times. MAYNARD (1974a) showed that the discontinuity in the electric field data obtained from OGO 6 double probe measurements is present even during extremely quiet times. It was then noted that the existence of the Harang discontinuity at quiet times would be difficult to recognize on the basis of other signatures, such as the H component reversal of ground magnetometer records.

It is also important to note that the reversal of the electric field cannot occur abruptly from northward to southward, but the northward-directed field would gradually rotate counterclockwise across the Harang discontinuity (MAYNARD, 1974a). KAMIDE (1978) stressed the importance of the predominance of the westward electric field in the Harang discontinuity 'region' in understanding the ionospheric current distribution in the premidnight sector, and showed a schematic diagram of latitudinal changes of the electric field in the vicinity of the Harang discontinuity It was emphasised that the 'Harang discontinuity region' is defined by the area with a finite width in which the westward component dominates over the north-south component; note that the electric field in the evening and morning sectors is dominated by its north-south component. The predominance of the westward field had been reported by WESTCOTT *et al* (1969) and BANKS *et al.* (1973). Their studies were based on barium cloud release experiments and the Chatanika radar, respectively. MAYNARD (1974b) further reported that the latitudinal width varies in conjunction with magnetic activity; the width becomes smaller under disturbed conditions and broadens under quiet conditions. WEDDE *et al.* (1977) showed that when the Harang discontinuity is traversed by ground-based instruments, such as the incoherent scatter radar, the discontinuity region (*i e*, the region where the convection flow direction changes from westward through south to eastward), occurs over a fairly wide local time range, say, 1–2 hours. HORWITZ *et al.* (1978b) have recently examined the latitudinal distributions of the electric field configuration near the Harang discontinuity region which were compared with those of isointensity ΔH contours in latitude and time and with the north-south component of the interplanetary magnetic field. Fig. 9b shows an illustration of the electric field and ΔH distributions in response to the changes in the interplanetary magnetic field, in which the Harang discontinuity is clearly

seen. It has been argued by them that although previous observations of the electric field in the premidnight sector stressed the enhancement of the westward component following the southward turning of the interplanetary magnetic field, overall oval expansion in latitude as indicated in Fig. 9b may be far more conspicuous than the enhancement of the westward field which is only observed near midnight. Moreover, westward field enhancement in the midnight sector could result from the latitudinal shift of the electric field pattern near the Harang discontinuity without a major change in the gross structure of the electric field.

The westward field in the discontinuity region has been shown to be modulated in the presence of discrete auroras (BANKS *et al.*, 1974; RINO *et al.*, 1974). However, the ionospheric conductivity changes across the Harang discontinuity have not been observationally established yet, although WEDDE *et al.* (1977) have reported that for at least one event, the discontinuity encounter by the Chatanika radar is accompanied by an abrupt increase in electron precipitation, the most intense part being located slightly east of the center of the discontinuity. We note that the day dealt with by the WEDDE *et al.* (1977) paper featured continuous substorm activity, so that it is difficult to distinguish unambiguously the auroral particle injection due to the Harang discontinuity region itself (*i.e.*, spatial change) and that to a substorm-related energization (*i.e.*, temporal effect).

The problem of electric field in the Harang discontinuity region lies also in the nature of the discontinuity in the magnetosphere, in spite of the fact that several attempts have been made to map the discontinuity onto the equatorial plane of the magnetosphere (MAYNARD, 1974a; FAIRFIELD and MEAD, 1975; BREKKE, 1977). There is little doubt that the discontinuity represents the convection boundary dividing the eastward and westward plasma drifts in the magnetosphere. However, the question of why various phenomena (such as ionospheric currents, auroral features and other substorm dynamics) change their characters across the discontinuity is unanswered. From a statistical study of plasma behavior at the synchronous orbit, LEZNIAK and WINCKLER (1970) defined a 'fault line' near local midnight, west of which inflation of magnetic field occurs and east of which collapse of magnetic field is observed during substorms. MAYNARD (1974a) suggested that when the Harang discontinuity is mapped onto the magnetotail, it can be identified as the fault line. However, a question is how the fault line forms the well-known local time dependence of the Harang discontinuity, namely, a 'slant' boundary. To resolve this question, detailed studies, both observational and theoretical, may be needed as to the large-scale convection characteristics related to ionospheric conductivities and field-aligned currents.

BREKKE (1977) has recently indicated that the Harang discontinuity defined by the electric field reversal corresponds to the substorm injection boundary in the magnetosphere This identification was made by comparing the north-south component field reversal observed by the Chatanika radar with the encounter of the injection boundary by the ATS 5. It is noted, however, that the injection boundary observed by the ATS 5 (MCILWAIN, 1974; MAUK and MCILWAIN, 1974) and Explorer 45 (KONRADI *et al.*, 1975, 1976) can be mapped to the equatorward boundary of the auroral belt (KIVELSON, 1976; KAMIDE and WINNINGHAM, 1977), rather than to the Harang discontinuity.

It is finally remarked that a new tool for inferring the ionospheric electric field is Doppler backscatter radars (HALDOUPIS and SOFKO, 1976; SOLVANG *et al*, 1977), which measures the drift velocity of electron density irregularities. Data from the STARE system, together with ground magnetic data taken from the Scandinavia meridian chain of observatories operated by the University of Münster, should provide a comprehensive situation of the ionospheric electric field and current near the Harang discontinuity. GREENWALD *et al.* (1978) have shown an interesting example of the STARE radar data in which the eastward drifting region (southward electric field) penetrates to the north of the westward drifting region (northward field) in the evening sector. The fairly dense network of the Scandinavia magnetic station during the IMS period has a clear ability to yield quantitative information in the fine spatial variation of the auroral electrojets in the region covered by the STARE radar system (KÜPPERS *et al.*, 1978). Some preliminary reports of the comparison between the radar and magnetic data are described in Section 8

2.5.3. Parallel electric field

We have so far discussed the perpendicular electric field only, but strong evidence of the existence of the parallel electric field has recently been reported The understanding of the field-aligned electric field is one of the most exciting and significant subjects of substorm physics relating to acceleration of auroral particles (SHAWHAN *et al.*, 1978). WESCOTT *et al.* (1976) and MOZER *et al.* (1977) have independently shown measurements of parallel electric field in the altitude range of 2000–8000 km in auroral latitudes.

It is interesting to note that ZMUDA *et al.* (1974) pointed out that the motion of the transverse magnetic field of field-aligned currents leads to induced electric fields parallel to the main geomagnetic field

For summary of theoretical studies which predict the existence of such a field, the reader may refer to the review paper by TERASAWA (1979) in this issue.

2.5.4. Penetration of high-latitude electric field into low latitudes

It is one of the important problems associated with magnetospheric convection how the high-latitude origin electric field can penetrate deep into lower latitudes (SWIFT, 1971; VASYLIŪNAS, 1972; PELLAT and LAVAL, 1972; VOLLAND, 1973; JAGGI and WOLF, 1973; MALTSEV, 1974; WOLF, 1974; YASUHARA, 1975; KAMIDE and MATSUSHITA, 1978c). The observational study of low-latitude effects of substorm-associated electric fields appears, at present, to be only at its beginning (TESTUD *et al.*, 1975). CARPENTER and KIRCHHOFF (1975) found by comparing the electric fields observed by two incoherent scatter radars at Chatanika, Alaska, and Millstone Hill, Massachusetts, that daily variations at the two radar sites are quite similar. KIRCHHOFF and CARPENTER (1976) examined the daily variations in ionospheric drift velocities at Millstone Hill and found that daily variations of electric field during with high geomagnetic activity were different from those during low geomagnetic activity, and that the electric field data on disturbed days followed basically the usual convection pattern but they included large day-to-day variations. HARPER (1977a, b) used variations in the electric fields measured at Arecibo and variations in ground magnetic perturbations at a nearby observatory, San Juan, to discuss the origins of the ionospheric electric fields and currents at mid-latitudes during both quiet and disturbed periods. It was suggested that the variations in the ground magnetic field on the very disturbed days appear not to be primarily due to the ionospheric currents. On the other hand, CARPENTER and AKASOFU (1972) showed that the westward electric field in the plasmasphere inferred from radial motions of whistler ducts is considerably intensified during substorms. TESTUD *et al.* (1975) reported also an enhancement of the westward field observed by an incoherent scatter radar at St. Santin, France, but not all substorms cause the enhancement. BLANC *et al.* (1977) and BLANC (1978) have recently suggested that while low-latitude extension of the convection electric field is not associated with all the substorms, it occurs in conjunction with the development of the partial ring current, indicating that large dawn-dusk asymmetry in ionosphere-magnetosphere coupling during substorms may be responsible for the lack of electric field shielding in mid-latitudes. By examining the world occurrence of sudden storm commencements, ARAKI (1977) has suggested that it is possible for the electric field impressed on the high-latitude ionosphere to penetrate deep into the equatorial region. SMIDDY *et al.* (1977) have conducted a DC electric field experiment on a polar-orbiting satellite (S3-2). Intense localized electric fields directed poleward in the pre-midnight sector near the ionospheric projection of the plasmapause were shown to be related to substorm activity.

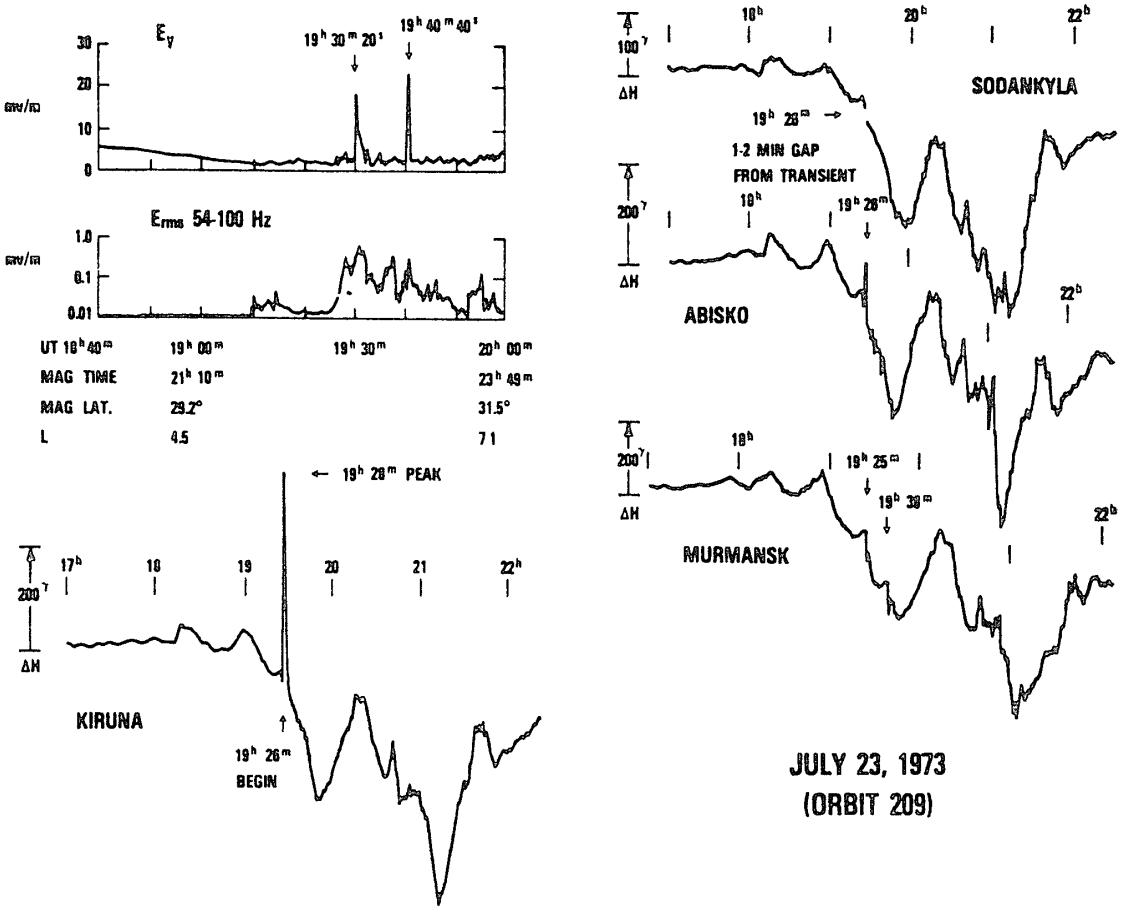

Fig. 10. Electric field observed by IMP 6 and simultaneous surface magnetograms (after AGGSON and HEPPNER, 1977)

2.5 5. Large transient electric field

The final topic of the high-latitude electric field relates to transient electric field events observed in the midnight sector at geocentric distances of 3 5–5 5 R_E with the long double-probe instrument carried by the IMP 6 satellite An example is shown in Fig 10, reproduced from Fig. 5 of AGGSON and HEPPNER (1977). These events usually have a total duration of 1 to several minutes, which occur under magnetically disturbed conditions, and in most cases can be associated with negative dH/dt excursions at magnetic observatories located near the foot of the field line intersecting IMP 6. AGGSON and HEPPNER (1977) then suggested that such transient electric fields provide an obvious mechanism for the impulsive acceleration and injection of plasma to populate the radiation belt

3. Auroral Particle Precipitation

The problems of precipitation patterns of auroral particles, their temporal

variations, and their energy spectra play a central role in high-latitude phenomena and magnetospheric processes. EATHER (1973) proposed that instead of the concept of the auroral oval defined statistically from visible auroras, the regions of particle precipitation that are subdivided by particle type and energy, would give a more physically meaningful framework for ordering a vast amount of geophysical data in high latitudes. During the period of 1973 to the present, a number of particle measurements have been carried out by low-altitude satellites, such as INJUN 5 (FRANK *et al.*, 1976), ISIS 1 and 2 (SHEPHERD *et al.*, 1973; WINNINGHAM and HEIKKILA, 1974; BURROWS, 1974; WINNINGHAM *et al.*, 1975; VENKATARANGE *et al.*, 1975; MCDIARMID *et al.*, 1975, 1976), DMSP (MISERA *et al.*, 1975; MENG, 1976; MENG *et al.*, 1977), ESRO (RIEDLER and BORG, 1972; HOLMGREN and APARICIO, 1973; DEEHR *et al.*, 1973; HULTQVIST, 1975), OGO 6 (WILLIAMS and TREFALL, 1973), and USAF 1971-089A (JOHNSON *et al.*, 1974; CAVERY, 1975; IMHOF *et al.*, 1975a), rockets in auroral region (REASONER and CHAPPELL, 1973; ARNOLDY and CHOY, 1973; BRYANT *et al.*, 1973; SHARP and HAYS, 1974; ARNOLDY *et al.*, 1974; REARWIN and HONES, 1974; WHALEN *et al.*, 1974; VIJ *et al.*, 1975; MILLER and WHALEN, 1976; ARNOLDY and LEWIS, 1977), and by ground-based optical instruments (MENDE and EATHER, 1975; SHEPHERD and EATHER, 1976; CHRISTENSEN *et al.*, 1977), and auroral X-ray measurements (KANGAS *et al.*, 1974, 1975; IMHOF *et al.*, 1975b; ROSSBERG, 1976; ROSENBERG *et al.*, 1977).

3.1. Diffuse and discrete auroral precipitations

One of the important findings in the auroral particle study is the identification of diffuse and discrete precipitations (WINNINGHAM *et al.*, 1975). The characteristics of both types of auroral particles are a complicated function of local time and latitude, and also of substorm time. HULTQVIST (1974) reviewed the characteristics of the auroral electrons and protons which impinge into these two auroral regions. HOLMGREN and APARICO (1973) and WILLIAMS and TREFALL (1976) have indicated that for >30 keV electrons, field-aligned precipitation can occasionally be observed in the evening and midnight sectors. PETERSON *et al.* (1977) have recently measured electron energy spectra extending to very low energy (~10 eV) in steady diffuse auroral forms by the AE-C and -D satellites.

The upper half of Fig. 11 (LUI *et al.*, 1977) shows both 5577 and 3915 Å photometer records which were taken from the ISIS 2 satellite. Both photometers show two peaks of intensity. The lower panel shows the spectrogram obtained by the same satellite for electrons and protons. Detailed inspection of these data

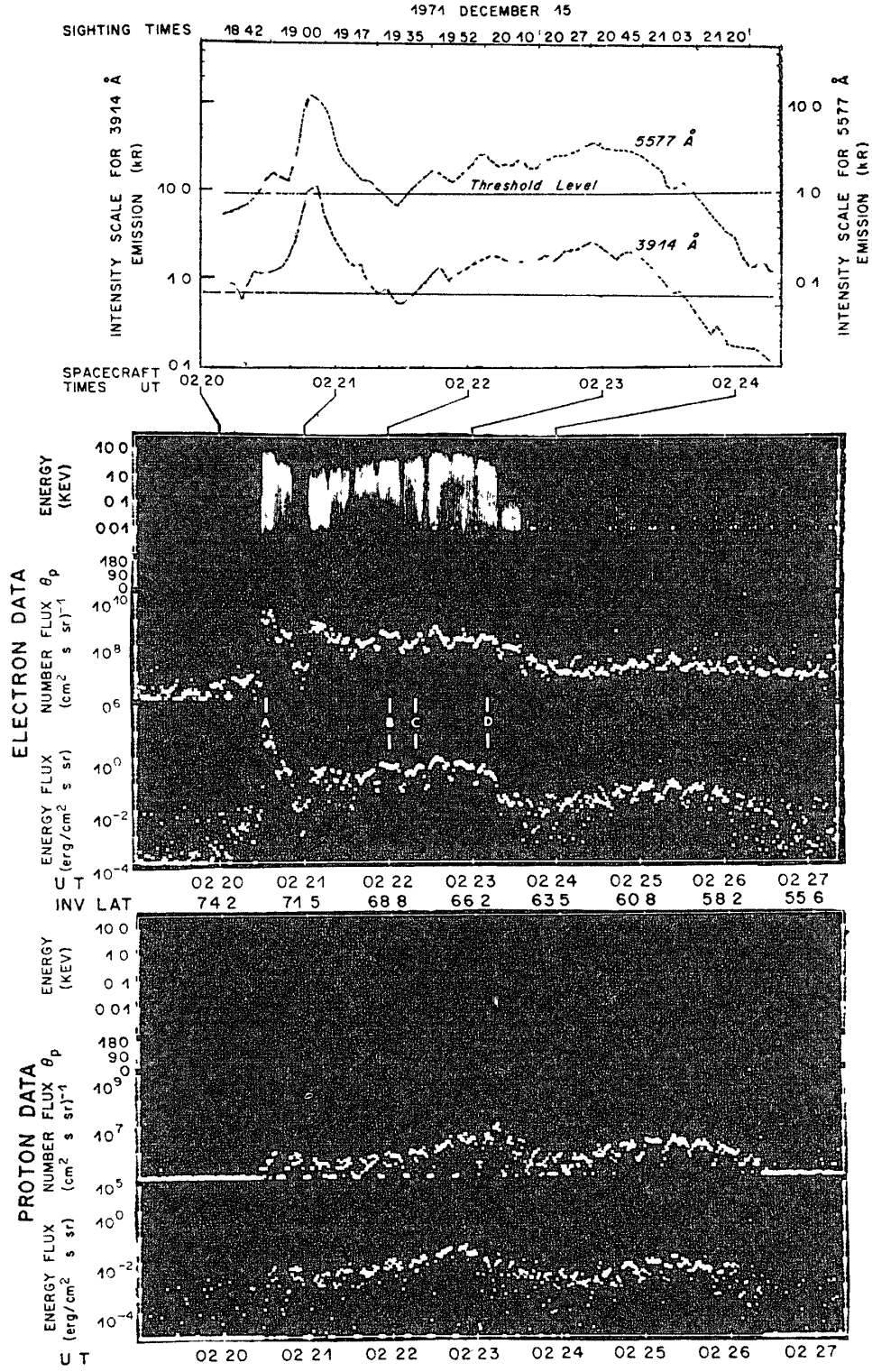

Fig. 11. Auroral intensity profiles along the magnetic projection of the satellite (ISIS 2) and the SPS electron and proton data on December 15, 1971 (after LUI et al., 1977).

indicates that the precipitation region can be divided into two regions. At the highest latitude end, there is a precipitation region in which both the intensity and energy of electrons are highly variable. Its latitudinal range is between 73.5° and 70.0° which corresponds to the region where discrete auroral arcs are present. Equatorward of this region, there is an extensive precipitation region with fairly uniform intensity, called the diffuse aurora. A very characteristic decrease of electron energies (*i.e.* softening of auroral particles) is seen toward the equatorward boundary.

Fig. 12 shows four energy spectra of auroral electrons which were taken at the times A, B, C and D indicated in Fig. 11. Lui *et al.* (1977) have shown by comparing the spectra A and D, which correspond to the discrete and diffuse auroral regions, respectively, that the most important difference between them is

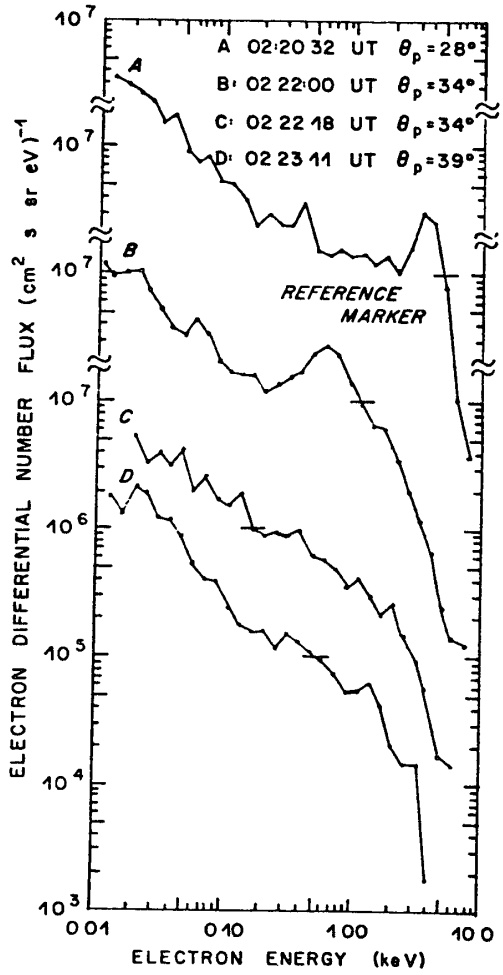

Fig. 12. Electron energy spectra taken from various locations within the region of auroral precipitation on December 15, 1971. Spectrum A is obtained within the discrete aurora, and B, C and D are obtained within the diffuse aurora (after Lui et al., 1977).

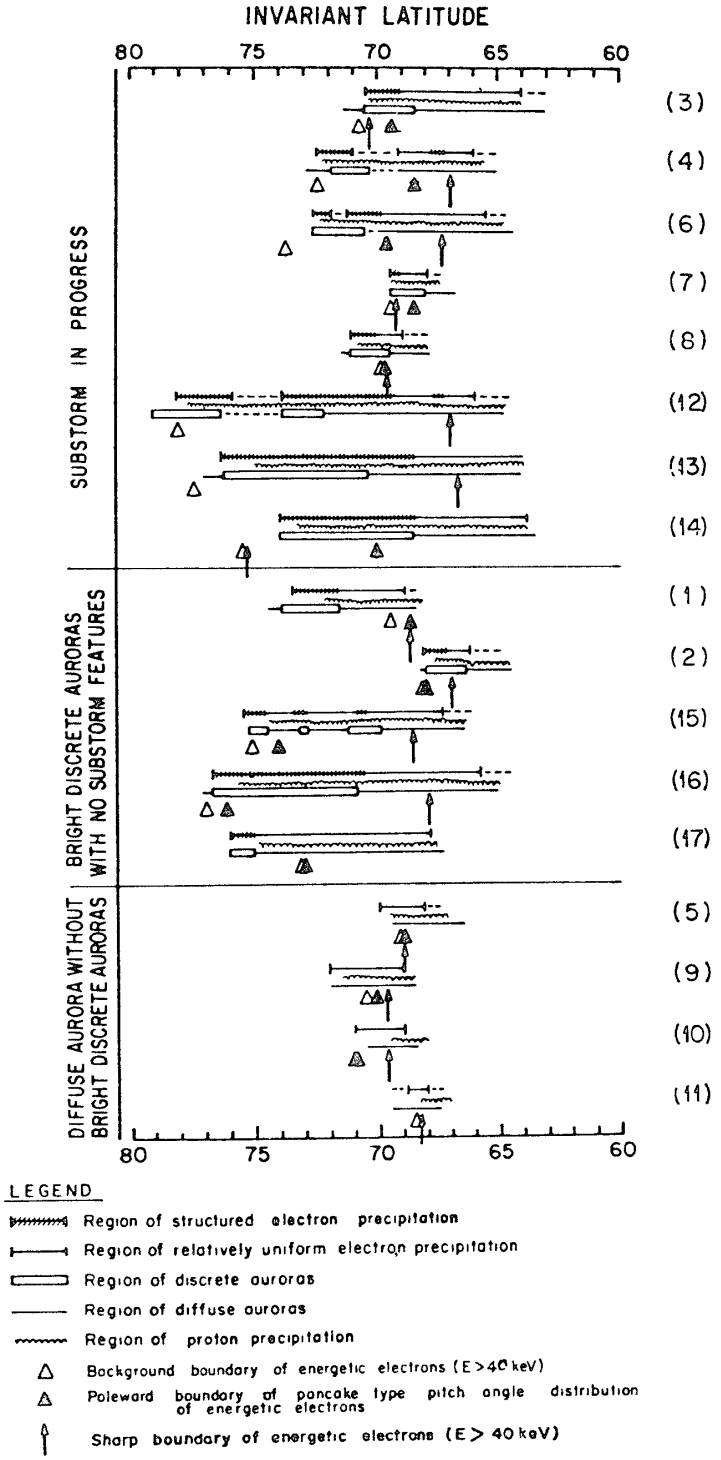

Fig. 13. Schematic illustration to summarize the results of comparison between regions of auroral and particle precipitation. Each satellite pass is represented by three lines to indicate the extent and characteristics of particle precipitation and the types of aurora (after LUI *et al , 1977)*

the presence of a peak of the flux at about 3.5 keV in A, whereas it is absent in D. Note that GURNETT and FRANK (1973) have already shown the existence of the diffuse, structureless precipitation in the region a little equatorward of inverted V precipitation region.

MENG *et al.* (1978) examined electron precipitations above the westward traveling surge, which is the domminant feature of the discrete aurora during substorms. The most spectacular precipitation feature is observed inside the main body of a surge where an unusually flat differential spectrum was observed, extending from 0.2 keV to at least 20 keV. Thus, the MENG *et al.*'s (1978) measurements indicate a substantial precipitation of energetic electrons above 20 keV inside a surge.

Fig. 13 shows a diagram to summarize the results of comparison between regions of auroras and particle precipitation. Each pass is represented by three lines to indicate the latitudinal extent and characteristics (for example, diffuse or discrete) of particle precipitation and aurora (LUI *et al.*, 1977). The general features are summarized as follows:

1) The region of discrete aurora corresponds to the region of highly structured electron precipitation where the electron differential energy spectra show prominent peaks within the energy range of 0.1–10 keV.

2) The diffuse aurora corresponds to the region of relatively uniform electron precipitation in which the pitch angle distribution is generally isotropic. Over the greater part of the diffuse auroral region the dominant contribution to the intensity is from low-energy (E_e<13 keV) electrons which carry energy fluxes in an order of magnitude larger than the low-energy (E_p<13 keV) protons. During substorms, precipitating electrons typically have monotonically decreasing energy spectra in the low-latitude portion of the diffuse aurora. Significant softening of the electron spectrum is seen at the equatorward boundary of the diffuse aurora.

Summarizing these results, Fig. 14 presents a schematic diagram illustrating the relationship between the plasma sheet and the two types of auroral precipitation for both quiet and substorm times (LUI *et al.*, 1977). The identification of the diffuse auroral region as the earthward (inner) termination of the plasma sheet at the auroral altitude is consistent with the works of LASSEN (1974), WINNINGHAM *et al.* (1975) and KAMIDE and WINNINGHAM (1977). This suggestion is also similar to that of EATHER *et al.* (1976) who identified the nightside 'soft' electron precipitation is a consequence of loss cone drizzle of plasma sheet electrons. Since the discrete auroras, such as auroral arcs, occur usually in the poleward portion of the diffuse aurora, the source can be reasonably inferred to lie on the geomag-

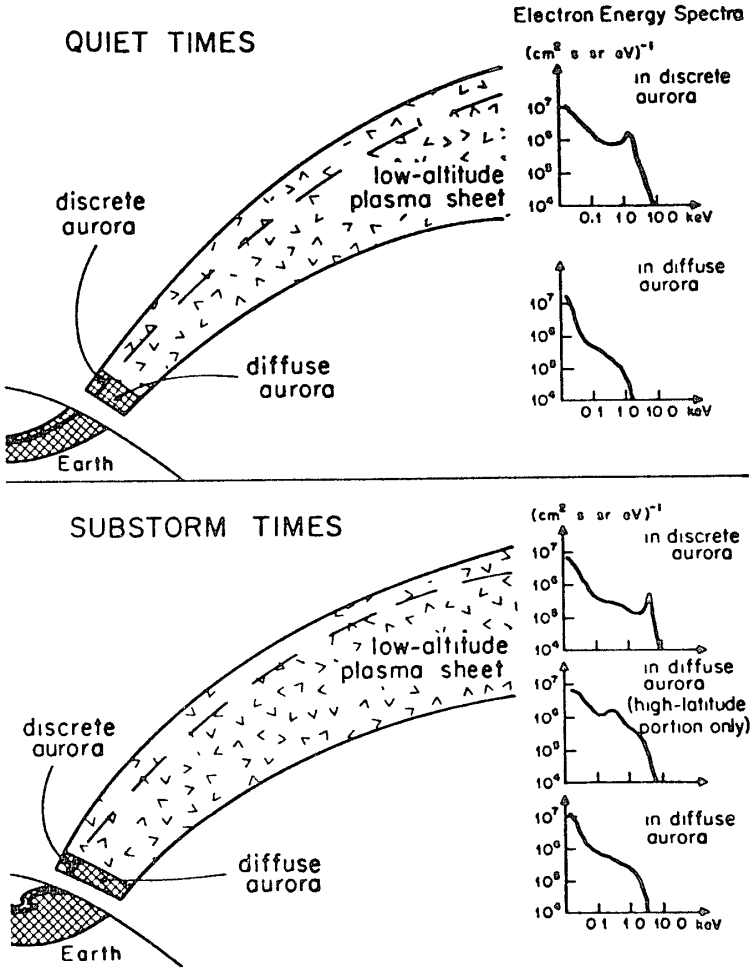

Fig. 14. Schematic diagram to illustrate the spatial relationship between the plasma sheet and the two types of aurora (after LUI *et al., 1977).*

netic field lines within the plasma sheet, near its poleward boundary, as illustrated in Fig. 14. This is one of the reasons that WINNINGHAM *et al.* (1975) referred to the intense and structured precipitation region as the boundary plasma sheet (BPS). LUI *et al.* (1977) have further noted that the different characteristics of particle precipitation within the discrete and diffuse auroral precipitations indicate that different acceleration mechanisms are operative in these two types of auroras. That is, the close resemblance of energy spectra between the plasma sheet electrons and the precipitating electrons within the diffuse aurora may suggest no need of significant acceleration processes for the production of the diffuse aurora, whereas strong acceleration mechanisms producing nearly monoenergetic spectra are required to account for the peaked component observed repeatedly in the discrete auroras.

DEEHR *et al.* (1976) made a correlative study, a simultaneous observation

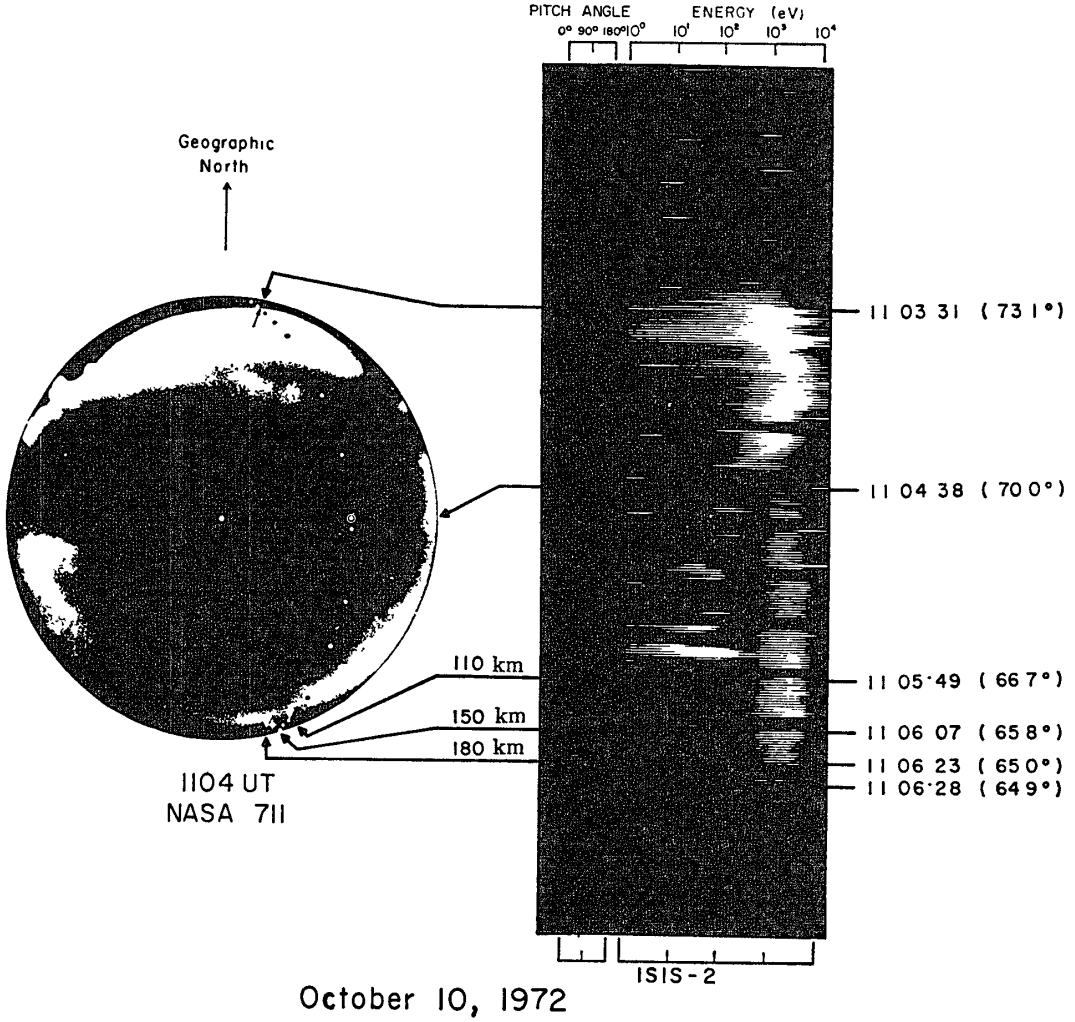

Fig. 15. All-sky camera record corresponding to the closest time of passage of the ISIS 2 satellite whose SPS data are displayed on the righthand side. The path of the satellite is projected downward along magnetic field lines to a 110 km altitude and shown as dots on the all-sky photograph (after DEEHR *et al., 1976).*

of the two auroral regions, from above by the ISIS 2 satellite and from below by the NASA 711 aircraft, which provided the electron spectrogram and all-sky picture of auroras, respectively. Fig. 15 shows the all-sky photograph (at the left-hand side) and the electron spectrogram (at the right-hand side), both of which clearly distinguish two types of auroras; an active discrete aurora located poleward and the diffuse aurora covering the equatorward half of the sky. Similar correlative studies have been made by MIZERA *et al.* (1975), CAVARY (1975), and MENG (1976), and most recently by KAUFMANN *et al.* (1978) who compared electron measurements during a rocket flight over an active aurora with optical observations by all-sky cameras and a TV system.

Although HOFFMAN and BERKO (1971) showed a general agreement of the

shapes between the oval of visible auroras and that of high fluxes of low energy (~0.7 keV in their OGO 4 detector) electrons, CRAVEN (1970), HULTQVIST (1972), and RIEDLER (1972) showed that the precipitating pattern of electrons for energies higher than 1 keV differs considerably from the FELDSTEIN and STARKOV's (1967) auroral oval. A statistical examination of the precipitation pattern was conducted by McDIARMID *et al.* (1975, 1976) for various energies of electrons in the range of 150 eV to 210 keV. Very complicated patterns in 'magnetic local time and invariant latitude' coordinates even for such an averaged flux distribution are found.

KAMIDE and WINNINGHAM (1977) have utilized the electron spectrogram from a number of ISIS 1 and 2 passes to study the effects of the interplanetary magnetic field in the auroral oval. It was found that the north-south component of the interplanetary magnetic field plays the dominant role in controlling the shift of the equatorward boundary of the electron auroral oval. Fig. 16 shows the location of the boundary of the diffuse electron precipitation at different local times for three B_z component values of the IMF. There is a significant difference in the amount of the shift between the evening and morning sectors; *i.e.*, for the same decrease in B_z value, the boundary moves more equatorward in the morning sector than in the evening sector. It was also noted that when the obtained oval particle boundary was projected onto the equatorial plane of the magnetotail along model

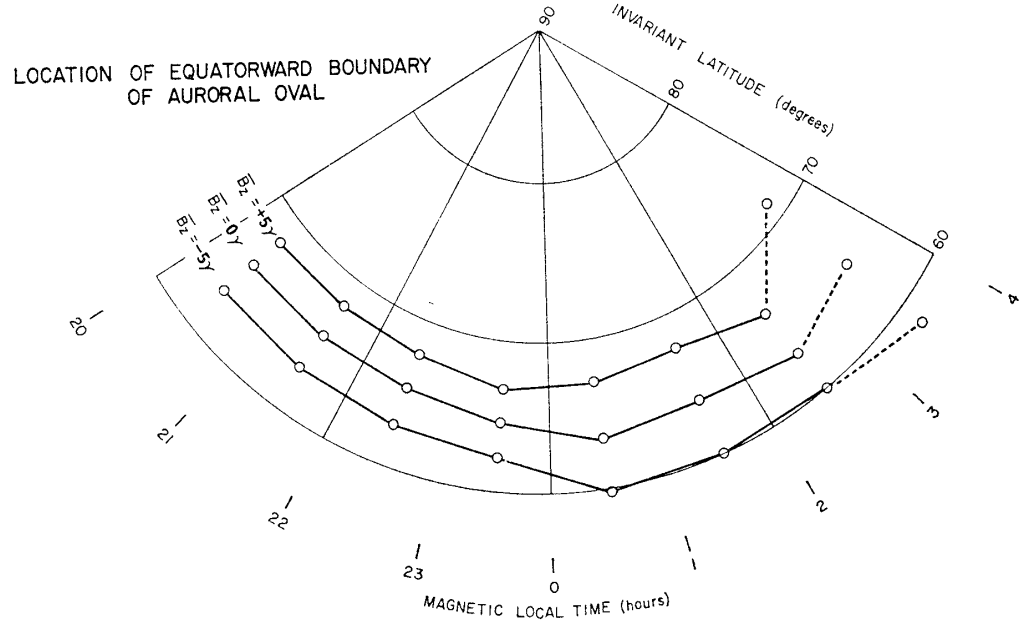

Fig 16 Location of the equatorward boundary of the diffuse electron precipitation at different local times in the dark sector for three B_z values of the IMF (after KAMIDE and WINNINGHAM, 1977)

magnetic field lines (MEAD and FAIRFIELD, 1975; FAIRFIELD and MEAD, 1975), good agreement was found between the projected boundary and the drift boundary (the Alfvén layer) of low-energy electrons in the presence of the dawn-dusk electric field. KAMIDE and WINNINGHAM (1977) interpreted this agreement to give new evidence showing that the diffuse electron precipitation that produces the diffuse aurora originates near and at the inner boundary of the plasma sheet. Substorm occurrence probability seen in the ISIS spectrograms was studied by KAMIDE *et al.* (1977a), who concluded that it increases as the auroral oval expands equatorward, in agreement with the suggestion by LUI *et al.* (1975).

Rocket-borne detectors can be used to examine in detail the pitch angle distribution of auroral particles as well as the differential energy spectra (*e.g.*, WHALEN and MCDIARMID, 1972; ARNOLDY and CHORY, 1973; SIVJEE and MCEWEN, 1976; LUNDIN, 1976; BRYANT *et al.*, 1978; KAUFMANN *et al.*, 1978). Peaks around a few keV in the energy spectra have been confirmed by a number of rocket observation. Such 'mono energetic' peaks overlap the 'continuum' which extends below 1 keV studied in detail by REASONER and CHAPPELL (1973), SHARP and HAYS (1974) and RAITT and SOJKA (1977). BOYD and DAVIS (1977) have shown that a narrow field-aligned component appears superimposed on a more isotropic electron distribution. EDMONSON *et al.* (1977) measured the spectrum of high energy precipitating electrons (2–26 keV) at the onset of a magnetic storm by a rocket borne experiment. The spectra show an unusual double-peaked distribution with maxima at near 5 and 17 keV, whose intensities vary independently during the sudden brightening of the aurora.

ARNOLDY (1974) reviewed the results of intense fluxes of field-aligned electrons (*i.e.*, peaked near zero-degree pitch angle). An intense field-aligned electron flux is often confined within a very narrow spectral range. Fig. 17 shows such an example in which an intense field-aligned electron flux of energy 2 keV is seen (ARNOLDY *et al.*, 1974). BOSQUED *et al.* (1974) showed that auroral electrons of energies 300 eV–5 keV indicated a large anisotropy while electrons of energies greater than 5 keV were almost isotropic. Note that most of the rocket observations were performed in the region of the discrete aurora, not of the diffuse aurora.

Inference of energies of precipitating electrons can be done with the aid of auroral emission measurements (*e.g.*, ZWICK and SHEPHERD, 1973; REES *et al.*, 1976; PIKE *et al.*, 1976; MOREELS *et al.*, 1976; KASTING and HAYS, 1977; BEITING and FELDMAN, 1978). DEEHR *et al.* (1973) made an extensive study of the electron energy flux and the resultant 4278 Å intensity on the basis of data from the ESRO satellite. MENDE and EATHER (1975) and PIKE *et al.* (1976) showed

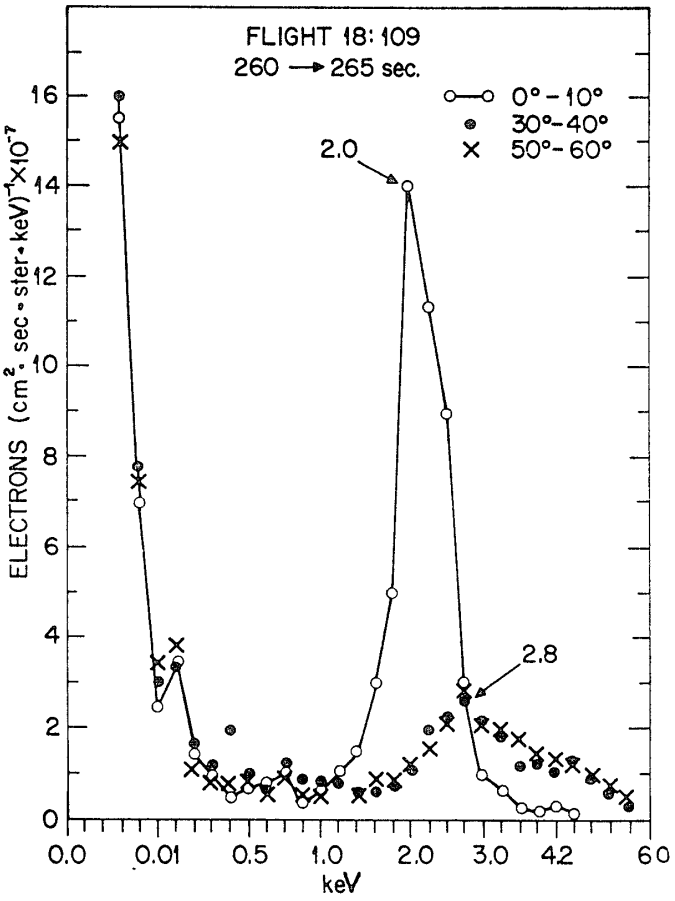

Fig. 17. Pitch-angle sorted spectra of auroral electrons (after ARNOLDY et al., 1974).

the gross precipitation patterns over the entire polar region, which are inferred from the spectroscopic observations. Most recently, VONDRAK and SEARS (1978) have made simultaneous radar and photometric measurements of the mean energy of precipitating electrons at Chatanika, Alaska, during a variety of auroral conditions. The radar observations of the altitude profile of electron density were used by them to obtain the differential energy spectrum of the precipitating electron flux NAGATA *et al.* (1975) used an enhancement in the *E* region electron density to infer the occurrence of the direct ionization by precipitating electrons. REES *et al.* (1977) have recently reported results of a coordinated auroral experiment involving the AE-C satellite and a sounding rocket Auroral primary electron fluxes measured by the satellite have been used in a model calculation, in which the electron density and OI emissions at 5577 and 6300 Å are obtained and found to be in good agreement with those observed by the rocket-borne instrument

3.2. Proton auroras

Earlier observation of hydrogen emissions showed that the hydrogen aurora

appears as an oval-shaped belt, but it is displaced with respect to the electron auroral oval. OGUTI (1973) and FUKUNISHI (1975) showed that in the morning sector, the proton aurora is located a little poleward of the electron auroral region, while it is located equatorward in the evening sector; see Fig. 18 which is reproduced from FUKUNISHI (1975). FUKUNISHI (1975) showed that in the morning sector, both the electron and proton auroras overlap during quiet times, but the proton aurora appears poleward of the electron aurora during substorms. Both types of auroras occur presumably in the region of the westward electrojet in morning hours. Furthermore, KAMIDE and FUKUNISHI (1973) showed that the proton aurora is in general colocated with the eastward electrojet in the evening sector. We note here that caution should be exercised in interpreting the distribution of the hydrogen emission, since, as BELON *et al.* (1974) showed, a part

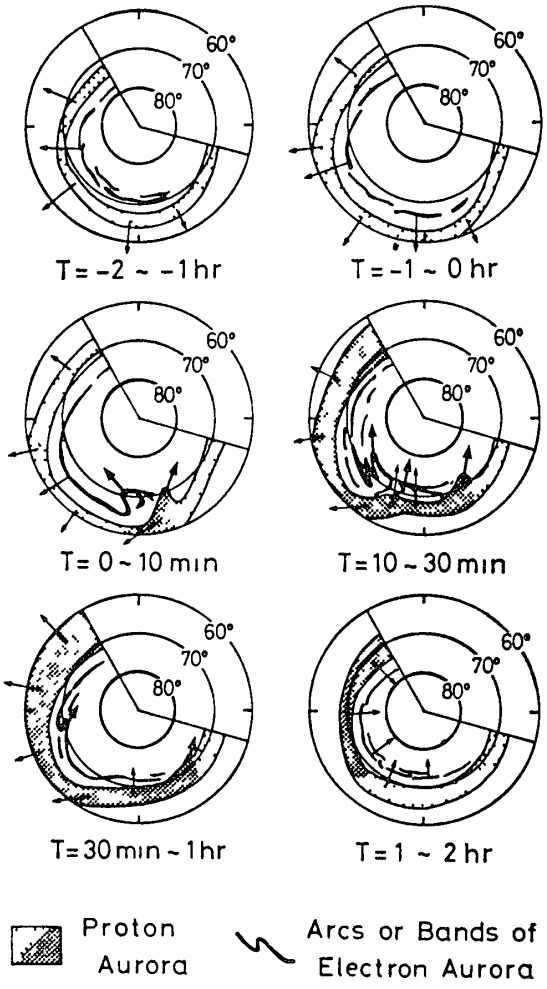

Fig 18 Schematic illustration of the development of the proton and electron auroral substorms (FUKUNISHI, 1975).

of the hydrogen emission might arise from the excitation of ambient hydrogen atoms impinged by auroral electrons Measurements of positive ion charge spectra were also conducted with an ion charge spectrometer on board sounding rockets (LYNCH *et al.*, 1976, 1977).

On the other hand, direct observations of precipitating protons by polar-orbiting satellites, such as ESRO and ISIS, have most comprehensively been made by HULTQVIST *et al.* (1974). SORAAS *et al.* (1974) also made a rocket observation of auroral protons and the H_β emission in a post-breakup auroral glow. A somewhat interesting conclusion emphasized by HULTQVIST *et al.* (1974) is that the general precipitation pattern of protons is quite similar to that of electrons, a results being contrast to the observation by FUKUNISHI (1975). Particularly, large differences of the latitudinal distributions of the electron and proton precipitation do not occur during quiet conditions and there is a large-scale correlation between variations in proton and electron fluxes. It should also be noted that LUI *et al.* (1973, 1977) emphasized the importance of low-energy electrons from 100 eV to 10 keV in the region of the diffuse aurora in the equatorial half of the evening auroral oval, where proton aurora is advocated by FUKUNISHI (1973, 1975).

HULTQVIST (1975) noted from an examination of the longitudinal distribution of the precipitation fluxes of low (<10 keV) energy particles that there is no essential asymmetry between dawn and dusk, indicating that the responsible particles are not injected into a narrow sector around midnight, but are generally injected over the total dark sector and are subject to an immediate precipitation before they can drift over appreciable longitude.

3.3. Precipitation in the polar cap and dayside cusp

Auroral particle precipitation in the polar cap has most extensively been studied by WINNINGHAM and HEIKKILA (1974). After an extensive analysis of the ISIS satellite spectrograms, they put forward the terms 'polar rain' and 'polar shower' to express, respectively, a fairly uniform precipitation of soft (~100 eV) electrons and a structured electron precipitation with energies of about 1 keV inside the polar cap. It was suggested that the polar shower is responsible for discrete auroras in the polar cap which is greatly enhanced in conjunction with substorm activity; such an intensified shower is called 'polar squall' by WINNINGHAM and HEIKKILA (1974).

The precipitation of electrons with energies below 1 keV (corresponding to the polar rain) over the entire polar cap in association with the interplanetary magnetic field has recently attracted considerable attention (*e.g.*, FENNELL *et al.*,

1975; YEAGER and FRANK, 1976; FOSTER and BURROWS, 1976, 1977; MENG and KROEHL, 1977; see also the recent review paper by MIZERA and FENNELL, 1978). FENNELL *et al.* (1975) suggested that the uniform polar cap precipitation during quiet times consists of interplanetary-origin electrons having direct access to the polar cap through the magnetotail. YEAGER and FRANK (1976) found a correlation between the intensity of these low-energy electrons in the northern tail lobe and the interplanetary magnetic field directed away from the sun.

Using precipitating electron data from the DMSP satellite, MENG and KROEHL (1977) showed evidence revealing significant enhancements (as large as two orders of magnitude) during magnetic storms over the quiet-time level of flux. A strong asymmetry between the northern and southern hemispheres was also observed. Moreover, MENG *et al.* (1977) reported a clear indication of the existence of the dawn-dusk gradient of the flux distribution in the polar cap, the direction of the gradient being dependent on the B_y component of the IMF. An example of electron precipitation over the northern polar cap region observed by the DMSP 32 satellite is shown in Fig. 19, in which a distinct asymmetric precipitation is noticed at the 200 eV channel. This character has a striking similarity to the distribution of the magnitude of the dawn-dusk component of the electric field in the polar cap obtained by HEPPNER (1973). Simultaneous examinations of electric fields and electron precipitation intensity are urgently needed. FOSTER and BURROWS (1977) have recently indicated the possibility for low-energy electrons over the polar cap to be at times accelerated and trapped by a large-scale potential barrier in the magnetotail. It was proposed that if the effective potential difference at the barrier fluctuates randomly, a fraction of the fluxes accelerated toward the earth beyond the barrier may be trapped between the barrier and the earth. Auroral particle precipitation in the polar cap during sudden commencement has also been examined by LASSEN and WEILL (1976).

Electron spectra observed in the dayside cusp region are usually to peak below 100 eV, and proton spectra peak near 1 keV (DOERING *et al.*, 1975, 1976; MCEWEN, 1977; MOE *et al.*, 1977; WINNINGHAM *et al.*, 1977; POTEMRA *et al.*, 1977, 1978; DALY and WHALEN, 1978; KINTNER *et al.*, 1978). CRAVEN and FRANK (1976) determined that the electrons in this region are strongly field-aligned and similar to the inverted V's observed at later local times. Recent observations by CRAVEN and FRANK (1978) suggest that the polar-cusp electron intensities are regulated also by the sign of the latitude of the interplanetary magnetic field. Recent reports by ROSENBAUER *et al.* (1975), HAERENDEL and PASCHMANN (1975), PASCHMANN *et al.* (1976), HANSEN *et al.* (1976), and BAVASSANO-CATTANEO and

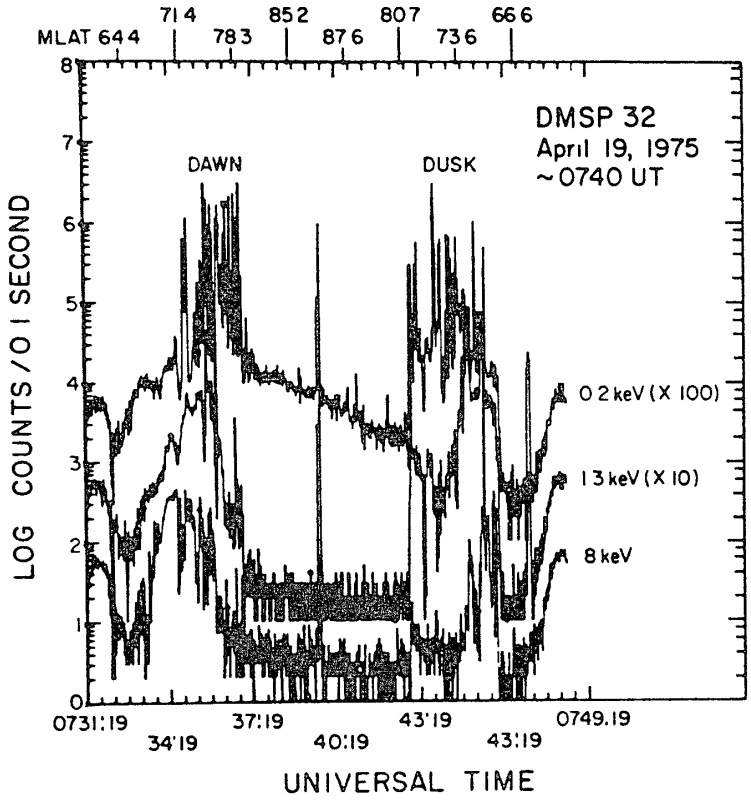

Fig 19 An example of the low-energy electron precipitation over the northern polar region observed by the DMSP 32 satellite The satellite crossed the northern polar cap from the dawn sector to the dusk sector, and the auroral intense precipitation was observed over the auroral oval near 73° magnetic latitude in both morning and evening sectors. Over the polar cap a distinct asymmetric precipitation was detected at 200 eV along the dawn-dusk meridian; no significant fluxes were observed at energies higher than 1 keV over the polar cap (after MENG et al., 1977)

FORMISANO (1978) of flowing plasma in the polar cusp are relevant to the question of access of solar wind particles to the magnetosphere; see also EASTMAN *et al.* (1976), and HEIKKILA (1975, 1978). CROOKER (1977a, b) has indicated that the 'entry layer' for the solar wind particles is a permanent feature which extends across the dayside and along the flanks to large distances down the tail on field lines between extensions of the northern and southern polar cusps Ion measurements obtained by the AE-C satellite were used to show systematic variations of the cusp ion evergy as a function of latitude, which are consistent with an injection of solar wind protons through magnetic merging at the dayside magnetopause (REIFF *et al*, 1977, HILL and REIFF, 1977) Cusp phenomena at the ionospheric level such as electron density enhancements, were studied by UNGSTRUP *et al.* (1975), OLESEN *et al.* (1976), TITHERIDGE (1976), WHITTEKER (1976), and CHACKO and MENDILLO (1977).

4. Aurora

The distribution of visible auroras can be observed by ground-based all-sky cameras and TV systems, airborne all-sky cameras, and satellite scanners from above the pole. Previous studies of the distribution and forms of auroras had relied principally upon all-sky cameras. An all-sky camera has only a limited 'field of view' and often fails to detect the diffuse aurora, thus even the combination of the IGY all-sky camera network being not extensive enough to provide the opportunity to observe the distribution of luminous auroras over the entire polar region. There is no doubt that auroral physics has been advanced to a significant extent by studies of photographs from a scanning camera aboard the ISIS 2 and DMSP satellites (ANGER *et al.*, 1973a, b, 1978; SHEPHERD *et al.*, 1973; ANGER and LUI, 1973; LUI *et al.*, 1973; LUI and ANGER, 1973; PIKE and WHALEN, 1974; SNYDER *et al.*, 1974; ROGERS *et al.*, 1974; SNYDER and AKASOFU, 1974; MIZERA *et al.*, 1975). This type of camera reconstructs a map of auroral luminosity from horizon-to-horizon scans of the earth by a photometer sweeping perpendicular to the orbital path. Efforts have been made to improve computer programs for transforming the obtained data into various coordinate systems and for producing latitude profiles of auroral intensities at different local times (MURPHREE and ANGER, 1977; HAYS and ANGER, 1977; HARRISON and ANGER, 1977a, b). Reviews on the development of recent morphological studies of the aurora have been published by AKASOFU (1974a, 1976) and JONES (1974). The similarity between the terrestrial auroral substorm and dynamic processes in solar flares has also been stressed by NAGATA (1975) and OBAYASHI (1975). A search for auroral type dynamics in solar flares has been attempted (DE FEITER, 1975; BECKERS *et al.*, 1977). The scanner data have revealed several new auroral characteristics which had not been clearly recognized by all-sky camera studies; see AKASOFU (1974a) for details. Furthermore, it is now possible to identify the position of the auroral electrojets and the field-aligned currents with respect to the pattern of large-scale auroral display, observed from the satellites. In this section, we review briefly the recent progress of the optical aurora made by the new techniques, as well as some new features of the dynamical small-scale aurora obtained by TV and all-sky camera observations.

4.1. Diffuse and discrete auroras

AKASOFU (1974a) examined how various auroral patterns (such as rayed arcs, patches, torches, Ω bands) in the combined all-sky camera records are

represented by the large-scale structure in the satellite-viewed pictures. During a prolonged interval (say, >12 hrs) of the northward interplanetary magnetic field, the size of the auroral oval is approaching to its minimum size with low visible brightness (AKASOFU, 1975), namely auroral activity is very 'quiet'. Based on several montage photographs of the DMSP auroral forms, AKASOFU (1976) also examined overall features of auroral characteristics in different local time sectors. Emerged from these studies is a schematic distribution pattern in Fig 20 showing the main characteristics of auroras during an auroral substorm.

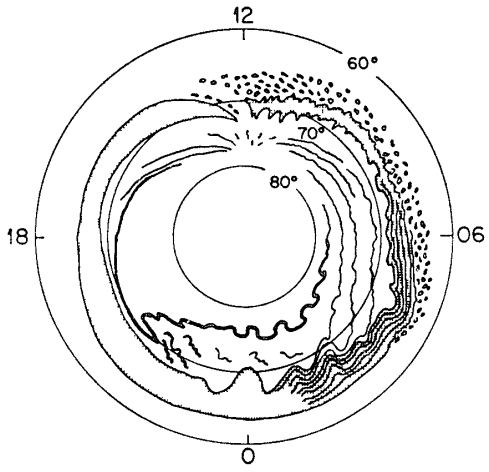

Fig. 20. Schematic diagram showing the main characteristics of auroras during the typical auroral substorm. Discrete arcs are indicated by lines and the diffuse auroral regions are shaded (after AKASOFU, 1976).

As previously discussed in terms of auroral particle precipitation, there are essentially two auroral belts, diffuse and discrete auroras (AKASOFU, 1974a). According to AKASOFU (1977), the diffuse aurora can be defined as a broad band of auroral luminosity with a width of, at least, several tens of kilometers which is separated from the discrete aurora. The diffuse auroral belt has been studied in detail by LUI and ANGER (1973), SHEPHERD *et al.* (1973), LUI *et al.* (1973), PIKE and WHALEN (1974), and SNYDER *et al.* (1974). The diffuse aurora often covers a significant part of the field of view of an all-sky camera, making it difficult to recognize its presence from a single ground station. Thus, the FELDSTEN and STARKOV's (1967) auroral oval does not necessarily represent accurately the distribution of the diffuse aurora particularly in the evening sector. The fact that the region of the diffuse aurora covers a large latitudinal range well beyond the view of a single all-sky camera makes also it difficult to obtain the global distribution of the diffuse aurora However, all-sky cameras carried by two aircrafts, one

located in the northern hemisphere and the other in the southern hemisphere, might be used to study the structure of the diffuse aurora (STENBAEK-NIELSEN *et al.*, 1973). It was found that the diffuse aurora contains complicated fine structures and that such fine structures in one hemisphere can be identified in the other hemisphere. This character of the diffuse aurora contrasts with that of the discrete aurora, of which conjugacy breaks down at times during intense substorms.

It should be also noted that the poleward boundary of the diffuse aurora develops in various wavy forms, such as omega (Ω) bands and torch structures. Fig. 21 shows an example of well-developed torch-like structures during an intense

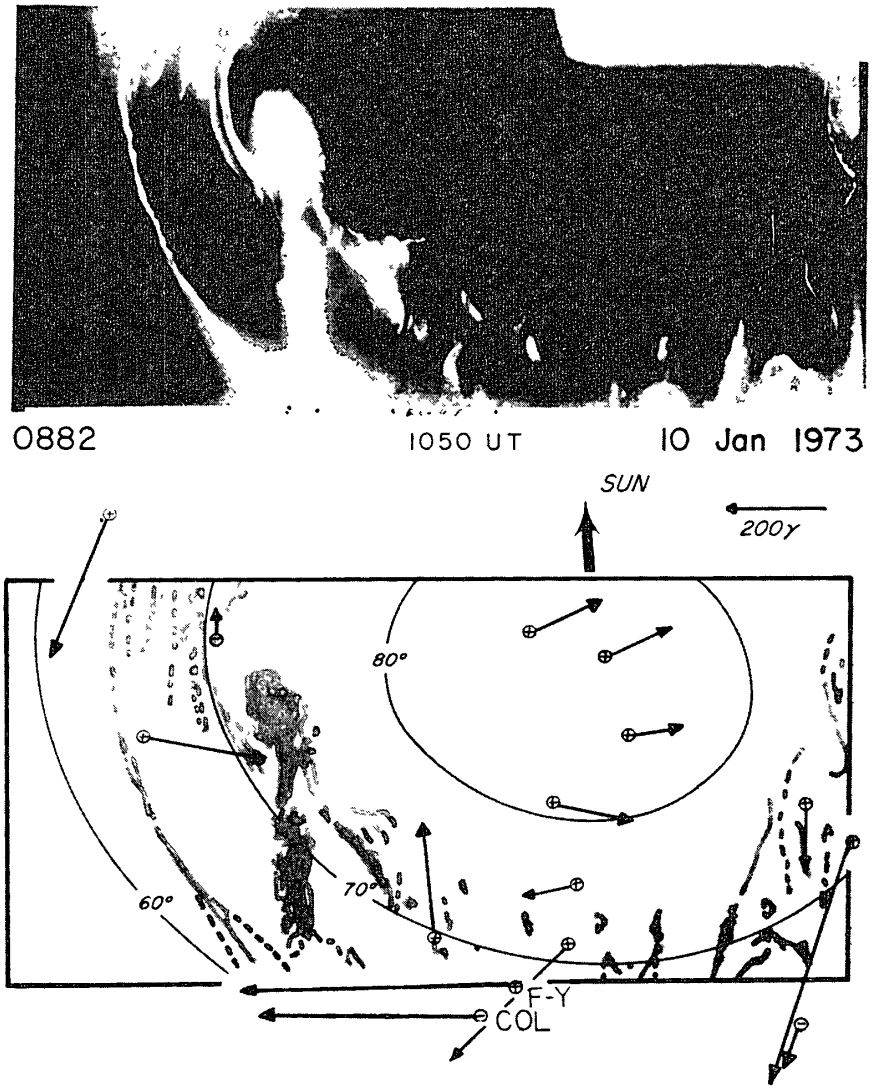

Fig. 21. DMSP auroral imagery and the equivalent overhead current vectors. The signs of the geomagnetic Z component are also indicated (after KAMIDE and AKASOFU, 1975).

substorm (AKASOFU, 1974a), together with the distributions of the equivalent ionospheric current (KAMIDE and AKASOFU, 1975). In contrast with the complex configurations of the poleward portion, a striking feature is the remarkable smoothness and continuity of the equatorial boundary of the diffuse aurora. This boundary tends to align most closely along L-shells when the auroral oval is largest in diameter, it is more oval-like when the diameter of the auroral oval is smallest (DAVIS, 1974). Note that ANGER *et al.* (1978) observed arc-like auroral emissions equatorward of this boundary, apparently in the ionospheric trough region.

Table 1, taken from AKASOFU (1977), summarizes some difference in morphological features of the discrete and diffuse auroras. It seems likely that the diffuse aurora constitutes a broad background region in which discrete auroras are embeded. It is not easy to distinguish both types of auroras from all-sky camera photographs The equatorward edge of the diffuse aurora appears often like a homogeneous arc. AKASOFU (1974a) noted that in the *morning* sector, the diffuse aurora tends to develop into several discrete auroras, some of the latter spread over the morning half of the polar cap and become the polar cap aurora. It is interesting to point out that there is a particular type of polar cap arc which lies parallel to auroral oval arcs in the *evening* sector and which bends away from the oval to the usual sun-earth line near the poleward boundary of the oval (MENG and AKASOFU, 1976). WHALEN *et al.* (1977) and PIKE *et al.* (1977) have recently shown that both discrete and diffuse components are contained in a band of enhanced 6300 Å emission extended over 2–10° in latitude in the midnight sector.

In studying the ISIS 2 scanning photometer data, ANGER and MURPHREE

Table 1 Discrete and diffuse auroras

	Discrete aurora	Diffuse aurora
Morphological features	A discrete aurora is a curtain-like structure and appears as a single arc or is separated from other arcs by a dark space of order of a few tens of kilometers in width	A diffuse aurora is either a broad band of luminosity at least several tens of kilometers in width or a group of discrete auroras which are closely packed along a rather narrow east-west belt Patchy auroras develop in the diffuse aurora The mantle aurora and the hydrogen aurora may belong to the diffuse aurora
Conjugacy	Varying degree of conjugacy.	Appears to be conjugate
Particle precipitation	Inverted V precipitation	A broad and relatively uniform precipitation
Energy spectrum	Considerably variable and has a peaked component, in addition to the power law and the Maxwellian components	Relatively constant, becoming soft near the poleward and equatorward edges The spectrum has the power law and the Maxwellian components

(1976) have placed their emphasis on auroral morphology rather than auroral dynamics, since satellite auroral imagery is inherently of a 'snapshot' character, providing of itself virtually no information on the temporal development of auroras. It was found that auroral arcs lie within the diffuse aurora, not outside of it, contrasting with the previous conclusions by SNYDER *et al.* (1974) and SNYDER and AKASOFU (1974) that there is often a clear separation between the discrete and diffuse auroras. It was thought by ANGER and MURPHREE (1976) that the apparent discrepancy is probably a result of the finite intensity threshold (~2 kR) of the DMSP satellites (BERKEY and KAMIDE, 1976).

Finally, the following four points are worthwhile to note concerning the diffuse aurora: (1) The terms mantle aurora (SANDFORD, 1968), continuous aurora (PIKE and WHALEN, 1974), and the present diffuse aurora are essentially interchangeable, in the sense that they all express the continuous and relatively uniform belt of auroral emissions, which is persistently present even without discrete auroras. (2) One of the prominent features of the diffuse aurora when viewed from a global perspective is its well-defined equatorward boundary (LUI and ANGER, 1973; CREUTZBERG, 1976). ANGER and MURPHREE (1976) cautioned that the auroral intensity does not actually cut off as shaply as one might expect from looking at the satellite pictures, because each has a specific intensity threshold. (3) Patchy aurora can be formed in the diffuse aurora (see Table 1), and pulsating aurora is a subset of the class of the patchy aurora. SIREN (1975) showed using DMSP photographs that pulsating auroras can occur at times on the poleward, leading edge of a midnight sector surge. We note in this connection that although the identification of the diffuse aurora in the evening sector is relatively easy, it is difficult to define it exclusively in the morning sector where complicated post-breakup auroral signatures are generally observed. (4) It is still unclear where the first indication of an auroral substorm, *viz.*, the auroral breakup, begins, although the first brightening occurs near an arc located between the diffuse and discrete auroras in the midnight sector. It is interesting to note in this respect that OGUTI (1973) suggested that the breakup may start when an electron aurora, which has split from the high-latitude arc, comes into contact with the hydrogen emission, indicating that if the electron and proton auroras are assumed to occur respectively at ionospheric projections of the plasma sheet and the proton trapping region, the onset of the auroral breakup is related to the close approach of these two regions in the magnetosphere. PELLINEN and HEIKKILA (1977) have recently conducted detailed observation of the onset of auroral breakup using rapid sequences of all-sky cameras and fast meridian scans by photometers, and have found

that the breakup is preceded by moderate brightening, followed by fading of the auroral intensity lasting one or two minutes. LUI and BURROWS (1978) have suggested using fortuitous polar passes of the ISIS 2 satellite that the substorm triggering process occurs on closed magnetic field lines well within the outer and inner edges of the plasma sheet.

4.2. Global auroral features and currents

It is now possible by examining coincident data to identify the position of the auroral electrojets and field-aligned currents with respect to the pattern of large-scale auroral displays observed from the satellites (*e.g.*, WEBER *et al.*, 1977). It should be noted, however, that because the satellite auroral imagery is available only once per each orbital period (~100 min, for the DMSP and ISIS 2 satellites) which is of the order of the lifetime of one substorm, the progressive change of auroral features and of the corresponding electrojet response must await the availability of a series of photographs from a satellite with an eccentric orbit, capable of observing the entire polar region continuously for several hours. There is little doubt that the Japanese satellite 'Kyokko', launched in February 1978, is an ideal for this purpose.

KAMIDE and AKASOFU (1975) studied DMSP satellite auroral photographs and the simultaneous ground magnetic records from a number of polar stations.

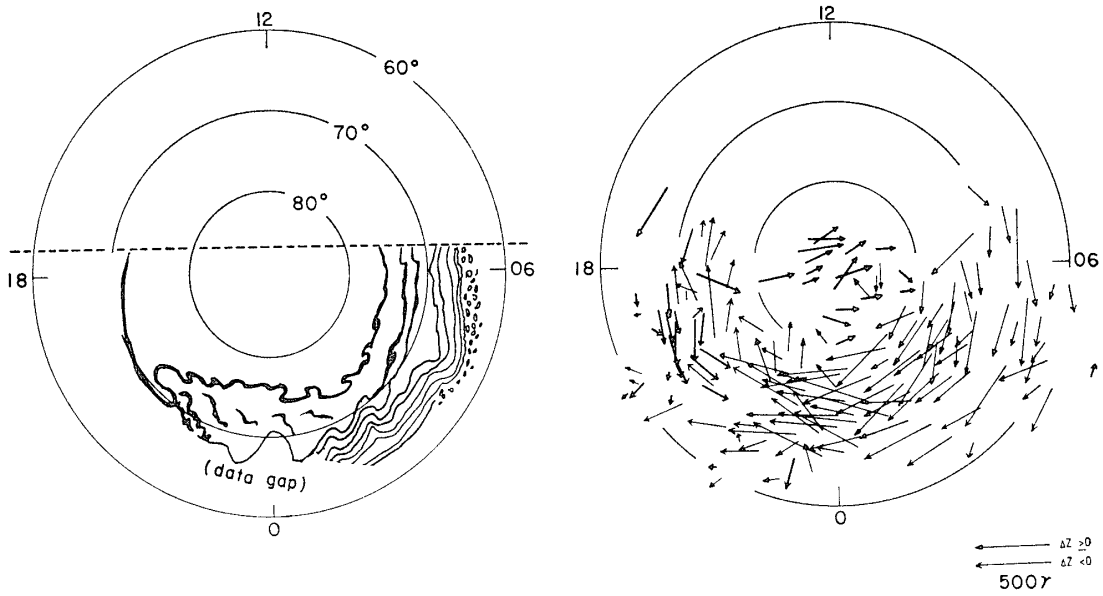

Fig 22 Schematic diagram of auroral features during the typical auroral substorm and the distribution of equivalent current vectors with reference to the auroral features. The magnitude of each current vector is normalized for the maximum magnitude of the magnetic perturbation of 500 nT (KAMIDE and AKASOFU, 1975).

By examining the distribution of the equivalent ionospheric current vectors with respect to the auroral configuration, it is inferred that there are two electrojets, eastward and westward, flowing along the visible auroral display. The reversal of the current direction occurs near the equatorward boundary of the auroral belt across the midnight meridian; eastward in the evening sector and westward in the midnight and morning sectors. The locus of the reversal was originally used by HEPPNER (1972d) to define the Harang discontinuity (HARANG, 1946). In Fig. 22, we show a schematic diagram of auroral characteristic features which is a composite of the major features appearing on a large number of DMSP photographs (AKASOFU and SNYDER, 1974). Note that this diagram shows the notable asymmetry with respect to the midnight meridian. Structured discrete auroras are active near the poleward boundary of the auroral oval, especially in the premidnight sector, whereas the diffuse aurora delineates a relatively stable equatorward boundary of the auroral belt. Using this auroral oval as the 'normalized' reference, the equivalent current vectors are also plotted in Fig. 22 for the total of 19 satellite passes which took place near the maximum phase of substorms. Fig. 22 confirms that the westward electrojet is most intense in midnight and early morning hours and that it does not end in the midnight meridian, but extends into the evening sector along the auroral oval. This is somewhat different from what the SD current system (CHAPMAN, 1935) indicates. The latitudinal width of the area where the westward electrojet effect is observed in the morning sector is much larger than that in the evening sector. In the diffuse auroral region, the eastward electrojet is a common feature in the evening sector.

WALLIS *et al.* (1976) have recently made a similar study of the spatial relationship between the ISIS 2 large-scale auroral display and the auroral electrojets, determined from the Canadian meridian chain of magnetometer data. They defined the latitudinal limits of auroral emissions in the evening sector on the basis of the auroral intensity at 3914 Å and 5577 Å. Summary of auroral electrojet locations and boundaries of auroral precipitation inferred from data of the auroral scanning photometer for 19 selected passes of the ISIS 2 satellite is shown in Fig. 23. It is seen that the eastward electrojet is contained within, and may be narrower than, the latitude range of auroral emission. It was also found that although discrete auroral arcs within the electrojet may produce enhanced conductivity in their vicinity, this does not necessarily lead to enhanced ionospheric current densities, implying the importance of the electric field in determining the current intensity.

KAMIDE *et al.* (1978) utilized magnetic field data from the TRIAD satellite

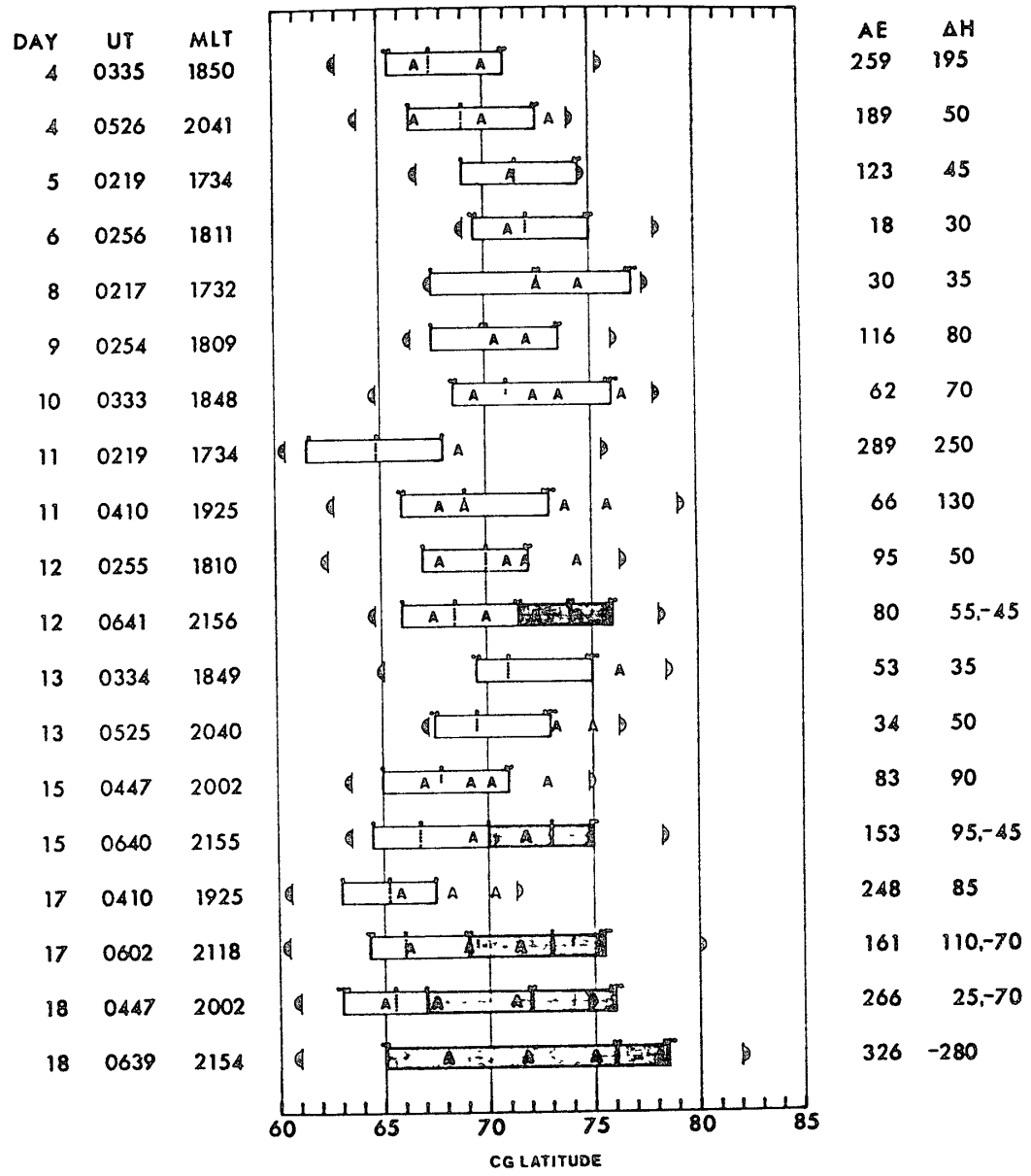

Fig 23 Summary of auroral electrojet locations and boundaries of auroral precipitation inferred from auroral scanning photometer data. Deduced locations for the auroral electrojets are shown by boxes The latitudes of the Z=0 crossovers are shown by the vertical dotted lines (after WALLIS et al., 1976).

at 800 km to define the boundaries of field-aligned currents when auroral luminosity along the same meridian was scanned by the ISIS 2 satellite. Fig. 24 shows ISIS 2 auroral photographs of the 5577 Å emission with a corrected geomagnetic 'latitude-longitude' grid This particular trajectory occurred during the maximum phase of an intense substorm There is an indication of a bright, westward traveling surge near 280° corrected geomagnetic longitude Along the TRIAD satellite

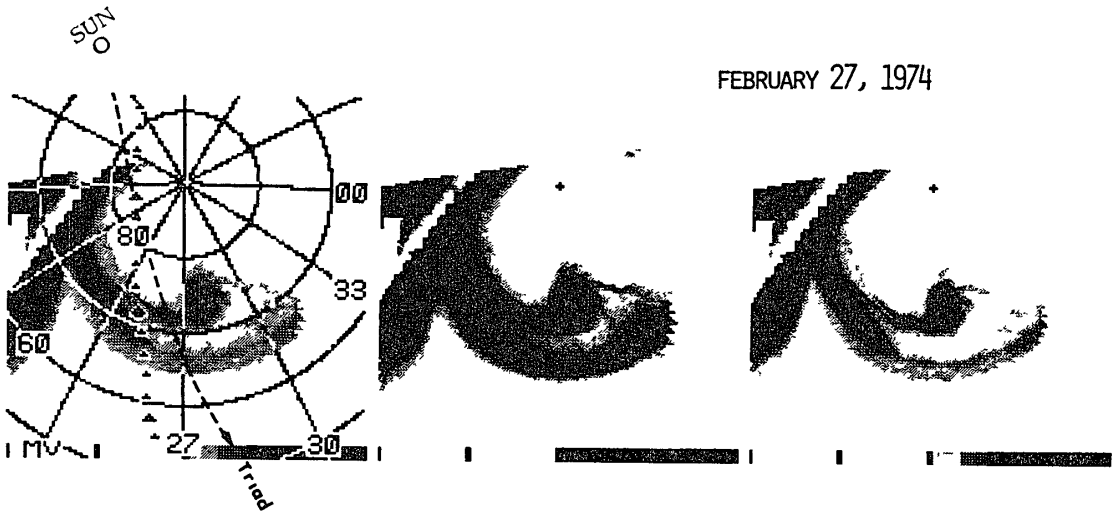

Fig. 24. Auroral scanning photometer data (5577 Å) transformed into a corrected geomagnetic coordinate system and shown in negative format. The range of luminosity represented by gray shades from white to black spans 0.60–1.55 kR in the left picture, 0.97–1 36 kR in the center picture, and 1.17–1.55 kR in the right picture (after KAMIDE et al., 1978).

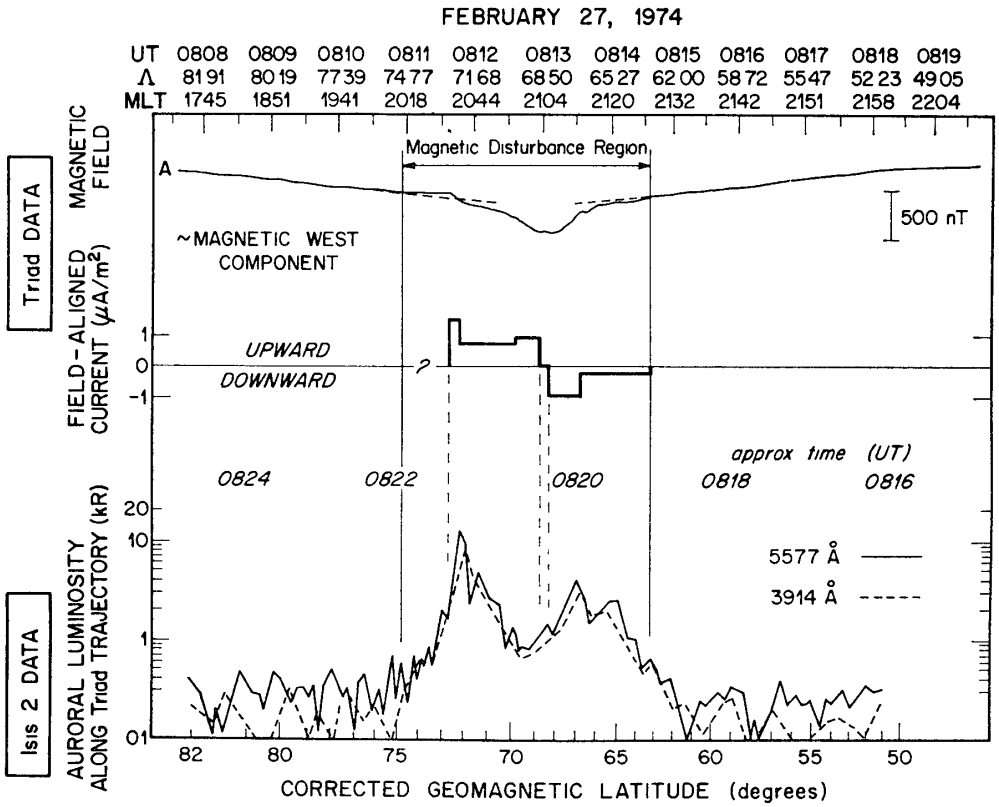

Fig. 25. TRIAD magnetometer data, the estimated field-aligned current density, and logarithmic latitudinal profiles of auroral intensity along the TRIAD subtrack (after KAMIDE et al., 1978).

trajectory (shown by a dashed line) there are two main auroral luminosity regions; the equatorward auroral distribution with its well-defined equatorward boundary and a poleward region which is connected to the westward traveling surge. Intense narrow structures can be seen in the latter region and thus it is reasonable to identify the poleward luminosity as the discrete aurora. The equatorward aurora has a fairly uniform distribution with latitude and can therefore be identified as the diffuse aurora. Available ground magnetic data showed northward perturbations in the equatorward auroral region, indicating that the eastward electrojet was flowing in the region occupied by the diffuse aurora. Unfortunately, there was no ground magnetic observatory whose data are available in the region of the poleward portion of the auroral display. A detailed comparison of the inferred field-aligned currents and the auroral luminosity along the TRIAD subtrack is given in Fig 25, which shows the TRIAD magnetometer record and the logarithmic profile of albedo corrected intensities along the TRIAD trajectory. It is seen that some structure can occur in the diffuse auroral region and may be due to discrete arcs (in the sense described by WALLIS *et al.*, 1976) imbeded in the diffuse aurora. It is evident that the luminosity does not go to zero between the diffuse and discrete auroras. KAMIDE *et al.* (1978) pointed out that in the evening sector, the latitudinal boundaries of the major portion of the field-aligned currents line up very well with the auroral luminosity boundaries of 1–2 kR at both the poleward and equatorward sides of the auroral distribution, and that the boundary between the upward and downward field-aligned currents generally occurs at the minimum in the auroral luminosity profile.

4.3. Polar cap and midday auroras

'Sun-aligned arc' in the polar cap is another aspect of spectacular auroral features. As described by LASSEN (1972) and STARKOV *et al.* (1973), these arcs are found in long, narrow regions (30 to 200 km with a typical value of 70 km) having an approximate orientation toward the noon sector on the polar cusp (cleft). AKASOFU and YASUHARA (1973) showed that the 6300 Å radiation is richer in polar cap auroras than in auroral-oval auroras. AKASOFU (1974b) presented midday red aurora enhanced greatly during a large magnetic storm. Observations of these arcs have recently been made also by means of equipments flown in ISIS 2 (ANGER *et al*, 1974) and DMSP (MENG and AKASOFU, 1976) satellites. BERKEY *et al.* (1976) have shown by the use of DMSP photographs that the interplanetary magnetic field is directed generally northward when such arcs appear in the polar cap.

ISMAIL *et al.* (1977) have recently made an extensive study of the characteristics of sun-aligned arcs based on observations made between 1971 and 1975 by the auroral scanning photometer on board the ISIS 2 satellite, which is suitable for the study of auroral features because of the capability of obtaining data nearly simultaneously from a large portion of the polar cap. In Fig. 26, the observed positions of the sun-aligned arcs from 36 polar passes are plotted, in which it is noticeable that although their characteristic orientation is roughly in the solar direction, individual arcs can be curved. It was also found that there is a '2:1' asymmetry in the occurrence frequency between the morning and evening sectors

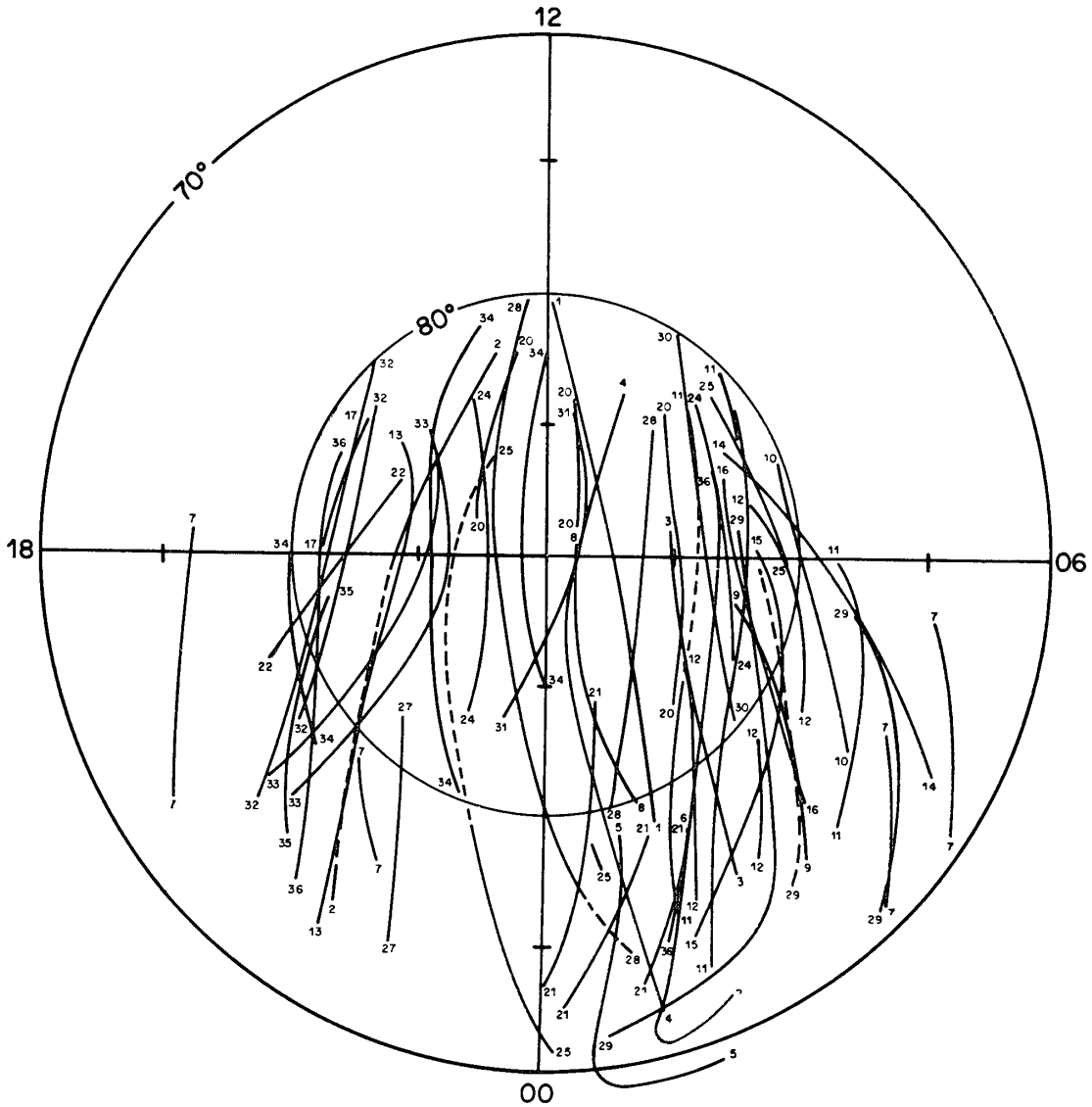

Fig. 26. Observed positions of the sun-aligned auroral arcs in the northern polar cap plotted on a corrected geomagnetic coordinate system (after ISMAIL et al., 1977).

of the polar cap. ISMAIL *et al.* (1977) claimed that this morning-evening asymmetry does not result from an experimental bias, for in all cases almost the entire polar cap was scanned by the photometer. There are several candidates which could cause the asymmetry, such as the differences in the lifetime and motion of the morning-side and evening-side arcs. It is, however, interesting to examine the simultaneous B_y component of the interplanetary magnetic field, since MENG *et al* (1977) found the morning-evening asymmetry of the low-energy (<1 keV) electron fluxes having a clear dependence on the B_y component of the interplanetary magnetic field

There is in general an anticorrelation between the occurrence of the polar cap arcs and the magnetic activity, the sun-aligned arcs can be usually found only during quiet period without substorm activity The polar cap is often completely void of such polar cap auroras during an intense substorm It is then one of the future problems to clarify how the sun-aligned arcs behave before and just at the onset of a substorm. In other words, it should be cleared up how the sun-aligned arcs disappear as the substorm grows The disadvantage of the experiments by polar-orbiting satellites is its inability to provide information about temporal variations in association with auroral-oval arcs during substorm activity

On the other hand, the midday part of the auroral oval was shown to be a band of 2°–5° wide in latitude, in which 6300 Å emission is greatly enhanced, growing discrete arcs According to ISIS 2 observation by SHEPHERD and THIRKETTLE (1973) and SHEPHERD *et al* (1973), the maximum intensity of the 6300 Å emission was a little more than 2 kR. DERBLOM (1975) noted that the 6300 Å emission in the dayside cusp region is accompanied by hydrogen emissions SNYDER and AKASOFU (1976) found a definite tendency for the midday arcs to converge toward the poleward boundary of the auroral oval in the noon sector, indicating that the auroras in the day and night sectors arise from different regions despite the fact that they both form a well-defined singly connected auroral oval Longitudinal extent of the polar cusp has been discussed in terms of the dayside auroras (ZAITZEVA and PUDOVKIN, 1976)

4.4. Small-scale auroras

Although the large-scale auroral distribution provides a crucial clue in unveiling the global structure of the ionospheric and magnetospheric system and its dynamic processes in conjunction with substorm occurrence, there are characteristic small-scale auroral displays as well whose dynamic behaviors are important in understanding the causative acceleration mechanisms in the magnetospheric and

ionospheric systems (LYATSKAYA and LYATSKY, 1973; OGUTI, 1975a; VOROBJEV *et al.*, 1976). OGUTI (1975b) found a resemblance between global auroral pattern (such as the westward traveling surge and bulge) and smaller-scale structures observed by the DMSP satellite and a highly sensitive TV camera, respectively. Auroral infrasonic waves (WILSON, 1973, 1974, 1975) are generated by small-scale auroras moving supersonically. Recently, JOHNSON (1976) has shown that numerous infrasonic waves were recorded even during a period of fairly low geomagnetic activity.

In such small-scale auroras, irregular, quasi-periodic and periodic temporal variations are observed which involve both motion and modulation of intensity (*e.g.*, BREKKE, 1972; SØRENSEN *et al.*, 1973; OGUTI, 1975c). The dynamics of the small-scale, highly variable auroras have been studied by OGUTI (1974a) and PEMBERTON and SHEPHERD (1975) using TV imagery device and photometers, respectively. By the use of highly sensitive TV camera records as well as data of all-sky cameras and meridian scanning photometers at Syowa Station, Antarctica, OGUTI (1974b) showed motions of individual discrete auroral forms to have a clockwise sense of rotation (as viewed from below the southern pole) and con-

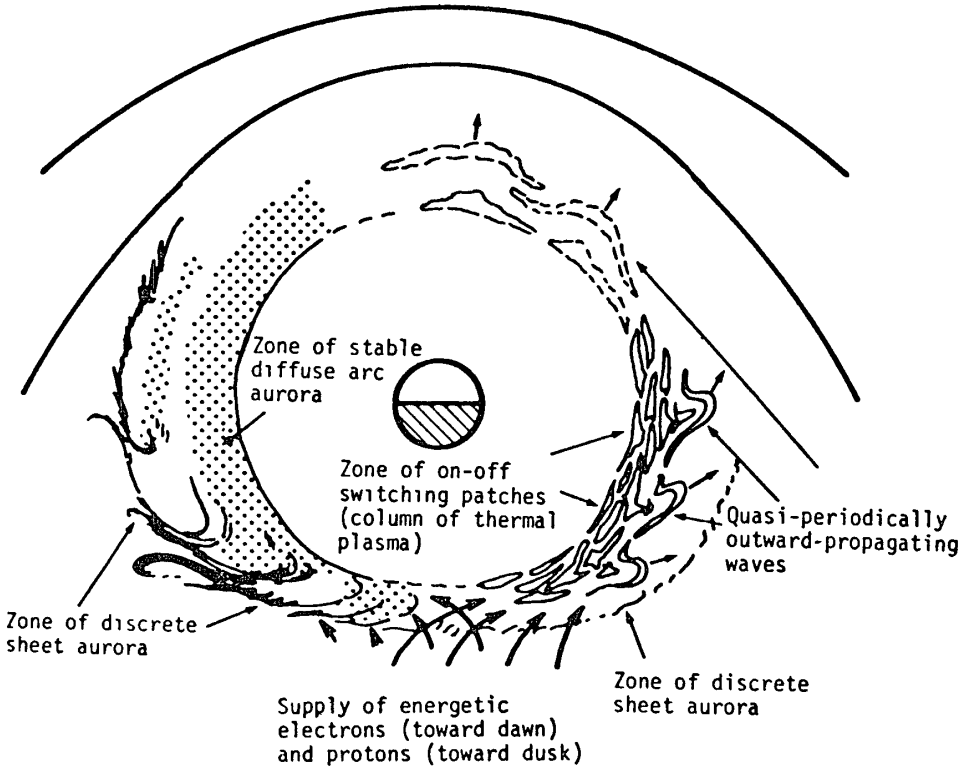

Fig. 27. Schematic illustration of the magnetospheric structure and the corresponding auroral characteristics deduced from auroral morphology (after OGUTI, 1976).

cluded that the auroral electron precipitation is related to the production of negative charge excess

On-off switching (or pulsation) aurora is one of the characteristics of auroral display in the dawn sector during the post-breakup phase of substorms (see THOMAS *et al*, 1973; OGUTI, 1975). OGUTI and WATANABE (1976) showed that the rapid poleward propagation of the switch-on region occurs in association with a particular type of geomagnetic pulsations in the dawn sector of the auroral zone. The morphological features of the on-off switching auroras as well as the large-scale auroras are summarized in Fig. 27, which was presented by OGUTI (1976). It was noted that particles responsible for the auroral precipitation in the dusk may 'drizzle', whereas in the dawn sector, they precipitate like 'rain'.

Extensive observations at College, Alaska, with all-sky TV cameras supplemented by observation with narrow-field TV cameras, all-sky cameras, and images from the DMSP satellites were conducted by ROYRVIK and DAVIS (1977) who have shown that pulsating auroras are broadly distributed along the auroral oval

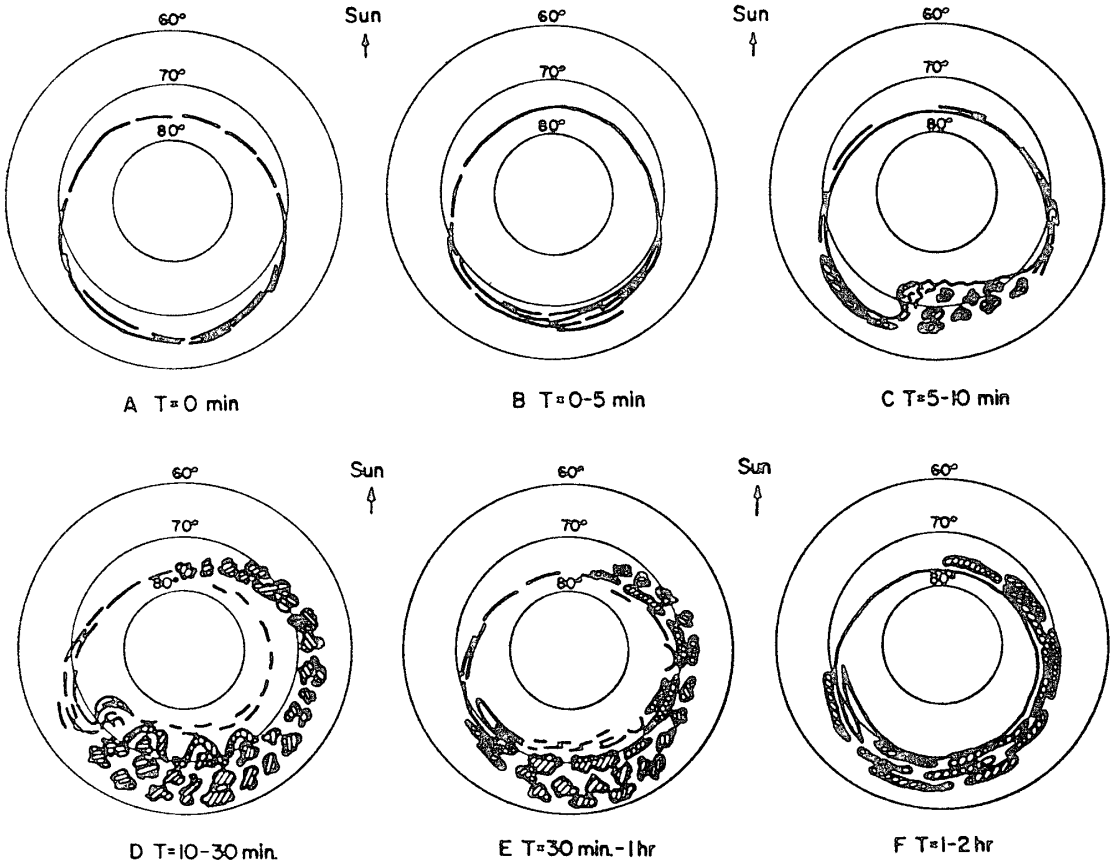

Fig 28 Schematic diagram illustrating the development of an auroral substorm, emphasizing the development of pulsating auroras which are indicated by hatched region (after ROYRVIK and DAVIS, 1977)

thoughout much of the auroral substorms. It was pointed out that although pulsating auroras occur extensively in the morning sector of the oval during the post-breakup phase of the substorm, pulsations in the auroral intensity extend eastward even to around the dayside during periods of large disturbances and they are also observed near the equatorward boundary of the evening sector. ROYRVIK and DAVIS (1977) have given a schematic diagram illustrating how pulsating auroras develop in the framework of the large-scale auroral substorm presented by AKASOFU (1964). This is shown in Fig. 28, which is reproduced from Fig. 15 of ROYRVIK and DAVIS (1977). The great variability in the pulsating behavior, as discussed by them, suggests that the occurrence and the nature of pulsations are determined by localized parameters with large temporal and spatial variations. Recent measurements by BROWN *et al.* (1976) demonstrated that the altitude of the lower border during the 'on' phase of pulsation auroras is mainly in the range of 50–100 km, implying that a substantial portion of the energy of causative electrons is in the range of 10–100 keV, in general agreement with satellite measurements of particle fluxes over pulsating auroras by FRANK *et al.* (1976).

The frequent appearance of spiral forms of 20 to 1300 km diameter is another aspect of the active auroral display. The availability of auroral imagery from the ISIS and DMSP satellites has allowed an improved mean to identity the morphology of the spiral auroras over ground-based conventional all-sky photographs. DAVIS and HALLINAN (1976) have made an extensive examination of the spiral auroras and found that clockwise (viewed anti-parallel to $\boldsymbol{B}$) spirals, appearing singly or in spiral sheets, are a common part of the auroral display, which occur in the evening and midnight sectors between the equatorward boundary of the aurora and geomagnetic latitude 85° during substorms. HALLINAN (1976) suggested that spirals in the aurora imply the existence of upward field-aligned current. It is interesting to note that DAVIS and HALLINAN (1976) state that the events called 'pseudo-breakups' or 'local substorms' are developments of auroral spirals.

4.5. Auroral distribution and electric field

The problem of how the electric field varies in the vicinity of a discrete auroral arc is still a matter of serious discussion, as described in Section 2. This is so at least partially, because it has been difficult to identify different types of auroral forms in each of the reported observations. Auroral forms and their motions are complex functions of both local time and latitude, as well as substorm time. It is presently judged by individual observers whether the observed particular type aurora is an independent discrete auroral arc or just local enhancement of bright-

ness within diffuse aurora. In this section we examine how variations in the large-scale electric field are related to large-scale auroral activity.

On the basis of the Chatanika radar data, DOUPNIK *et al.* (1972), BANKS *et al.* (1973, 1974) and RINO *et al.* (1974) studied this problem. It was found that a large northward electric field is observed in the evening sector when a substorm is in progress in the midnight sector and that a large increase of the westward electric field is associated with the passage of a westward traveling surge in the poleward sky of the radar site. It was also observed by RINO *et al.* (1974) that the enhancements in the westward electric field were coincident with an equatorward expansion of the instantaneous auroral oval.

Extensive observations of the electric field by balloon-borne probes let MOZER (1973c) conclude that the westward component of the electric field develops about one hour prior to the onset of the expansive phase of substorms, while an southward component grows at the expansive onset. Note that MOZER (1973c) did not examine the simultaneous auroral data to identify the expansion of substorms, while KELLEY *et al.* (1971) showed the growth of the westward component is well correlated with an equatorward motion of auroral forms, the speed of auroras being estimated from E/B. Recently, HORWITZ *et al.* (1978a) have shown, using DMSP auroral photographs, that the strong westward electric field near the leading western edge or nose of the westward traveling surge is one of the signatures of the Harang discontinuity, which divides regions of northward and southward electric fields on the western and eastern sides, respectively. It appears that associated with the southward turning of the interplanetary magnetic field, which occurs prior to a particular type of substorm sequences (KAMIDE and MATSUSHITA, 1978a), the entire auroral oval expands equatorward, thus making the westward field observable at the radar site fixed on the earth's surface.

AKASOFU *et al* (1974) have shown, using plasma flux and magnetic field changes at the synchronous distance (ATS 5) and ground-based all-sky auroral photographs near the 'foot' of ATS 5, that specific auroral activity in specific local times can be interpreted by specific particle features at the synchronous distance by taking into account the configuration of the plasma sheet and drifts of the plasma sheet particles. Analysis of ATS 5 particle spectrograms and simultaneous meridian-scanning photometer data obtained at the 'foot' of the ATS 5 field line has revealed that a persistent zone of weak aurora is related to steady plasma-sheet drizzle, and the equatorward edge of this aurora delineates field lines threading the inner edge of the plasmer sheet (EATHER *et al*, 1976) MENDE and SHELLEY (1976) have shown that the local injection of magnetospheric particle at synchro-

nous orbit generally produces structured auroras such as breakup events and westward traveling surges. Correlated observations of auroral substorms and the corresponding disturbances were reported by HONES *et al.* (1976).

4.6. Radar auroras

In recent years, workers have attempted to describe the radar aurora as a sequence of radar auroral substorms (BATES *et al.*, 1973; ECKLUND *et al.*, 1974; ROMICK *et al.*, 1974; UNWIN and KEYS, 1975; TSUNODA *et al.*, 1974, 1976b; TSUNODA and FREMOUW, 1976a, b; MOORCROFT and TSUNODA, 1978). Once the exact nature of plasma instabilities associated with the radar is understood, the radar becomes a powerful diagnostic tool in the study of the auroral substorm processes (MCDIARMID, 1976; GREENWALD, 1977, 1978; BREKKE *et al.*, 1977; MCDIARMID and MCNAMARA, 1978).

It appears that radar auroral irregularities are generated by various current-associated instabilities, such as the gradient drift and/or two-stream plasma instabilities. Both of these instabilities require a relative drift of the electrons and ions (see GREENWALD, 1974; WANG and TSUNODA, 1975; TSUNODA, 1976).

The correlation between the positions of the radar aurora and the auroral electrojets was found to be reasonably good (GREENWALD *et al.*, 1973; MCDIARMID *et al.*, 1976). PETERSON (1977, personal communication) has recently found that the maximum radar echoes originate in the center of the auroral electrojets. Fig. 29 shows an example of radar observation during a substorm by the Anchorage radar at 50 MHz (BALSLEY *et al.*, 1973), in which the location and its time shift of the radar echo are indicated together with magnetic records from the Alaska meridian chain of observations (GREENWALD *et al.*, 1975). The auroral echo seems to return from a little poleward of College between 0800 and 1000 UT when the center of an eastward electrojet is located there. Similarly, the onset of the substorm and the subsequent poleward expansion of the westward electrojet seen in the latitude variation of the H and Z component magnetic perturbations can also be identified as a motion of radar auroral forms. GRAY and ECKLAND (1974) have further shown that there is often a good linear relationship between the total horizontal disturbance and the square root of the range-integrated backscattered power. In these studies ground-based magnetometers were used to deduce the general location, extent and intensity of the electrojet currents. However, because of limited magnetometer coverage and unknown ground induction effects, it was not possible to define the electrojet intensity uniquely. Most recently, SIREN *et al.* (1977) have found, in the comparisons of auroral electrojet parameters measured

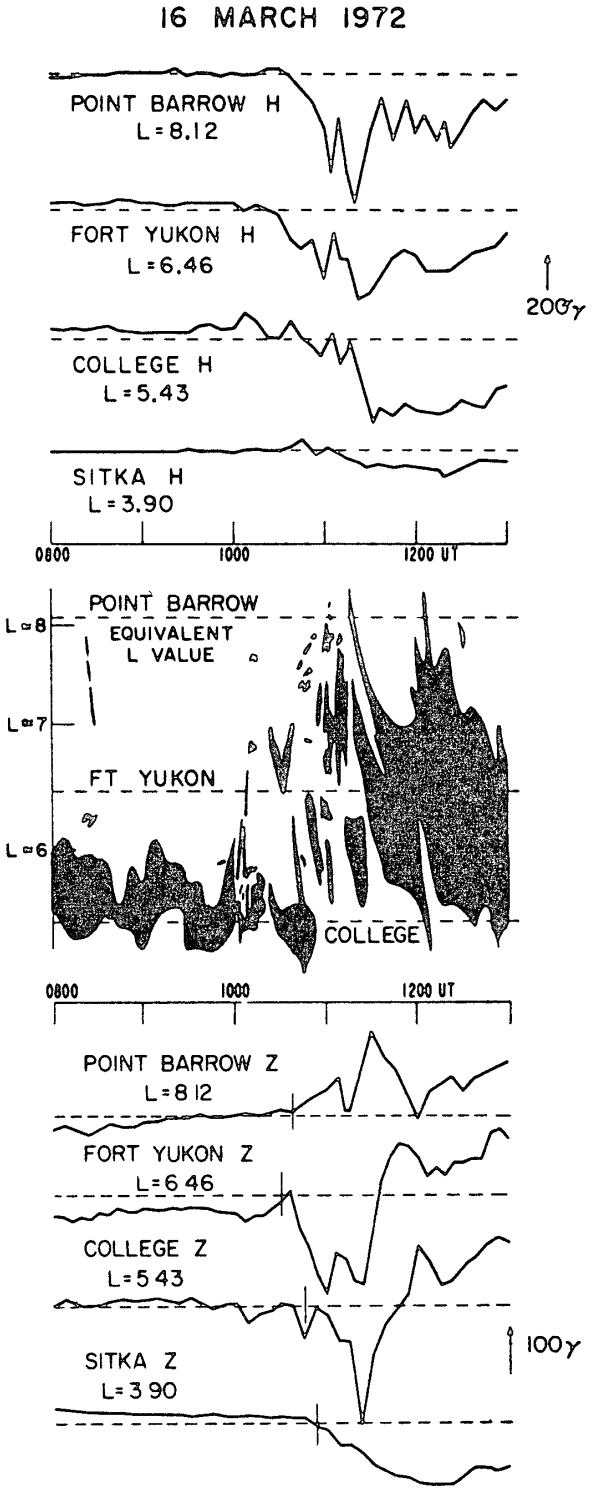

Fig 29 Auroral radar backscattered power and magnetic records in the H and Z components from four Alaska observatories (after GREENWALD et al , 1975)

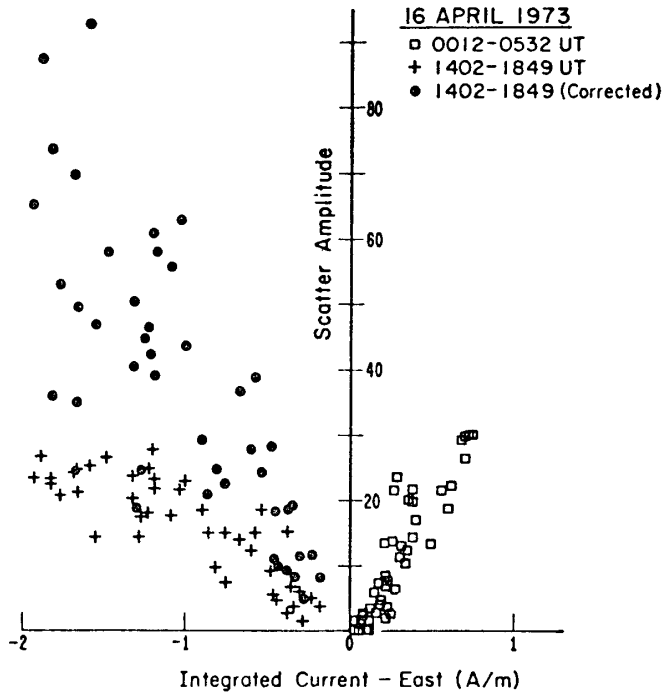

Fig 30. Eastward current density obtained by the Chatanika radar plotted against the backscatter amplitude observed in a comparable area by the Anchorage auroral radar The pluses correspond to the observed scatter amplitudes in the morning period, and the closed circles are the same data corrected for absorption (after SIREN *et al , 1977)*

by the Chatanika incoherent scatter radar with VHF backscatter observed in a comparable area by the 50 MHz radar, that the east-west electrojet current intensity is the parameter that correlates best with the amplitude of the backscatter irregularities. Fig. 30 shows the backscatter amplitude observed by the radar plotted against the height-integrated east-west current density (SIREN *et al.*, 1977), for evening and morning sectors separately, indicated by different symbols. Also shown is the corrected backscatter amplitude by taking the ionospheric *D* region absorption into account occurring in concert with the morning electrojet. If the amplitude is thus corrected for absorption effects, the scatter of points varies linearly with either eastward or westward current density with the same slope for both periods.

The correlation between the positions of the radio and visual auroras is not necessarily good (*e.g.*, MCDIARMID *et al* , 1976) A possible explanation is that the electric field is important rather than other parameters, such as the ionospheric electron density and conductivities. TSUNODA (1975) and TSUNODA and PRESNELL (1976) have found using the data from a 398-MHz backscatter radar located at Homer, Alaska, that when the electric field strength is greater than 30 mV/m,

the auroral radar echo intensity is always positively correlated with the electric field intensity, regardless of the electron density.

It should be noted that there are at least two types of radar echoes, discrete and diffuse. TSUNODA *et al.* (1976b) have shown that diffuse auroral echoes can be used to map the spatial distribution of the eastward electrojet and that discrete

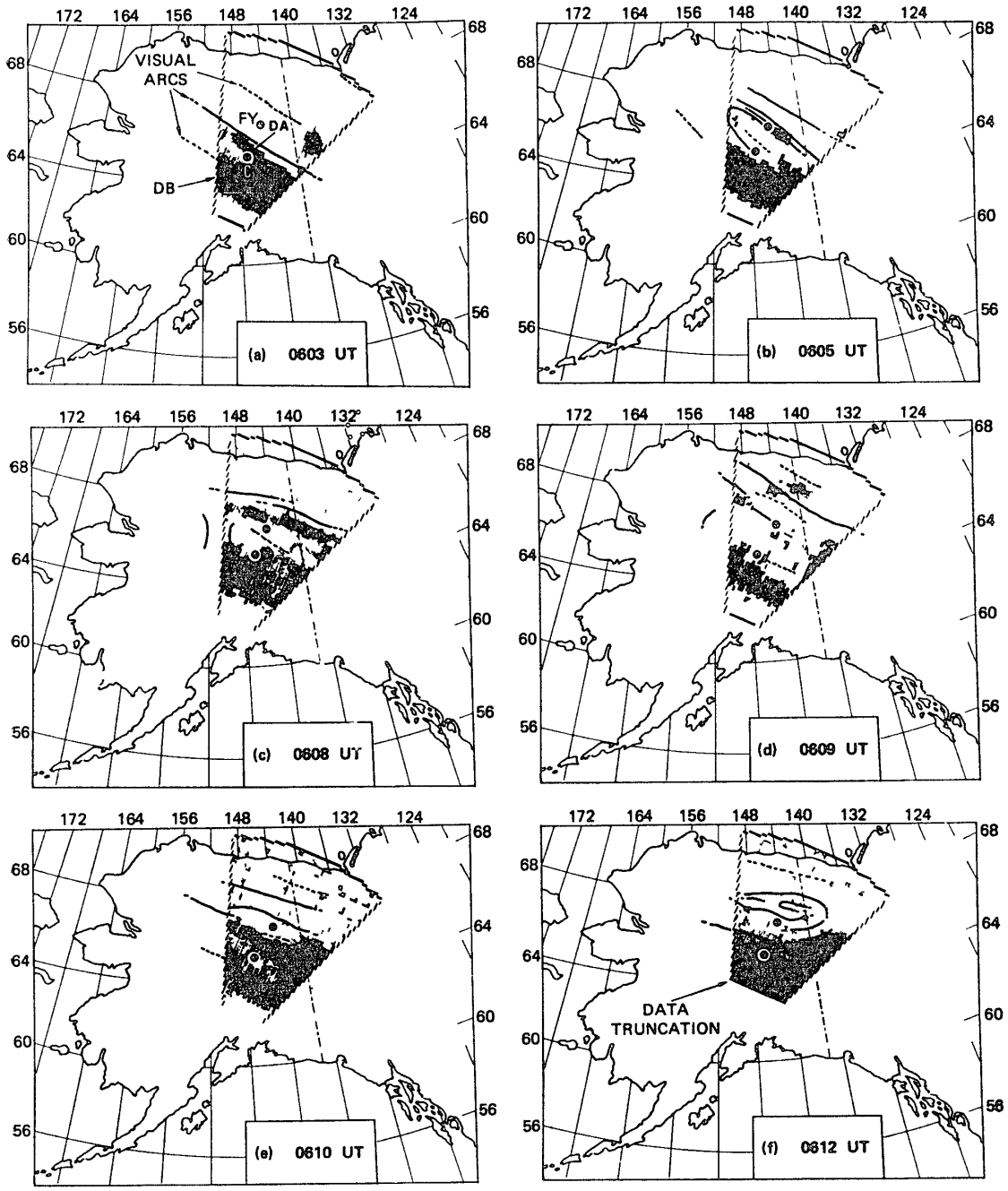

Fig. 31. Maps comparing the radar and visual auroras during the expansive phase of a substorm (after TSUNODA et al , 1976b)

visual auroral arcs are almost invariably to occur poleward of the eastward electrojet. Fig. 31 shows consecutive maps comparing the radar and visual auroras during the expansive phase of a substorm (TSUNODA *et al.*, 1976b). It is seen that when discrete radar echoes are observed, they are associated only with bright visual arcs. Furthermore, they noted that the association is usually confined to only the most equatorward visual arcs located closest to the poleward boundary of the eastward electrojet, namely near the equatorward edge of the westward electrojet. TSUNODA *et al.* (1976a) have also found that the evening diffuse radar aurora is collocated with the downward field-aligned currents, consistent with the observation that the downward currents flow generally into the region of the eastward electrojet (KAMIDE and AKASOFU, 1976). It was uncomfortable to hear, during the preparation of this manuscript, that the Stanford Research Institute International in Menlo Park, California, decided to close the radar facilities at Homer, Alaska, because of the lack of financial support (TSUNODA, 1978, personal communication).

For the International Magnetospheric Study (IMS), the Max-Planck Institut für Aeronomie at Lindau/FRG is operating the Scandinavian Twin Auroral Radar Experiment (STARE) which consists of two nearly idential backscatter radars located in Finland and Norway (GREENWALD *et al.*, 1977). Data from the STARE system, along with ground magnetometer data in the same region should provide a comprehensive picture of the relationship between the auroral electrojets and the electric fields. Results from a preliminary composition are given in Section 8.

5. Ionospheric Conductivity

Using suitable models for the neutral atmospheric densities and the ion-neutral particle collision frequency, it is possible to compute ionospheric electrical conductivities from measured electron density profiles. The altitude dependent Hall (σ_H) and Pedersen (σ_P) conductivities are defined by the expressions

$$\sigma_H = \frac{N_e e}{B}\left(\frac{\Omega_i^2}{\Omega_i^2+\nu_i^2} - \frac{\Omega_e^2}{\Omega_e^2+\nu_e^2}\right)$$

$$\sigma_P = \frac{N_e e}{B}\left(\frac{\Omega_i \nu_i}{\Omega_i^2+\nu_i^2} - \frac{\Omega_e \nu_e}{\Omega_e^2+\nu_e^2}\right)$$

where N_e is the electron density, e is the electronic charge, B is the magnetic field intensity, $\Omega_{i,e}=eB/m_{i,e}$ is the gyrofrequency, and $\nu_{i,e}$ is the ion (or electron) and neutral collision frequency.

On the basis of the Chatanika radar observations of the electron density profiles and atmospheric models tabulated by BANKS and KOCKARTS (1973),

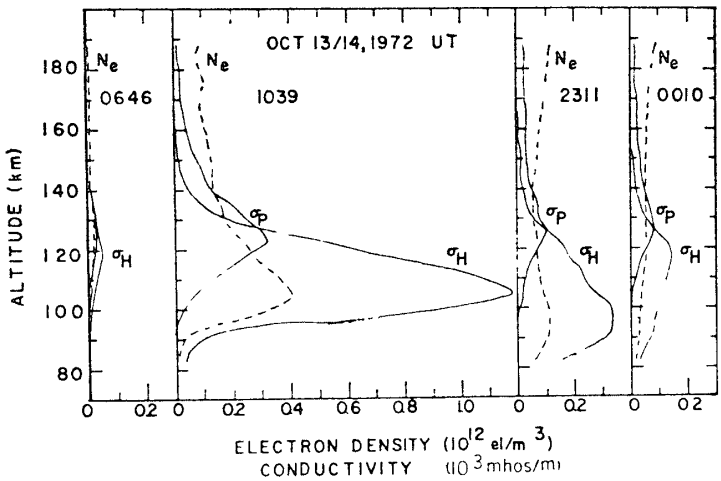

Fig. 32. Altitude profiles for the electron density N_e, the Pedersen conductivity σ_P, and the Hall conductivity σ_H for a quiet evening time, a disturbed nighttime, a disturbed daytime, and a quiet daytime, order being from left to right (after BREKKE *et al., 1974)*

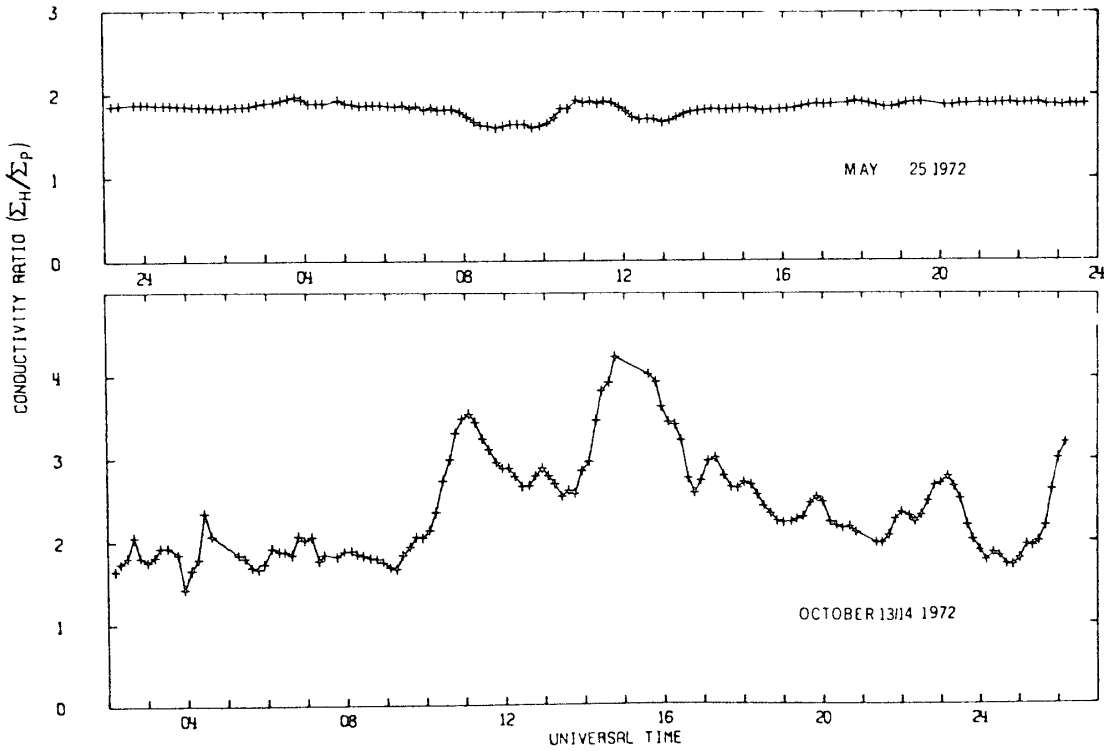

Fig 33 The ratio of the height-integrated Hall to Pedersen conductivities for a very quiet day (top) and a strongly disturbed day (bottom) (after BREKKE *et al , 1974)*

BREKKE *et al.* (1974) obtained the typical altitude dependence of the radar-measured electron density and the derived conductivities, which are shown in Fig 32. It can be seen that the height-integrated Hall conductivity (Σ_H) emphasizes

the electron density in the region below 125 km, whereas the Pedersen conductivity (Σ_P) obtains its maximum contribution between 125 and 110 km. Fig. 33 illustrates the daily variation in the ratio Σ_H/Σ_P for two different days, one very quiet and the other strongly disturbed (BREKKE *et al.*, 1974). For the quiet day the ratio is fairly constant being close to 2, while during the disturbed day, several peaks occur corresponding to substorm activity. The ratio between the two conductivities gives a crude first approximation to the energy of the precipitating particles (REES, 1963), since energetic auroral electrons penetrating the atmosphere reach different altitude levels depending on their energy. BANKS and DOUPNIK (1975) noted that the ionospheric conductivities during an extremely quiet day reflect a dominance of normal EUV produced ionization and vary strongly with solar zenith angle. The errors in the deduced conductivities from the Chatanika radar observations are estimated to be of the order 10–20%, most of which results from the uncertainties in the atmospheric model.

Latitudinal distributions of the height-integrated conductivities have been measured with the Chatanika radar for the range of invariant latitudes 63° to 68° (WEDDE *et al.*, 1977; HORWITZ *et al.*, 1978b). It was found that the local time transition between the diffuse precipitation-conductivity zone in the evening sector (Σ_P=8–12 mho, Σ_H=16–24 mho) and the harder, active precipitation-conductivity

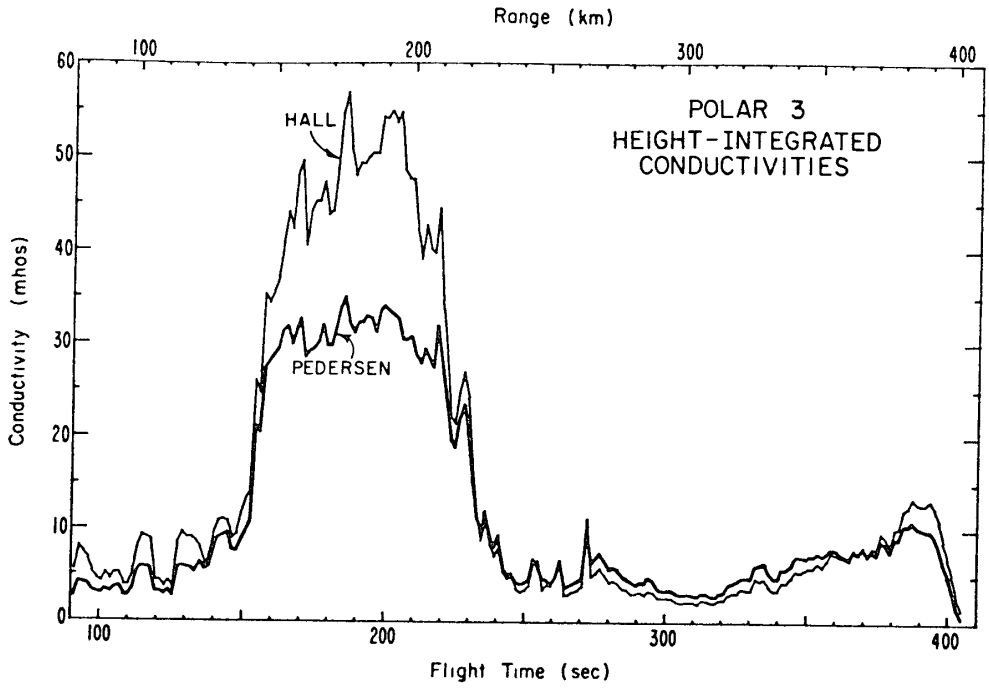

Fig. 34. Height-integrated Hall and Pedersen conductivities as computed throughout the rocket flight of Polar 3 over an auroral arc (after EVANS et al., 1977).

zone in the midnight and morning sector (Σ_P=10–16 mho, Σ_H=20–60 mho) coincides with the Harang discontinuity defined by the electric field reversal.

EVANS *et al.* (1977) utilized the auroral electron data obtained during a sounding rocket flight over a stable auroral arc as an input to a computation of the Hall and Pedersen conductivities. They used a different atmospheric model (see BOSTROM, 1973; JONES and REES, 1973) from that used by BREKKE *et al.* (1974). Fig. 34 displays the height-integrated conductivities during the rocket flight, where the strip of highly conducting ionosphere associated with the major auroral arc is clearly seen. The change in the ratio of the two conductivities from a value of 1.4 above the auroral form to 0.8 further northward is a manifestation of the softening of the auroral electron spectrum outside the arc

6. Ionospheric Current

As described in Sections 2 and 5, the recent new techniques allow one to derive the height-integrated conductivities and electric fields from high-quality measurements of the electron density and plasma drift in the ionosphere. Knowledge of these quantities leads to a description of the ionospheric currents and thus to a clear demonstration of local time changes of the auroral electrojets and their relationship with intensities of the electric field and field-aligned currents. Thus, it was the first time in the history of ionospheric physics and geomagnetism, data from the incoherent scatter radar at Chatanika, Alaska, made it possible to deduce continuously the ionospheric current density (BREKKE *et al.*, 1974, BANKS and DOUPNIK, 1975).

6.1. Ionospheric currents and ground magnetic perturbations

Several attempts have been made to correlate the deduced ionospheric currents with ground magnetic perturbations, confirming that ionospheric currents, called the auroral electrojets, can account for most of the H component perturbations at auroral latitudes (BREKKE *et al.*, 1974; KAMIDE and BREKKE, 1975; KAMIDE *et al.*, 1976a; DOUPNIK *et al.*, 1977).

Fig 35 shows an example of the eastward and northward components of the deduced height-integrated ionospheric currents together with the H and D components from the College magnetogram for a very quiet day (BREKKE *et al.*, 1974). In agreement with the fairly smooth behavior in both the conductivities and electric fields, only small variations exist in the calculated ionospheric currents. A small positive bay of about 40 nT is seen in the H component between 0630 and

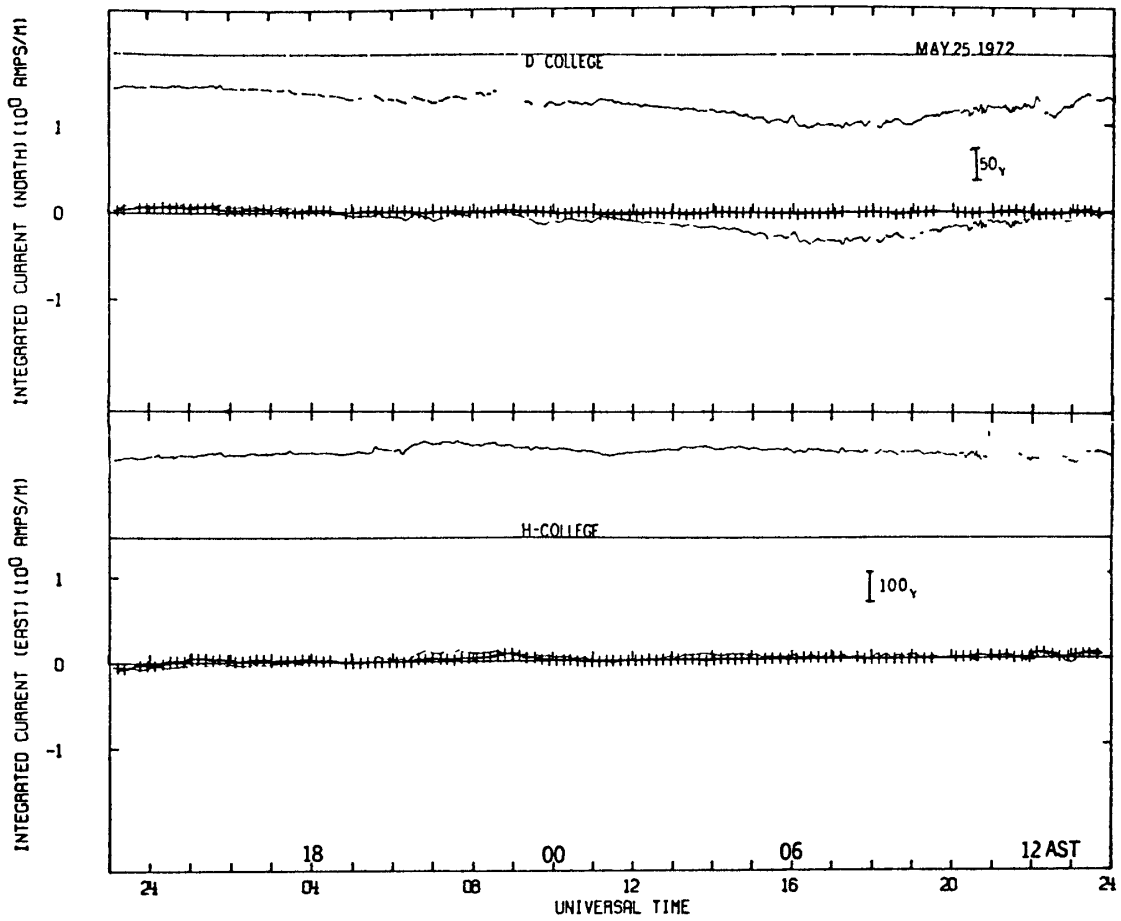

Fig. 35. Height-integrated ionospheric currents in geomagnetic coordinates and the H and D component magnetic reords at College (after BREKKE *et al., 1974).*

0930 UT and is reproduced by the calculated eastward ionospheric current. In the morning hours (1200–2200 UT), there is a large eastward deflection in the *D* component that is not reproduced by the ionospheric currents. BREKKE *et al.* (1974) suggested that this discrepancy might be removed by considering field-aligned currents flowing toward the earth from the dawnside magnetopause and flowing outward to the dusk side magnetopause from the afternoon sector of the auroral oval (KAWASAKI and AKASOFU, 1973), by assuming that College is normally located south of the auroral oval during daytime.

Fig. 36a gives another example of the ionospheric currents in the northward and eastward components at Chatanika together with the corresponding magnetic traces of the *H* and *D* components observed at Poker Flat, which is only 3 km north of the radar site. Moderate magnetic disturbances were observed all day. In the figure the ordinate scales are given in such a way that 1 A/m in the current density and 400 nT in the magnetic perturbations are represented by the same

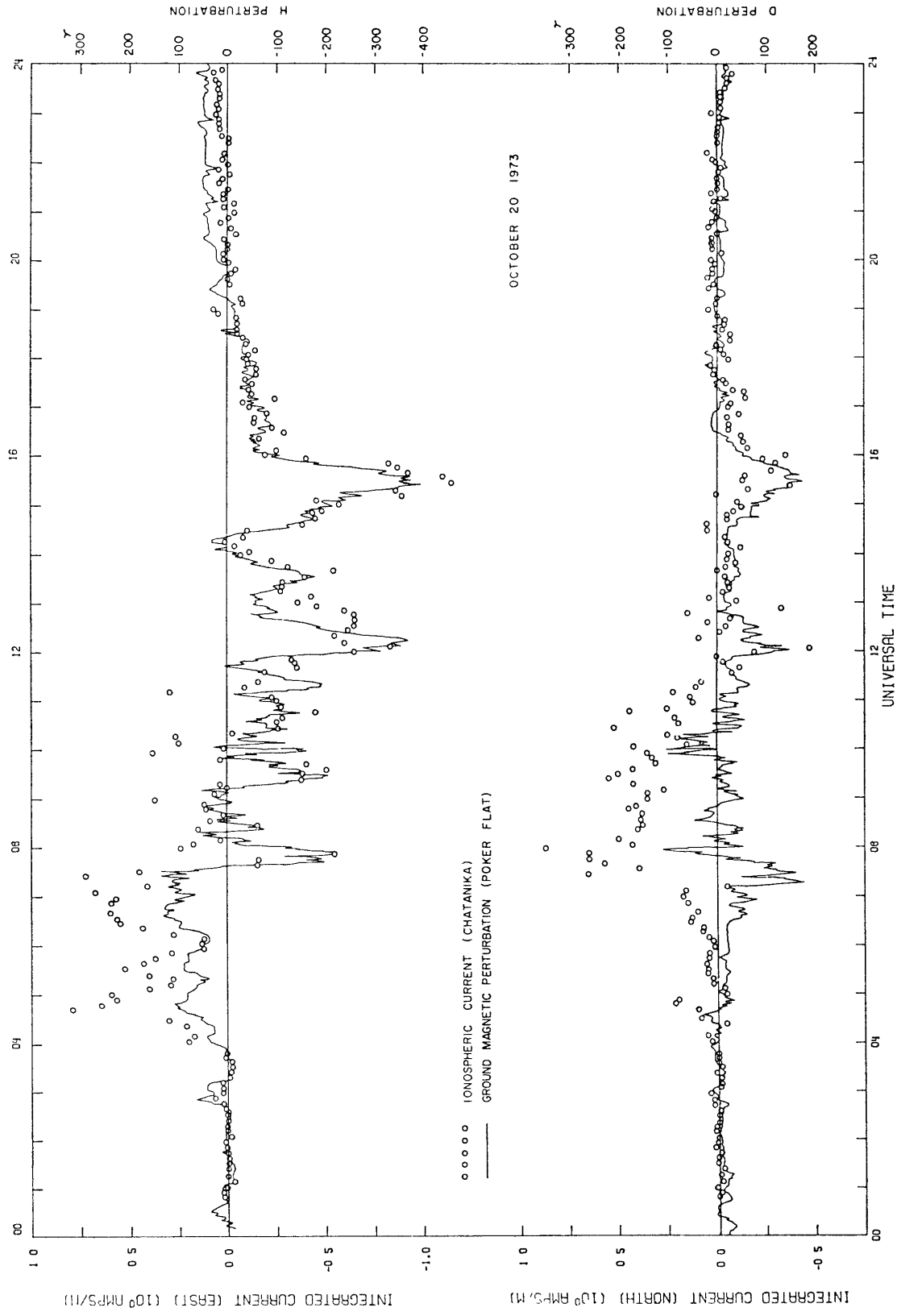

Fig 36a Height-integrated ionospheric currents (circles) and the corresponding ground magnetic records (after KAMIDE et al., 1976a).

scale length. Time variations of the east-west current density are quite similar to the corresponding variations in the H component of the geomagnetic field near the radar site. There are some disagreements, in magnitude, between the two quantities during the period 0400–0730 UT, but they can be reasonably explained by the fact that the eastward electrojet had a small latitudinal width during that period. It can be said that the total intensity of the eastward current was much less than that of the westward electrojet in midnight and morning hours. The relationships between the north-south current density and the ground D component appear, however, to be more complicated. From about 0500 UT, the Chatanika radar observed a gradual increase of the northward current followed by a sudden intensification of it at about 0730 UT. Until about 1130 UT, the ionospheric current has essentially a northward component, regardless of the change of the sign in the D component. The disagreement between the north-south ionospheric current and ground D is most serious prior to local midnight, except for the short time intervals of 0750–0850 UT and 0950–1020 UT. That is, there are many periods in which the Chatanika radar data give results completely contrary to the observed D perturbations on the earth's surface.

On the other hand, the disagreement becomes less serious in the morning sector. There are, at least, two eastward deviations ($\Delta D>0$) at Poker Flat which occurred at about 1145 and 1420 UT associated with intense negative H bays. It is noted that these eastward perturbations were observed at all the Alaska observatories except Sitka along the meridian, which are caused by the southward ionospheric current actually observed at Chatanika.

These characteristics may be more clearly seen in the vector representation at four instances (two of them were observed in the evening sector and the other two in the morning sector). In Fig. 36b, we show the vector $\boldsymbol{J}$ of the deduced ionospheric current at Chatanika and the magnetic perturbation vector $\Delta \boldsymbol{F}$ in the horizontal plane ($\Delta F=\sqrt{\Delta H^2+\Delta D^2}$) observed at Poker Flat, along with the predicted direction of $\Delta \boldsymbol{F}$ (assuming that it results purely from the observed overhead ionospheric current $\boldsymbol{J}$). Disturbance vectors at Point Barrow and Fort Yukon are also given for comparison. At 0730 UT, when a typical positive H bay was in progress at Poker Flat, the strong westward electrojet was flowing in higher latitudes, as seen in the negative H bays at Point Barrow and Fort Yukon. The radar measurement indicates that the ionospheric current was directed northeastward, thus the expected ΔF on the earth's surface should be directed northwestward ($\Delta H>0$, $\Delta D<0$), as illustrated by the dashed line. However, the actually observed vector $\Delta \boldsymbol{F}$ was directed northeastward ($\Delta H>0$, $\Delta D>0$).

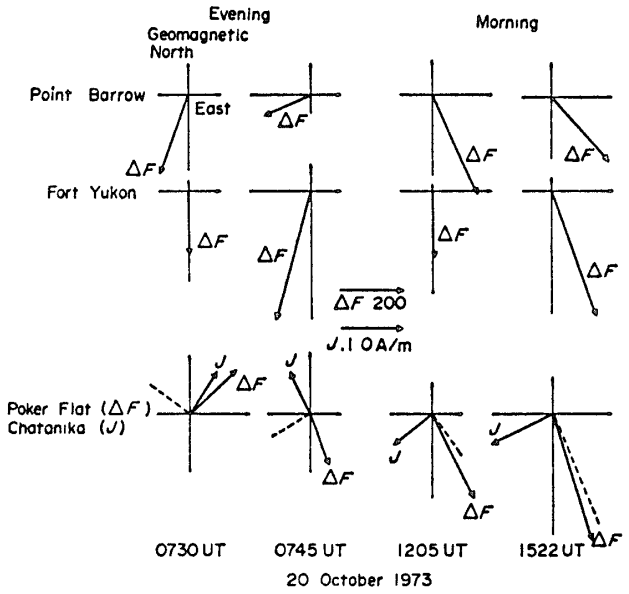

Fig. 36b. Vector J of the deduced ionospheric current and the magnetic perturbation vector ΔF in the horizontal plane. The dashed line represents the predicted direction of ΔF assuming that it results purely from the observed overhead ionospheric current J (after KAMIDE et al., 1976a).

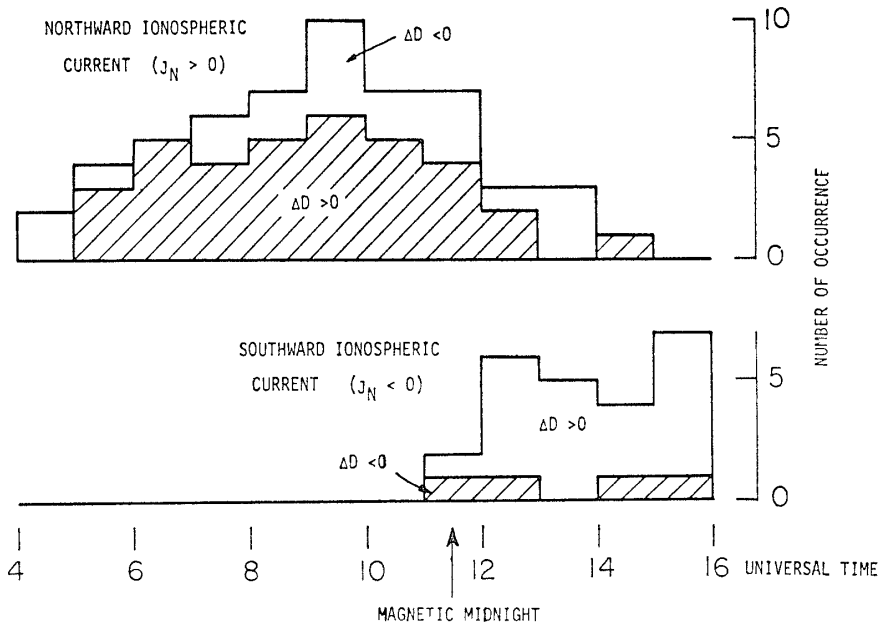

Fig 37. Occurrence frequency of the northward (top) or southward (bottom) ionospheric current and the corresponding geomagnetic D perturbation as a function of universal time. The occurrence of the D event, which cannot be explained solely by the ionospheric current, is hatched (after KAMIDE et al , 1976a).

At 0745 UT, the ground perturbations in the H component at all the three stations were negative, whereas the D perturbation at Poker Flat was positive, and was negative at higher latitudes. Again there is a large discrepancy between the predicted and the observed ΔF. The angle between these two vectors is almost 90° for both cases.

In morning hours, however, the direction of ΔF, predicted based on the deduced ionospheric current vector, agrees reasonably well with that observed at Poker Flat for both cases at 1205 and 1522 UT which were during the maximum phase of the two substorms.

An attempt has been made to confirm statistically the above relationship between the north-south ionospheric current deduced from the radar observations and the ground D perturbation on the basis of data for ten disturbed days when the radar was operated. In the analysis, only clearly-defined perturbations in the north-south component of the ionospheric current during each UT interval were taken, ignoring rapid fluctuations with periods of a few minutes.

In Fig. 37, the occurrence frequency of the northward or southward ionospheric current and the corresponding magnetic deviation in the D component are shown as a function of UT. It is generally seen that the northward ionospheric currents prevail in the evening sector, whereas the southward currents prevail in the morning sector. If the ionospheric current in the north-south direction is the main source of the ground magnetic perturbations in the D component (as the east-west ionospheric current is so for the H perturbation), then we should have expected that there would be a corresponding predominance of the westward and the eastward deviations in the evening and morning sectors, respectively. The occurrence of the D perturbations, which cannot be explained by the ionospheric current on this background, is hatched. The eastward ($\Delta D>0$) deviation is a common feature, independent of the local time at Poker Flat and College. This suggests that the main part of the ground D perturbation in the evening sector is not caused by ionospheric currents but probably by field-aligned currents. Then, why does the ground ΔD observation suggest the incorrect direction of the current in the evening sector? This contradiction is at least partially solved by a finding that the intensities of the upward and the downward field-aligned currents are, in general, not equal (YASUHARA *et al.*, 1975). After qualitative considerations, KAMIDE *et al.* (1976a) have proposed a current flow model including both ionospheric and field-aligned currents. This is shown in Fig. 38. The dashed line represents the Harang discontinuity which divides the region of the eastward current from the region of the westward current in the evening sector. On the equatorward

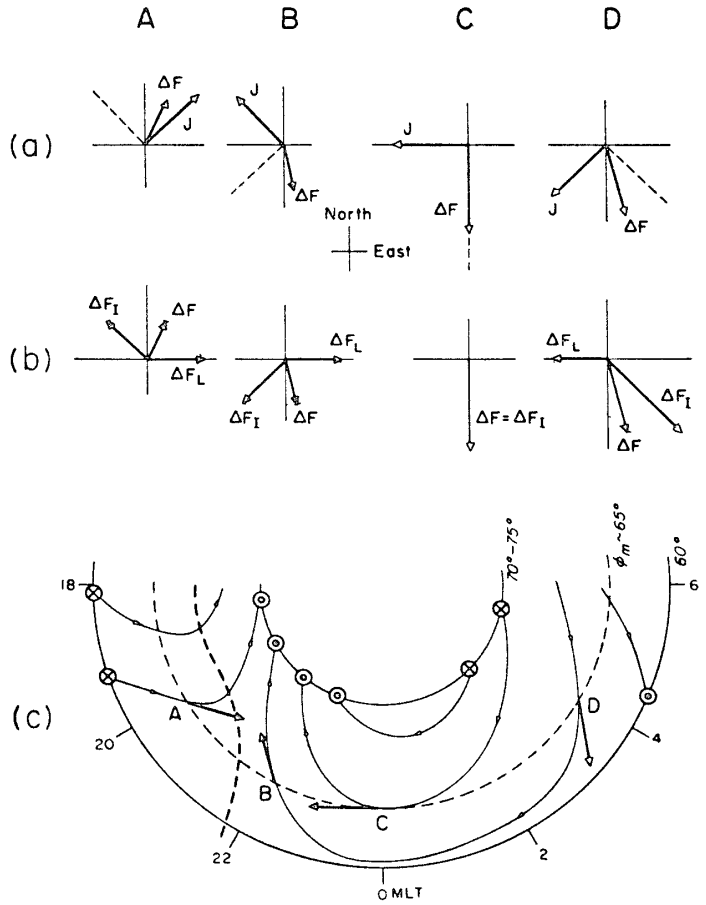

Fig 38. Schematic drawing of ionospheric current flow, together with the Harang discontinuity (dashed line) (after KAMIDE et al , 1976a)

side of the discontinuity, the ionospheric current flows northeastward, as can be seen in the examples at 0730 UT (Fig. 36b). On the other hand, the direction of the ionospheric current on the poleward side is northwestward; this can be seen in the vectors at 0745 UT (Fig. 36b). These should not be confused with the equivalent current vectors derived from the ground magnetic perturbations.

Recently, rocket measurements of the electric field vectors and the electron density profile have made it possible to deduce the ionospheric currents EVANS *et al.* (1977) obtained, as shown in Fig. 39, the pattern of the height-integrated ionospheric currents with respect to the location of an auroral arc in the evening sector It is seen that the eastward current in and near the auroral arc has a northward component as well

6.2. Overhead ionospheric current approximation

There have been several conventionally used methods to infer the ionospheric current density One of the most popular methods is the infinite overhead current

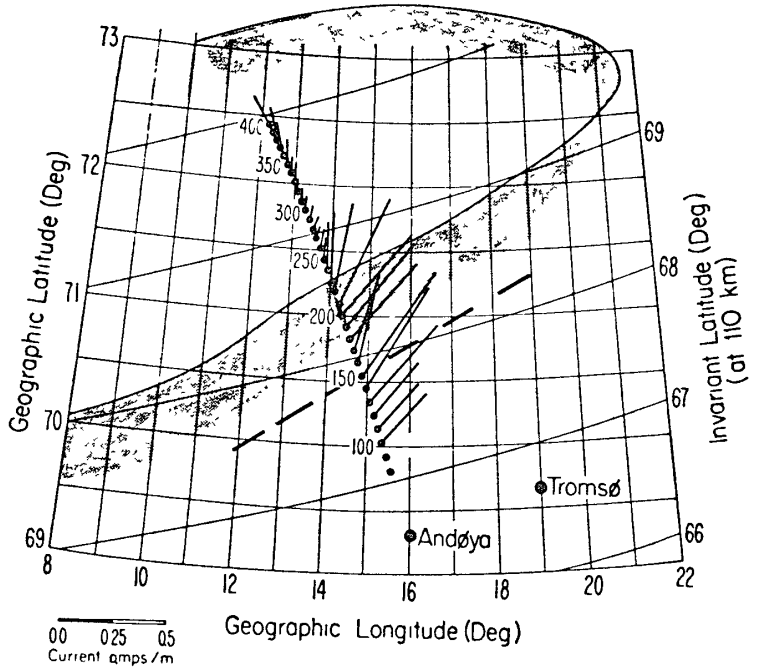

Fig. 39. Auroral electrojet current pattern which shows the relationship with the visual auroral forms. The dashed line marks the orientation and location of the southern edge of the main auroral form (after EVANS et al., 1977).

approximation (see NAGATA and FUKUSHIMA, 1971). The determination of an equivalent overhead current vector has usually been made by converting the magnitude (in nT) of the horizontal magnetic perturbation at the point of observation on the earth's surface into the overhead current density (in amperes per kilometer) by assuming that geomagnetic disturbances are produced by an infinite, uniform sheet current. Such an assumption is undoubtedly unrealistic, since it is well known that polar substorms are characterized by localized currents called the auroral electrojets.

KAMIDE and BREKKE (1975) examined how well the use of the equivalent ionospheric current approximation can reproduce the height-integrated ionospheric current density deduced by the Chatanika incoherent scatter radar data. Fig. 40 shows the relationship between the ground H perturbation at Poker Flat and the height-integrated current density in the east-west component at Chatanika for 36 positive and negative H bays. For comparison, the linear relations based on the infinite overhead current approximation for $k=1$, 2/3, and 1/2 are also given. Note that $k=1$ corresponds to the particular assumption that there is no induction current within a flat earth and $k=1/2$ corresponds to an infinite sheet current above a perfectly conducting flat earth. In Fig. 40 it is clear that even the extreme approximation ($k=1$) underestimates the current density by a large factor. Note

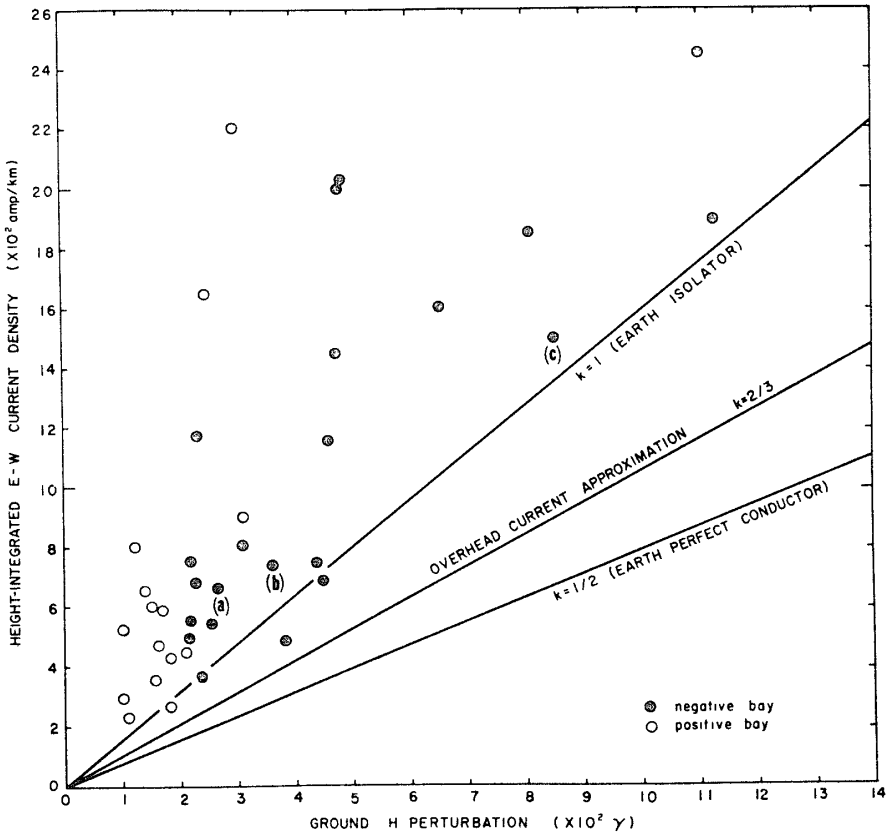

Fig 40. Relationship between the ionospheric east-west current density provided by the Chatanika radar observations and the magnitude of the corresponding geomagnetic H perturbations on the ground. The lines show the expectable current density based on the overhead current approximation for three different values of correction factor k of the induction effect within the earth (after KAMIDE and BREKKE, 1975).

that whereas for an infinite sheet current one would expect $1/2<k<1$ and a spatially constant k, this is not so for an electrojet flowing in the finite area. Note also in Fig 40 that there is a significant difference in this relationship between positive and negative bays

It is important to note that the overhead current approximation almost always underestimates the current density by a factor of 2 or more. Thus, great caution should be exercised in estimating the ionospheric current intensity on the basis of this approximation. As discussed in detail by KAMIDE and BREKKE (1975), some obvious causes for the underestimation are (1) the latitudinal width of the auroral electrojet, (2) the distance from the center of the electrojet, (3) the latitudinal dependence (*i.e.*, gradient) of the current density, and (4) field-aligned current effects.

6.3. Altitude dependence of ionospheric currents

A sounding rocket (launched into a westward electrojet) measurement of the ion flow velocity and the electric field by the double probe was performed by BERING *et al.* (1973). BERING and MOZER (1975) have shown that altitudes above 140 km the electric fields deduced from the two data sets agree to an accuracy within the uncertainties of the two measurements. The difference between the two data at altitudes below 140 km provides an *in situ* measurement of the ionospheric current density. It was shown that a maximum current density of 5×10^{-6} A/m^2 was observed at an altitude of 110 km in the westward electrojet.

More recently, high-resolution (~10 km) measurements of the ionospheric electric fields have been made possible at the Chatanika incoherent scatter radar (RINO *et al.*, 1977). Fig. 41 shows height-versus-time vector plots in geomagnetic coordinates of the deduced current density. Of particular interest is the height variation of the current, in both magnitude and direction. During the geomagnetically active period from 1130 to 1600 UT in the morning sector, one can see a concentration of the electrojet at the lower altitudes with a tendency of the currents to rotate to the southwest at the higher altitudes, particularly near 1300 and 1400 UT.

KAMIDE and BREKKE (1977) have made a similar study, in which the intensity contours of the ionospheric current density are obtained as functions of altitude (from 85 to 185 km) and universal time, as shown in Fig. 42. The following two points of interest are noted: (1) The dashed line indicates the altitude of the maximum current density as a function of time. It is seen that the altitude dependence of the eastward electrojet was rather stable in the evening sector even when it grew in conjunction with substorms. In the midnight and morning sectors, however, it became intermittently lower in conjunction with the growth of the current that is a signature of the substorm intensification. (2) The current center of the eastward electrojet is located at higher altitudes than that of the westward electrojet. The average altitude of the maximum current density at the peak time of the eastward electrojet is 119.1 km, while that for the westward electrojet is 101.6 km.

These results may not be unexpected, if we combine previously observed different characteristics associated with the eastward and westward electrojets. The eastward electrojet is probably associated with the diffuse aurora caused by relatively low energy particles. In that region the Hall and Pedersen conductivities seem to change in unison. In the westward electrojet region, however, there are large changes in the Hall conductivity with only small increases in the Pedersen

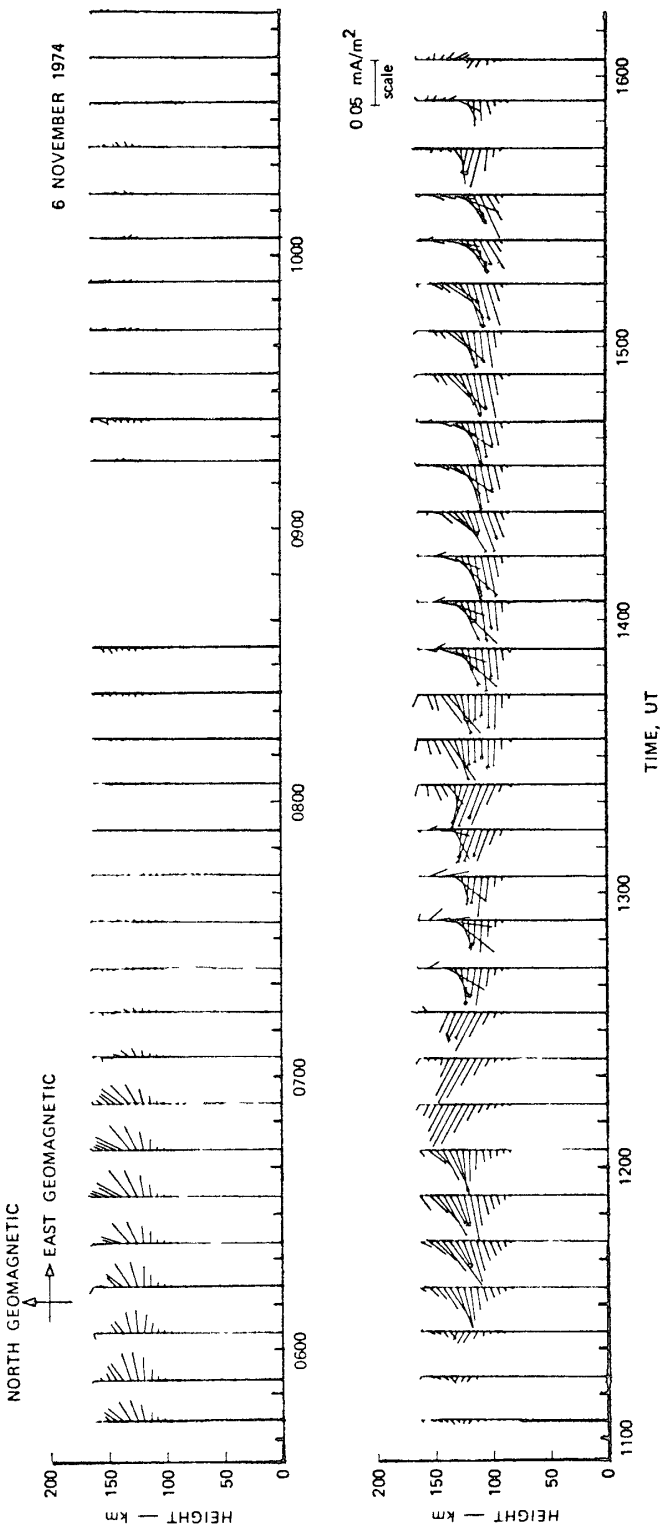

Fig. 41 Ionospheric current vectors obtained from the Chatanika radar observations as functions of altitude and universal time (after RINO *et al*., *1977).*

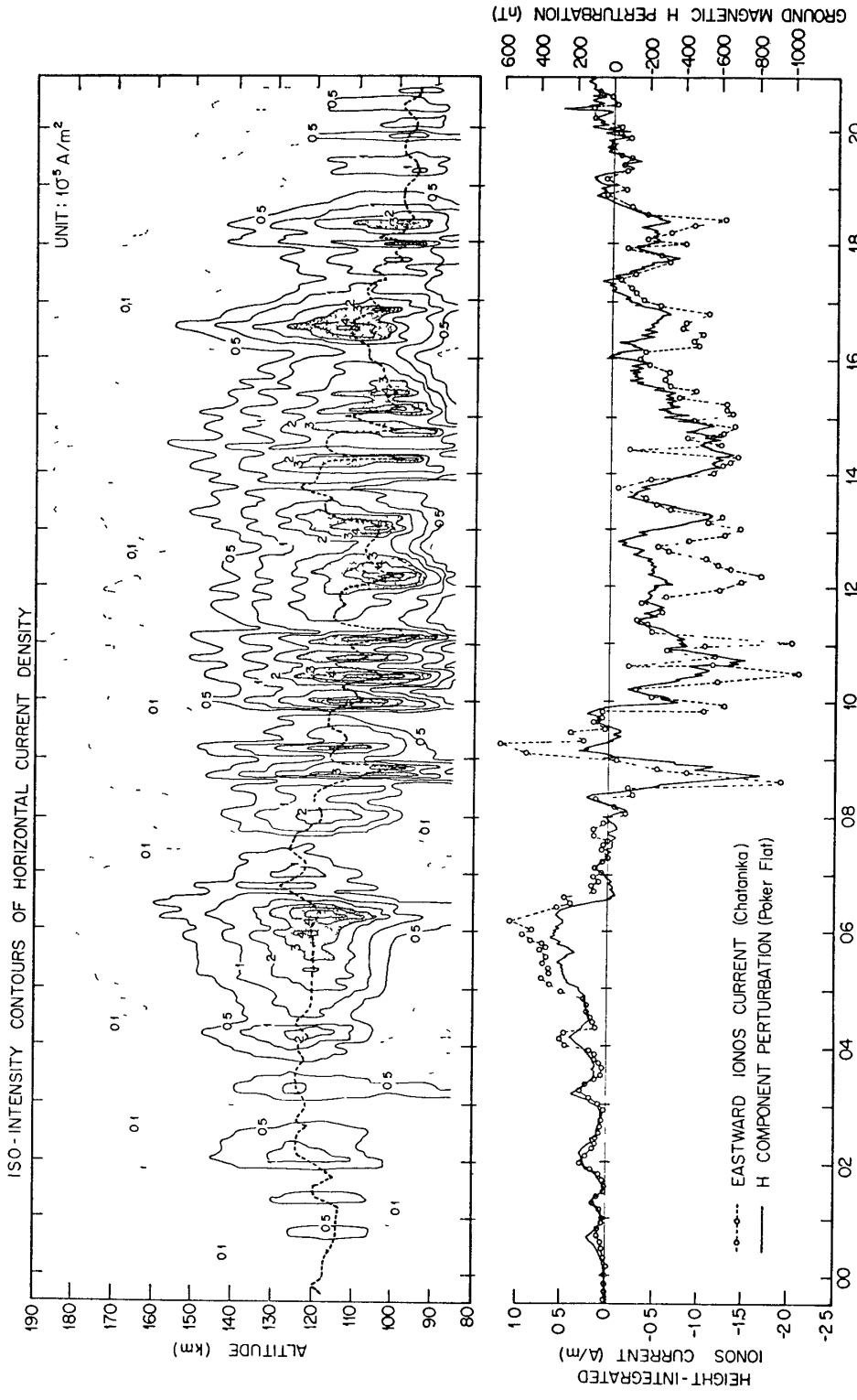

Fig 42 Altitude profile of horizontal ionospheric current density as a function of universal time deduced from the Chatanika radar observations. Contour unit is 10^{-5} A/m^2. The height-integrated ionospheric current in the geomagnetic east component and the corresponding H component magnetic perturbation at Poker Flat (the nearest station to the radar site) are also shown (after KAMIDE and BREKKE, 1977).

conductivity, implying the sporadic precipitation of particles with energies of several keV and above.

7. Field-Aligned Current

The importance of field-aligned currents -Birkeland currents- in magnetospheric and auroral physics was suggested by BIRKELAND (1908) and ALFVÉN (1939) a long time ago, but it is only in the last decade that their presence has been confirmed with particle and magnetic field observations acquired from a variety of rocket and satellite instruments. A relatively large number of review papers (ARNOLDY, 1974; ARMSTRONG, 1974; ANDERSON and VONDRAK, 1975; CLOUTIER and ANDERSON, 1975; SUGIURA, 1976; RUSSELL, 1977; POTEMRA, 1977) have been published on the observations of the field-aligned currents and their relations to auroral display and energetic particle precipitation. The observations of the field-aligned currents can be classified into three groups in terms of the regions where the measurements are made; rocket observations at ionospheric altitude, low altitude (<3000 km) observations by polar-orbiting satellites, and observations in the magnetosphere. Among these have been the observations in the auroral and polar cap regions acquired with a two-axis magnetometer on board the AZUR satellite (THEILE and PRAETORIUS, 1973); the three-axis measurements by the IMP 4 and 5 satellites in the magnetotail (FAIRFIELD, 1973); the three-axis magnetic field measurements on the OGO-5 satellite at altitudes $>4\,R_E$ (SUGIURA, 1975); simultaneous measurements of precipitating electrons and magnetic fluctuations from OGO 4 at altitudes between 412 and 908 km (BERKO, 1973; BERKO and HOFFMAN, 1974; BERKO *et al*, 1975), and at synchronous altitudes with the ATS 1 satellite (IIJIMA, 1974).

7.1. Gross field-aligned current pattern

FAIRFIELD (1973) and IIJIMA (1974) studied manifestations of the field-aligned currents in the magnetosphere and their gross patterns as functions of local time and substorm activity using magnetometer data of the IMP 4 and 5 and ATS 1 satellites, respectively. As BIRKELAND (1908) suggested, the westward electrojet which is the dominant feature of a polar substorm, can be thought to be connected to a pair of the field-aligned currents originating in the magnetosphere; they are directed toward the earth in the morning sector and away from the earth in the evening sector. When these currents are intensified in harmony with the growth of magnetospheric substorms, one would expect an eastward deflection of the magnetic field in the morning sector of the high latitude lobe of the magnetotail

and a westward deflection in the evening sector. FAIRFIELD (1973) showed that this is indeed observed by satellites in the magnetotail during substorms. Fig. 43 shows an example of such magnetic changes in the evening sector; the upper part of this figure is taken from FAIRFIELD's (1973) Fig. 4. It is seen that the large negative D perturbation at 0015 UT occurred in association with a substorm recorded at Leirvogur. It should be noted, however, that this sudden change in the D component did not occur at the onset time of the substorm; it represents rather a spatial change. Note that the D change indicates the encounter of the

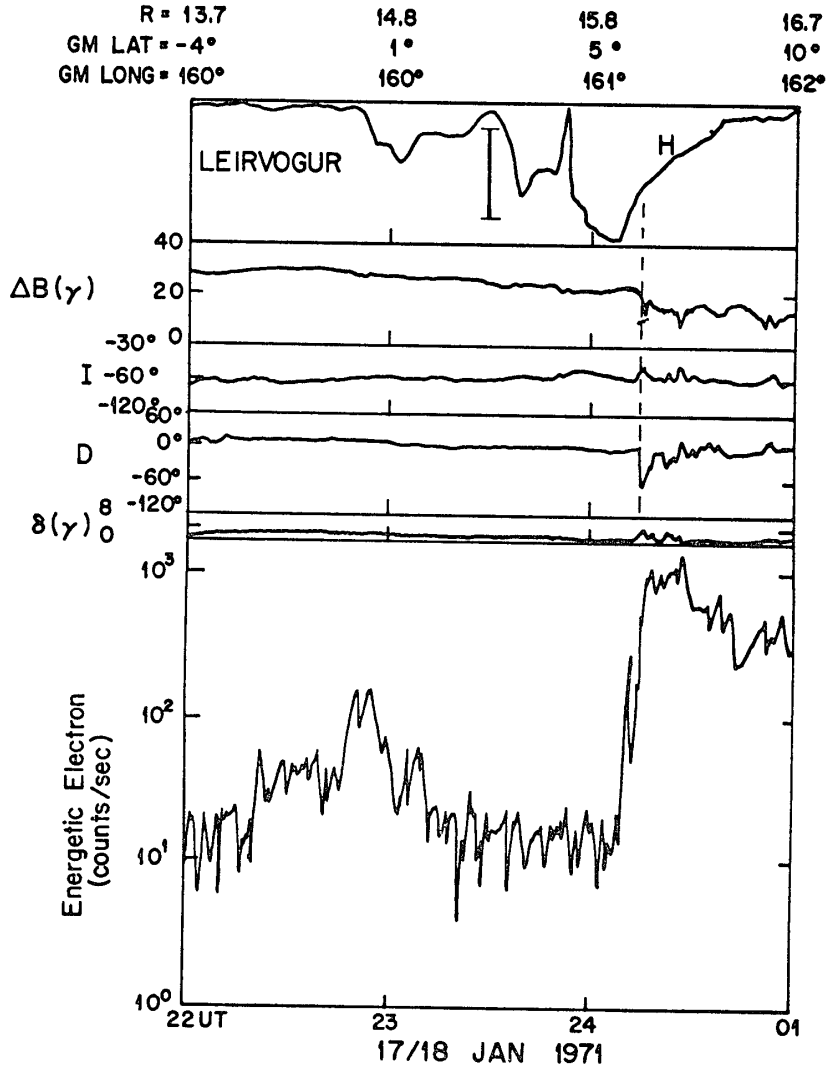

Fig. 43. Magnetic field and energetic electron flux observations in the magnetotail during substorms. The H component magnetic record from the midnight auroral zone station is also shown. Note that a large deflection of the magnetic vector occurs at the moment when the satellite is submerged in the expanding plasma sheet (after FAIRFIELD, 1973; and courtesy of MENG).

satellite with the expanding plasma sheet boundary. Indeed, the simultaneous energetic electron data (the bottom of the figure) show a considerable increase at the time of the magnetic deflection (MENG, 1977, personal communication; see also AKASOFU, 1977). These observations may indicate that the corresponding magnetic deflection can be observed only in a limited region near the plasma sheet boundary, not in the entire region of the magnetotail. Implications of it are now under study by the author. Fig. 44 shows the locations of the *D* events observed by the satellite projected to the earth surface along with the statistical auroral oval (FAIRFIELD, 1973). It is noticeable that the directions of the inferred field-aligned currents are systematically separated by different local time sectors with respect to premidnight hour. IIJIMA (1974) reached the similar configuration of the gross pattern of the field-aligned currents in the nightside magnetosphere.

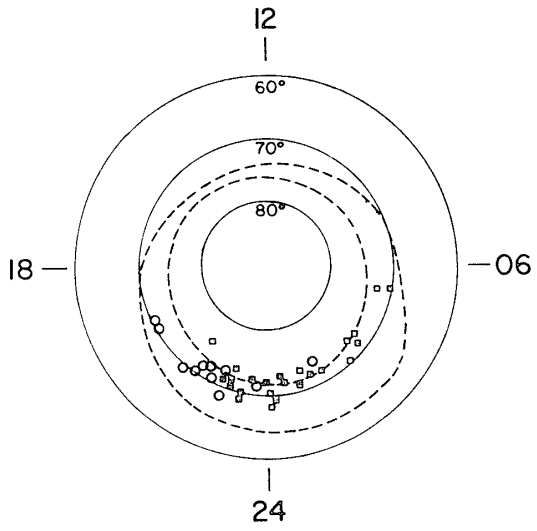

Fig. 44 Locations of field-aligned current events, which are most frequently seen near midnight and near the northern boundary of the auroral oval (dashed line) (after FAIRFIELD, 1973)

BERKO *et al.* (1975) compared statistically the regions where high fluxes of field-aligned 2.3 keV precipitations were observed (from BERKO, 1973), regions where the OGO 4 magnetometer recorded fluctuations (BURTON *et al*, 1969) and region where ZMUDA *et al* (1970) observed large transverse magnetic disturbances. Fig 45 (BERKO *et al*, 1975) indicates that all these regions share the spatial feature of an oval-shaped auroral belt in which the lower boundary is located at higher latitudes during the dayside hours than during the near-midnight hours It was noted that upward field-aligned currents in late evening hours were detected

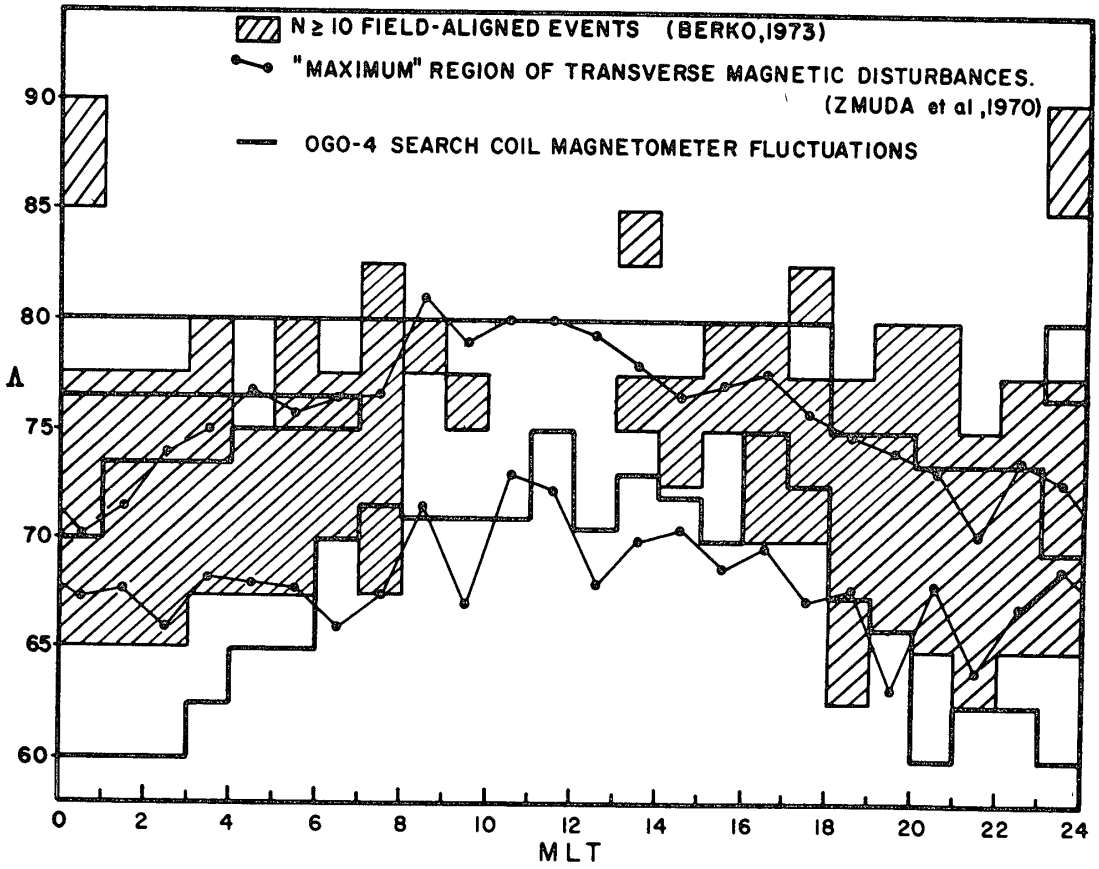

Fig. 45. Comparison of regions where field-aligned 2.3 keV electron precipitation was observed by OGO 4 (BERKO, 1973) with the regions where OGO 4 search coil magnetometer fluctuations were observed (BURTON et al., 1969), and where transverse magnetic disturbances were observed by ZMUDA et al., (1970) (after BERKO et al., 1975).

in the region of high field-aligned particle precipitation occurrence, and that most of the current in this region was carried by particles with energies greater than 0.7 keV. Simultaneous measurements of low-energy electrons and magnetic fluctuations from the low-altitude polar-orbiting satellite by BERKO *et al.* (1975) indicate that dayside field-aligned currents consist primarily of electrons with energies of less than 1 keV. BERKO and HOFFMAN (1974) examined the dependence of field-aligned current occurrence on season and altitude by using electron precipitation data from more than 7500 orbits of OGO 4, and found that the highest probability occurs when the measurements were made at altitudes near 800 km to 900 km during the winter season.

THEILE and PRAETORIUS (1973) described the results of an analysis of two component magnetometer data on board the AZUR satellite, which is in polar orbit at 400 to 3000 km altitudes. It was shown that the regions of transverse

magnetic perturbations coincide with the regions of measured emission of 3914 Å radiation, presumably excited by precipitating auroral electrons.

An extensive survey of magnetic fields has most recently been carried out by MCPHERRON and BARFIELD (1978) with instruments on board the ATS 6 satellite. It was statistically shown that the above configuration of the field-aligned currents exists permanently and enhances in accordance with geomagnetic activity. This means that the main part of the field-aligned currents is generally located outside the synchronous distance. They have also pointed out that in interpreting the magnetic signature of the field-aligned currents at the synchronous orbit, it is necessary to take into account the difference between the magnetic equator (where no field-aligned currents signature can be expected) and geographic equator (where a synchronous satellite is located).

7.2. TRIAD satellite observations

The TRIAD satellite, launched into a nearly circular polar orbit at 800 km altitude in November 1972, is the first satellite that carries a tri-axial, high-resolution magnetometer, allowing us to determine the current flow directions, spatial distribution, and intensities of field-aligned currents at all magnetic local times. The characteristics of the TRIAD magnetometer experiment have been described

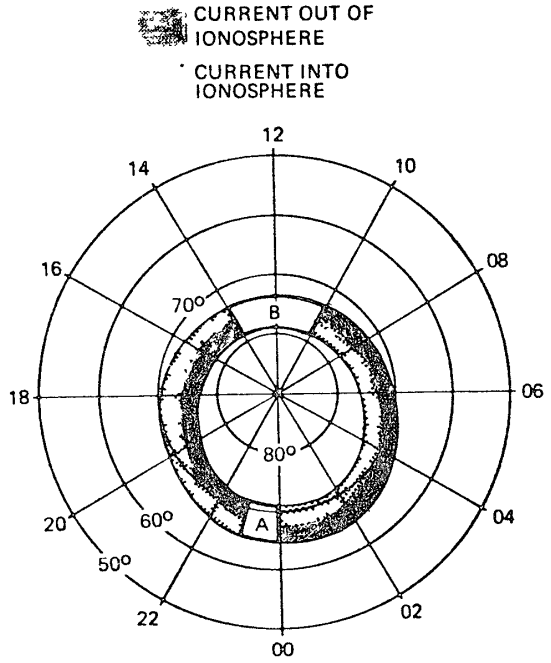

Fig 46 Diurnal flow pattern of field-aligned currents along the auroral oval observed by the TRIAD satellite. A, both types of current patterns found in this region B, irregular region (after ZMUDA and ARUSTRONG, 1974b).

in detail by ARMSTRONG and ZMUDA (1973), along with sample magnetometer records. ARMSTRONG (1974) noted that in most cases, the total magnetic perturbation vector at auroral latitudes is transverse to the main field to within experimental sensitivity, confirming the earlier suggestion that the magnetic perturbations result from field-aligned currents.

According to ZMUDA and ARMSTRONG (1974a), in the evening sector (1400 MLT through dusk to 2300 MLT) the magnetic field perturbation is eastward, indicating a current flow away from the earth at the poleward part and a flow toward the earth at the equatorward part of the disturbance region. The current direction is reversed in the morning sector (2400 MLT through dawn to 1000 MLT). Either set can appear in the transition period, 2300–2400 MLT. From 1000 through noon to 1400 MLT, the magnetic variations are still transverse but

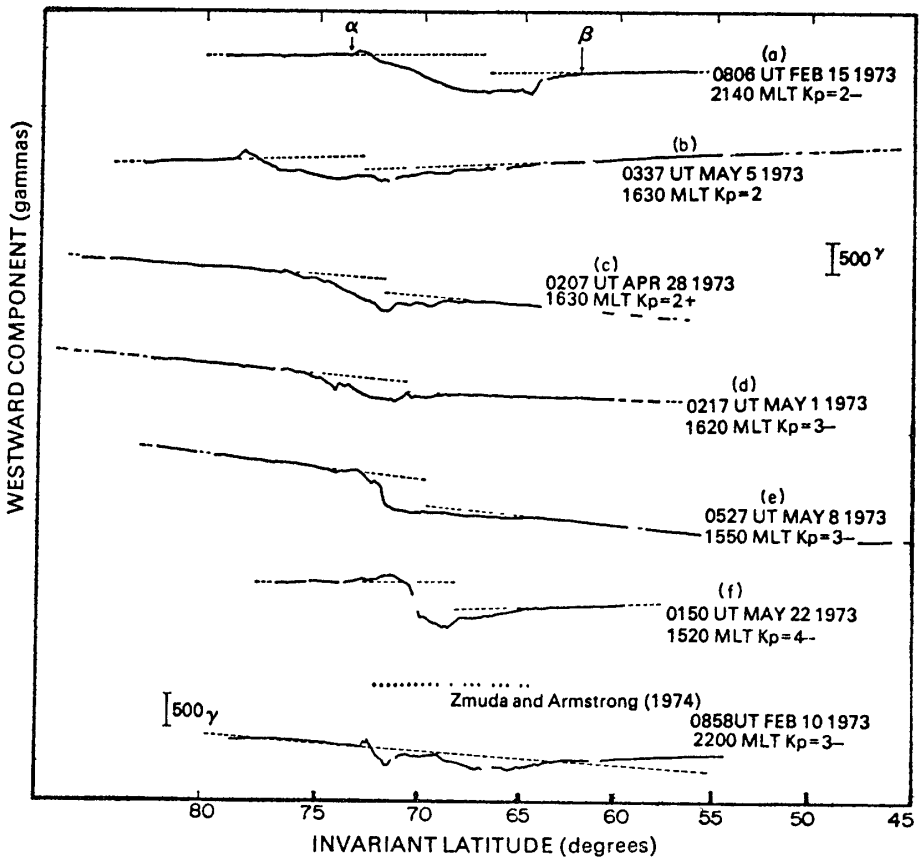

Fig. 47. Typical examples of the magnetic field perturbations observed by TRIAD; the invariant latitude is shown at the bottom. The dashed lines are extrapolation from both the poleward and equatorward portions of the traces. The arrows α and β on the top trace indicate the poleward and equatorward edges of the perturbation region. The last trace is one of the examples studied by ZMUDA and ARMSTRONG (1974b) in which the dashed line shows their base line (after YASUHARA et al., 1975)

are relatively irregular. The diurnal flow pattern is schematically shown in Fig. 46, which is reproduced from Fig. 9 of ZMUDA and ARMSTRONG (1974b).

Such paired field-aligned currents of oppositely directed flow have been further examined by the same authors. It was shown that the current densities of the two oppositely-directed field-aligned currents are essentially equal (ZMUDA and ARMSTRONG, 1974b), considering a lack of shift in base line level of the east-west component of the magnetic perturbation in passing through the current flow region. However, YASUHARA *et al.* (1975) have claimed that cases of the equality of the oppositely directed current intensities does not exist more often than cases of the inequality do. They have shown several 'typical' examples of the magnetic field perturbations observed by TRIAD (see Fig. 47), in which the eastward deviation does not recover fully at the end of the data; namely, the trace does not merge with the extrapolated line from the poleward side. This tendency can be explained by supposing that the intensities of the inflow and the outflow currents are not equal. Unfortunately, the opportunity had not occurred to discuss this 'basic' difference between conclusions by ZMUDA and ARMSTRONG (1974b) and YASUHARA *et al* (1975) before tragic deaths of ZMUDA and ARMSTRONG in 1974, in spite of the fact that the study of the configuration of the field-aligned currents began as a joint project by all of them.

Fig. 48 shows the relationship between the upward and inward field-aligned

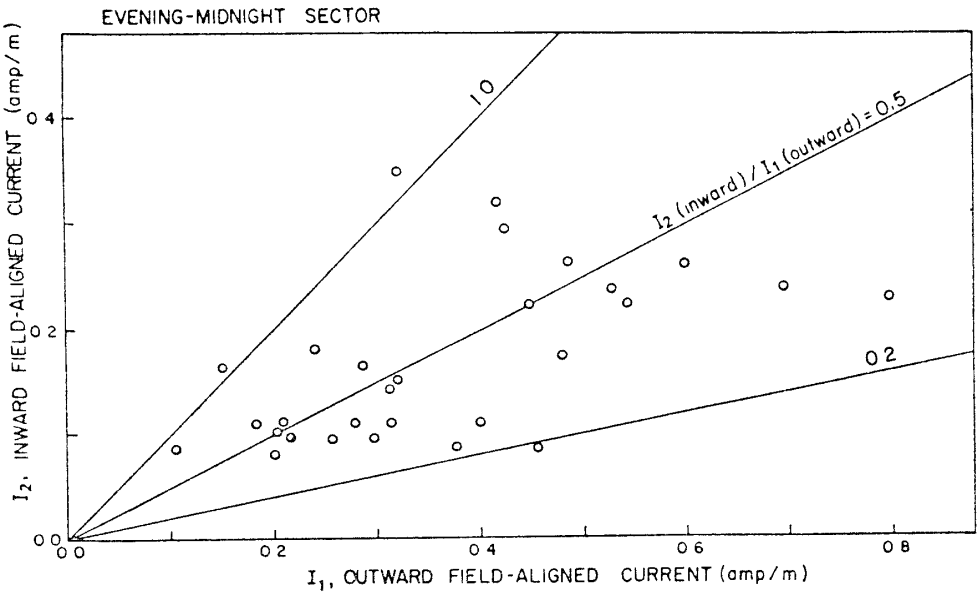

Fig 48 Relation between the intensities of the poleward and equatorward field-aligned currents All these data points are from passes in the evening-midnight sector (after YASUHARA et al , 1975)

currents in the evening sector, together with three lines giving the ratio between these currents. Although the ratio varies considerably, most points lie between the two lines 1.0 and 0.2 indicative of the upward current being generally greater than the downward current. YASUHARA *et al.* (1975) and YASUHARA and AKASOFU (1977) conducted extensive numerical calculations to examine how the observed distribution and intensity of the field-aligned currents are related to ionospheric currents and electric fields for specific models of the ionospheric conductivities.

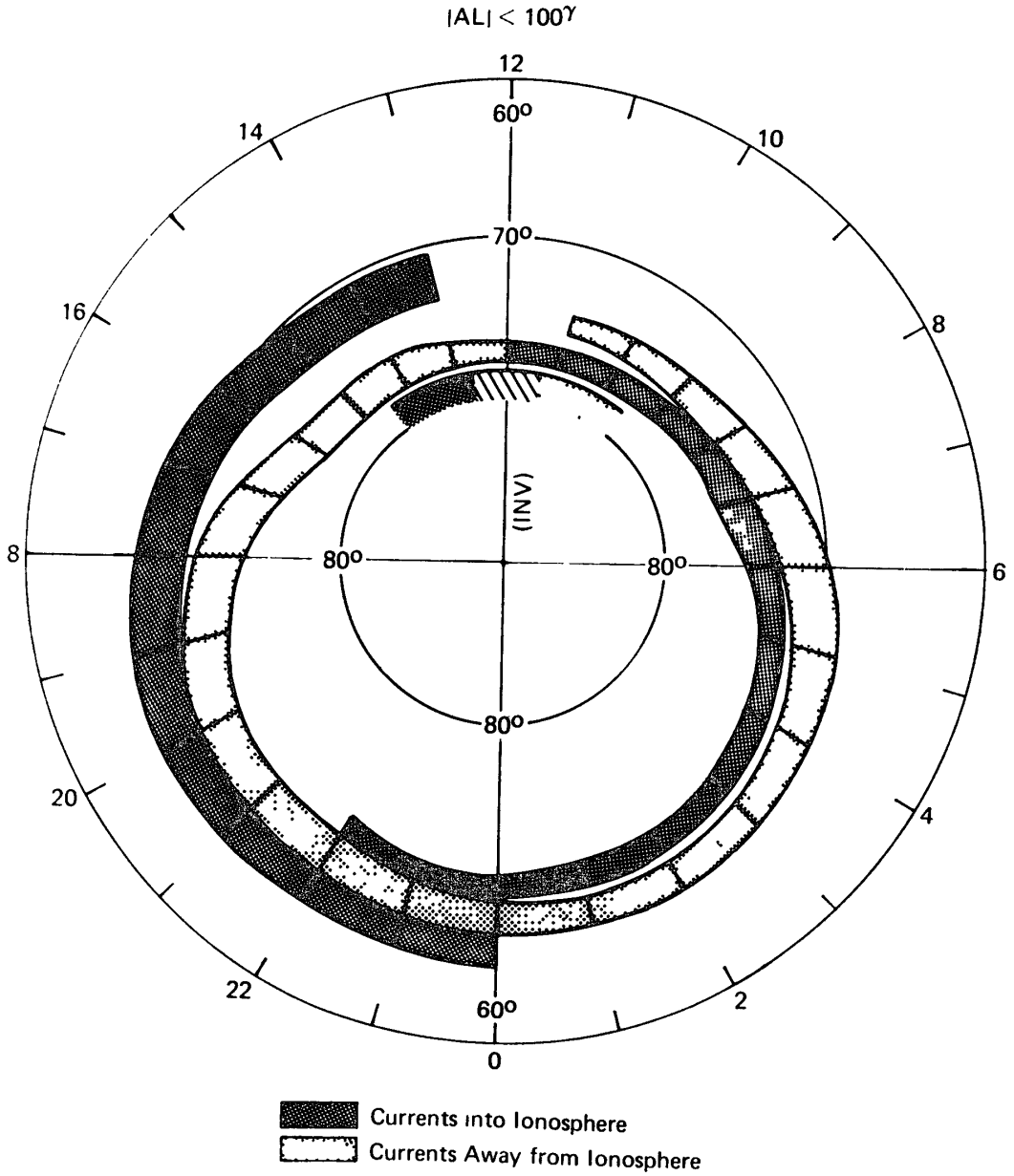

Fig 49. Spatial distribution and flow directions of large-scale field-aligned currents determined from data obtained on 493 TRAID passes during weakly disturbed conditions (after IIJIMA and POTEMRA, 1976b).

By means of the OGO 5 magnetometer data, SUGIURA (1975) has found the existence of the paired field-aligned currents in the magnetosphere. In the nightside magnetosphere, the polar cap boundary was identified by a sudden transition from a dipolar field to a more tail-like configuration, at which a field-aligned current layer exists.

There have been well documented definitive studies carried out by SUGIURA and POTEMRA (1976) and IIJIMA and POTEMRA (1976a, b) using bulk data from the TRIAD satellite. Fig. 49 shows a summary of the average distribution in 'MLT and invariant latitude' coordinates of the large-scale field-aligned currents determined from TRIAD magnetometer data obtained on 493 passes during weakly disturbed conditions (IIJIMA and POTEMRA, 1976b). As summarized by POTEMRA (1977), the principal features include the following: (1) Field-aligned currents are concentrated in two major areas which encircle the geomagnetic pole, regions 1 and 2. The region 1 field-aligned currents flow into the ionosphere in the morning sector and away from the ionosphere in the evening sector, whereas the region 2 currents flow in the opposite direction at any given local time. (2) The areas of maximum current density in region 1 are approximately coincident with

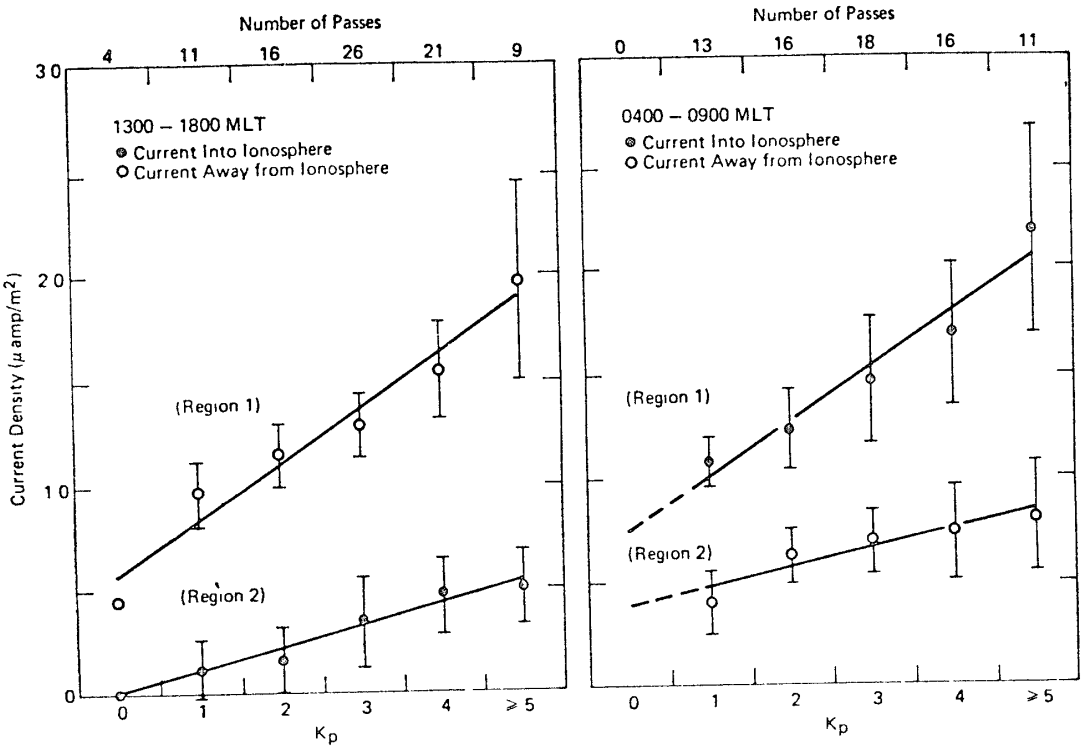

Fig 50. Relationship between field-aligned current densities and the general level of geomagnetic activity in the forenoon and afternoon sectors (after IIJIMA and POTEMRA, 1976a).

the location of the foci of the S_q^p current system; see Fig. 49. (3) The currents in region 1 are statistically larger than the currents in region 2 at all local times, indicating an unbalanced or 'net' current flow on one side of the two regions. (4) The region 1 currents appear to persist even during very low geomagnetic activity with a value of current density $\gtrsim 0.6\times10^{-6}$ A/m^2 for K_p=0; see Fig. 50. (5) A region of field-aligned currents has been discovered in the dayside between 1000 and 1400 MLT and poleward of region 1 between ~78° and 81° invariant latitude. These 'cusp' field-aligned currents (called the region 3 currents) flow away from the ionosphere in the pre-noon sector and into the ionosphere in the post-noon sector.

Fig. 51 shows the local time dependence of the field-aligned current intensities after IIJIMA and POTEMRA (1976a). It should be noted, however, that since all the TRIAD data were acquired only at College, Alaska on a real time basis to construct Fig. 51 and thus a particular local time when the satellite passes near

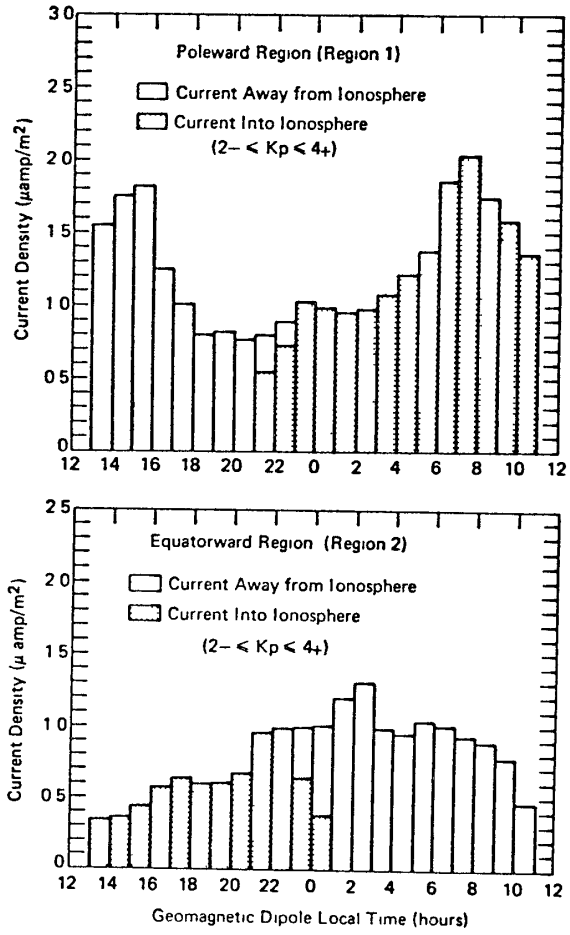

Fig. 51. Diurnal distribution of field-aligned current densities in regions 1 and 2 (after IIJIMA and POTEMRA, 1976a).

College is given by a particular season, the obtained local time variations of the field-aligned current intensity include the seasonal effects (if any) as well.

7.3. ISIS 2 satellite observations

Simultaneous particle and magnetic field measurements made on the ISIS 2 satellite have been reported by BURROWS *et al.* (1976), KLUMPAR *et al.* (1976) and MCDIARMID *et al.* (1977). The ISIS 2 satellite is in a nearly circular polar orbit at an altitude of approximately 1400 km. The energetic particle experiment

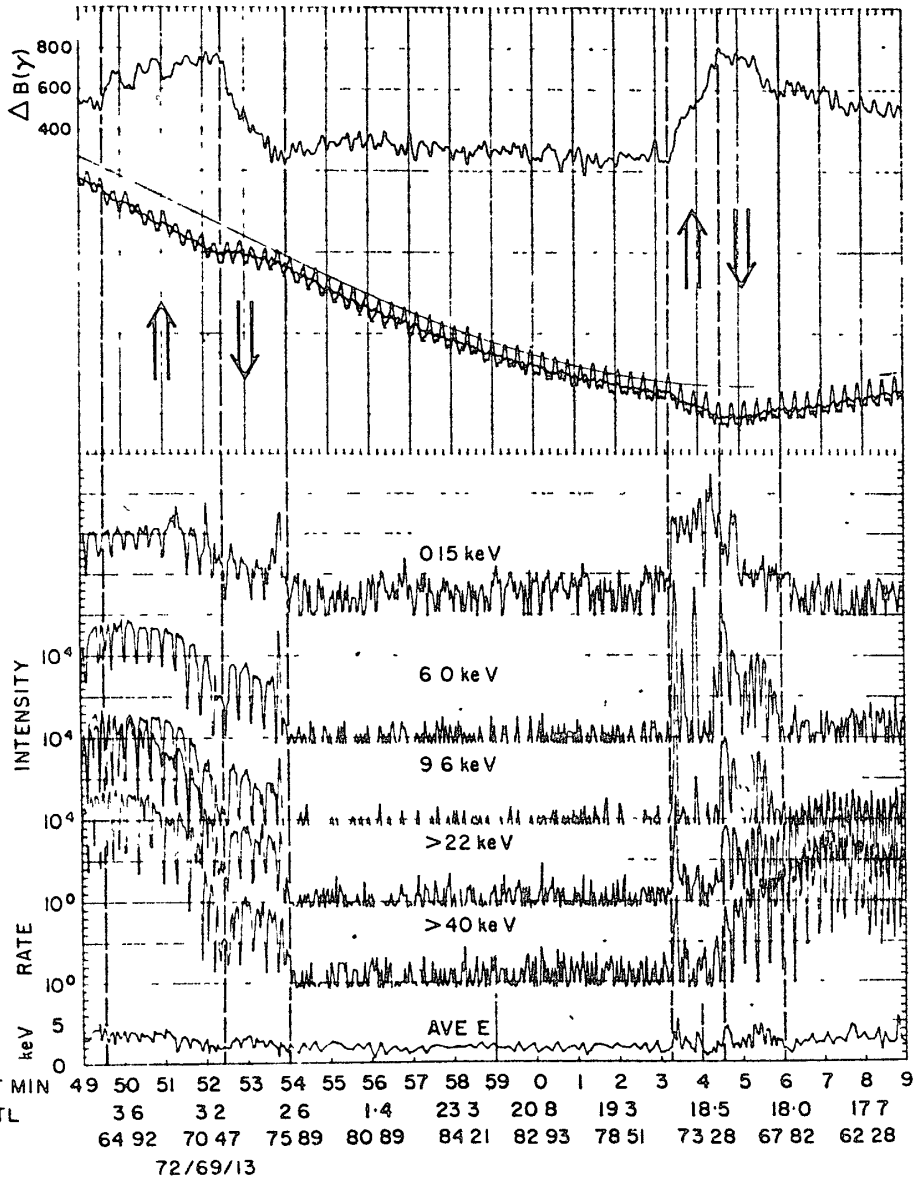

Fig 52. Example of a dawn-dusk pass in which field-aligned current directions are shown by arrows. Electron fluxes at five different energies are also shown. The average electron energy in keV is shown at the bottom on a linear scale (after MCDIARMID et al , 1977)

on board includes an electrostatic analyzer measuring particle fluxes in the energy range from 0.15 keV to 10 keV in 8 channels and a Geiger counter with an electron energy threshold of 22 keV (VENKATARANGAN *et al.*, 1975). All of these detectors have narrowly collimated field of view and look in a direction perpendicular to the spin axis whose direction can be changed. The satellite instrumentation also includes an orthogonally mounted system of flux-gate magnetometers, two of which have their axes aligned in the direction of the spin axis.

KLUMPAR *et al.* (1976) presented sample data of simultaneous magnetic field signatures of field-aligned currents and comprehensive charged particle measurement, and found that in the post-midnight sector, the equatorward region of upward field-aligned current flow is coincident with the region of nearly isotropic precipitation of kilovolt electrons. They also noted that the poleward region of downward-directed current flow is often associated with fluxes of low energy electrons, some having pitch angles near 180° with sufficient upward flux to account for the current density obtained from the simultaneously observed magnetic field perturbation.

About 300 satellite passes in local time intervals of 6 hours centered on the dawn and dusk meridions were examined by MCDIARMID *et al.* (1977). Fig. 52 shows a dawn-dusk pass in which magnetic field perturbations corresponding to the typical field-aligned current pattern are observed. The field perturbation shown in the upper panel of the figure was obtained as the observed field minus a model field (IGRF 1965.0 model). As indicated by arrows, the field perturbation can be modeled by two oppositely-directed field-aligned current sheets in both the morning and the evening sectors. In this example the currents are not again balanced; instead, a net current flows into the ionosphere on the morning side and out of the ionosphere on the evening side, in agreement with the results of YASUHARA *et al.* (1975) and IIJIMA and POTEMRA (1976a). In comparing the field and particle measurements it is evident that the high-latitude upward current in the evening sector coincides with the high-latitude part of the plasma sheet, called the boundary plasma sheet (BPS) by WINNINGHAM *et al.* (1975). It is characterized by highly structured particle fluxes and is the region in which inverted V's and discrete auroras are observed.

MCDIARMID *et al.* (1978) have most recently shown similar examples, but in these cases, with a more reliable method of determining the base line for the magnetic field. Fig. 53a shows an example in which the parts of the ΔB plot at low latitudes on both sides of the pole are flat, indicating the agreement between the shapes of the measured and calculated fields in these regions. The arrows indicate the high and low latitude extent of the negative perturbation on both the

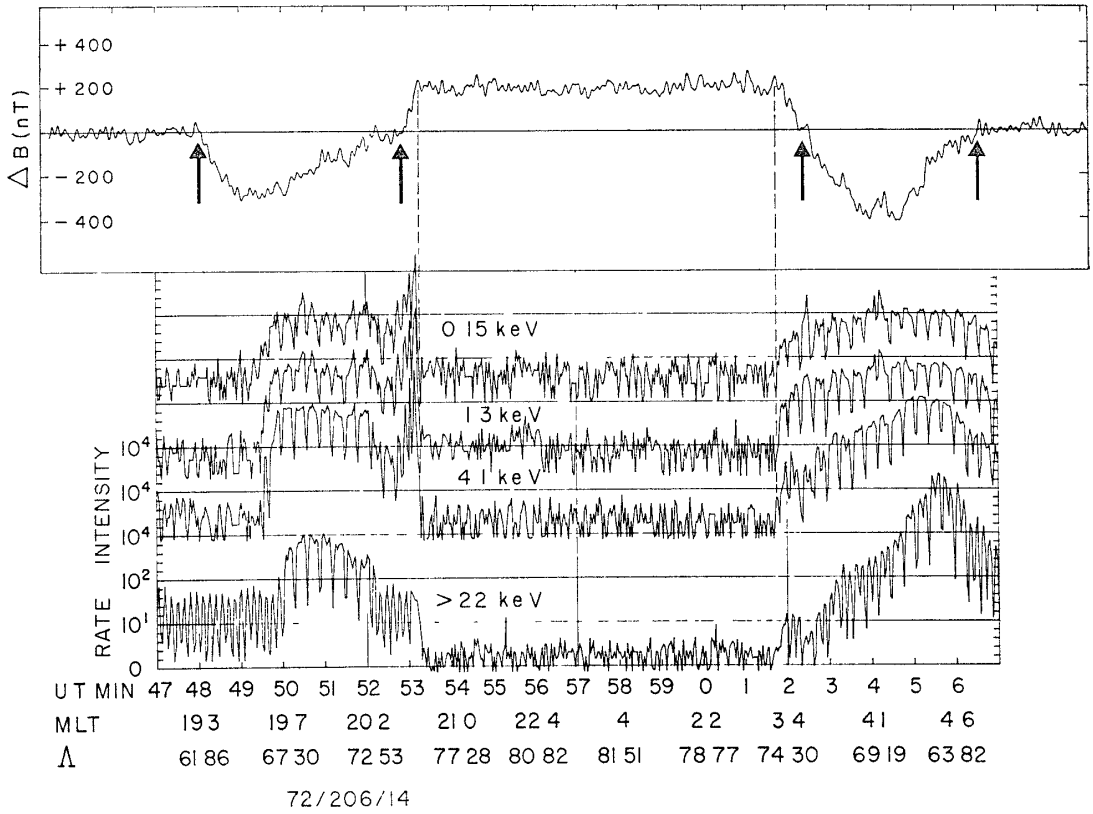

Fig. 53a. Example of a dusk-dawn pass showing one component of the magnetic field perturbation ΔB and electron intensity profiles for a number of different energies (after McDIARMID et al , 1978).

dawn and dusk sides of the pole as well as the low latitude edge of the positive perturbation. The dashed vertical lines indicate the high latitude edge of the plasma sheet determined from the latitude where the 1.3 keV electron channel reaches its background level It is seen that the plasma sheet extends poleward of the location where the magnetic perturbation changes its sign.

McDIARMID *et al* (1977) also found that in a few percent of the morning side passes, the current pattern is reversed; that is, the high-latitude current is upward, and the low-latitude part downward Fig 53b shows an example of these along with the corresponding charged particle measurements. It was noted that these perturbations are observed only at times when the interplanetary magnetic field has a strong northward component, and they are found at latitudes above those usually associated with field-aligned currents.

7.4. Projection of the field-aligned current region into the magnetosphere

It may be possible to discuss magnetospheric processes by projecting the region of the observed large-scale field-aligned current onto the equatorial plane

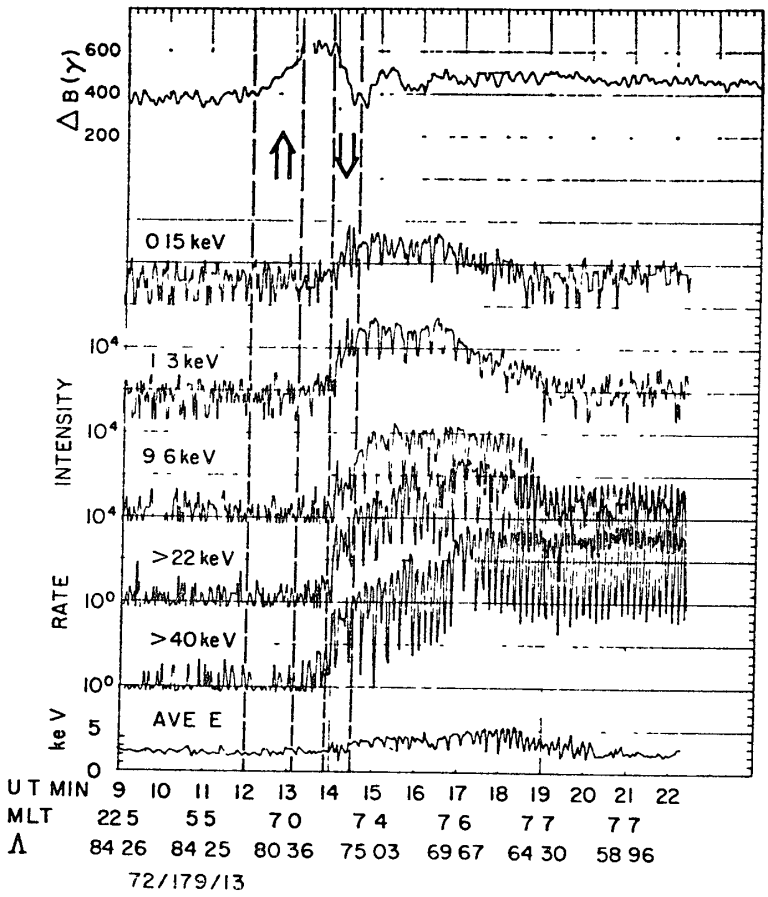

Fig. 53b. Example of a morning pass in which the current directions are reversed in comparison with those shown in Fig. 52 (after McDiarmid et al., 1977).

of the magnetosphere. Boström (1975) demonstrated that assuming only the pressure gradient being associated with the observed field-aligned currents, the direction of pressure gradients can be obtained in the equatorial plane of the magnetosphere. The required gradient in the magnetosphere for the observed field-aligned current distribution was obtained. Rostoker and Boström (1976) stressed the importance of the inertia of plasma motion capable of driving the large-scale field-aligned currents of 'balanced' upward and downward component.

Using the spatial distribution and flow direction pattern of the field-aligned currents determined by Iijima and Potemra (1976a), Potemra (1977) has attempted to map these current regions to the equatorial plane along field lines of magnetic field model of Mead and Fairfield (1975) and Fairfield and Mead (1975) for conditions corresponding to quiet and disturbed conditions. In Fig. 54, the regions of the large-scale field-aligned currents are indicated along with the boundary of the inner edge of the plasma sheet. It is noticed that the boundary between the flow direction of the field-aligned currents on the dusk side statistically

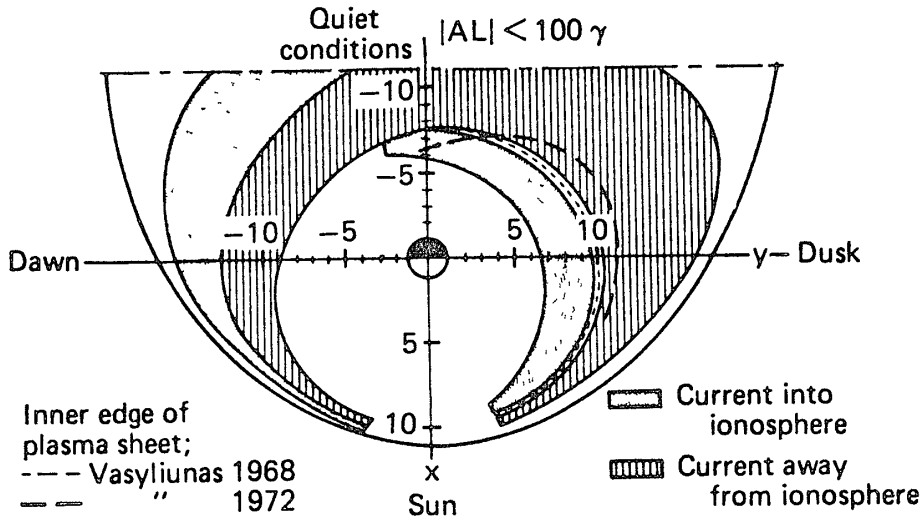

Fig. 54. The projection of the regions of large-scale field-aligned currents onto the equatorial plane (after POTEMRA, 1977)

coincides with the earthward edge of the plasma sheet. POTEMRA (1977) emphasized that on the dusk side the field-aligned currents flow away from the ionosphere maps to the region within the plasma sheet The flow of electrons from the plasma sheet to the auroral region can adquately account for the flow pattern of these currents. On the other hand, field-aligned current flow into the auroral ionosphere on the dusk side maps to a region to the earthward side of the plasma sheet boundary, where no electrons are available for transport to the auroral region. Thus it may well be that upgoing low-energy electrons from the ionosphere carry the downward field-aligned current in the equatorward half of the evening auroral belt.

SUGIURA (1975) suggested that the region 1 currents are associated with the distant boundaries of the plasma sheet, while the region 2 currents should close via the equatorial (ring) currents in the magnetosphere.

7.5. Field-aligned currents as divergence of ionospheric currents

As discussed by ANDERSON and VONDRAK (1975), there are three possible methods for current detection in the ionosphere and magnetosphere· (1) count charge carriers, (2) measure curl B, and (3) measure E and σ; where B is the magnetic induction, E is the electric field, and σ is the electric conductivity. Thus far, only techniques (1) and (2) have been described, while (3) has been used to examine horizontal (perpendicular to B) currents in the ionosphere (BREKKE *et al*, 1974). The Chatanika incoherent scatter radar is ideal for the purpose of deducing ionospheric current densities by means of (3). DE LA BEAUJARDIERE *et al.* (1977) have attempted a technique of the one-dimensional divergence to

estimate the field-aligned current density in the vicinity of an east-west aligned auroral arc which moved in the north-south direction, so that even one point measurement could see the spatial variation.

In the work of KAMIDE and HORWITZ (1978), an attempt has been made to describe a technique for deducing field-aligned current densities from ground-based measurements of the horizontal ionospheric currents at two or more latitudes using the Chatanika incoherent scatter radar. By computing a one-dimensional divergence of the current in a suitable coordinate system, an estimate of the field-aligned current density is obtained. In addition, a direct comparison was made between the Chatanika radar estimates and those from simultaneous TRIAD satellite passes over Chatanika. Fig. 55a shows the ionospheric current at three invariant latitudes, in which the following points of interest are noted: First, the horizontal current is generally northeastward in the evening sector, and southwestward in the morning sector. The eastward and westward auroral electrojets in evening and morning hours thus have respectively northward and southward components as well. Second, the transitions from the evening to morning features in the north-south and east-west components do not necessarily occur at the same time. In the region where the east-west component changes its sign (*e.g.*, at the Harang discontinuity), an intense northward current prevails at all three latitudes. This predominance is caused by the westward electric field and the Hall conductivity (see the data of HORWITZ *et al.*, 1978a). Third, the main features of the currents at the three latitudes are generally similar, but sizable latitudinal variations can be seen on several occasions. For example, at about 0635 UT, the eastward current component was about 2 A/m at $\Lambda=66.1°$, but was only 1 A/m over Chatanika, and 0.5 A/m at $\Lambda=64.2°$.

The currents in Fig. 55a were used by KAMIDE and HORWITZ (1978) to estimate the field-aligned current densities by assuming that current variations along the auroral oval are negligible. The alignment angle α with respect to the latitude circle was obtained by averaging α from the $Q=0$ through $Q=7$ ovals given by FELDSTEIN and STARKOV (1967). The average field-aligned current densities between $\Lambda=64.9°$ and 66.1° and between 64 2° and 64 9° are shown in Fig. 55b Also shown are the current densities computed under an alternative assumption, that $J_{\parallel}$ results entirely from a divergence of the Pedersen current ($=\mathrm{div}\,(\Sigma_P E)$). The general agreement between the two estimates points up the fact that the electric field usually points perpendicular to the auroral oval and that most of the $J_{\parallel}$ obtained in this way is due to divergence of the Pedersen current.

The salient features are: (1) The magnitudes of the field-aligned current

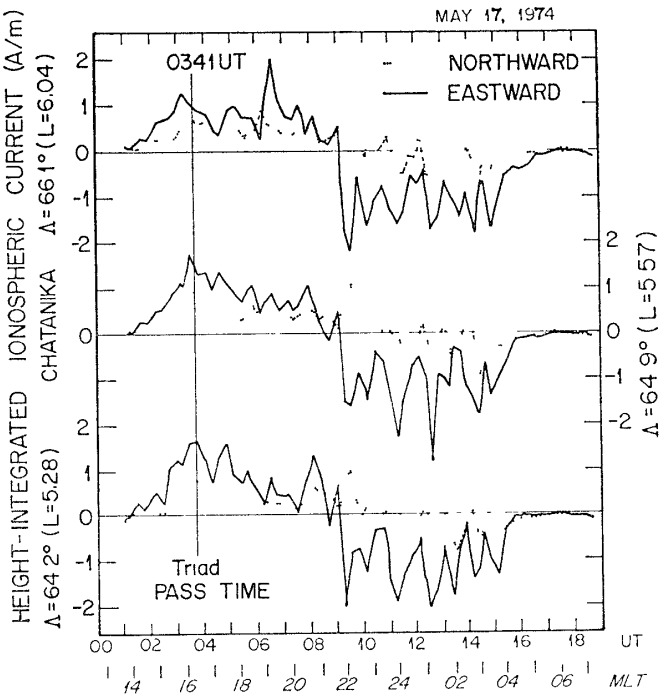

Fig. 55a *Northward and eastward components (in geomagnetic coordinates) of height-integrated ionospheric currents at three latitudes (after* KAMIDE *and* HORWITZ, *1978).*

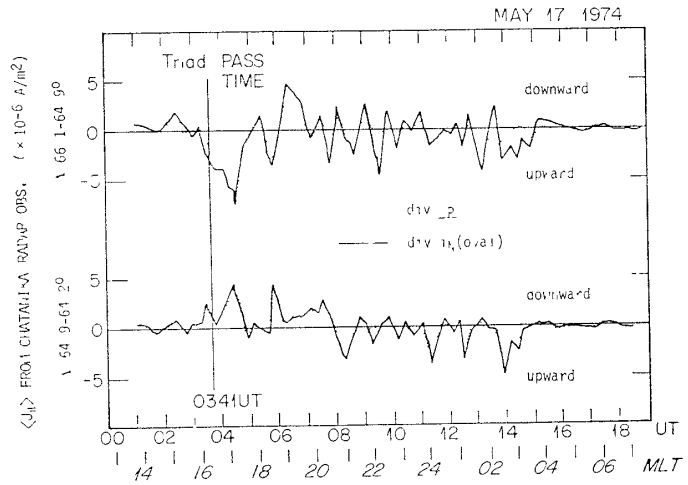

Fig. 55b *Field-aligned current densities estimated from the horizontal ionospheric currents shown in (Fig 55a) Solid lines represent the current densities which are the divergence of the horizontal current in the direction perpendicular to the statistical auroral oval, whereas dotted lines are obtained by the divergence of the Pedersen current alone (after* KAMIDE *and* HORWITZ, *1978).*

densities, $10^{-6}-10^{-5}$ A/m^2, are comparable to those observed with other techniques, such as rocket and satellite detectors. (2) The currents tend to be directed upward in the morning sector in a latitudinal range near Chatanika. Equatorward of Chatanika, the currents are directed generally downward in the evening sector. This sense corresponds to the equatorward half of the field-aligned current system constructed on the basis of TRIAD data (ZMUDA and ARMSTRONG, 1974b), which is expected to be present at these latitudes under moderately disturbed conditions (see Fig. 2 of IIJIMA and POTEMRA, 1976a). The currents were highly irregular in the midnight sector (0900–1300 UT) perhaps due to real fluctuations as well as to more complicated current structure invalidating the procedure used to complete the field-aligned currents. (3) Intensifications of the field-aligned currents appear to be associated with substorm activity as observed in high-latitude ground magnetic disturbances in the midnight sector (not shown here). (4) During periods of very large disturbances, the poleward half of the field-aligned sheet current system expands equatorward to the vicinity of the radar.

7.6. Field-aligned currents and auroras

It is one of the important problems of auroral physics how the field-aligned currents are related to different auroral features. This has a crucial importance for understanding some of the dominant physical processes occurring in the upper atmosphere in association with precipitating and upgoing particles, and relates closely to the questions of 'what are the main charge carriers responsible for the field-aligned currents?' and 'where do these particles originate?'

7.6.1. Large-scale field-aligned currents

ARMSTRONG *et al.* (1975) examined the spatial relationship between field-aligned currents and auroras for a few TRIAD satellite passes, and found that the poleward discrete arc marks the northernmost boundary of the field-aligned current region. It was also found that all the visible arcs lie within the latitudinal region occupied by the field-aligned current flows. KAMIDE and AKASOFU (1976a) examined a number of such simultaneous satellite and ground-based observations, with special reference to discrete and diffuse auroras. Fig. 56 shows, from left to right, the TRIAD magnetometer data in the standard format (ARMSTRONG and ZMUDA, 1973), the satellite trajectory at a 110 km level and the distribution of auroras over Alaska, and the all-sky camera photographs taken from the four Alaska meridian chain sites at 0631 UT on March 7, 1973. The direction of the three sensors, A, B, and Z, is indicated at the top of the middle diagram.

The satellite passed over Alaska around the maximum epoch of a weak

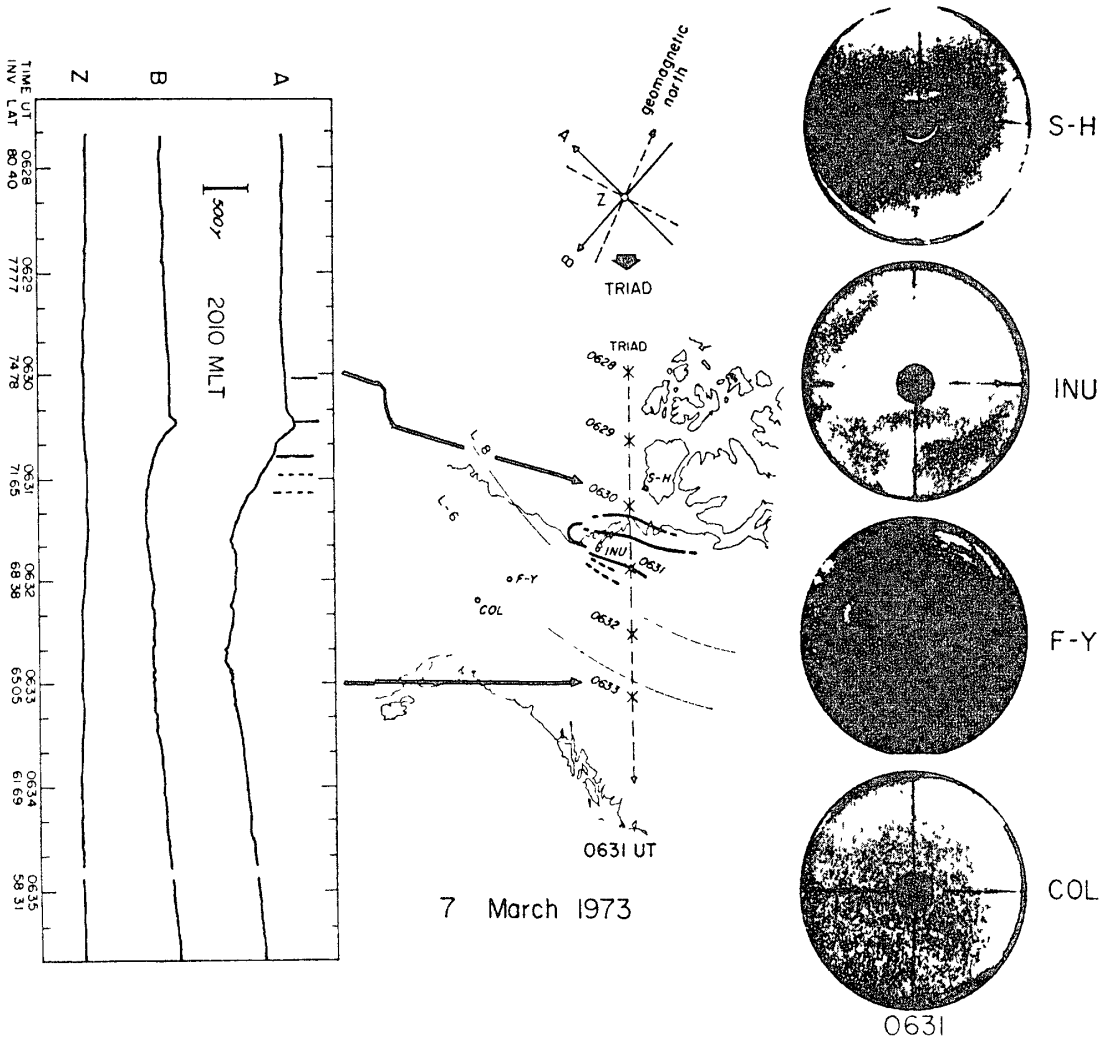

Fig 56. TRIAD magnetometer data in the A, B and Z coordinates, the satellite pass over Alaska together with the locations of auroral arcs, and the all-sky camera photographs taken from a chain of four Alaska meridian observatories Less bright arcs are shown by dashed lines (after KAMIDE and AKASOFU, 1976a)

substorm (AL=−282 nT). Note that the increase (or decrease) of the magnetic perturbation in the A sensor is produced by a downward (or upward) field-aligned current It is seen that the east-west magnetic deviation does not recover fully after crossing the auroral oval. This can be explained by the unequal intensities of the upward and downward field-aligned currents; the upward current was more intense than the downward current in this case.

It can be seen from the all-sky photographs that a weak surge was passing a little north of Inuvik at that time and that the satellite passed over it between 0630 and 0631 UT. Both Fort Yukon and College had a very clear sky at that

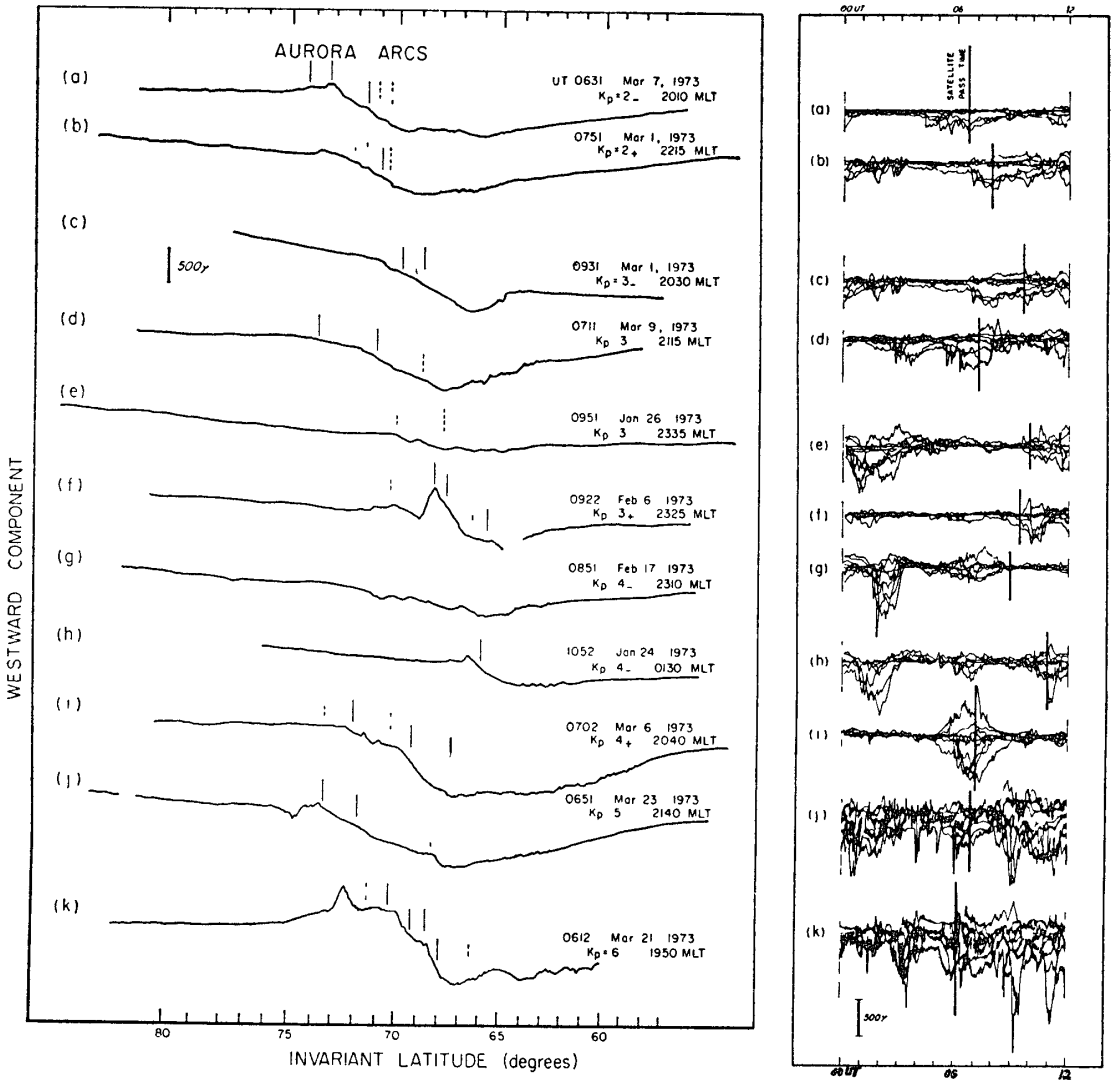

Fig 57. TRIAD magnetometer data in the A sensor (approximately in the geomagnetic east-west direction) as functions of the invariant latitude, along with the locations of the discrete arc crossing, and the superposed H component magnetic records from nine auroral zone observations (after KAMIDE and AKASOFU, 1976a).

time, but it was difficult to determine the distribution of the diffuse aurora. It was only at about 0645 UT that the diffuse aurora was clearly seen in the northern sky of Fort Yukon. In Fig 56 we show the location of the auroral arcs determined from the all-sky camera data, assuming the height of the auroras to be 110 km, together with the TRIAD trajectory. The three northern arcs were directly crossed by the satellite, but the two faint southern arcs did not appear to be crossed by the satellite; locations of the southern arcs were thus extrapolated along constant L curves to the satellite trajectory. Their locations are also indicated in the TRIAD record. It is noted that the poleward arc marks the northernmost boundary of

the field-aligned current region and that all other arcs are confined within the latitudinal region of the upward field-aligned current (Λ=73.1°−69 8°).

In Fig. 57 we combine the TRIAD magnetometer (A sensor) data together with the locations of the arc crossing. On the right-hand side the superposed H component magnetic records from nine auroral zone stations are shown to indicate magnetic activity during a few hours before and after the passage time, which is marked by a vertical line. Most of the data were taken during evening hours in MLT, but the corresponding magnetic conditions (expressed by the K_P index) are quite different. There is a significant latitudinal expansion of the field-aligned current region as magnetic activity increases

With this gross feature in mind the figure shows that (1) discrete arcs are, in general, confined within the region of the upward field-aligned current and (2) no discrete arcs are seen in the region of the downward field-aligned current except for one arc in the last example (0612 UT on March 21, 1973) which was very faint. Although the all-sky camera photographs available for some of the present data sets were not conclusive in identifying the diffuse aurora, it appears that the region of the donward field-aligned current corresponds to the region of the diffuse aurora. These conclusions are a little more specific than ARMSTRONG *et al.*'s (1975) conclusion in that they found that visible auroras are located within the latitudinal regime of the field-aligned currents.

However, it is difficult in those study using the all-sky camera data to associate individual arcs with the irregular features of the TRIAD magnetic perturbations, which presumably indicate concentrated upward and downward currents within the large-scale upward field-aligned current region

Most recently, KAMIDE and ROSTOKER (1977) have made an extensive study of the spatial relationship of the field-aligned currents to the distribution of nightside auroras on the basis of nearly simultaneous sets of the TRIAD magnetometer data and auroral imagery and information on precipitating electrons in the energy range between 200 eV and 20 keV obtained from the DMSP satellites. In Figs. 58 and 59, we show such comparisons for morning and evening sectors, respectively. The distribution of vectors of ground magnetic perturbations at the DMSP passage time is also given. It is noticed in Fig 58 that optical auroras appear to be confined to the region of the field-aligned currents as defined by the TRIAD data KAMIDE and ROSTOKER (1977) noted that the downward current flow in the morning sector occurs in a region of auroral luminosity generated by precipitating electrons, but the strength of the downward current and the auroral intensity are anticorrelated On the other hand, the region of the upward field-aligned current coincides well

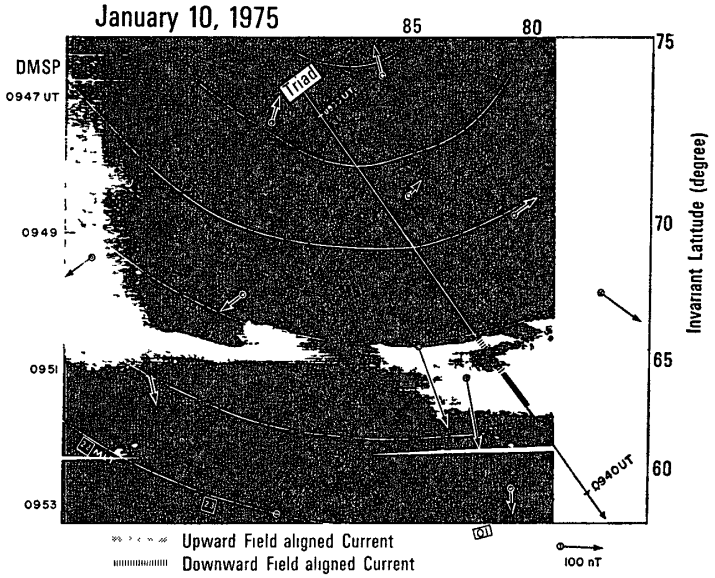

Fig. 58. DMSP auroral imagery data for a morning pass together with the magnetic perturbation vectors, measured at ground observatories. The trajectory of the TRIAD satellite is also indicated along with the field-aligned current direction (upward or downward) inferred from the TRIAD magnetometer record (after KAMIDE *and* ROSTOKER, *1977).*

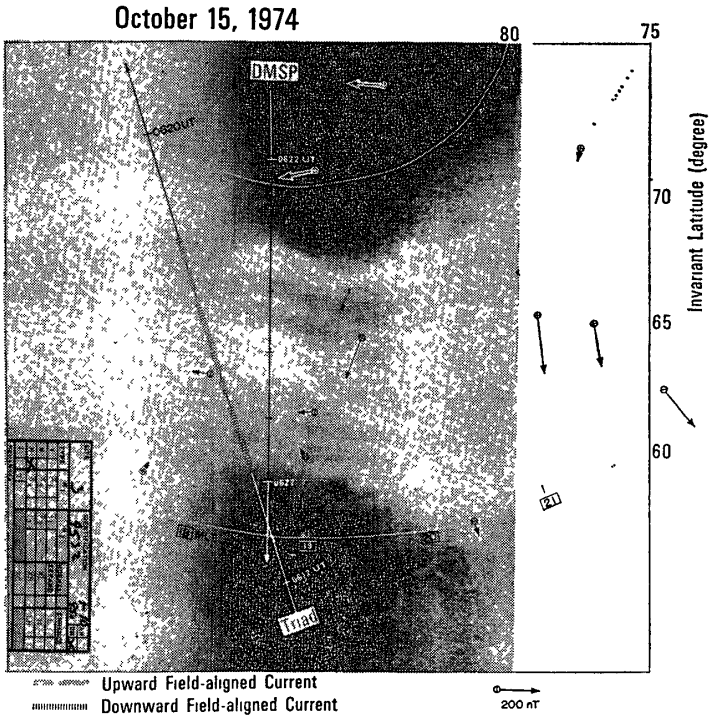

Fig. 59. DMSP auroral data for an evenings pass together in the magnetic perturbation vectors measured at ground observatories The trajectories of the DMSP (southbound) and TRIAD (northbound) satellites are also indicated along with the field-aligned current directions inferred from the TRIAD magnetometer records (after KAMIDE *and* ROSTOKER, *1977).*

with the region of the visible aurora in the equatorward half of the morning auroral belt.

An evening example of the DMSP imagery and the corresponding distribution of the field-aligned currents is shown in Fig. 59, in which both a bright westward traveling aurora near 2000 MLT with several arcs extending into early evening hours and a diffuse aurora are seen. Although the poleward boundary of the diffuse aurora merges into the discrete aurora in a complicated fashion, its equatorward boundary delineates an oval-shaped belt. A striking feature is that there are several high-latitude smaller-scale field-aligned current regions (of 100 km latitudinal extent or less) which may correspond to the discrete arcs visible in the DMSP data. These smaller-scale current features do not always seem to coincide with a discrete arc. This was interpreted by KAMIDE and ROSTOKER (1977) as being attributable to the north-south motion of the discrete arc (or the relatively short lifetime of any discrete arc) and the time separation between the DMSP and TRIAD passes. The weak downward field-aligned current with density of less than 1×10^{-6} A/m^2 is collocated with the diffuse aurora and the eastward electrojet.

Fig. 60 shows the differential electron fluxes for three selected energies along the DMSP trajectory. The northernmost arc corresponds to the sharp rise of the electron flux from the background level in the polar cap at all energy channels, for example, an increase by a factor of about 10 in the 0.2- and 8.0-keV channels. Such a good correlation cannot be found for other auroral arcs. In particular, there are no visible auroral arcs apparent for the enhancement in 0.2-keV electrons which peaked at about 72.4° and 71 0° corrected geomagnetic latitude (almost identical to the invariant latitude in this sector). It is found, however, that each auroral are coincides well with an increase in the energy flux more than 10^0 erg/cm^2·s·sr, indicated by the dashed line in Fig. 60.

The differential energy spectra for the discrete arcs (not shown here) are typical in that inside the arcs, a distinct spectral peak about 10^8–10^9 el/cm·s·sr·keV can be seen near 1–8 keV which is superposed on a softer spectrum (*cf*, MENG, 1976).

The diffuse aurora is also characterized by the electron precipitation It is seen that the equatorward boundary of the diffuse aurora can be determined by that of the 8-keV electron precipitation, in agreement with the result by MENG (1976). The energy flux of the precipitating electrons in the diffuse aurora is about 1 order of magnitude lower than that for the discrete aurora.

The latitudinal profile of the electron number flux is shown at the bottom. On the right-hand side of the figure the scale of the estimated current density is

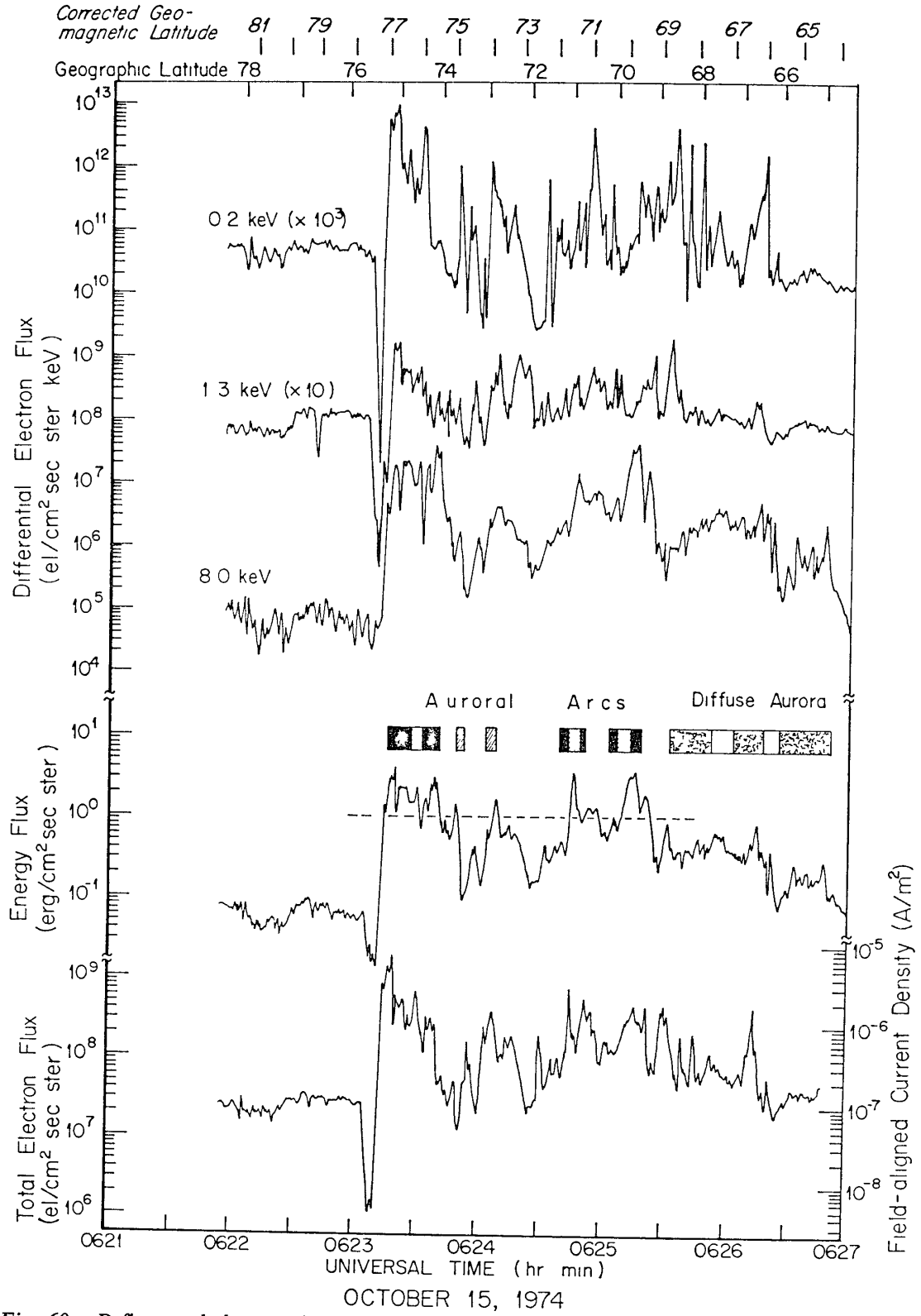

Fig. 60. Differential electron flux for three selected energy channels, the precipitating electron energy flux integrated from 0.2 to 20 keV, and the total electron number flux for the DMSP pass shown in Fig. 59. The auroral distribution along the DMSP subtrack is also indicated in negative (after KAMIDE *and* ROSTOKER, *1977).*

given. In comparing the field-aligned current densities inferred from the TRIAD magnetic perturbation it may be said that the upward field-aligned currents in the region of the discrete auroral arcs can be explained by the precipitating electrons.

Two other points seem worthwhile to be noted.

1) Before the satellite encountered the sudden increase in the electron precipitation corresponding to the northernmost arc, a sharp decrease in the electron flux, especially at low energies (0.2 and 1.3 keV), was observed An intense downward current was also detected by the TRIAD satellite in this region, and this current may be carried by upward flowing thermal electrons escaping from the ionosphere.

2) Although considerable upward field-aligned currents are carried by the precipitating electrons in the diffuse aurora region, a net downward field-aligned current is actually flowing in that latitudinal regime, indicating that upgoing ionospheric electrons may well be carrying the downward current (similar to the conclusions for the downward current flowing in the poleward portion of the morning sector auroral oval). It is interesting to note that recent sounding rockets and polar-orbiting satellites observed upward flowing fluxes of particles in the auroral latitudes (WHALEN *et al.*, 1978; GHIELMETTI *et al.*, 1978).

7.6 2 Small-scale field-aligned currents

We note that a great deal of work has been carried out over the last few years using rocket-borne particle and magnetic field detectors to estimate small-scale (<100 km) field-aligned currents in and near auroral forms (*e g*, CAHILL *et al.*, 1974; KINTNER *et al.*, 1974). Some of the studies have been already reviewed by ARNOLDY (1974) and ANDERSON and VONDRAK (1975), and so only the main results which relate closely to the gross field-aligned currents and auroras are noted in this paper. Measurements of field-aligned currents by sounding rockets have several advantages over the measurements by polar-orbiting satellites, in spite of the shorter range that rockets can traverse as compared with satellites Rocket observations can give the finest spatial detail concerning the particle precipitation and the magnetic field configuration in association with selected auroral forms.

ARNOLDY and CHOY (1973) discussed the role of low-energy electrons measured on rocket flights into breakup auroras. It was found that the net flux of these soft electrons was upward on the poleward side of the visible aurora, which coincides with the narrow sheet of downstreaming electrons. The authors suggested that the upgoing electrons are the main carriers of net downward field-aligned current that is the return of the upward current carried by more energetic

electrons to the south.

Field-aligned fluxes have also been measured by BRYANT *et al.* (1973), MAEHLUM and MOESTUE (1974), and BOSQUED *et al.* (1974), who reported a region of energetic and intense electron flux over auroral arcs.

Several sounding rockets over relatively stable auroral arcs were launched by the group at the Rice University, as summarized by ANDERSON and VONDRAK (1975) and ANDERSON and CLOUTIER (1975). These transmitted complete particle flux and simultaneous magnetic data. It was found that there are oppositely directed field-aligned current sheets associated with a bright auroral arc, in which the total number flux jumped abruptly and the energy of maximum flux rose to approximately 10 keV as the pitch angle distribution became more field-aligned at all energies (PAZICH and ANDERSON, 1975; SPIGER and ANDERSON, 1975; CASSERLY and CLOUTIER, 1975). Interpretation of the magnetic perturbations requires both vertical (field-aligned) and horizontal ionosphere currents. A total upward current coincided with the main arc and the region of intense electron precipitation, the measured electrons (0.5–20 keV) carrying a significant portion (15% to 50%) of the total upward current. The equal downward 'return' current was found to the south from the magnetic field data, although a net downward electron flux was measured in this region. Thus, the energy of the current carriers must be less than the lowest energy detectable by their instruments (0.5 keV).

SESIANO and CLOUTIER (1976) and CASSERLY (1977) found evidence for multiple pairs of anti-parallel current sheets associated with complicated discrete auroral systems. Sheet thickness ranged from 20 to 60 km.

Based on rocket measurements, models of the field-aligned currents near an auroral arc system have been put forward (VONDRAK, 1975; BURCH *et al.*, 1976; CARLSON and KELLEY, 1977). Fig. 61 shows two models constructed by VONDRAK (1975) and CARLSON and KELLEY (1977) in which the field-aligned currents are driven by the divergence of the horizontal currents arising from electric field gradients. These models differ from previous models by ATKINSON (1970) who considered the field-aligned currents to be driven by variations in the horizontal currents arising from conductivity gradients. The model of VONDRAK (1975) is able to explain the rocket observations in which vertical currents were found adjacent to an auroral arc in a region where no conductivity gradients were expected to be present.

7.6.3. Field-aligned currents and radar auroras

TSUNODA *et al.* (1976a) examined the spatial relationship of the evening radar aurora to the field-aligned currents by utilizing data collected with a 398-MHz

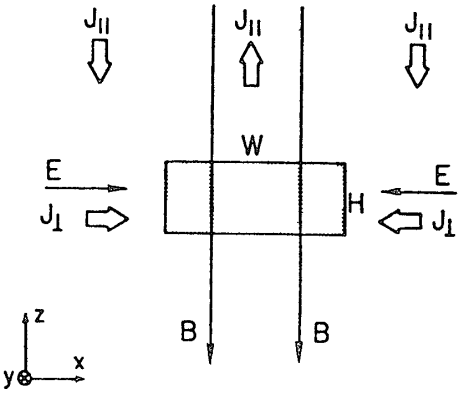

(a)

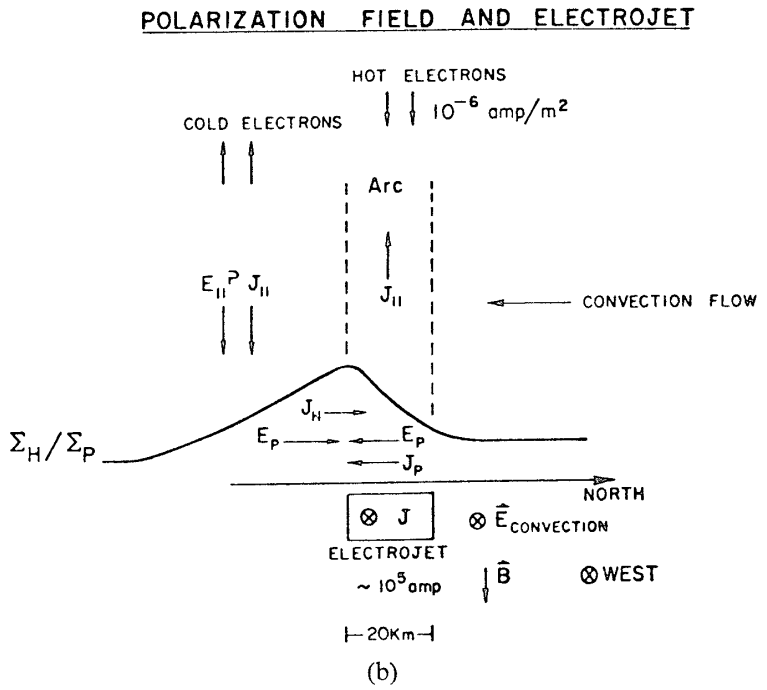

(b)

Fig. 61. (a) Model of an auroral arc system of north-south extent W and infinite east-west (y) extent proposed by VONDRAK *(1975), and (b) model of current and field in an auroral arc suggested by* CARLSON *and* KELLEY *(1977).*

radar located at Homer, Alaska, and with the TRIAD satellite. Fig. 62 represents an extensive analysis in which the distributions of the radar aurora and the visual aurora are shown together with the two transverse components of the magnetic perturbation at an 800 km altitude. It is clear that the poleward boundary of the radar diffuse band is coincident with the location of maximum perturbation of the TRIAD record, namely the boundary between the upward and downward field-aligned currents. It was noted that while the latitudinal extents of the radar echo and current regions are related, the downward current density is not necessarily proportional to the auroral echo strength; the TRIAD magnetometer data

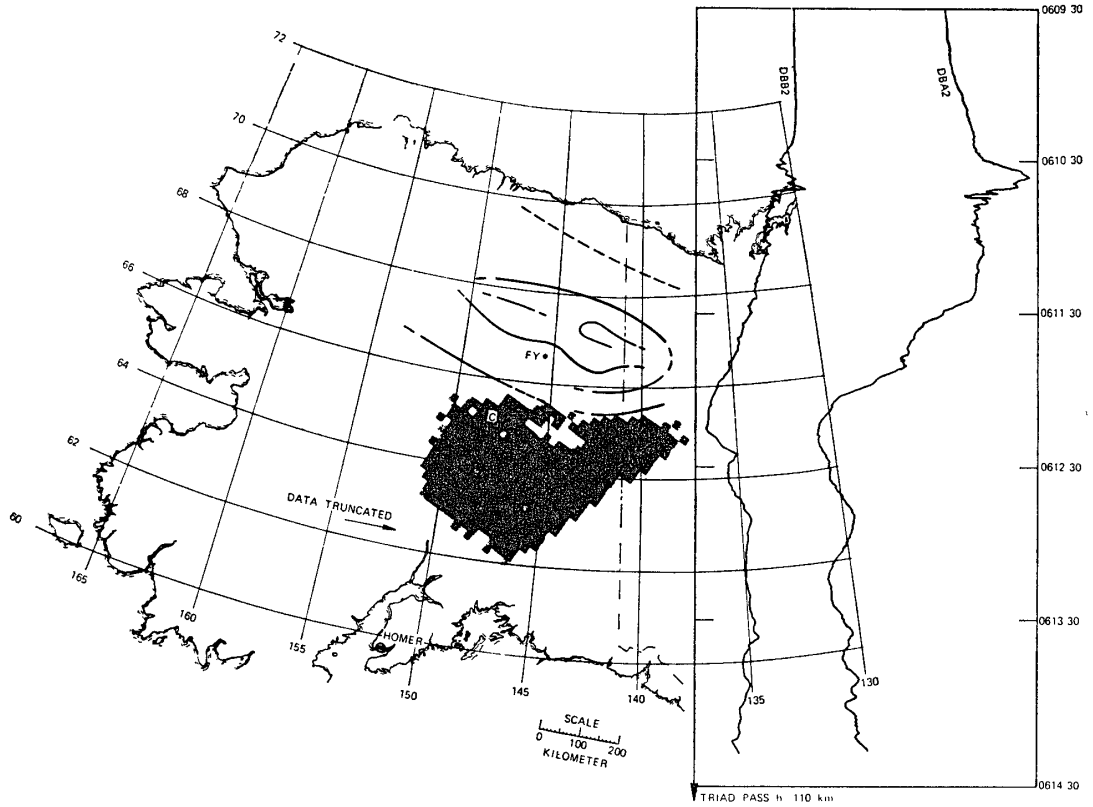

Fig. 62. Spatial relationships among the radar aurora, visual aurora, and field-aligned currents (after TSUNODA et al., 1976a).

contain oscillatory structure within the downward current region that does not appear to correspond to the auroral echo intensity. It was thus suggested by the authors that the downward field-aligned currents must be carried by precipitating protons and/or upward-moving low-energy electrons.

7.7. Field-aligned currents and the auroral electrojets

There had been no direct observation which indicates the link between the field-aligned currents and the auroral electrojets. Several 'equivalent' three-dimensional current systems had been inferred based primarily on magnetic observations made on the earth's surface, in which there is an inflow of current into the morning half of the auroral oval and an outflow from the evening half of the oval and these are connected through the westward electrojet. However, as described in the previous sections, recent satellite measurements indicated the existence of both upward and downward flows at all local times. Thus, the earlier current patterns must be revised considerably by taking into account the recent new findings of the configuration of the field-aligned currents which exhibits distortions during substorms, particularly in the region of the Harang discontinuity.

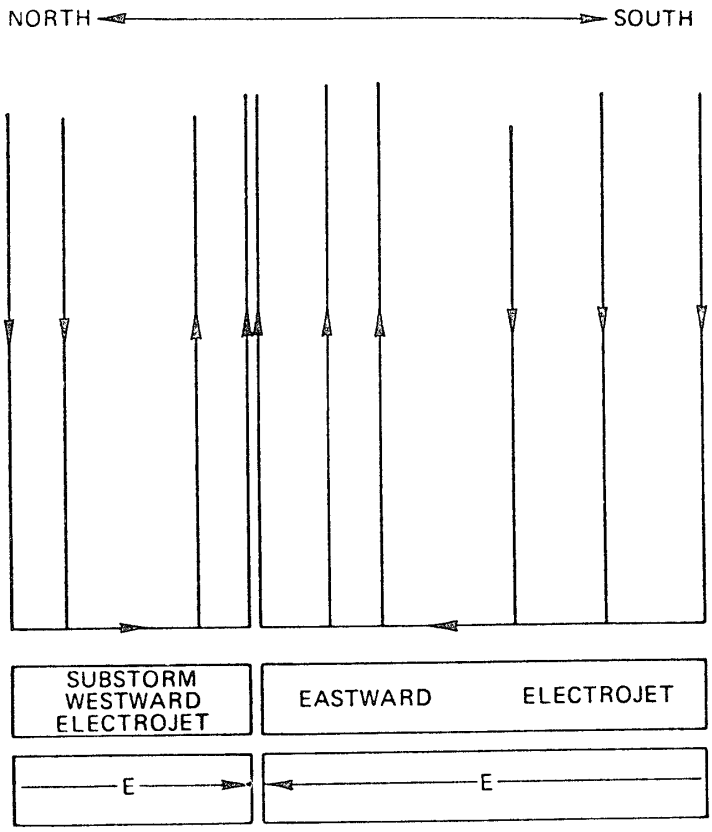

Fig 63. Schematic picture of the field-aligned current configuration in the substorm-disturbed evening sector inferred from the TRIAD data. The E field configuration is inferred from the direction of the auroral electrojet flow (after ROSTOKER et al., 1975).

ROSTOKER *et al.* (1975) examined the simultaneous magnetometer data from the TRIAD satellite and ground-based meridian chains of observatories. It was shown by the use of modeling techniques employed by KISABETH and ROSTOKER (1973) that a region of intense upward field-aligned current encompasses the boundary between the eastward and westward electrojets. They noted that there is a downward current flow both to the north and the south of the boundary between the two electrojets, *i e*, the Harang discontinuity Fig. 63 shows the schematic picture of the field-aligned current configuration in the substorm-disturbed evening sector, inferred by ROSTOKER *et al.* (1975). This configuration is interpreted in terms of the transition in electric field polarity at the boundary between the auroral belt and the polar cap, as reported by CAUFFMAN and CURNETT (1971) and BURCH *et al.* (1977)

IIJIMA and POTEMRA (1978) have shown that during periods when the westward electrojet has intruded deeply into the evening sector, the TRIAD magnetometer data exhibit complicated and fine-structured variations indicating the presence

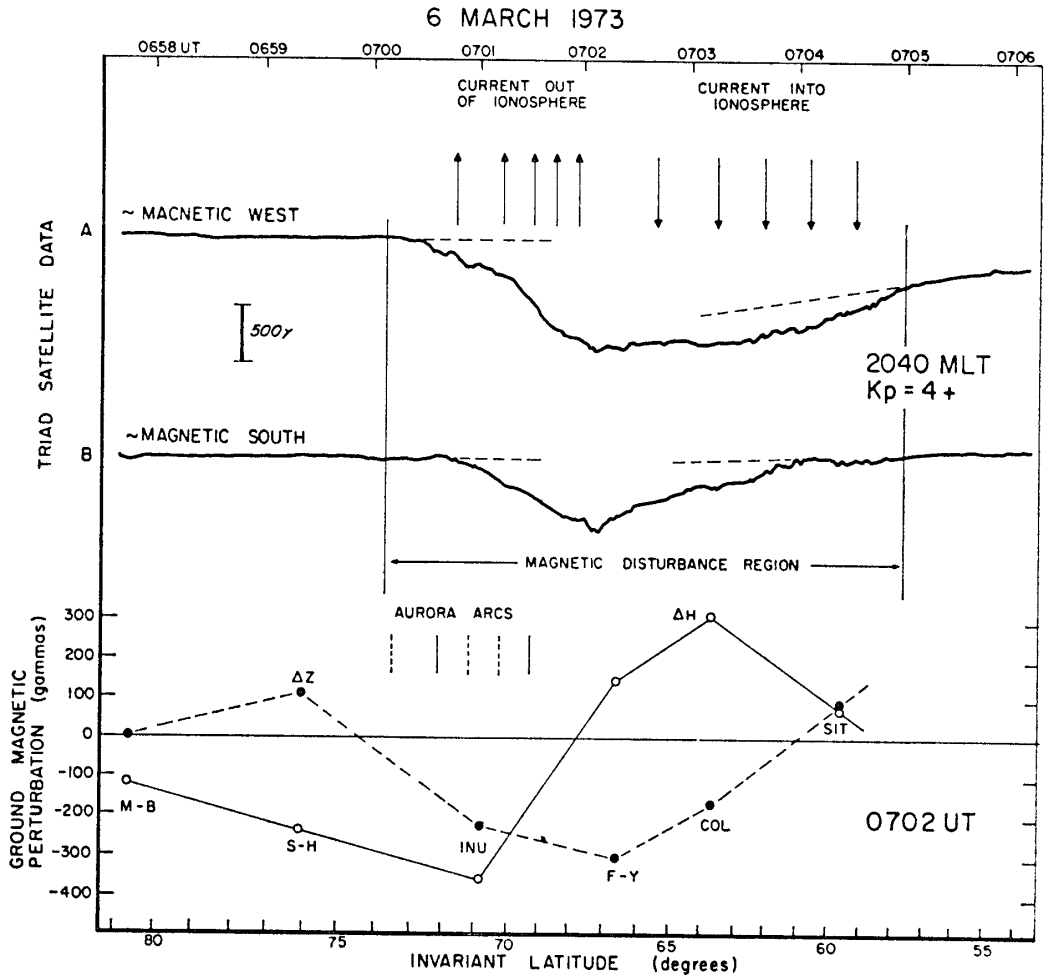

Fig. 64. Relationship between the field-aligned currents and the auroral electrojets. Note that the boundary of the upward and downward currents coincides approximately with the boundary of the region of positive and negative geomagnetic ΔH (after KAMIDE and AKASOFU, 1976b).

of complex field-aligned currents in the Harang discontinuity region. Nevertheless, the large-scale current configuration essentially consists of an upward field-aligned current surrounded on the north and south by downward currents, which is a simple superposition of morning-type and evening-type field-aligned current systems.

However, as pointed out by KAMIDE (1978), the loci defined by various methods (such as reversals of the electric field direction, currents, and ground magnetic perturbations) as the Harang discontinuity may not be coincident, in particular, when we note recent findings of the electric field which does not show an abrupt change in the north-south component but shows a gradual rotation in the finite region. KAMIDE and AKASOFU (1976b) have shown examples of the TRIAD magnetometer data and the simultaneous ground magnetic data from a meridian in which there can be seen no field-aligned current in the Harang discon-

tinuity, *i.e.*, the boundary between the eastward and westward electrojets. Fig. 64 shows the TRIAD data and the latitudinal profile of the ground H and Z perturbations, together with the locations of auroral arcs. Although ground-based observations of the magnetic vector distribution alone cannot provide uniquely the latitudinal position of the eastward and westward electrojets, we can infer the location of the center of each electrojet and the two-electrojet boundary with a reasonable accuracy ($<1°$ in latitude) by knowing the latitudinal profile of both the H and Z components (OLDENBURG, 1976, 1978). It is noticed in Fig 64 that the boundary between the upward and downward field-aligned currents coincides well with the boundary between the westward and eastward electrojets, which is inferred from the location of $\Delta H=0$ and ΔZ=minimum. It might be claimed that the electrojet pattern changes during the period when the TRIAD satellite traversed latitudinally over the electrojets. However, KAMIDE and AKASOFU (1976b) checked the latitude profile minute by minute and found that the electrojet boundary did not shift significantly In Fig 65, we show the equivalent overhead current vectors at four observatories along the meridian for the total of 35 TRIAD passes in the evening sector Also shown in the figure is the location of the boundary between the upward and downward field-aligned currents; on the poleward side of this boundary the upward current prevails, whereas the donward current prevails on the equatorward side It is seen that the westward and eastward currents are fairly well separated by the field-aligned current boundary, indicating that the Harang discontinuity, identified by the line separating the negative and positive H perturbations on the earth's surface, corresponds to a region in which no field-aligned current is present. This finding suggests a connection of the field-aligned currents with the auroral electrojets in the evening sector, which is quite different from what had been suggested in the earlier studies based on the ground magnetic observations alone. KAMIDE and FUKUSHIMA (1972), and CROOKER and MCPHERRON (1972) have put forward a model current system in which there is an upward field-aligned current at the eastern end of the eastward electrojet. The KAMIDE and AKASOFU's (1976b) current configuration includes rather the downward field-aligned current in the entire eastward electrojet region.

KAMIDE *et al.* (1976c) made a similar examination for the morning sector and found that during substorm periods, both the downward and the upward field-aligned currents generally occur inside the westward electrojet region It was suggested, however, that the observed inequality of the intensities of the upward and downward currents implies that their closure in the ionosphere cannot be completed in the same meridian in the morning sector and must have a large

westward component, that is the westward electrojet. In other words, the 'westward electrojet' in the morning sector should actually flow in the 'southwestward' direction.

7.8. Field-aligned currents in the cusp and polar cap

The large-scale characteristics of field-aligned currents in the dayside high-latitude region determined from magnetometer data from 200 passes of TRIAD was presented by IIJIMA and POTEMRA (1976b). It was found that these high-

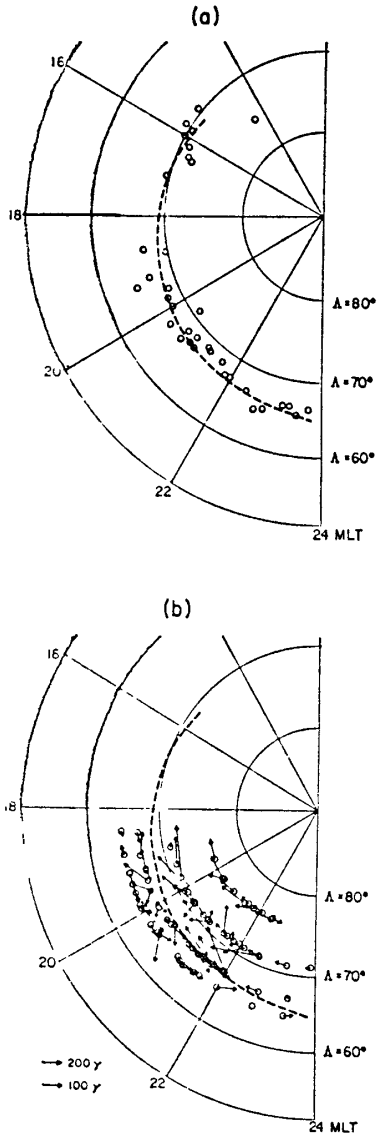

Fig. 65. (a) Observed boundary between the upward and downward field-aligned currents in the evening sector for 35 TRIAD satellite passes and (b) distribution of the equivalent ionospheric current vectors in the horizontal plane with reference to the location of the boundary of the upward and downward field-aligned currents (after KAMIDE and AKASOFU, 1976b)

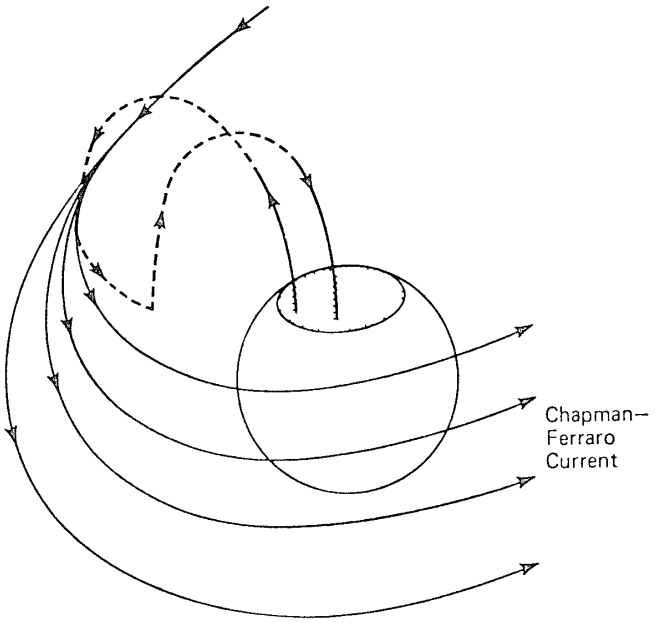

Fig 66. Schematic diagram illustrating the flow directions of the cusp region field-aligned currents (after IIJIMA and POTEMRA, 1976b).

latitude field-aligned currents are most often observed in the dayside sector between 0930 and 1430 MLT and are distributed between 78° and 80° invariant latitudes. They generally flow away from the forenoon ionosphere and into the afternoon ionosphere, being opposite to the permanent region 1 currents. Fig. 49 shows a summary of the distribution and flow directions of field-aligned currents (IIJIMA and POTEMRA, 1976b). It was also found that the intensity of these field-aligned currents increases as the interplanetary magnetic field increases in the southward direction, indicating that they may play an important role in the coupling between the interplanetary medium and the magnetosphere.

IIJIMA and POTEMRA (1976b) presented a diagram (shown in Fig. 66) illustrating the flow directions of the cusp field-aligned currents and their possible relation to the Chapman-Ferraro magnetospheric surface current. Note that the directions of the cusp field-aligned currents shown in this diagram are opposite to those hypothesized by RUSSELL *et al* (1974) to explain the 'erosion' of the magnetopause observed by their OGO 5 magnetometer.

Observations of the field-aligned currents near local magnetic noon have most recently been compared to the simultaneous ground magnetic observations which were made at the IMS meridian chain of observatories along the west coast of Greenland (WILHELM *et al*, 1978). They have reached a somewhat different conclusion as to the directions of the cusp field-aligned currents which are controlled by the azimuthal component B_y of the interplanetary magnetic field. Fig. 67 shows

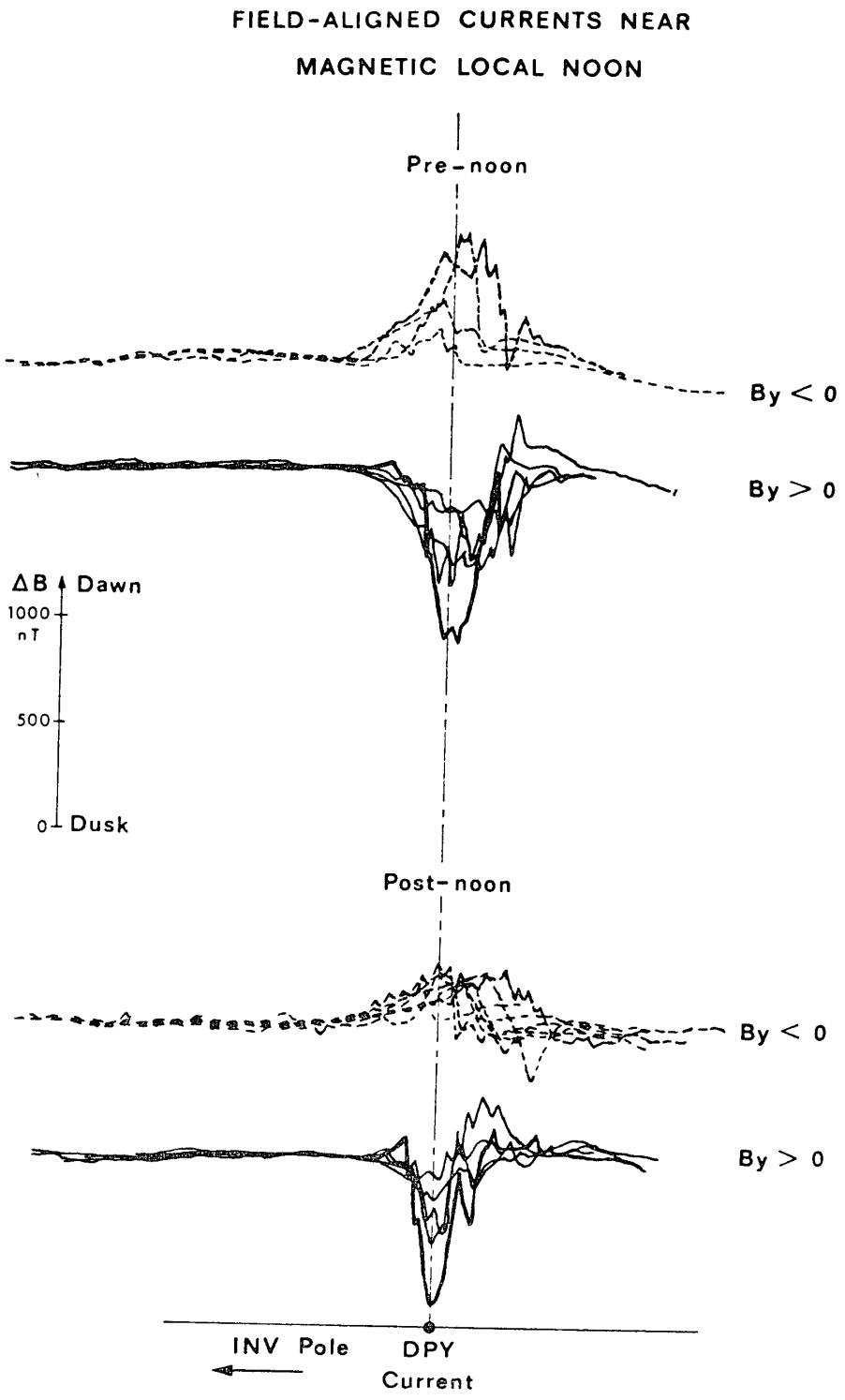

Fig. 67. TRIAD B-sensor (approximately in the geomagnetic east-west direction) obtained over Greenland near local noon. The latitude of the simultaneous DPY current (FRIIS-CHRISTENSEN and WILHJELM, 1975) was common for all passes (after WILHJELM et al., 1978).

TRIAD magnetometer data in the approximately east-west component which are grouped into four categories in terms of the B_y values (positive or negative) and local time sectors (forenoon or afternoon). It is seen that for $B_y>0$ the directions of the cusp field-aligned currents are downward in the forenoon sector and upward in the afternoon sector, whereas the directions are reversed when $B_y<0$, indicating that the current configuration presented by IIJIMA and POTEMRA (1976b) expresses only the cases corresponding to the negative B_y. This point needs further clarification

WILHJELM *et al* (1978) have also shown that the directions of the ionospheric currents inferred from the meridian magnetic observations depend upon the directions of the two field-aligned currents controlled by the interplanetary B_y values, in the sense consistent with the assumption that the ionospheric currents are the Hall currents associated with the field-aligned currents.

Structured field-aligned currents were detected in the dayside cusp region by FREDRICKS *et al.* (1973) and LEDLEY and FARTHING (1974). LEDLEY and FARTHING (1974) made vector magnetic field measurements by a sounding rocket flight and found structured field-aligned currents having a characteristic horizontal scale size of about 1 km.

Field-aligned currents in the polar cap have been examined in detail by SAFLEKOS *et al.* (1978), who referred to the magnetometer experiment on board the TRIAD satellite. In contrast to the magnetic variations associated with the large-scale field-aligned currents within the auroral oval, the magnetometer data in the polar cap indicate variations smaller in amplitude and over smaller latitude ranges It was found that such small-scale magnetic disturbances occur most frequently in the morning sector between 0300 and 0900 MLT, during a wide range of geomagnetic activity as seen in the K_p index. SAFLEKOS *et al.* (1978) also noted the occurrence frequency of the polar cap field-aligned currents, being correlated with the azimuthal direction of the interplanetary magnetic field; they are observed in the northern polar cap twice as often during periods when the IMF is directed away from the sun than when directed toward the sun.

MCDIARMID *et al.* (1978) have utilized the ISIS 2 magnetometer data in the dawn-dusk sectors of the polar cap. It was shown by them that the magnitude of the magnetic perturbations in the polar cap is correlated with both the Z and Y components of the interplanetary magnetic field. The perturbations are larger on the morning than the afternoon side when B_y is positive, and vice versa when B_y is negative. Fig. 68 shows such relationships, in which an asymmetry parameter is defined as the ratio of the difference to the sum of the dawn and dusk polar

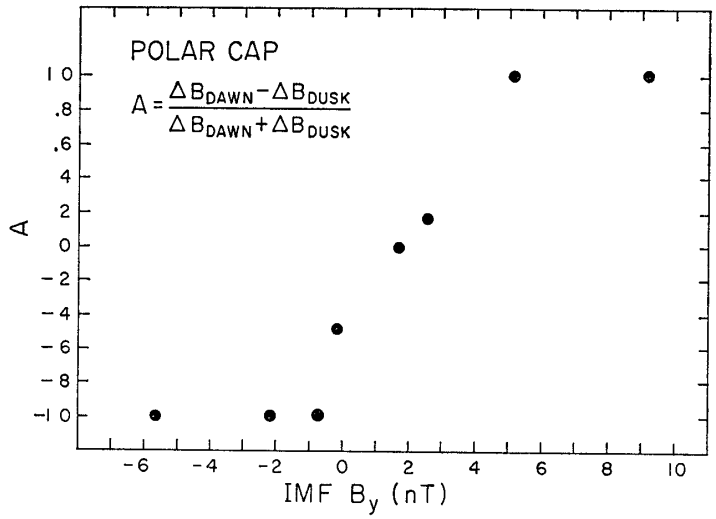

Fig. 68. Dawn-dusk asymmetry in the polar cap magnetic field perturbation plotted against the y component of the IMF (after McDiarmid et al., 1978).

cap perturbations; this is reproduced from their Fig. 5. The dawn and dusk perturbations are measured just poleward of the plasma sheet boundary determined from the simultaneous particle measurements. In spite of the poor statistics (namely, only eight passes are available for this comparison), it is clearly indicated that positive values of IMF B_y correspond to enhanced perturbations on the morning side of the polar cap, while negative B_y values correspond to enhanced perturbations on the evening side. Such a dependence is presumably related to the similar dependence of polar cap electric fields observed by Heppner (1972b) and Mozer *et al.* (1974), to the B_y dependence of low-energy electron precipitations observed by Meng *et al.* (1977), and to the magnetic variations in the polar cap dependent on the B_y sign shown by Friis-Christensen and Wilhjelm (1975).

8. Ground Magnetic Observations

Magnetic perturbations observed on the earth's surface arise mainly from the ionospheric and field-aligned currents (Kisabeth and Rostoker, 1977), as well as the induced current flowing within the earth. Although it is in principle impossible to separate the effects of these different current sources only from magnetic measurements made on the ground, it is important to clarify the global and local patterns of the ground magnetic perturbations when they are compared with other direct observations of the electric fields, and currents in the ionosphere and the magnetosphere (Fukushima and Kamide, 1973). In this section, we sum

up, for several relevant topics, recent progress in studies which are primarily based on ground magnetic data.

8.1. Potential contours for ground magnetic perturvations: Equivalent ionospheric current representation

Isointensity contour lines of magnetic potential for the ground magnetic perturbations can be regarded as streamlines of the equivalent ionospheric currents. The potential distribution for the ground magnetic perturbations observed at a worldwide set of observatories can theoretically be obtained by several methods. However, all these methods require a considerable amount of numerical calculations, so that it has been obtained mostly for the mean S_q field, whose pattern is less complicated than that of the substorm field (SUZUKI, 1978). In spite of the unrealistic assumption that the currents, including the auroral electrojets, lie in a plane sheet of uniform intensity with infinite width and length, the method of the equivalent overhead current approximation has conventionally and most widely been used in producing 'hand-drawn' contour maps of the ionospheric current lines (isopotential contours for the magnetic perturbation) and has been fairly successful in obtaining a gross pattern of the substorm current system (NAGATA and FUKUSHIMA, 1971). Note that it is sometimes extremely difficult to produce two-dimensional divergence-free streamlines, especially in high latitudes, owing to an inadequate distribution of the ground observatories.

Following BOSTRÖM (1971) who designed a comprehensive computer program for obtaining isopotential contours during polar magnetic substorms on the basis of magnetic data from 36 high-latitude observatories, KAMIDE *et al.* (1976d) have developed a new method of computer mapping of the potential contours giving us the opportunity to produce the equivalent ionospheric current system in any desired length of period with a fine time resolution. They have ascribed the process in obtaining the world potential to solving the two-dimensional Poisson equation in which the two-dimensional divergence of the ground magnetic perturbation is represented as the 'forcing' term. The obtained plot represents the extent of geomagnetic activity better than do geomagnetic activity indices. From the plot we can recognize both the global pattern and the intensity of the world magnetic perturbations. Since the computer method can plot the isopotential contour lines under a consistent assumption without any subjective prejudices, we can discuss several modes of the equivalent ionospheric current systems which have already been proposed by means of hand-drawn current patterns, and examine how the pattern changes progressively before, during, and after polar substorms. KAMIDE *et al.* (1976e)

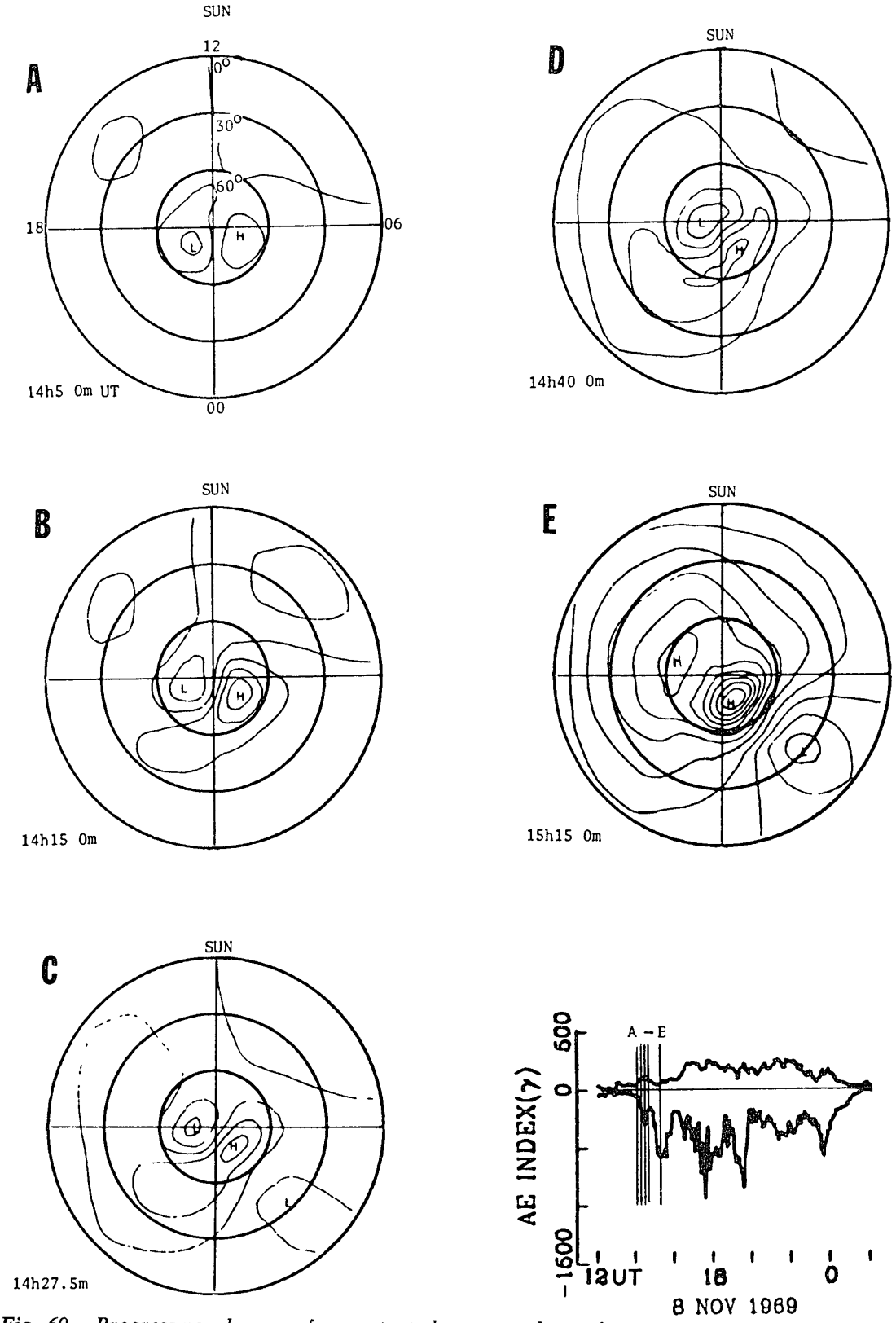

Fig. 69. Progressive change of isopotential contour lines during the period of succesive substorm activity. The AE index variation is also given with vertical lines indicating the corresponding epochs, A-E (after KAMIDE et al., 1976).

have made a movie film, each frame of which expresses the isopotential contours obtained from all the available magnetic records. Fig. 69 shows several frames of the movie for November 8, 1969, together with *AE* index variations. Although we must be careful in interpreting low-latitude and polar cap current lines as an indication of ionospheric currents (KAMIDE and MATSUSHITA, 1978b), most of the eastward and the westward auroral electrojets can be regarded as the real ionospheric currents (BREKKE *et al.*, 1974; KAMIDE and BREKKE, 1975). Thus, the equipotential contour maps are of great use in studying spatial and time changes of the auroral electrojets.

8.2. Distribution of world magnetic disturbances

Once we understand the origins of the ground magnetic perturbations in terms of various source currents, the ground observations have a great advantage in comparing with satellite observations since the magnetic field can be monitored at a large number of fixed points on a continuous basis.

From the observed magnetic perturbations at various auroral zone observatories, the *AE* indices can be derived, providing better measures of the effects of the auroral electrojets than any other geomagnetic activity indices. It is for this reason that the National Geophysical and Solar-Terrestrial Data Center of National Oceanic and Atmospheric Administration is undertaking a program of the compilation of the *AE* indices to provide the scientific community with a record of the electrojet activity (*e g.*, ALLEN, 1972). Using the published values, some statistical characteristics have been discussed.

ALLEN and KROEHL (1975) noted systematic patterns in the times of most frequent observation of extreme *H* component deviations by each observatory. Figs. 70a and b show the frequency distribution of, respectively, hourly *AL* and *AU* contribution by each observatory over universal time; UT times of geomagnetic midnight are also indicated It is seen that on the average, *AL* is most often derived from records of observatories located about 3 1/4 hours past local geomagnetic midnight and *AU* is most often derived from observatories located 6 1/2 hours before midnight. ALLEN and KROEHL (1975) also found secondary peaks near 1100 MLT which cannot be attributable to the ionospheric current patterns associated with substorms. In view of the fact that the substorm activity is most intense in the midnight sector, as seen in such dramatic auroral displays as the westward traveling surge and torch aurora, the above finding of the average *AL* peak located near 0300 MLT needs further clarification of whether or not it does really mean that the 'substorm' westward electrojet is most intense in the morning sector, not

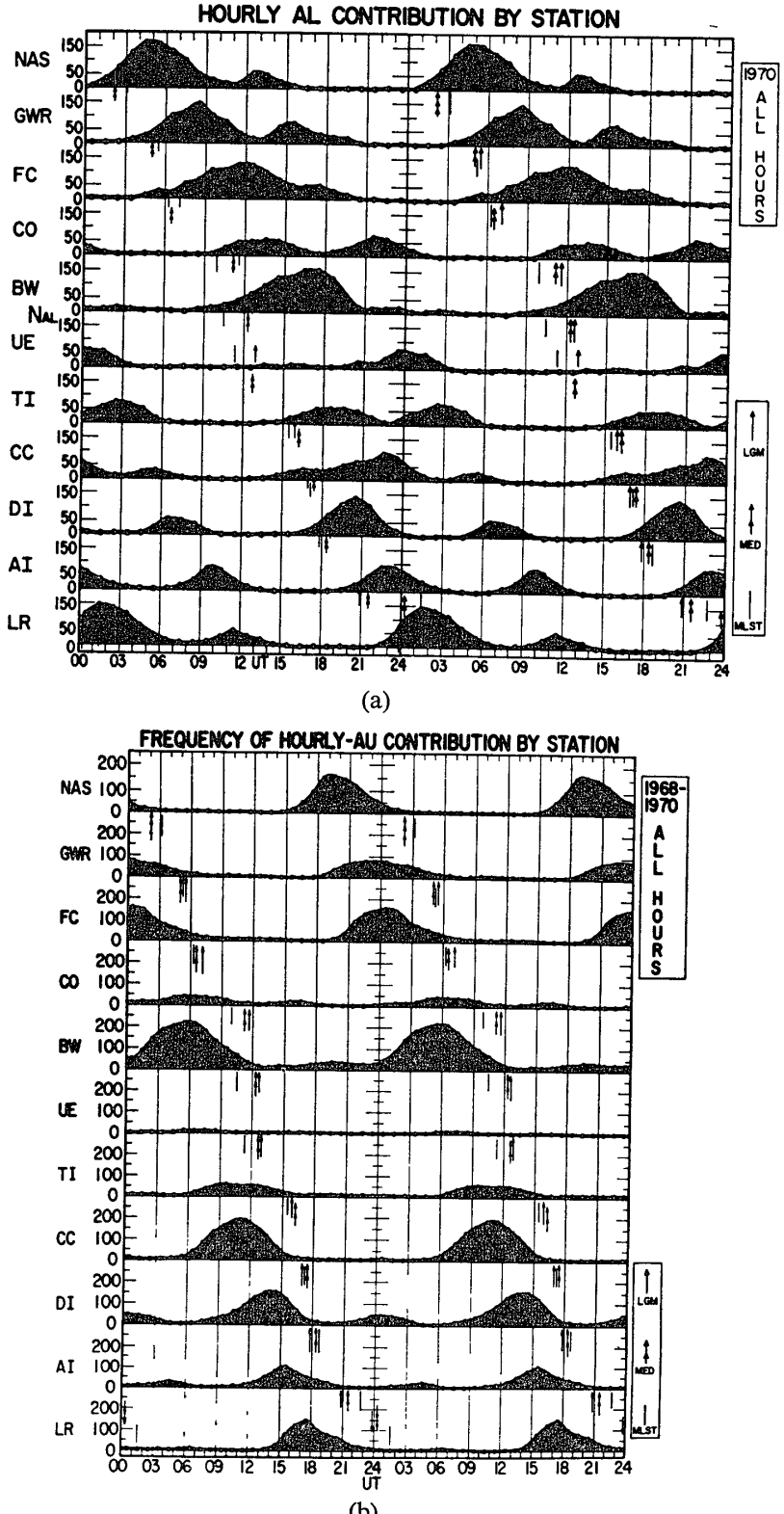

Fig. 70. (*a*) *Frequency of hourly AL contribution by each observatory. UT times of midnight local standard time (MLST), local geomagnetic midnight (LGM) and midnight eccentric dipole (MED) are marked for each observatory.* (*b*) *Same, but for AU (after* ALLEN *and* KROEHL, *1975*).

near midnight.

PERREAULT (1974), KAMIDE (1974), KANE (1974), SU and KONRADI (1974) and PERREAULT and AKASOFU (1978) have used the *AE* values and mid-latitude disturbances to correlate with several parameters of the interplanetary magnetic field (IMF). KOKUBUN (1972) and PATEL and DESAI (1973) reached a conclusion that the main phase of large magnetic storms is initiated by the southward turning of the IMF. CAAN *et al.* (1977) have shown that the amplitude of auroral-zone negative excursions is given as a function of the southward interplanetary magnetic field flux preceding the onsets of individual substorms. MENG *et al.* (1973) showed that although the highest correlation between the southward IMF and the *AE* index is obtained if the IMF leads *AE* by on average 30–60 min, this time lag is divergent considerably from one to another event. MURAYAMA and HAKAMADA (1975) made an extensive effort to find possible effects of solar wind parameters (the azimuthal component as well as the north-south component of the IMF, and solar wind velocity) on the enhancement of the *AE* indices. RUSSELL *et al.* (1974) found that the southward IMF had to exceed an apparent threshold level in order to trigger a storm main phase. BURTON *et al.* (1975a, b) showed that it is possible to predict storm activity solely from a knowledge of the velocity and density of the solar wind and the southward component of the IMF. Most recently, IYEMORI *et al.* (1978) have applied the Wiener's 'prediction' theory to reproduce reasonably well geomagnetic activity indices *AE* and D_{st}, indicating that the magnetosphere can be regarded as a 'linear' system against the solar wind as an input Polar cap magnetic disturbances in association with the IMF signatures have been reviewed by FELDSTEIN (1976) and MISHIN (1977). ROSTOKER *et al.* (1974) showed that the distribution of the equivalent current vectors during extremely quiet times consists essentially of the S_q^p type pattern.

IIJIMA (1973) indicated that on a disturbed day when the global geomagnetic activity is high but fairly steady, the substorm current system appears as an intensification of the DP 2 current system. This feature can be seen in Fig. 71 where the current distribution resembled the twin-vortex S_q^p current. TROSHICHEV *et al.* (1974) found that two basic current systems of substorm type and DP 2 type appear alternatively on a disturbed day. GIZLER *et al.* (1976) suggested using polar cap magnetic variations that DP 2 disturbances are associated with pure ionospheric currents, while substorm current system stems from a three-dimensional current loop.

Polar cap magnetic variations undergo a considerable modulation of the interplanetary magnetic field even when no substorm is in progress; see review articles

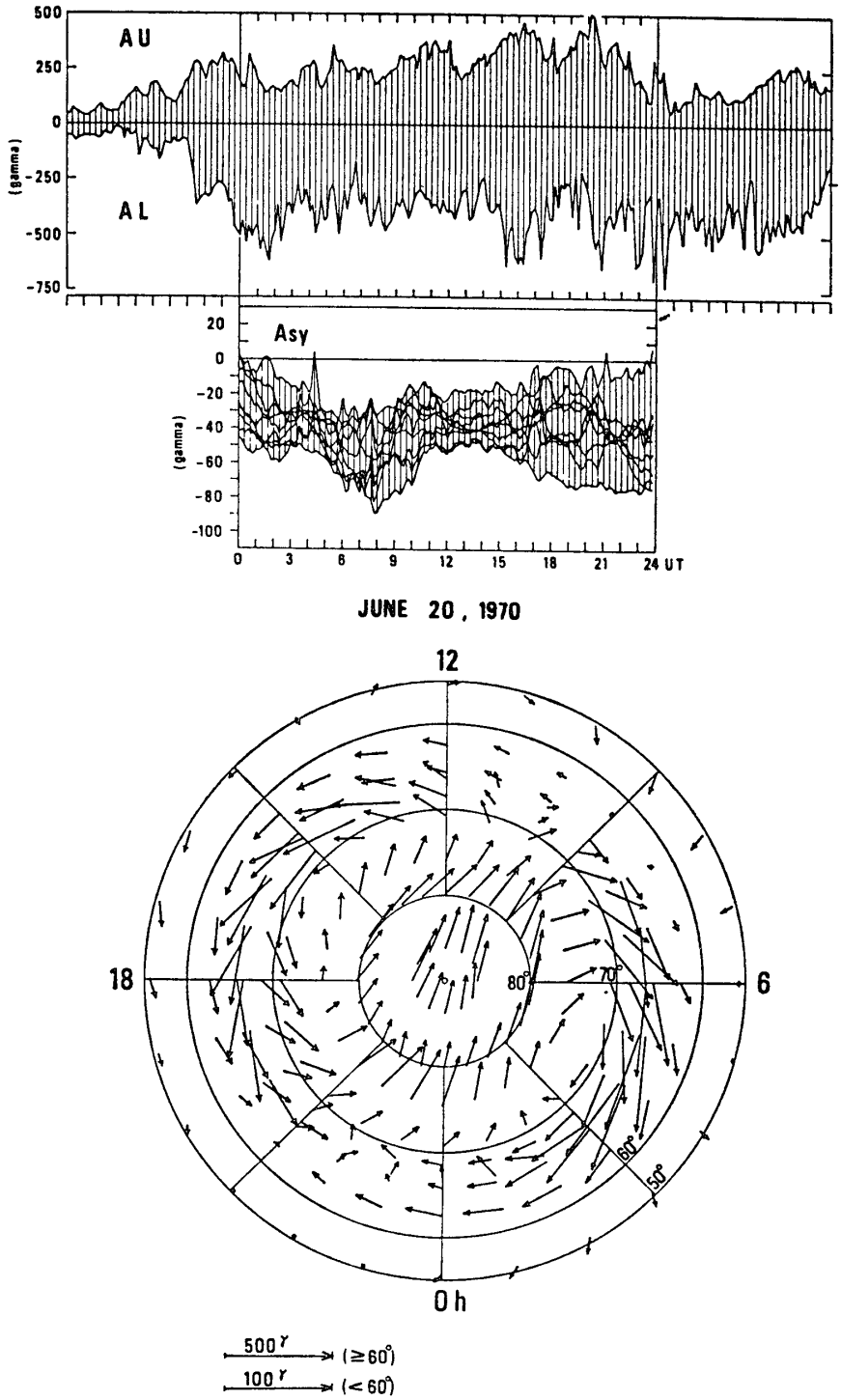

Fig 71. Distribution of the equivalent current vectors in high latitudes. A highly disturbed day is chosen as seen in the upper two panel expressing geomagnetic activity (after IIJIMA, 1973).

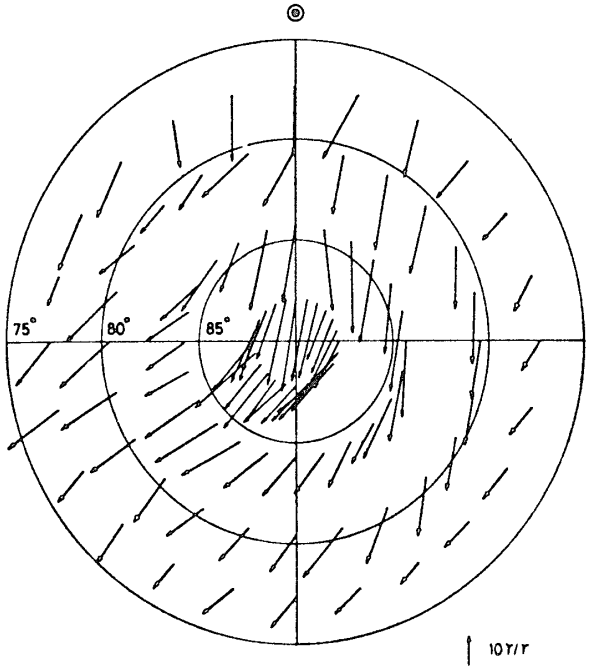

(a)

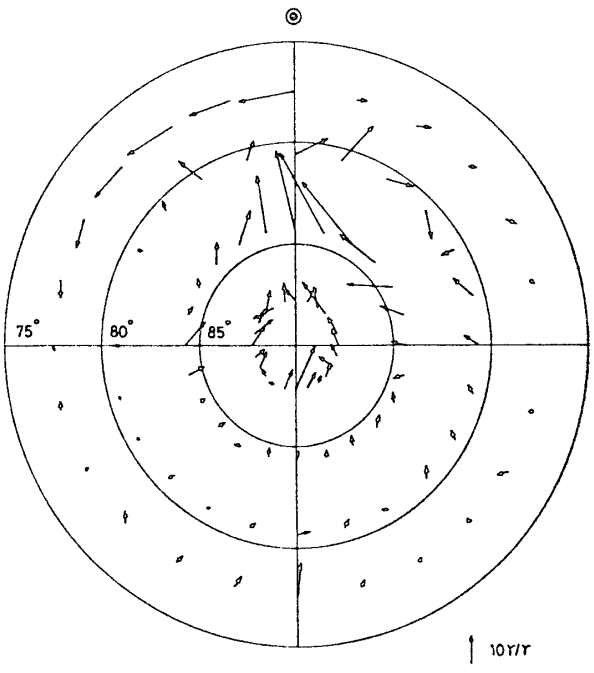

(b)

Fig 72. Equivalent current vectors with arrow directions reversed to indicate the direction of cross polar cap convective flow Part (a) pertains to southward IMF and part (b) to northward IMF. Note the remarkable reversal of convective flow from (a) to (b) in the dayside cleft region (after MAEZAWA, 1976).

by BURCH (1974) and NISHIDA (1975). A correlation of the eastward IMF and of sector structure ('away' or 'toward') with the polar cap magnetic field has been studied extensively by SVALGAAD (1973), CAMBELL and MATSUSHITA (1973), LANGEL (1973, 1974a, b), MATSUSHITA *et al.* (1973), BERTHELIER and CUÉRIN (1973), BERTHELIER *et al.* (1974), and SVALGAAD (1975); see also a review paper by MATSUSHITA (1978). To explain this correlation, in addition to the S_q^p current system, circular currents around the north and south poles were suggested by SVALGAAD (1973). MATSUSHITA *et al.* (1973) have shown that the S_q^p current pattern shifts toward the afternoon (early morning) side of the polar cap for the toward (away) sector structure. LANGEL (1974c, 1975) also examined the total magnetic field measured at the polar-orbiting satellites, OGO 2, 4 and 6, in relation to the interplanetary sector structure. MAEZAWA (1976) conducted a regression analysis of the polar cap field. Fig. 72 shows the effects of the northward and southward IMF conditions on the polar cap disturbances, shown as convection diagrams. The outstanding feature is the reversal in the direction of the convection flow between $+B_z$ and $-B_z$ occurring near the region of the noon polar cleft. A similar feature has been reported by KUZNETSOV and TROSHICHEV (1977). FRIIS-CHRISTENSEN and WILHJELM (1975) have pointed out that there is a marked reduction in the polar disturbances relating to the B_y component of the IMF from summer to winter compared to the similar behavior of the B_z related disturbances. This indicates that B_y and B_z have separate roles in producing the polar cap variations (KAWASAKI *et al.*, 1973).

8.3. Latitudinal profile of auroral electrojets

Quantitative modeling of ionospheric and magnetospheric currents to estimate the distribution of the auroral electrojets using meridian line magnetometer data has been discussed by OLDENBURG (1976, 1978). See also NOPPER and HERMANCE (1974) and HORNING *et al.* (1974) for a similar treatment of modeling of current systems. The structure of a sequence of substorms has determined and compared with other ground-based and satellite data of auroras and particle variations (ROSTOKER and KISABETH, 1973; ROSTOKER and HRON, 1975; ROSTOKER *et al.*, 1975, 1976; KISABETH and ROSTOKER, 1973, 1974; WALLIS *et al.*, 1976; MCDIARMID and HARRIS, 1976). CHEN and ROSTOKER (1974) have shown that the region of the Harang discontinuity is identifiable in the latitudinal profile of the D component perturbations. OLSON and ROSTOKER (1975, 1977) have found that the maximum amplitude of Pi2 pulsations occurs in general at the center of the substorm auroral electrojet. HUGHES and ROSTOKER (1977) have demon-

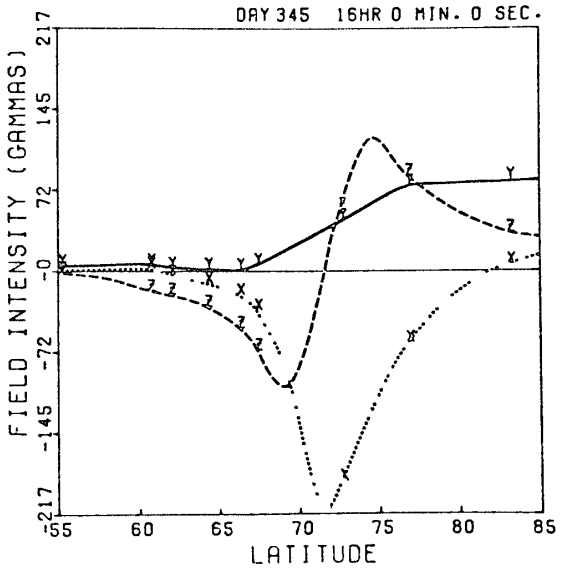

Fig. 73. Hourly average latitude profile of ground magnetic perturbation taken near local dawn. Latitude is given in corrected geomagnetic latitude (after HUGHES *and* ROSTOKER, *1977).*

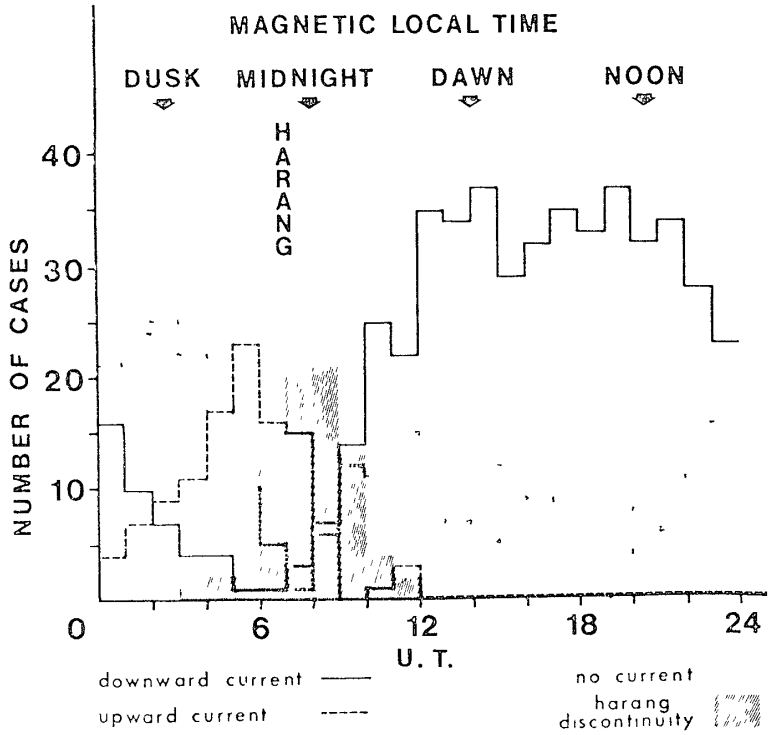

Fig 74. Histogram showing the distribution of net field-aligned current as a function of universal time (after HUGHES *and* ROSTOKER, *1977).*

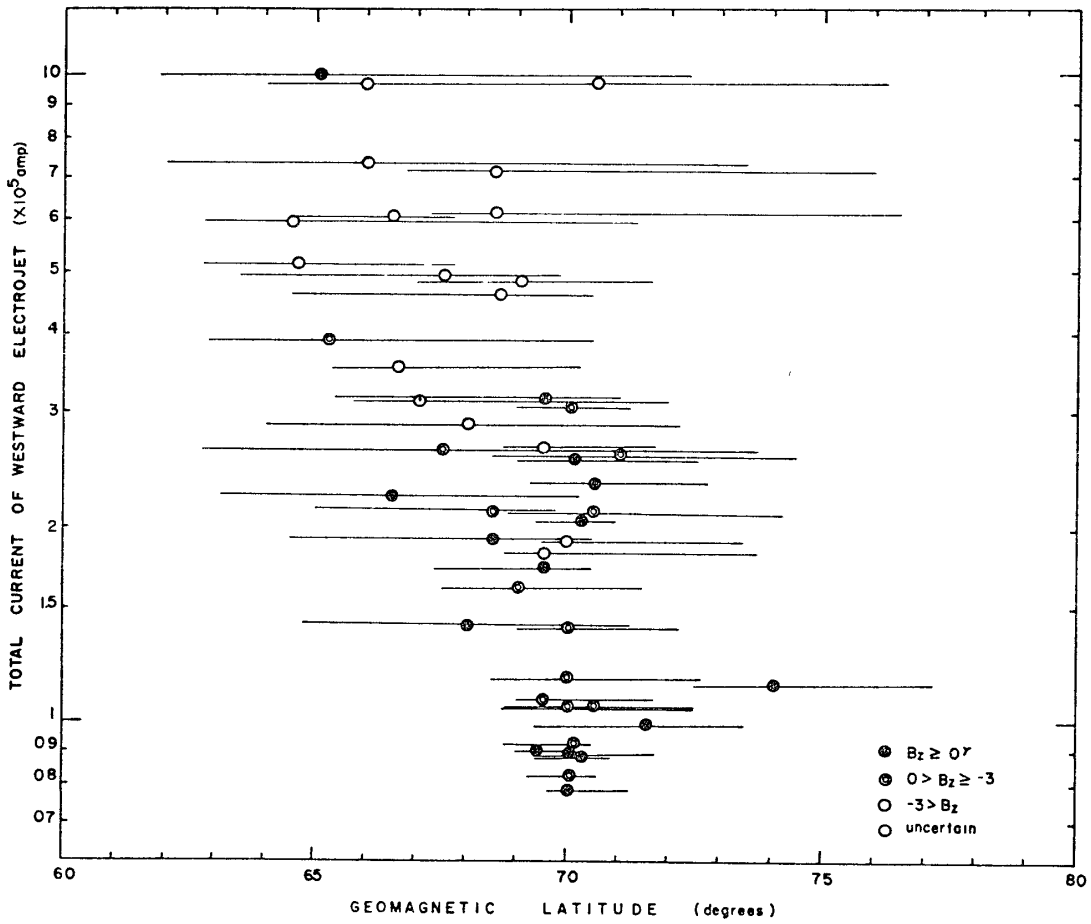

Fig. 75. Locations of the center of westward electrojet and its half-widths and the total intensity (after KAMIDE and AKASOFU, 1974).

strated that although effects of both ionospheric and field-aligned currents are involved in the ground magnetic perturbations, it is possible to find the ground-based signatures of the net field-aligned current flow using the latitudinal profile of the ground magnetic perturbations. Fig. 73 shows an example of such profiles taken near local magnetic dawn in which a clear level shift appears in the *D* component profile. The level shift, or step, exhibits the ground-based magnetic signature of the net field-aligned current flowing into the ionosphere. HUGHES and ROSTOKER (1977) have shown, using this technique, the diurnal variation of the net field-aligned currents. Fig. 74 is the histogram showing the distribution of the net field-aligned current as a function of universal time, along with approximate magnetic local time. It was noted that there is a remarkable similarity between the behavior of the field-aligned current flow as inferred from this diagram and the diurnal variation of the average electric field observed at auroral zone latitudes by MOZER and LUCHT (1974). Most recently, WINNINGHAM *et al.* (1978) and ROSTOKER

et al. (1978) have organized the ISIS 2 particle data in the framework of the latitudinal profile of the auroral electrojets It was found that precipitating energetic electrons are embeded within the poleword portion of the evening eastward electrojet.

KAMIDE and AKASOFU (1974) and AKASOFU and KAMIDE (1976) examined the total current of the auroral electrojet across the Alaska meridian as a functions of the interplanetary magnetic field for the maximum epoch of a number of substorms. Fig. 75 shows the relationship between the total current intensity and the central locations of the westward electrojet; different symbols are used to designate different IMF conditions. It is seen that the total current, location and width of the substorm electrojet are all related to the B_z component of the IMF. That is, for a larger negative B_z value, the total current and the latitudinal width are larger, and the center is located at a lower latitude, compared with the corresponding quantities for a positive B_z value. It is expected that the spatial and temporal changes of the auroral electrojets must be unveiled to a significant degree by the IMS meridian chains of magnetic observatories, now being successively operating at Alaska, Canada, Scandinavia, and Siberia.

As a contribution to the IMS, the University of Munster has installed a two-

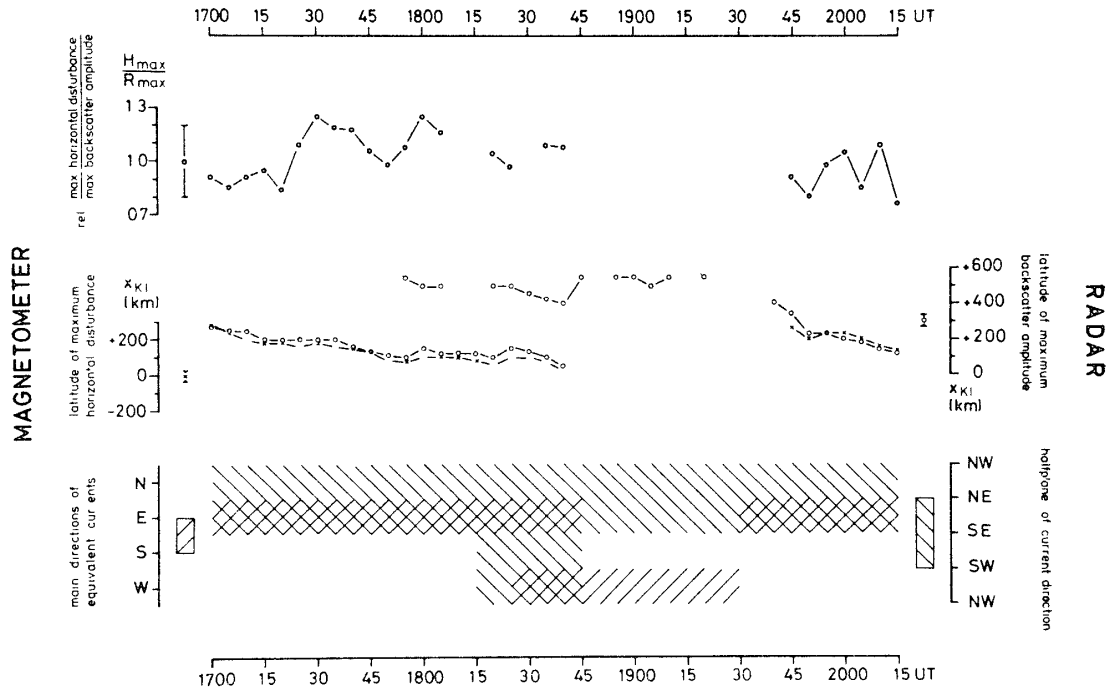

Fig 76. Comparison of magnetic and radar data The lower panel relates the main direction of the equivalent ionospheric current with the halfplane of allowable current direction consistent with the radar Doppler velocities (after BAUMJOHANN et al , 1978)

dimensional aray of 32 magnetometers in Northern Scandinavia constituting several meridian chains. As described in Section 4, the Max-Planck Institut für Aeronomie at Lindau is operating the STARE consiting of two backscatter radars which are sensitive to auroral irregularities occurring within the auroral electrojets. Fig. 76, reproduced from Fig. 3 of BAUMJOHANN *et al.* (1978), shows several comparisons of the magnetic and radar data during a moderately disturbed period. The middle set of curves in this figure illustrates a comparison of the latitudinal location of the maximum magnetic disturbance and the maximum backscatter amplitude as a function of time, which are represented by the crosses and circles, respectively. It is indicated that the maxima of the auroral electrojet and radar backscatter amplitude are at virtually the same latitudes, except for the interval 1840–1945 UT when the electrojet appears to be located well north of the Scandinavian network.

8.4. Substorm timing and complicated substorm development

There is no doubt that the magnetospheric substorm has been one of the most intensively studied geomagnetic phenomena. As noted by VASYLIUNAS and WOLF (1973), AKASOFU and KAN (1973), MCPHERRON (1974), and VASYLIUNAS (1976), there are at present several areas of controversy on some important aspects of substorm phenomena (HIRSHBERG and HOLZER, 1975; FEYNMAN, 1976). One cause of the controversy is the multiplicity of methods used to define substorm onset. This substorm timing is important for the establishment of cause-and-effect relationships among the various phenomena occurring during substorms (MCPHERRON *et al.*, 1973b; RUSSELL and MCPHERRON, 1973; KOKUBUN and IIJIMA, 1975; PYTTE *et al.*, 1976, 1978a, b; AKASOFU, 1977). As discussed by CAAN *et al.* (1973), inadequate intercalibration among the different techniques of onset determination exacerbates this controversy problem. The ground-based substorm signatures most frequently used include the brightening and poleward expansion of auroral bulge (AKASOFU, 1974), negative magnetic excursions in the auroral zone (KOKUBUN *et al.*, 1977), positive magnetic bays at mid-latitudes (CLAUER and MCPHERRON, 1974a, b; CAAN *et al.*, 1975), and Pi2 magnetic pulsations at auroral latitudes (SAITO, 1974; KAMIDE *et al.*, 1974) and at mid-latitudes (SAKURAI and SAITO, 1976; SAITO *et al.*, 1976a, b). It seems likely that some of these signatures may only be associated with specific subclasses of all substorm events (KAMIDE and MATSUSHITA, 1978a). An important point we have to realize is that any results obtained from a particular subclass of observations may be valid only within the assumptions employed in choosing that data set. It is interesting to note in this connection that SAITO *et al.* (1976b) have recently contended that the most

practical and best method to identify the substorm onset is to use mid-latitude Pi2, giving the identical time frame as determined by the original tool for defining the onset, the auroral breakup.

Since the first morphological description of the polar magnetic and auroral substorms by AKASOFU (1964, 1968), the significant improvement of a denser network of ground observatories and the availability of satellite records have made it possible to detail several substorm features in a more complicated way (VOROBIEV and REZHENOV, 1973; HONES *et al.*, 1973, NISHIDA and HONES, 1974; KISABETH and ROSTOKER, 1974; KAWASAKI *et al.*, 1974; JOHNSTONE *et al.*, 1974; KAMIDE *et al.*, 1975; NISHIDA and NAGAYAMA, 1975; KAMIDE and MCILWAIN, 1975; LUI *et al.*, 1976; KAMIDE *et al.*, 1977; PYTTE *et al.*, 1978a). Some of complex features associated with substorm development have been represented by a series of discrete step-like development of the substorm-disturbed region (WIENS and ROSTOKER, 1975), and multiple onsets of substorm current system (PYTTE *et al.*, 1976b, c). It was argued that substorm activity expands westward at intervals of 10–20 minutes, causing a sequence of auroral electrojet and surge intensifications that occur progressively farther and farther west.

9. Concluding Remarks

Interest in understanding the high-latitude electromagnetic phenomena has recently increased to a significant degree. This is primarily because of the recent availability of new techniques for measuring many physical quantities in the polar ionosphere, as well as of a growing realization that this region plays a principal role in large-scale magnetospheric processes This review paper was begun for the purpose of synthesizing the recent progress in studies of the electric fields and currents in the polar ionosphere made during the period 1973—present, and, hopefully, of combining the various complicated findings into a consistent view Some agreeable interpretations have been found in a variety of observational evidence, but there are still many areas which are not satisfactorily settled in terms of basic physical concepts, or which hold a considerable controversy. One of the difficulties in deducing the possible causes that can consistently explain the observed characteristics lies in the fact that all the natural phenomena occurring in this region are controlled by many unknown conditions; we cannot repeat the same experiment again and again under the constant conditions. We, thus, may often fail to find an crucial parameter which influences the whole system of the ionosphere and magnetosphere. Nevertheless, it may be useful to summarize the present status of

what we have learned in the new findings and what we need to clarify in the future. We think that the most important points are as follows:

9.1. Substorm current systems

Perhaps, one of the most fruitful efforts during the last few years is an attempt to construct a possible configuration of the three-dimensional current system for the magnetospheric substorm by integrating the findings of the ground-based and rocket-satellite observations of the electric fields and currents in the polar ionosphere obtained during the last several years. Various three-dimensional current systems associated with the magnetospheric substorm have been proposed in the past. Several theoretical studies have also been carried out on the relationship between the field-aligned currents and the ionospheric electric fields, and of their magnetic effects (*e.g.*, FUKUSHIMA, 1971, 1974, 1975, 1976; KAWASAKI and FUKUSHIMA, 1974; SATO, 1974, 1976). There are two possible current configurations, as pointed out by BOSTRÖM (1964), Type I and Type II, as schematically illustrated in Fig. 77. Type I was originally proposed by BIRKELAND (1908) and includes an inflow of currents into the morning half of the auroral oval and an outflow from the evening oval. Those field-aligned currents are connected through the westward electrojet. More recently, several three-dimensional current systems for the polar magnetic substorm have been inferred on the basis of the distribution

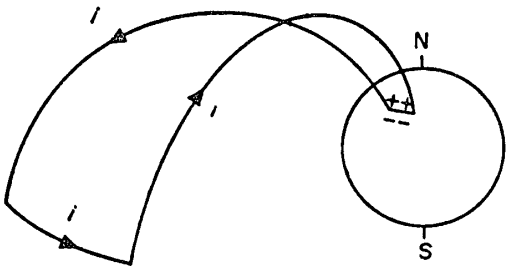

Type I

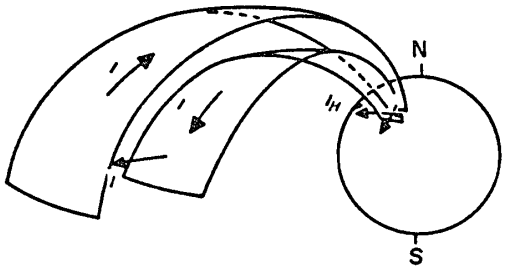

Type II

Fig. 77. Two possible configurations of field-aligned currents as pointed out by BOSTROM (1964).

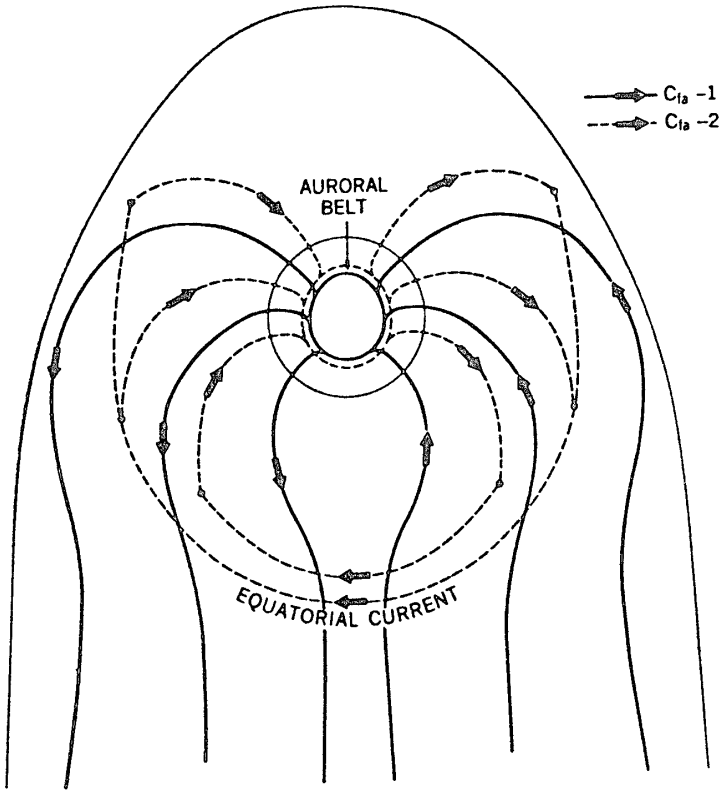

Fig. 78. Model of field-aligned current systems C_{fa}-1 and C_{fa}-2, which flow in the polar cap boundary layer, and on the low-latitude side of the auroral belt, respectively (after SUGIURA, 1975).

of magnetic perturbation vectors on the earth's surface. As pointed out by SUGIURA (1975), all of them can be classified as Type I, which further can be grouped into two categories; (1) the system containing a short-circuit of a part of the magnetotail current, and (2) the system with a closure through the partial ring current Models proposed by AKASOFU (1972) and MCPHERRON *et al* (1973) belong to (1), and those by AKASOFU and MENG (1969), MENG and AKASOFU (1969), and BONNEVIER *et al.* (1970) belong to (2). However, these models deal only with the westward electrojet in the dark sector The models put forward by KAMIDE and FUKUSHIMA (1972) and CROOKER and MCPHERRON (1972) include both types of current systems (1) and (2), as well as the eastward electrojet; they suggested that the westward electrojet results from the disruption of the magnetotail current, whereas the eastward electrojet is connected to the partial ring current through field-aligned currents ROSTOKER (1974a) presented a model in which a small-scale (in the sense of its longitudinal extent) field-aligned current in the Harang discontinuity region is emphasized

In Type II current system, an east-west electrojet is generated between the

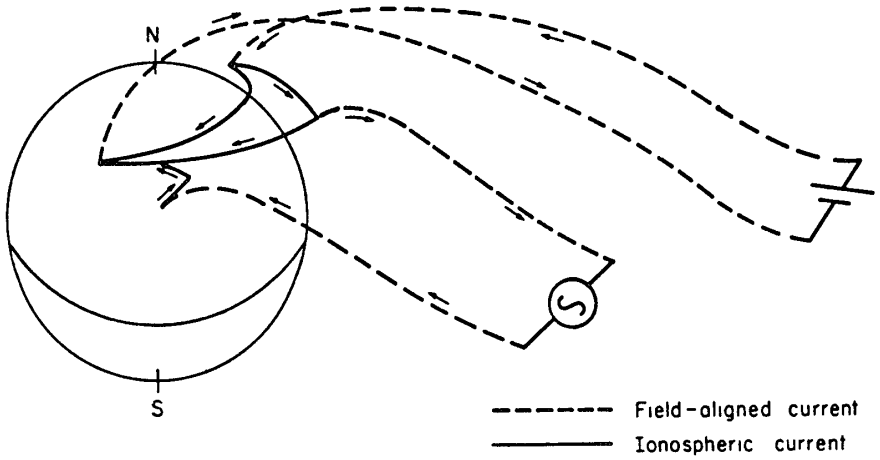

Fig. 79. Model of the connection between ionospheric and field-aligned currents (after YASUHARA et al., 1975).

feet of the field-aligned currents. ZMUDA and ARMSTRONG (1974b) and PARK (1975) considered two pairs of such field-aligned currents, one in the morning sector and the other (with the reversed current direction) in the evening sector.

SUGIURA (1975) has proposed a qualitative model of the field-aligned current configuration in which two current systems ($C_{fa}-1$ and $C_{fa}-2$) are connected to different regions of the magnetosphere, as shown in Fig. 78. Based on high-altitude observations of magnetic fields by OGO 5, it has been concluded that the polar cap boundary can be identified by a sudden transition from a dipolar to a more tail-like magnetic configuration, while the magnetic field in the region where the lower-latitude field-aligned current layer is situated is essentially meridional, indicating that the equatorial current closure of the latter current must be via the equatorial ring current. However, it was difficult to discuss how these two current systems interact in the ionosphere only from the observations in the magnetotail.

A numerical calculation of the ionospheric current pattern made by YASUHARA *et al.* (1975) can be used to check which configuration (Type I or II) of the ionospheric closures of the field-aligned currents is consistent with the results of the recent field-aligned current observations. They have reached a model current system as schematically shown in Fig. 79. It was suggested that the real situation appears to be a complicated combination of the Types I and II systems and that the relative importance of each of the closures depends chiefly on the ionospheric conductivity distribution. It was also discussed that although the closure of the currents in the magnetosphere equatorial-plane is essentially azimuthal, the north-south connection can occur in the ionosphere depending on the Pedersen and Hall conductivity ratio.

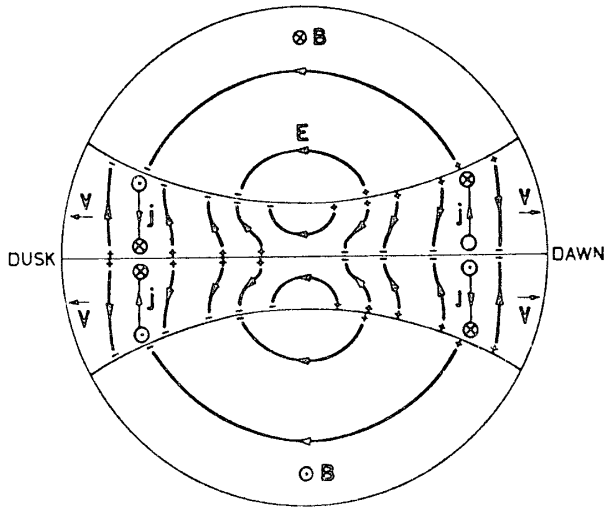

Fig 80 Electric field configuration in the magnetotail projected on the cross-section area of the magnetotail (after ROSTOKER and BOSTROM, 1976)

On the other hand, ROSTOKER and BOSTRÖM (1976) have developed a mechanism in which a meridional closure of the currents in the magnetosphere is associated with convective motion of plasma in the magnetotail, see also BOSTROM (1975). It was demonstrated that the gross field-aligned currents can be driven by energy supplied by the braking of this convective motion of the plasma sheet particles as they drift toward the flanks of the magnetosphere ROSTOKER and BOSTROM (1976) have shown the expectable configuration of the electric field in the cross section of the magnetotail, which is consistent with our current knowledge of the electric field in the ionosphere (see Section 2), and with the assumption that magnetic field lines are nearly equipotential. Fig 80 is reproduced from their Fig. 4, in which the basic character is seen such that away from the center of the tail, most of the electric field is directed normal to the neutral sheet, indicating that toward the flanks of the tail the dominant direction of convective flow is parallel to the neutral sheet and toward the boundary between the magnetotail and magnetosheath. It was also discussed that since the closure currents of the field-aligned current loops flow in directions opposite to the electric field, the current region in the tail has the character of an electric generator.

KAMIDE *et al.* (1976b) have reached an empirical model of the three-dimensional current system for the magnetospheric substorm which satisfies the recent new observations of the electric fields and currents in the ionosphere. In Fig 81, we show a schematic illustration of their model, in which the shaded area represents the region of the westward electrojet, that is the dominant feature of the polar substorm. From nearly simultaneous observations of the field-aligned currents,

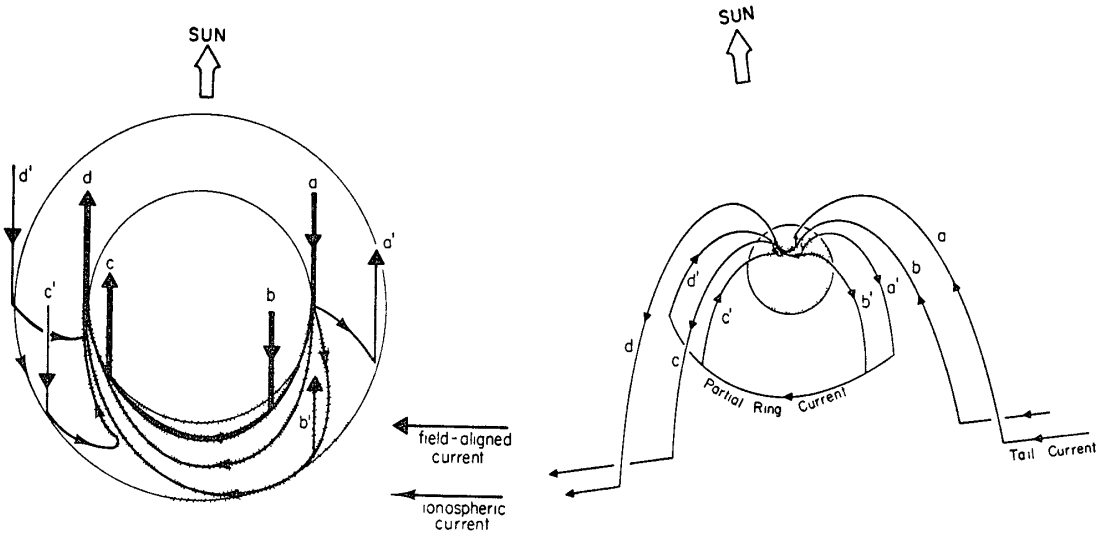

Fig. 81. (a) Model current system for the magnetospheric substorm. The dotted area represents the region of the westward electrojet and (b) schematic illustration of the three-dimensional current model for the magnetospheric substorm (after KAMIDE *et al., 1976b*)

the auroral electrojets, and the auroral distribution, KAMIDE and ROSTOKER (1977) have added the association of this current system with various types of auroras. According to their current configuration, the westward electrojet flows approximately along the active westward traveling surge in the evening sector, as well as along the entire diffuse aurora in the morning sector. The latitudinal width of the westward electrojet is much larger in the morning sector than that in the evening sector. The eastward electrojet flows equatorward of the westward electrojet in the evening sector, namely along the diffuse aurora. There is no significant ionospheric return current from the electrojets in the polar cap (HEPPNER *et al.*, 1971) and in mid-latitudes. Thus, the electrojet currents must mostly be supplied by the field-aligned currents.

The westward electrojet in Fig 81 is fed by the field-aligned currents in the way suggested by BIRKELAND in 1908 (shown by thick lines), but a significant part of the downward field-aligned current (represented by a) in the morning sector flows southwestward, and then flows out of the ionosphere as the upward currents (a′ and b′). This is in agreement with the observations made by the Chatanika radar and the TRIAD satellite. In particular, the radar measurements suggest that the westward electrojet has a large southward deflection in the morning sector.

It can be seen that the current pattern is much more complicated in the

evening sector than in the morning sector. There are downward field-aligned currents (c′ and d′) in the area of the eastward electrojet. The intense upward currents (c and d) are connected with the westward electrojet and also with the northward ionospheric current, which is eventually connected to the inward field-aligned currents through the eastward electrojet. Thus, the total intensity of the upward field-aligned currents is much more intense than that of the inward currents, as observed by the TRIAD satellite (YASUHARA *et al*, 1975; IIJIMA and POTEMRA, 1976a). This current configuration is also in good agreement with the radar observations which show that the northward ionospheric current prevails in the evening sector, regardless of the sign of the east-west ionospheric current Some previous models suggested the existence of an upward field-aligned current at the eastern end of the eastward electrojet (KAMIDE and FUKUSHIMA, 1972; CROOKER and MCPHERRON, 1972), whereas in the present model the downward current is associated with the eastward electrojet throughout evening hours. This conclusion is based on the new results from a detailed comparison of the TRIAD data with the corresponding ground magnetic records. It is seen that the eastward electrojet flows northeastward as it approaches the midnight sector and eventually is connected to the westward electrojet The general current pattern is also consistent with the current configuration reached by HUGHES and ROSTOKER (1977).

9.2. Collocation of aurora and current boundaries

Recent studies of the auroral oval and the current configuration contained within its bounds have yielded the following information

1) The convection eastward electrojet is confined within the diffuse auroral oval in the evening sector (WALLIS *et al.*, 1976). The equatorward portion of the eastward portion of the eastward electrojet is penetrated by downward field-aligned current, while the poleward edge of the eastward electrojet region is associated with upward current flow (ARMSTRONG *et al.*, 1975). The region poleward of the eastward electrojet is the site of upward field-aligned current flow, discrete auroral arcs, and westward ionospheric current flow (KAMIDE and AKASOFU, 1976b).

2) The convection westward electrojet is penetrated by downward flowing field-aligned currents in the poleward portion and upward flowing field-aligned currents in the equatorward portion (KAMIDE *et al*, 1976a; IIJIMA and POTEMRA, 1978).

3) In substorm-disturbed regions in the evening sector the westward electrojet penetrates toward dusk along the poleward edge of the eastward (steady state)

electrojet. Field-aligned currents are downward at the poleward edge of the westward electrojet and in the equatorward portion of the eastward electrojet, and are upward between these two regions (ROSTOKER *et al.*, 1975).

KAMIDE and ROSTOKER (1977) have indicated that the auroral electrojets are more tightly confined to the region of auroral luminosity than was indicated by WALLIS (1976), who noted significant auroral luminosity outside of the predicted boundaries of the auroral electrojet. Albedo corrections of the ISIS 2 photometer data have now made the auroral and electrojet boundaries more coincident (see notes added in proof to the work of WALLIS *et al.*, 1976). In addition, it is likely that the auroral luminosity would have to rise above some threshold before adequate conductivity to support a significant electrojet current could be achieved. The ISIS 2 photometer is capable of sensing luminosity about 0.5–1 kR (see BERKEY and KAMIDE, 1976), while the threshold for DMSP is 2–3 kR. It is reasonable to expect that while luminosities below 1 kR are indicative of the presence of auroras, they do not imply the existence of significant ionospheric electrojet current (KAMIDE *et al.*, 1978).

9.3. Carriers of field-aligned currents

KAMIDE and ROSTOKER (1977) have indicated that significant downward current flow may occur in regions of low auroral luminosity, whereas upward current flow appears to be related to intense auroral features such as discrete arcs. These features are particularly noticeable for the morning sector westward electrojet in the course of a substorm. On the basis of these observations it is suggested that downward flowing field-aligned current is carried by ionospheric electrons moving upward into the magnetosphere, while upward flowing current is carried by the precipitating keV electrons responsible for *E* region auroral luminosity. The suggestion that downward field-aligned current is carried by upward moving low-energy (thermal) ionospheric electrons is in agreement with the results of ARNOLDY and CHOY (1973), who observed, by a series of rocket detectors, the upward streaming of electrons of energy less than a few hundred eV poleward of a main auroral luminosity. KLUMPAR *et al.* (1976) also observed low-energy electrons having pitch angles near 180° and with sufficient flux to account for the field-aligned current density measured simultaneously by the ISIS 2 magnetometer.

In evaluating the ability of energetic electrons to carry enough current to account for the observed level of magnetic perturbation we note that KLUMPAR *et al.* (1976) indicated on the basis of simultaneous magnetic signatures of the field-aligned currents and electron measurement (5 eV to 15 keV) that the pre-

cipitation of kilovolt electrons can account for the magnitude of the upward field-aligned current in the equatorward half of the morning auroral belt. This suggestion also agrees with those of EVANS *et al.* (1977) and CARLSON and KELLEY (1977) in that the precipitating keV electrons constitute the upward field-aligned current within bright auroral arcs. However, there are two points we have to note here. First, SUGIURA and POTEMRA (1976) claimed that the electron flux given by MCDIARMID *et al.* (1975) on the basis of the results from energetic particle detector experiment on the ISIS 2 satellite is insufficient to carry the field-aligned current densities estimated from the TRIAD magnetometer observations However, it seems that owing to the averaging processes in deriving the isointensity contours in magnetic 'latitude-local time' coordinates, the electron flux given by MCDIARMID *et al.* (1975) might be somewhat smaller than the actual electron flux that can often be found in a narrow region in association with structured bright auroras. Second, most of the rocket observations of the field-aligned current have indicated that in the vicinity of individual auroral arcs the precipitating electrons with energies between approximately 500 eV and 20 keV can carry a significant fraction of the upward field-aligned current (see review papers by ARNOLDY, 1974 and ANDERSON and VONDRAK, 1975). However, some rocket data (*e g*, PAZICH and ANDERSON, 1975; SPIGER and ANDERSON, 1975) showed that although a total upward current coincides with the main arc, the measured precipitating electrons (0.5–20 keV) carry only a small fraction (<15%) of the upward current necessary to produce the simultaneously observed magnetic signatures We believe that this apparent discrepancy may be accounted for by taking into account the difference either in altitude (*i e.*, 100–200 km for the rocket measurements) or in spatial resolution (*i.e*, less than 5 km for rocket observations) or both

The diffuse aurora in evening hours delineating the equatorward half of the auroral oval is the persistent feature. Compared with the structured discrete aurora in the poleward half of the auroral oval, the diffuse aurora is less structured and relatively stable It has been found that the downward field-aligned current is collocated with the diffuse aurora. This correspondence is not unexpected, combining all independent past observations that the downward field-aligned current flows in the latitudinal regime within the eastward electrojet (KAMIDE and AKASOFU, 1976b), that the diffuse radar aurora is associated with the eastward electrojet and is confined in the region of the downward field-aligned current (TSUNODA *et al.*, 1976a, c), and that the upward field-aligned current is located in the discrete aurora region (ARMSTRONG *et al.*, 1975, KAMIDE and AKASOFU, 1976a).

Since it is difficult to identify the boundaries of the diffuse aurora in all-sky camera records, a direct comparison of the diffuse aurora and the downward field-aligned current has long been desired. However, it is important to note that discrete auroral arcs may be immersed in the diffuse aurora and in the region of the northward electric field, particularly in the poleward portion of the diffuse auroral oval (WALLIS *et al.*, 1976; DE LA BEAUJARDIERE *et al.*, 1977). On the basis of the results of ARMSTRONG *et al.* (1975) we would contend that in the evening sector, discrete arcs often carry the upward current flow in the poleward portion of the eastward electrojet and in the region poleward of the eastward electrojet where substorm-associated currents are known to flow.

Insofar as the current carriers for diffuse auroral region in the evening sector are concerned, a plausible candidate both for carrying the downward field-aligned current and for the production of the diffuse aurora might be precipitating positive ions. However, there is evidence that although both precipitating electrons and protons are observed in the diffuse aurora region, the 5 eV to 15 keV protons carry only 0.1–0.01 of the field-aligned current carried by the electrons over the same energy range (WINNINGHAM *et al.*, 1975; LUI *et al.*, 1977). Thus the precipitating protons are not suitable for the downward current, and this leads us to speculate that upward flowing thermal electrons are the most likely current carriers. KLUMPAR (1976) suggested that isotropic keV electrons originating in the plasma sheet give rise to the diffuse aurora. MENG (1976) has shown that the energy spectrum of the diffuse aurora during quiet periods is characterized by nearly constant differential fluxes from 0.2 to about 8 keV with a sharp cutoff above 8 keV and that the energy flux is about 0.1 erg/cm^2·s·sr. The characteristics observed by KAMIDE and ROSTOKER (1977) are essentially the same as MENG's (1976) observation, except that energy density during substorms increases by a factor of 5 or more.

9.4. Current flow associated with different auroral forms

One obvious uncertainty in the studies of high-latitude current pattern is the relationship between the smaller-scale current systems observed by the rockets near individual auroral forms and the larger-scale current systems detected by polar-orbiting satellites. As suggested by ANDERSON and VONDRAK (1975), it is necessary to design either rockets or longer-range satellites which can scan the entire auroral belt with high data rates supported by optical observations of auroral fine structures.

At present, our knowledge concerning the relationship between current flow

and different auroral forms may be summarized as follows: In the evening sector the westward traveling surge is one of the typical substorm features (MENG *et al.*, 1978), in which the intense upward field-aligned current is present which is carried by precipitating keV electrons. The westward extremity of the main body of the surge often has bright discrete arcs emanating attached to it which occupy the region to the west. Each of these arcs is the site of intense upward current flow, and occasionally there will be downward current flow adjacent to the discrete arcs where the current is carried by upward flowing thermal electrons of ionospheric origin. Particular emphasis should be placed on the downward field-aligned current just outside the poleward edge of the discrete aurora (KAMIDE and ROSTOKER, 1977). The latitudinal width of the downward current region ranges from 0.1° to 1°. Since the current is associated with no precipitating electron flux, the most plausible candidate for the current carrier is upward moving ionospheric electrons. A net streaming out of the ionosphere poleward of auroral forms was indeed observed by rocket detectors (CHOY *et al.*, 1971; ARNOLDY and CHOY, 1973). In the morning sector, the upward current in the equatorward half of the field-aligned current belt is collocated with bright auroras. It is contended that although there is no direct particle observation in this region, precipitating electrons are responsible for both the upward current and visible auroras, just the same as in the region of the intense upward field-aligned current in the evening sector. On the other hand, however, the aurora luminosity has no correlation with the intensity of the downward field-aligned current, a result suggesting that the current is again carried by ionospheric thermal electrons.

9.5. Future problems

The review presented here may suggest that recent observations by means of several new techniques made it possible to *begin* to unfold many complex phenomena occurring in the polar ionosphere and to unveil now the cause of the ionospheric and magnetospheric processes. However, we are still far from providing successful answers to many problems of dynamical processes and there even emerge some essential questions in the recent new findings. We list some of these questions:

1) What are the sources of the ionospheric electric fields during both quiet and disturbed times? Recent reliable measurements by means of several different techniques have revealed the existence of the characteristic diurnal variations of the auroral zone electric field. It is directed northward and southward in the evening and morning sectors, respectively. The predominance of the westward

field in between has also been detected near the midnight sector. These features are consistent with the two-cell convection pattern. However, there is no agreement in various data sets as to the significance and nature of the small-scale electric fields, in particular, in the east-west component associated with complicated auroral forms. For a fruitful determination of the electric field behavior in understanding the sources of the spatial and temporal structure of the electric fields in auroral latitudes, it may be necessary to make a comparison of the electric field with other ionospheric quantities, such as the electron density, field-aligned currents, and ionospheric conductivities, as well as the magnetic field and auroral distribution. Some results of the study along this direction have been reported by DE LA BEAUJARDIERE *et al.* (1977).

2) What are the roles of magnetospheric convection and field-aligned currents in the course of a magnetospheric substorm? If one assumes that auroral-zone magnetic field lines are electrical equipotential, one can use the observed electric field topology to study the large-scale convective motion in the magnetosphere. There is no doubt that various ionospheric and magnetospheric phenomena depend upon how the magnetospheric plasma convection varies during magnetospheric substorms. In the midnight sector, the westward electric field drives the magnetotail plasma inward toward the earth; this motion in the ring current and plasma sheet regions appears to be closely related to a drastic change of the magnetospheric configuration observed during substorms. Thus, by examining the electric field variations throughout a substorm, it may be possible to deduce the roles of the convection that is the major process in the magnetosphere. The field-aligned currents that connect the ionospheric and magnetospheric currents play also a dominant role. It may be needed to combine recent observations of the distribution and substorm changes of the large-scale electric field configuration, field-aligned currents and ionospheric conductivities in order to interpret observed complicated processes and expectable phenomena in terms of theoretical consequences of particle distribution resulting from the electric potential distribution in the magnetosphere. It is interesting to note that RICHMOND (1976) has recently suggested that the electric field source at middle and low latitudes on quiet days is primarily of ionospheric dynamo origin.

3) Where do auroral particles originate and what processes accelerate these particles? Although there seems a general agreement on the energy distribution of precipitating auroral particles for the discrete aurora in that plasma sheet electrons are accelerated along the auroral zone field lines, it is unclear in which part of the plasma sheet (near inner edge, central part, or high-latitude boundary?)

these particles originate and what acceleration mechanism is effective to produce the abrupt increase in population of the auroral particles at the onset of a substorm. It is also important to examine how the magnetic energy is converted to the substorm energy dissipated in the polar ionosphere It remains to be answered how the tail current disruption occurs, that results in a large induced electric field (KAN and AKASOFU, 1978).

4) What is the auroral oval? The 'classical' auroral oval (or belt), which is defined as the locus of high frequency of visible auroral appearance (FELDSTEIN, 1966), has been used extensively to order geophysical data. EATHER (1973) has pointed out several pitfalls in this usage in that the most relevant 'coordinate' is the instantaneous region of both visual and subvisual auroral emissions. Most recently, HOLZWORTH and MENG (1975), and MENG *et al.* (1977) have shown that the instantaneous auroral distribution during quiet periods is more similar in shape to a 'auroral circle' rather than is expected from the term 'auroral oval'. The dynamical response of the 'instantaneous' auroral oval defined by the global auroral and electron distribution to the interplanetary magnetic field and substorm activity has been 'statistically' examined by LUI *et al* (1975), HOLZWORTH and MENG (1975), and KAMIDE and WINNINGHAM (1977). One must make a serious effort to examine the physical meaning of the auroral oval, and the relationship of the auroral oval with the injection boundary in the magnetotail (MCILWAIN, 1974)

5) What is the Harang discontinuity? There is confusion as to the spatial structure of the Harang discontinuity (KAMIDE, 1978). Although MAYNARD (1974b) has indicated from a study of satellite electric field data that the Harang discontinuity has a finite thickness, it is important to determine how fine structure within the Harang discontinuity 'region' relates the ionospheric processes in conjunction with the growth of a substorm (J. FOSTER, 1978, personal communication). At present even the characteristic features of particle precipitation, optical auroras and field-aligned currents are unclear

6) How are field-aligned currents related to the auroral distribution during extremely quiet times? As described in the previous sections, recent works have revealed the existence of two belts expressing latitudinally separated features of auroras and field-aligned currents The two regions of auroras (diffuse and discrete) coincide generally with the two regions of the field-aligned currents (upward and downward) in the dark sector. However, there arises apparently one puzzling problem when quiet-time features are considered Auroral observations have shown that the diffuse auroral precipitation on the *equatorward* side of the nightime

(21–03 MLT) auroral oval is a persistent feature (WINNINGHAM *et al.*, 1975), although the precipitation belt tends to shift poleward (up to 70° invariant latitude) during very quiet times (KAMIDE and WINNINGHAM, 1977). On the other hand, only the *poleward* portion of the field-aligned current (downward and upward in the morning and evening sectors, respectively) remains during extremely quiet periods as shown by IIJIMA and POTEMRA (1976a), who have then suggested that the S_q^p current should be supplied by that field-aligned current system.

A remark is given here on the use of ground magnetic records in inferring the source currents. A number of 'equivalent' ionospheric current systems have hitherto been put forward to explain the particular types of magnetic perturbations observed on the earth's surface. The question arises then whether these proposed equivalent current patterns represent a real flow of the ionospheric currents or they are just a convenient expression of ground magnetic field potential caused by other currents, such as field-aligned and ring currents in more distant magnetosphere (FUKUSHIMA and KAMIDE, 1973a, b). The Chatanika radar observations of the ionospheric electric fields and conductivities have made it possible to conclude that the H component magnetic perturbations in the auroral latitudes are produced primarily by the ionospheric east-west current (BREKKE *et al.*, 1974; KAMIDE and BREKKE, 1975). However, there are two opposite suggestions concerning the origin of the D component perturbations: KISABETH and ROSTOKER (1973) have indicated that the positive D changes near the westward traveling surge are caused by the southward ionospheric current, whereas KAMIDE *et al.* (1976a) have suggested that these changes are ascribable mainly to an upward field-aligned current flowing into the bright auroral area. As to the ground magnetic disturbances in the polar cap, HEPPNER *et al.* (1971) concluded that the comparison between vectors of observed electric fields and the ground magnetic perturbations argues against attributing the polar cap magnetic disturbances to the ionospheric currents for any combinations of the assumed Pedersen and Hall conductivities. Based on the barium release experiments, MIKKELSON *et al.* (1975) have reached the similar conclusion.

Recently, however, PRIMDAHL and SPANGSLEV (1977) have shown the results of rockets measurements of electric and magnetic fields in the sunlit part of the polar cap in which it was suggested that the ionospheric Hall current strength and the ground-based magnetic perturbations fitted well together. To resolve this apparent paradox, it is important to examine both experimentally and theoretically what conditions are required to reproduce the observed characteristics of the polar cap magnetic disturbances, and, at the same time, great caution must be employed

in interpreting the polar cap magnetic disturbances as an indication of changes in the dawn-dusk electric field without paying much attention to the possible magnetic effects of the field-aligned currents. It is also urgently needed to make an effort to combine the observed non-uniform distributions of the electric field (HEPPNER, 1973), low-energy electron precipitation (MENG *et al.*, 1977), magnetic field disturbances (SVALGAARD, 1973; FRIIS-CHRISTENSEN and WILHJELM, 1975), and the recent theoretical calculations including day-night conductivity gradients (ATKINSON and HUTCHISON, 1978; KAMIDE and MATSUSHITA, 1978b).

Acknowledgments

It is a pleasure to acknowledge helpful discussions with Drs Y. INOUE and T IIJIMA throughout the preparation of this paper. Special thanks are due to Mr. R. FUJII for his inestimable assistance in the editorial work. I would like to thank the colleagues and also the editors and publishers of various journals for their kind permission to reproduce the illustrations used in this paper. They are detailed as follows: Drs T. L. AGGSON (NASA Goddard Space Flight Center), S.-I. AKASOFU (University of Alaska), J. H. ALLEN (National Oceanic and Atmospheric Administration), R. L. ARNOLDY (University of New Hampshire), W. BAUMJOHANN (University of Munster), A. BREKKE (University of Tromsø), F. W BERKO (NASA Goddard Space Flight Center), C. W. CARLSON (University of California at Berkeley), T. N. DAVIS (University of Alaska), C S DEEHR (University of Alaska), O. DE LA BEAUJARDIERE (Stanford Research Institute International), D. S. EVANS (National Oceanic and Atmospheric Administration), D. H. FAIRFIELD (NASA Goddard Space Flight Center), H FUKUNISHI (National Institute of Polar Research), R. A. GREENWALD (Max-Planck Institut fur Aeronomie at Lindau/Harz), D A GURNETT (University of Iowa), J. P HEPPNER (NASA Goddard Space Flight Center), R. G. HOFFMAN (NASA Goddard Space Flight Center), J L. HORWITZ (NASA Marshall Space Flight Center), T J. HUGHES (University of Alberta), T. IIJIMA (University of Tokyo), S ISMAIL (University of Calgary), A T. Y. LUI (Johns Hopkins University), K MAEZAWA (University of Tokyo), N. C MAYNARD (NASA Goddard Space Flight Center), I. B. MCDIARMID (National Research Council of Canada), C-I MENG (Johns Hopkins University), F S. MOZER (University of California at Berkeley), T. OGUTI (University of Tokyo), T A. POTEMRA (Johns Hopkins University), C L RINO (Stanford Research Institute International), G ROSTOKER (University of Alberta), J. C SIREN (University of Maryland), M. SUGIURA (NASA Goddard

Space Flight Center), R. T. TSUNODA (Stanford Research Institute International), R. R. VONDRAK (Stanford Research Institute International), J. WILHJELM (Danish Meteorological Institute), V. M. VASYLUINAS (Max-Planck Institut für Aeronomie at Lindau/Harz), and D. D. WALLIS (National Research Council of Canada); and American Geophysical Union (for the reproduction of illustrations from the Journal of Geophysical Research), Deutsche Geophysikalische Gesellschaft (Journal of Geophysik), Pergamon Press Ltd. (Planetary and Space Science), and D. Reidel Publishing Co. (Space Science Reviews, Particles and Fields in the Magnetosphere, and Dynamical and Chemical Coupling).

This work was supported in part by National Institute of Polar Research.

References

AGGSON, T. L. (1969): Probe measurement of electric field in space. Atmospheric Emission, ed. by B. M. MCCORMAC and A. OMHOLT. New York, Van Nostrand Reinhold, 305–310.

AGGSON, T. L. and HEPPNER, J. P. (1977): Observations of large transient magnetospheric electric fields. J. Geophys. Res., **82**, 5155–5164.

AKASOFU, S.-I (1964) The development of the auroral substorm. Planet. Space Sci., **12**, 273–290.

AKASOFU, S.-I. (1968). Polar and Magnetospheric Substorms. Dordrecht, D. Reidel, 280 p. (Astrophys. Space Sci. Lib., Vol. 11)

AKASOFU, S-I. (1972). Magnetospheric substorms· A model. Solar-Terrestrial Physics, ed. by E. R. DYER. Dordrecht, D. Reidel, 131–151 (Astrophys. Space Sci. Lib., Vol. 29).

AKASOFU, S.-I. (1974a): A study of auroral displays photographed from the DMSP-2 satellite and from the Alaska meridian chain of stations. Space Sci. Rev., **16**, 617–725.

AKASOFU, S-I. (1974b): The midday red aurora observed at the South Pole on August 5, 1972. J. Geophys. Res., **79**, 2904–2910.

AKASOFU, S.-I. (1974c). The aurora and the magnetosphere. Planet. Space Sci., **22**, 885–923.

AKASOFU, S.-I. (1974d): Discrete, continuous and diffuse auroras. Planet. Space Sci., **22**, 1723–1726.

AKASOFU, S-I. (1975): The roles of the north-south component of the interplanetary magnetic field on large-scale auroral dynamics observed by the DMSP satellite. Planet. Space Sci., **23**, 1349–1354.

AKASOFU, S.-I. (1976). Recent progress in studies of DMSP auroral photographs. Space Sci. Rev, **19**, 169–215.

AKASOFU, S.-I. (1977): Physics of Magnetospheric Substorms. Dordrecht, D. Reidel. 599 p.

AKASOFU, S.-I. and KAMIDE, Y. (1976): Substorm energy. Planet. Space Sci, **24**, 223–227.

AKASOFU, S.-I. and KAN, J. R. (1973) Some new thoughts on magnetospheric substorms. Radio Sci., **8**, 1049–1057.

AKASOFU, S-I. and MENG, C.-I. (1969). A study of polar magnetic substorms. J. Geophys. Res, **74**, 293–313.

AKASOFU, S.-I. and YASUHARA, F. (1973). Red auroras in the morning sector. J Geophys.

Res, **78**, 3027–3032.

AKASOFU, S.-I, DEFOREST, S. and MCILWAIN, C. E. (1974) Auroral displays near the 'foot' of the field line of the ATS-5 satellite. Planet. Space Sci., **22**, 25–40.

AKASOFU, S -I., PERREAULT, P. D., YASUHARA, F. and MENG, C.-I. (1973). Auroral substorms and the interplanetary magnetic field. J. Geophys. Res, **78**, 7490–7508.

ALFVÉN, H. (1939): A theory of magnetic storms and of the aurorae, 1. Kgl. Sv. Vetenskapsakad. Handl., Ser. 3, **18**, 1–39 (Partial reprint, EOS; Trans. Am. Geophys Union, **51**, 181–193, 1970).

ALLEN, J. H. (1972): Auroral electrojet magnetic activity indices (AE) for 1970. Rep. UAG-22, WDC-A, NOAA, Boulder, Colorado, U.S A., 146 p.

ALLEN, J. H and KROEHL, H. W. (1975)· Spatial and temporal distributions of magnetic effects of auroral electrojets as derived from *AE* indices. J. Geophys. Res., **80**, 3667–3677.

AMUNDSEN, R., AARSNES, K., LINDALEN, H R. and SORAAS, F. (1973). High latitude electron and proton precipitation at different local times and magnetic activity. J. Atmos. Terr. Phys, **35**, 2191–2199.

AMUNDSEN, R., SORAAS, F. and AARSNES, K (1975). Cleft signature in proton fluxes above 100 keV. J. Geophys. Res., **80**, 685–689.

ANDERSON, H R. and CLOUTIER, P. A. (1975): Simultaneous measurements of auroral particles and electric currents by a rocket-borne instrument system Introductory remarks J. Geophys. Res., **80**, 2146–2151.

ANDERSON, H R. and VONDRAK, R. R. (1975): Observations of Birkeland currents at auroral latitudes Rev Geophys. Space Phys, **13**, 243.

ANDREWS, M. K. and STROMMAN, J. R. (1973): Simultaneous observations of low energy electron fluxes and the polar red emission at 6300 Å. J. Atmos. Terr. Phys., **35**, 537–545.

ANGER, C. D. and LUI, A. T. Y. (1973): A global view at the polar region on 18 December 1971. Planet. Space Sci., **21**, 873–878.

ANGER, C. D. and MURPHREE, J. S (1976) ISIS-2 satellite imagery and auroral morphology. Magnetospheric Particles and Fields, ed. by B. M. MCCORMAC. Dordrecht, D. Reidel, 223–234 (Astrophys. Space Sci Lib., Vol. 58).

ANGER, C. D., FANCOTT, T., MCNALLY, J. and KERR, H. S. (1973a): The Isis-2 scanning auroral photometer. Appl. Opt., **12**, 1753–1759.

ANGER, C D, LUI, A. T. Y. and AKASOFU, S.-I. (1973b) Observations of the auroral oval and westward traveling surge from the Isis 2 satellite and the Alaska meridian all-sky cameras. J. Geophys. Res., **78**, 3020–3026.

ANGER, C D., SAWCHUK, W. and SHEPHERD, G. G. (1974). Polar cap optical aurora seen from ISIS-2. Magnetospheric Physics, ed. by B. M. MCCORMAC. Dordrecht, D Reidel, 357–368 (Astrophys. Space Sci. Lib., Vol. 44).

ANGER, C. D., MOSHUPI, M. C., WALLIS, D. D., MURPHREE, J S, BRACE, L. H. and SHEPHERD, G. G. (1978) Detached auroral arcs in the trough region To be published in J. Geophys. Res, **83**.

ARAKI, T. (1977) Global structure of geomagnetic sudden commencements. Planet Space Sci., **25**, 373–384.

ARMSTRONG, J. C. (1974) Field-aligned currents in the magnetosphere. Magnetospheric Physics, ed by B. M. MCCORMAC. Dordrecht, D. Reidel, 155–175 (Astrophys Space

Sci. Lib., Vol. 44).

ARMSTRONG, J. C. and ZMUDA, A. J. (1973): Triaxial magnetic measurements of field-aligned currents at 800 km in the auroral region: Initial results. J. Geophys. Res, **78**, 6802–6807.

ARMSTRONG, J. C., AKASOFU, S.-I. and ROSTOKER, G. (1975): A comparison of satellite observations of Birkeland currents with ground observations of visible aurora and ionospheric currents. J. Geophys. Res., **80**, 575–586.

ARNOLDY, R. L. (1974): Auroral particle precipitation and Birkeland currents. Rev. Geophys. Space Phys., **12**, 217–231.

ARNOLDY, R. L. and CHOY, L. W. (1973): Auroral electrons of energy less than 1 keV observed at rocket altitudes. J. Geophys. Res., **78**, 2187–2200.

ARNOLDY, R. L. and LEWIS, P. B. (1977): Correlation of ground-based and topside photometric observations with auroral electron spectra measurements at rocket altitudes. J. Geophys Res., **82**, 5563–5572.

ARNOLDY, R. L., HENDRICKSON, R. A. and WINCKLER, J. R. (1975): Echo 2: Observations at Fort Churchill of a 4-keV peak in low-level electron precipitation. J. Geophys. Res., **80**, 2316–2318.

ARNOLDY, R. L., LEWIS, P. B. and ISAACSON, P. O. (1974): Field-aligned auroral electron fluxes. J. Geophys. Res., **79**, 4208–4221.

ATKINSON, G. (1970): Auroral arcs· Results of the interaction of a dynamic magnetosphere with the ionosphere. J. Geophys. Res., **75**, 4746–4755.

ATKINSON, G. (1972): Magnetospheric flow and substorms. Magnetosphere-Ionosphere Interactions, ed by K. FOLKESTAD. Oslo, Universitetsforlaget, 203–213.

ATKINSON, G. (1973): A proposed experiment to determine if field-aligned currents close by polarization currents. J. Geophys. Res., **78**, 7549–7751.

ATKINSON, G. and HUTCHISON, D. (1978): Effect of the day night ionospheric conductivity gradient on polar cap convective flow. J. Geophys. Res., **83**, 725–729.

AXFORD, W. I. and HINES, C. O. (1961): A unifying theory of high-latitude geophysical phenomena and geomagnetic storms. Can. J. Phys., **39**, 1433–1464.

BALSLEY, B. B., ECKLUND, W. L. and GREENWALD, R. A. (1973): VHF Doppler spectra of radar echoes associated with visual auroral form: Observations and implications. J. Geophys. Res., **78**, 1681–1687.

BANKS, P. M. and DOUPNIK, J. R. (1975): A review of auroral zone electro-dynamics deduced from incoherent scatter radar observations. J. Atmos. Terr. Phys., **37**, 951–999.

BANKS, P. M. and KOCKARTS, G. (1973): Aeronomy, Part A. New York, Academic Press, 430 p.

BANKS, P. M., DOUPNIK, J. R. and AKASOFU, S.-I. (1973): Electric field observations by incoherent scatter radar in the auroral zone. J. Geophys. Res., **78**, 6607–6622.

BANKS, P. M., RINO, C. L. and WICKWAR, V. B. (1974): Incoherent scatter radar observations of westward electric fields and plasma densities in the auroral ionosphere, 1. J. Geophys. Res., **79**, 187–198.

BARON, M. J. (1974): Electron densities within aurorae and other auroral *E* region characteristics. Radio Sci., **9**, 341–350.

BARON, M. J., DE LA BEAUJARDIERE, O. and CRAIG, B. (1970): Project 617 Radar Readiness Achievement Program, Part A, Data Processing and Analysis. Final report, contracts

DASA 01-67-C-0019 and DASA 2519-1, SRI Project 6291 Menlo Park, Calif, Stanford Res Inst, 120 p

BATES, H F. and HUNSUCKER, R. D (1974): Quiet and disturbed electron density profiles in the auroral zone ionosphere. Radio Sci, **9**, 455–465.

BATES, H. F, AKASOFU, S.-I., KIMBALL, D. S and HODGES, J C (1973) First results from the north polar auroral radar J Geophys. Res., **78**, 3857–3864

BAUMJOHANN, W, GREENWALD, R. A. and KUPPERS, F. (1978) Joint magnetometer array and radar backscatter observations of auroral currents in northern Scandinavia J Geophys., **44**, 373–383

BAVASSANO-CATTANEO, M. B and FORMISANO, V. (1978) Low energy electrons and protons in the magnetosphere. Planet. Space Sci, **26**, 51–58.

BECKERS, J. M., GILLIAM, L. B. and STERN, D. P (1977) A search for auroral type motions in solar flares. J. Geophys. Res., **82**, 1915–1918.

BEITING III, E J. and FELDMAN, P. D. (1978). A search for nitric oxide gamma band emission in an aurora. Geophys. Res. Lett., **5**, 51–53

BELON, A. E, ROMICK, G J. and STRINGER, W J. (1974) Proton precipitation during the auroral breakup Planet Space Sci, **22**, 735–742

BERING, E A. and MOZER, F. S. (1975)· A measurement of perpendicular current density in an aurora. J. Geophys. Res., **80**, 3961–3972.

BERING, E. A., BENBROOK, J. R. and SHELDON, W. R (1977) Investigation of the electric field below 80 km from a parachute-deployed payload. J. Geophys Res, **82**, 1925–1929.

BERING, E A, KELLEY, M. C., MOZER, F. S and FAHLESON, U. V (1973) Theory and operation of the split Langmuir probe. Planet. Space Sci, **21**, 1983–2001.

BERKEY, F. T and KAMIDE, Y (1976) On the distribution of global auroras during intervals of magnetospheic quiet J. Geophys. Res., **81**, 4701–4714.

BERKEY, F T, COGGER, L. L, ISMAIL, S and KAMIDE, Y (1976) Evidence for a correlation between sun-aligned arcs and the interplanetary magnetic field direction. Geophys Res Lett, **3**, 145–148.

BERKEY, F T, DRIATSKIY, V. M, HENRIKSEN, K, HULTQVIST, B., JELLY, D, SHCHUKA, T I., THEANDER, A and YLINIEMI, J. (1974) A synoptic investigation of particle precipitation dynamics for 60 substorms in IQSY (1964–65) and IASY (1969) Planet Space Sci, **22**, 255–307.

BERKO, F W (1973) Distribution and characteristics of high latitude field-aligned electron precipitation. J Geophys. Res, **78**, 1615–1618

BERKO, F W and HOFFMAN, R A (1974). Dependence of field-aligned electron precipitation occurrence on season and altitude J Geophys. Res, **79**, 3749–3754.

BERKO, F W, HOFFMAN, R A, BURTON, R. K and HOLZER, R E (1975) Simultaneous particle and field observations of field-aligned currents J Geophys Res, **80**, 37–46.

BERTHELIER, A and GUERIN, C (1973) Influence of the polarity of the interplanetary magnetic field on magnetic activity at high latitudes Space Res, **13**, 661–670

BERTHELIER, A, BERTHELIER, J. J. and GUERIN, C. (1974). The effect of the east-west component of the interplanetary magnetic field on magnetospheric convection as deduced from magnetic perturbations at high latitudes. J Geophys Res., **79**, 3187–3192.

BIRKELAND, K. (1908) The Norwegian Aurora Polaris Expedition 1902–1903. **1**, Christiana,

Aschehoug, 80 p.

BLANC, M (1978): Midlatitude convection electric fields and their relation to ring current development. Geophys. Res. Lett., **5**, 203–206.

BLANC, M., MMAYENC, P., BAUER, P. and TAIEB, C. (1977): Electric field induced drifts from the French incoherent scatter facility. J. Geophys. Res., **82**, 87–97.

BOSQUED, J M. and REME, H. (1974): Evidence of energy dependent mechanisms for the precipitation of auroral electrons. Planet. Space Sci., **22**, 1279–1288.

BOSQUED, J. M., CARDONA, G. and RÈME, H. (1974): Auroral electron fluxes parallel to the geomagnetic field lines. J. Geophys. Res., **79**, 98–104.

BOSTROM, R. (1964) A model of the auroral electrojet. J. Geophys. Res, **69**, 4983–4999.

BOSTROM, R (1971) Polar magnetic substorms. The Radiating Atmosphere, ed. by B. M. MCCORMAC Dordrecht, D. Reidel, 357–370 (Astrophys. Space Sci. Lib., Vol. 24).

BOSTROM, R (1973) Electrodynamics of the ionosphere. Cosmical Geophysics, ed. by A. EGELAND *et al* Oslo, Universitetsforlaget, 276.

BOSTROM, R. (1975a): Mechanisms for driving Birkeland currents. Physics of the Hot Plasma in the Magnetosphere, ed. by B. HULTQVIST and L. STENFLO. New York, Plenum Press, 341–351.

BOSTROM, R. (1975b) Current Systems in the Magnetosphere and Ionosphere. Publ. TRITA-EPP-75-18, Stockholm, Dep. of Plasma Phys., Roy. Inst. of Technol, 28 p.

BOYD, J. S. and DAVIS, T. N. (1977): Rocket measurements of electrons in a system of multiple auroral arcs. J. Geophys. Res, **82**, 1197–1205.

BREKKE, A. (1972) The frequency of pulsating aurora and its relationship to other characteristic parameters. Planet. Space Sci., **20**, 285–289.

BREKKE, A. (1977a): Auroral effects on neutral dynamics. Dynamical and Chemical Coupling between the Neutral and Ionized Atmosphere, ed. by B. GRANDAL and J. A. HOLTET. Dordrecht, D. Reidel, 313–336.

BREKKE, A. (1977b) The relationship between the Harang discontinuity and the substorm injection boundary. Planet. Space Sci, **25**, 1119–1129.

BREKKE, A, DOUPNIK, J. R and BANKS, P. M. (1973): A preliminary study of the neutral wind in the auroral *E* region. J Geophys. Res., **78**, 8235–8250.

BREKKE, A, DOUPNIK, J. R. and BANKS, P. M. (1974a) Incoherent scatter measurement of *E* region conductivities and current in the auroral zone. J. Geophys. Res, **79**, 3773–3790.

BREKKE, A., DOUPNIK, J. R. and BANKS, P. M. (1974b): Observations of neutral winds in the auroral *E* region during the magnetospheric storm of August 3–9, 1972. J. Geophys. Res, **79**, 2448–2456.

BREKKE, A, TSUNODA, R. T and BARON, M. J (1977) On auroral electrojet curvature and the interpretation of azimuth-scan, radar Doppler data. Radio Sci., **12**, 141–148

BROWN, N B., DAVIS, T. N., HALLINAN, T. J. and STENBAEK-NIELSEN, H C. (1976) Altitude of pulsating aurora determined by a new instrumental techniques. Geophys. Res Lett, **3**, 403–405

BROWN, R. R (1978) On the poleward expansion of ionospheric absorption regions triggered by sudden commencements of geomagnetic storms. J. Geophys Res, **83**, 1169–1172

BRYANT, D. A., COURTIER, G. M. and BENNETT, G. (1973). Electron intensities over two auroral arcs. Planet. Space Sci, **21**, 165–177.

BRYANT, D A., HALL, S. D and LEPINE, D R (1978): Electron acceleration in an array of auroral arcs. Planet. Space Sci., **26**, 81–89.

BRYANT, D A, SMITH, M. J. and COURTIER, G. M. (1975)· Distant modulation of electron intensity during the expansion phase of an auroral substorm. Planet. Space Sci., **23**, 867–878.

BURCH, J. L. (1972a) Precipitation of low-energy electrons at high latitudes· Effects of interplanetary magnetic field and dipole tilt angle. J. Geophys. Res, **77**, 6696–6707.

BURCH, J L (1972b)· Preconditions for the triggering of polar magnetic substorms by storm sudden commencements J. Geophys. Res, **77**, 5629–5632.

BURCH, J L (1973a) Effects of interplanetary magnetic sector structure on auroral zone and polar cap magnetic activity. J. Geophys. Res, **78**, 1047–1057.

BURCH, J. L. (1973b): High-latitude proton precipitation and light ion density profiles occurring the magnetic storm initial phase. J. Geophys Res, **78**, 6569–6578.

BURCH, J. L (1973c) Rate of erosion of dayside magnetic flux based on a quantitative study of the dependence of polar cusp latitude on the interplanetary magnetic field. Radio Sci., **8**, 955–964.

BURCH, J L. (1974). Observations of interaction between interplanetary and geomagnetic fields Rev. Geophys Space Phys., **12**, 363–378.

BURCH, J. L and HOFFMAN, R. A. (1974): AGU/NASA topical conference on electrodynamics of substorms and magnetic storms (Report). EOS, Trans, Am. Geophys Union, **55**, 971–977

BURCH, J L., LENNARTSSON, W, HANSON, W. B, HEELIS, R. A, HOFFMAN, J H and HOFFMAN, R A. (1976) Properties of steplike shear flow reversals observed in the auroral plasma by Atmospheric Explorer C. J. Geophys. Res., **81**, 3886–3896

BURLAGA, L F and LEPPING, R. P (1977) The causes of recurrent geomagnetic storms. Planet. Space Sci, **25**, 1151–1161.

BURROWS, J R. (1974) The plasma sheet in the evening sector. Magnetospheric Physics, ed by B. M. MCCORMAC. Dordrecht, D Reidel, 179–188 (Astrophys Space Sci Lib., Vol. 44).

BURROWS, J R, WILSON, M D. and MCDIARMID, I B. (1976) Simultaneous field aligned current and charged particle measurements in the cleft. Magnetospheric Particles and Fields, ed by B M. MCCORMAC. Dordrecht, D Reidel, 111–124 (Astrophys. Space Sci. Lib, Vol. 58).

BURTON, R K, HOLZER, R. E. and SMITH, E J. (1969) Intense magnetic impulses and chorus observed in the auroral zone during particle precipitation (Abstract) EOS, Trans, Am. Geophys Union, **50**, 292.

BURTON, R K, MCPHERRON, R. L. and RUSSELL, C. T (1975a) An empirical relationship between interplanetary conditions and D_{st} J Geophys Res, **80**, 4204–4214.

BURTON, R K., MCPHERRON, R L. and RUSSELL, C. T. (1975b): The terrestrial magnetosphere. A half-wave rectifier of the interplanetary electric field. Science, **189**, 717–718

CAAN, M N, MCPHERRON, R. L. and RUSSELL, C. T. (1973)· Solar wind and substorm-related changes in the lobes of the geomagnetic tail. J. Geophys. Res., **78**, 8087–8096.

CAAN, M N, MCPHERRON, R. L. and RUSSELL, C. T. (1978)· The statistical magnetic signatures of magnetospheric substorms To be published in Planet. Space Sci., **26**.

CAAN, M N, MCPHERRON, R. L and RUSSELL, C. T. (1975) Magnetospheric substorms:

A computerized determination and analysis. Publ. 1380–58, Los Angeles, Inst. Geophys. Planet. Phys., Univ. Calif., 120 p.

CAAN, M. N., MCPHERRON, R. L. and RUSSELL, C. T. (1977): Characteristics of the association between the interplanetary magnetic field and substorms. J. Geophys. Res, **82**, 4837–4840.

CAHILL, L. J., POTTER, W. E., KINTNER, P. M., ARNOLDY, R. L. and CHOY, L. W. (1974)· Field-aligned currents and the auroral electrojet. J. Geophys. Res., **79**, 3147–3154.

CAMPBELL, W. H. and MATSUSHITA, S. (1973): Correspondence of solar field sector direction and polar cap geomagnetic field changes for 1965. J. Geophys. Res., **78**, 2079–2087.

CARLSON, C. W. and KELLEY, M. C. (1977): Observation and interpretation of particle and electric field measurements inside and adjacent to an active auroral arc. J. Geophys Res, **82**, 2349–2357.

CARPENTER, D. L. and AKASOFU, S-I. (1972): Two substorm studies of relations between westward electric fields in the outer plasmasphere, auroral activity, and geomagnetic perturbations. J. Geophys. Res., **77**, 6854–6863.

CARPENTER, L A. and KIRCHHOFF, V. W. (1975): Comparison of high-latitude and mid-latitude ionospheric electric fields. J. Geophys. Res., **80**, 1810–1814.

CASSERLY, R. T., Jr. (1977). Observation of a structured auroral field-aligned current system. J. Geophys. Res, **82**, 155–163.

CASSERLY, R. T, Jr. and CLOUTIER, P. A. (1975)· Rocket-based magnetic observations of auroral Birkeland currents in association with a structured auroral arc. J. Geophys Res, **80**, 2165–2168

CAUFFMAN, D. P. and GURNETT, D. A. (1971): Double-probe measurements of convection electric fields with the INJUN 5 satellite. J. Geophys. Res., **76**, 6014–6027.

CAUFFMAN, D. P. and GURNETT, D. A. (1972): Satellite measurements of high latitude convection electric fields. Space Sci. Rev., **13**, 369–408.

CAVARLY, R. S. (1975): Observations from a chain of all-sky cameras coordinated with satellite auroral zone particle precipitation. M S. Thesis, University of Alaska, Fairbanks, 78 p.

CHACKO, C. C. and MENDILLO, M. (1977): Electron density enhancements in the *F* region beneath the magnetospheric cusp. J. Geophys. Res., **82**, 4757–4762.

CHAPMAN, S (1935) The electric current-system of magnetic storms. J. Geophys. Res, **40**, 349–365.

CHEN, A. J. and ROSTOKER, G. (1974)· Auroral-polar currents during periods of moderate magnetospheric activity. Planet. Space Sci., **22**, 1101–1115.

CHOY, L. W, ARNOLDY, R L., POTTER, W., KINTNER, P. and CAHILL, L. J. (1971)· Field-aligned particle currents near an auroral arc. J. Geophys. Res., **76**, 8279–8298

CHRISTENSEN, A B., ROMICK, G. J and SIVJEE, G. G. (1977): Auroral OI (989 Å) and OI (1027 Å) emissions. J. Geophys. Res., **82**, 4997–5004

CLAUER, C R and MCPHERRON, R. L (1974a) Mapping of the local time-universal time development of magnetospheric substorms using mid-latitude magnetic observations J. Geophys. Res., **79**, 2811–2820.

CLAUER, C. R. and MCPHERRON, R. L. (1974b). Variability of mid-latitude magnetic parameters used to characterize magnetospheric substorms J. Geophys. Res., **79**, 2898–2900.

CLOUTIER, P. A. and ANDERSON, H. R. (1975). Observations of Birkeland currents. Space

Sci. Rev , 17, 563–587

CLOUTIER, P A , SANDEL, B R , ANDERSON, H. R , PAZICH, P M and SPIGER, R J. (1973)· Measurement of auroral Birkeland currents and energetic particle fluxes. J. Geophys Res , 78, 640–647

CORNWALL, J M (1974) Magnetosphere dynamics with artificial plasma clouds Space Sci Rev , 15, 641–699.

CRAVEN, J. D. (1970) A survey of low-energy electron energy fluxes over the northern auroral regions with satellite INJUN-4. J. Geophys Res., 75, 2468–2480.

CRAVEN, J D and FRANK, L. A. (1976): Electron angular distributions above the dayside auroral oval. J Geophys Res., 81, 1695–1699.

CRAVEN, J D and FRANK, L A. (1978)· Energization of polar-cusp electrons at the noon meridian. J Geophys. Res., 83, 2127–2131.

CREUTZBERG, F (1976) Morphology and dynamics of the instantaneous auroral oval. Magnetospheric Particles and Fields, ed. by B. M. MCCORMAC Dordrecht, D Reidel, 235–246 (Astrophys Space Sci Lib., Vol 58)

CROOKER, N U (1975) Solar wind-magnetosphere coupling. Rev Geophys. Space Phys , 13, 955–975

CROOKER, N U (1977a) Explorer 33 entry layer observations. J. Geophys. Res , 82, 515–522.

CROOKER, N U (1977b). The magnetospheric boundary layers A geometrically explicit model. J. Geophys. Res., 82, 3629–3635.

CROOKER, N U and MCPHERRON, R L (1972) On the distinction between the auroral electrojet and partial ring current systems. J Geophys Res , 77, 6886–6892

CUMMINGS, W D (1966): Asymmetric ring currents and the low-latitude disturbance daily variation. J. Geophys Res., 71, 4495–4503.

DALY, P W and WHALEN, B A. (1978). Rocket-borne measurements of particles and ion convection in dayside aurora. J. Geophys Res , 83, 2195–2199.

DAVIS, T N. (1974). Auroral morphology based on DAPP photographs (Abstract) EOS, Trans., Am Geophys. Union, 55, 1008.

DAVIS, T. N. and HALLINAN, T. J. (1976) Auroral spirals, 1 Observations. J Geophys. Res , 81, 3953–3965.

DAVIS, T N. and PARTHASARATHY, R. (1967): The relationship between polar magnetic activity DP and growth of the geomagnetic ring current. J. Geophys. Res , 72, 5825–5836.

DAVIS, T. N and WALLIS, D D. (1972) Observations ionospheric motions using barium ion cloud Space Res , 12, 935.

DEEHR, C S , WINNINGHAM, J D , YASUHARA, F and AKASOFU, S -I (1976) Simultaneous observations of discrete and diffuse auroral by the Isis 2 satellite and airborne instruments J Geophys Res , 81, 5527–5535.

DEEHR, C. S., BGELAND, A , AARSNES, K , AMUNDSEN, R , LINDALEN, H. R , SORAAS, F., DALZIEL, R , SMITH, P , THOMAS, G R , STAUNING, P , BORG, H.. GUSTAFSSON, G , HOLMGREN, L A., RIEDLER, W , RAITT, J , SKOVLI, G , WEDDE, T. and JAESCHKE, R. (1973) Particle and auroral observations from the ESRO 1/AURORAE satellite. J Atmos Terr. Phys , 35, 1979–1993.

DE FEITER, L D (1975) Chromospheric flares or chromospheric aurorae? Space Sci Rev., 17, 181–193

DE LA BEAUJARDIERE, O., VONDRAK, R. and BARON, M. (1977): Radar observations of electric fields and currents associated with auroral arcs. J. Geophys. Res., **82**, 5051–5061.

DERBLOM, H. (1975): Observed characteristics of polar cleft H_α and OI emission. Planet. Space Sci., **23**, 1053–1058.

DOERING, J. P., PETERSON, W. K., BOSTROM, C. O. and ARMSTRONG, J. C. (1975) Measurement of low-energy electrons in the day airglow and day-side auroral zone from AE-C. J. Geophys. Res , **80**, 3934–3944.

DOERING, J. P., POTEMRA, T. A., PETERSON, W. K. and BOSTROM, C O. (1976): Characteristic energy spectra of 1– to 500 eV electrons observed in the high-latitude ionosphere from AE-C. J. Geophys Res., **81**, 5507–5516.

DOUPNIK, J. R., BREKKE, A. and BANKS, P. M. (1977): Incoherent scatter radar observations during three sudden commencements and a Pc 5 event on August 4, 1972. J. Geophys. Res., **82**, 499–514

DOUPNIK, J. R., BANKS, P. M , BARON, M. J., RINO, C. L. and PETRICEKS, J. (1972): Direct measurements of plasma drift velocities at high magnetic latitudes. J. Geophys Res , **77**, 4268–4279.

EASTMAN, T. E., HONES, E. W., Jr., BAME, S. J and ASBRIDGE, J. R. (1976): The magnetospheric boundary layer, Site of plasma, momentum and energy transfer from the magnetocheath into the magnetosphere. Geophys. Res. Lett , **3**, 685–687.

EATHER, R H. (1973): The auroral oval—A reevaluation. Rev. Geophys. Space Phys., **11**, 155–170.

EATHER, R H and MENDE, S. B. (1973). Substorm effects in auroral spectra. J. Geophys. Res., **78**, 7515–7520.

EATHER, R. H., MENDE, S. B. and JUDGE, R. J. R. (1976): Plasma injection at synchronous orbit and spatial and temporal auroral morphology. J. Geophys. Res., **81**, 2805–2824.

ECKLUND, W. L , BALSLEY, B. B. and CARTER, D. A. (1977): A preliminary comparison of *F*-region plasma drifts and *E*-region irregularity drifts in the auroral zone. J. Geophys. Res , **82**, 195–197.

ECKLUND, W. L., BALSLEY, B. B. and GREENWALD, R. A. (1973): Doppler spectra of diffuse radar auroral. J. Geophys. Res , **78**, 4797–4800.

ECKLUND, W. L., BALSLEY, B. B. and GREENWALD, R. A. (1975): Crossed beam measurements of the diffuse radar aurora. J. Geophys. Res., **80**, 1805–1809.

ECKLUND, W. L., CARTER, D. A., KEYS, J. G. and UNWIN, R. S. (1974) Conjugate auroral radar observations of a substorm. J. Geophys. Res., **79**, 3211–3213.

EDMONSON, D. A., PETERSON, W. K., DOERING, J. P. and FELDMAN, P. D. (1977): High resolution electron energy spectra in an active aurora at the onset of the magnetic storm of March 26, 1976. Geophys. Res. Lett., **4**, 75–77.

EDWARDS, T., BRYANT, D. A., SMITH, M. J., FAHLSON, U., FÄLTHAMMER, C.-G. and PEDERSEN, A. (1976) Electric fields and energetic particle participation in an auroral arc. Magnetospheric Particles and Fields, ed. by B. M. MCCORMAC. Dordrecht, D. Reidel, 285–289 (Astrophys. Space Sci. Lib., Vol. 58).

EVANS, D. S. (1974): Precipitating electron fluxes formed by a magnetic field aligned potential difference. J. Geophys. Res., **79**, 2853–2858.

EVANS, D. S (1975) Evidence for the low altitude acceleration of auroral particles. Physics

of the Hot Plasma in the Magnetosphere, ed by B HULTQVIST and L STENFLO New York, Plenum Press, 319–330.

EVANS, D S, MAYNARD, N C, TRPIM, J., JACOBSEN, T. and EGELAND, A (1977): Auroral vector electric field and particle comparisons, 2. Electrodynamics of an arc J Geophys Res, **82**, 2235–2244.

FAIRFIELD, D. H. (1973) Magnetic field signatures of substorms on high-latitude field lines in the nighttime magnetosphere J Geophys Res, **78**, 1553–1562

FAIRFIELD, D H and MEAD, G D (1975) Magnetospheric mapping with a quantitative geomagnetic field model J. Geophys. Res, **80**, 535–542

FELDMAN, P D. and DOERING, J. P (1975) Auroral electrons and the optical emissions of nitrogen J. Geophys Res., **80**, 2808–2812.

FELDSTEIN, Y. I. (1966) Peculiarities in the auroral distribution and magnetic disturbance distribution in high latitudes caused by the asymmetrical form of the magnetosphere. Planet Space Sci, **14**, 121–130

FELDSTEIN, Y I. (1976): Magnetic field variations in the polar region during magnetically quiet periods and interplanetary magnetic fields. Space Sci Rev, **18**, 777–861

FELDSTEIN, Y I and STARKOV, G V (1967) Dynamics of auroral belt and polar geomagnetic disturbances Planet. Space Sci., **15**, 209–229.

FENNELL, J F, MIZERA, P. F and CROLEY, D. R. (1975) Low energy polar cap electrons during quiet times. Proc. 14th Int. Conf Cosmic Rays, 1267–1278.

FEYNMAN, J (1976): Substorms and the interplanetary magnetic field J Geophys Res, **81**, 5551–5555

FOSTER, J. C. and BURROWS, J. R (1976)· Electron fluxes over the polar cap, 1. Intense keV fluxes during poststorm quieting. J Geophys. Res., **81**, 6016–6028

FOSTER, J C. and BURROWS, J. R. (1977): Electron fluxes over the polar cap, 2 Electron trapping and energization on open field lines. J. Geophys. Res, **82**, 5165–5174

FRANK, L A and GURNETT, D A. (1971) Distribution of plasmas and electric fields over the auroral zones and polar caps J. Geophys Res, **76**, 6829–6846

FRANK, L A, SAFLEKOS, N. A and ACKERSON, K. L (1976) Electron precipitation in the postmidnight sector of the auroral zones. J Geophys. Res, **81**, 155–167.

FREDRICKS, R. W, SCARF, F. L. and RUSSELL, C. T. (1973)· Field-aligned currents, plasma waves and anomalous resistivity in the disturbed polar cusp. J Geophys Res, **78**, 2133–2141

FRIIS-CHRISTENSEN, E. and WILHJELM, J. (1975) Polar cap currents for different directions of the interplanetary magnetic field in the Y-Z plane J Geophys Res, **80**, 1248–1260

FUKUNISHI, H (1973) Constitution of proton aurora and electron aurora substorms, Part II Dynamical morphology of proton aurora and electron aurora substorms and phenomenological model for magnetospheric substorms JARE Sci. Rep, Ser. A (Aeronomy), **11**, 19–78

FUKUNISHI, H. (1975): Dynamic relationship between proton and electron auroral substorms J Geophys. Res, **80**, 553–574

FUKUNISHI, H. and TOHMATSU, T (1973) Constitution of proton aurora and electron aurora substorms, Part I. Meridian-scanning photometric system for proton auroras and electron auroras JARE Sci Rep, Ser A (Aeronomy), **11**, 6–18.

FUKUSHIMA, N. (1971): Electric current systems for polar substorms and their magnetic effect below and above the ionosphere. Radio Sci., **6**, 269–275.

FUKUSHIMA, N. (1974): Equivalent current pattern for a field-aligned current into the auroral belt of enhanced electric conductivity. Rep. Ionos. Space Res. Jpn., **28**, 207–214.

FUKUSHIMA, N. (1975): Equivalent current pattern for a field-aligned current into the auroral belt of enhanced electric conductivity, Part III. Case of open field lines on the poleward side and closed field lines on the equatorward side of the auroral belt. Rep. Ionos Space Res. Jpn., **29**, 39–43.

FUKUSHIMA, N. (1976): Generalized theorem for no ground magnetic effect of vertical currents connected with Pedersen currents in the uniform-conductivity ionosphere. Rep. Ionos. Space Res. Jpn., **30**, 35–40.

FUKUSHIMA, N. and KAMIDE, Y. (1973a): Partial ring current models for worldwide geomagnetic disturbances. Rev. Geophys. Space Phys, **11**, 795–853.

FUKUSHIMA, N. and KAMIDE, Y. (1973b) Contribution of magnetospheric bays and S_q fields: A comment on partial ring-current models. Radio Sci., **8**, 1013–1017.

GHIELMETTI, A. G, JOHNSON, R. G., SHARP, R. D. and SHELLEY, E. G. (1978): The latitudinal, diurnal, and altitudinal distributions of upward flowing energetic ions of ionospheric origin. Geophys. Res. Lett, **5**, 59–62.

GIZLER, N. A., KUZNETSOV, B. M., SERGEEV, V. A. and TROSHICHEV, O. A. (1976): The sources of the polar cap and low latitude bay-like disturbances during substorms. Planet. Space Sci., **24**, 1133–1139.

GRAY, A. M. and ECKLUND, W. L. (1974): The Anchorage, Alaska real-time auroral radar monitor: System description and some preliminary analyses. NOAA Tech. Rep. ERL 306–AL 9, Boulder, Colorado, U.S.A., 25 p.

GREBOWSKY, J. M., CHEN, A. J. and TAYLOR, H. A., Jr. (1976): High-latitude troughs and the polar cap boundary. J. Geophys. Res., **81**, 690–694.

GREENWALD, R. A. (1974): Diffuse radar aurora and the gradient-drift instability. J. Geophys. Res., **79**, 4807–4810.

GREENWALD, R. A. (1977): Recent advances in the use of radar auroral backscatter to measure ionospheric electric fields. Dynamical and Chemical Coupling between the Neutral and Ionized Atmosphere, ed. by B. GRANDAL and J. A. HOLTET. Dordrecht, D. Reidel, 291–312.

GREENWALD, R A. (1978): An alternative explanation of the Doppler spectra of current-driven plasma instabilities. Preprint MPAE-W-04-78-06, Katlenburg-Lindau, Max-Planck Institut fur Aeronomie, 28 p.

GREENWALD, R. A. and ECKLUND, W. L. (1975): A new look at radar auroral motions. J. Geophys. Res., **80**, 3642–3648.

GREENWALD, R. A., ECKLUND, W. L. and BALSLEY, B. B. (1973). Auroral currents, irregularities and luminosity. J. Geophys. Res., **78**, 8193–8203.

GREENWALD, R. A., ECKLUND, W. L. and BALSLEY, B. B. (1975): Radar observations of auroral electrojet currents. J. Geophys. Res., **80**, 3635–3641.

GREENWALD, R. A., WEISS, W., NIELSEN, E. and THOMSON, N. R. (1978): STARE—a new radar auroral backscatter experiment in northern Scandinavia. Radio Sci., **13**, 1021–1039.

GUREVICH, A. V, KRYLOV, A. L. and TSEDILINA, E. E. (1976): Electric fields in the earth's magnetosphere and ionosphere. Space Sci. Rev., **19**, 59–160.

GURNETT, D A (1972a) INJUN 5 observations of magnetospheric electric fields and plasma convection Earth's Magnetospheric Processes, ed by B M McCORMAC Dordrecht, D Reidel, 233–253 (Astrophys Space Sci Lib, Vol. 32).

GURNETT, D. A (1972b) Electric field and plasma observations in the magnetosphere Critical Problems of Magnetospheric Physics, ed by E. R DYER Washington, IUCSTP, National Academy of Sciences, 123–138

GURNETT, D A. and AKASOFU, S-I (1974) Electric and magnetic field observations during a substorm on February 24, 1970. J. Geophys Res, **79**, 3197–3200.

GURNETT, D A and FRANK, L A. (1973)· Observed relationship between electric fields and auroral particle precipitation. J. Geophys Res., **78**, 145–170

HAERENDEL, G and PASCHMANN, G. (1975) Entry of solar wind plasma into the magnetosphere Physics of the Hot Plasma in the Magnetosphere, ed by B. HULTQVIST and L STENFLO New York, Plenum Press, 23–35.

HAERENDEL, G., LUST, R and RIEGER, E. (1967)· Motion of artificial ion clouds in the upper atmosphere Planet. Space Sci., **15**, 1–18

HALDOUPIS, C and SOFKO, G (1976)· Doppler spectrum of 42 MHz auroral backscatter. Can J Phys, **54**, 1571–1578

HALLINAN, T J (1976) Auroral spirals, 2. Theory. J. Geophys Res, **81**, 3959–3965.

HANSON, W. B and HEELIS, R A. (1975). Techniques for measuring bulk gas motions from satellites Space Sci Instrum, **1**, 493–524

HANSON, W B, ZUCCARO, D. R, LIPPINCOTT, C R and SANATANI, S (1973) The retarding potential analyzer on Atmospheric Explorer Radio Sci., **8**, 333–342.

HANSEN, A M., BAHNSEN, A. and D'ANGELO, N (1976) The cusp-magnetosheath interface. J Geophys Res, **81**, 556–561

HARANG, L. (1946) The mean field of disturbance of polar geomagnetic storms Terr. Mag, **51**, 353–380

HARGREAVES, J. K. (1974)· Dynamics of auroral absorption in the midnight sector Planet. Space Sci., **22**, 1427–1441.

HARGREAVES, J. K., CHIVERS, H. J. A. and AXFORD, W. I. (1975): The development of the substorm in auroral radio absorption. Planet. Space Sci., **23**, 905–911.

HARPER, R. M. (1977a)· A comparison of ionospheric currents, magnetic variations and electric fields at Arecibo. J. Geophys. Res., **82**, 3233–3242.

HARPER, R M. (1977b)· Tidal winds in the 100- to 200-km region at Arecibo. J. Geophys Res, **82**, 3243–3253.

HARRISON, A. W. and ANGER, C. D. (1977a)· Spectral albedo corrections to ISIS 2 satellite auroral photometer data. Can. J. Phys., **55**, 663–670

HARRISON, A. W. and ANGER, C. D. (1977b)· Earth albedo effects in satellite auroral photometry Can. J Phys, **55**, 929–936.

HAUGE, R. and SORAAS, F. (1975) Precipitation of >115 keV protons in the evening and forenoon sectors in relation to the magnetic activity. Planet Space Sci, **23**, 1141–1154

HAYS, P. B. and ANGER, C. D (1978) The influence of ground scattering on satellite auroral observation. Appl. Opt, **17**, 1898–1905.

HEELIS, R A., HANSON, W. B. and BURCH, J. L (1976)· Ion convection velocity reversals in the dayside cleft J. Geophys Res, **81**, 3803–3809

HEIKKILA, W J. (1975) Is there an electrostafic field tangential to the dayside magnetopause and neutral line? Geophys. Res. Lett., **2**, 154–158.

HEIKKILA, W. J. (1978)· Electric field topology near the dayside magnetopause. J Geophys. Res , **83**, 1071–1077.

HENRIKSEN, K., DEEHR, C. S. and ROMICK, G. J. (1977) Lunar influence on the occurrence of aurora. J Geophys. Res., **82**, 2842–2848.

HEPPNER, J. P. (1972a) Electric field variations during substorms. Planet. Space Sci , **20**, 1475–1498.

HEPPNER, J. P. (1972b): Polar cap electric field distributions related to the interplanetary magnetic field direction. J. Geophys. Res., **77**, 4877–4887.

HEPPNER, J. P. (1972c): Electric fields in the magnetosphere. Critical Problems of Magnetospheric Physics, ed. by E. R. DYER. Washington, IUCSTP, National Academy of Sciences, 107–122.

HEPPNER, J. P. (1972d) The Harang discontinuity in auroral belt ionospheric currents Geofys. Publ., **29**, 105–120.

HEPPNER, J P. (1973)· High latitude electric fields and the modulations related to interplanetary magnetic field parameters. Radio Sci., **8**, 933–948.

HEPPNER, J. P. (1977): Empirical models of high latitude electric field J. Geophys. Res , **82**, 1115–1125.

HEPPNER, J. P., STOLARIK, J. D. and WESCOTT, E. M. (1971): Electric field measurements and the identification of current causing magnetic disturbances in the polar cap. J. Geophys. Res , **76**, 6028–6053.

HILL, T. W. and REIFF, P. H (1977)· Evidence of magnetospheric cusp proton acceleration by magnetic merging at the dayside magnetopause. J. Geophys. Res., **82**, 3623–3630.

HIRSHBERG, J. and HOLZER, T. E. (1975): Relationship between the interplanetary magnetic field and 'isolated substorms'. J. Geophys. Res., **80**, 3553–3556.

HOFFMAN, R. A. and BERKO, F. W. (1971): Primary electron influx to dayside auroral oval. J. Geophys. Res., **76**, 2967–2976.

HOFFMAN, R. A. and BURCH, J. L. (1973): Electron precipitation patterns and substorm morphology. J. Geophys. Res , **78**, 2867–2884.

HOLMGREU, L. A. and APARICIO, B. (1973): Field aligned electron anisotropies observed by the ESRO-1A (Aurorae) satellite. Space Res., **13**, 555–575.

HOLZWORTH, R. H. and MENG, C.-I. (1975). Mathematical representation of the auroral oval. Geophys. Res. Lett., **2**, 377–382.

HOLZWORTH, R. H., BERTHELIER, J. J., CULLERS, D. K., FAHLESON, U. V., FALTHAMMER, C.-G., HUDSON, M. K., JALONEN, L., KELLEY, M. C., KELLOGG, P. J., TANSKANEN, P., TEMERIN, M. and MOZER, F S. (1977): The large-scale ionospheric electric field· Its variation with magnetic activity and relation to terrestrial kilometric radiation. J. Geophys. Res , **82**, 2735–2744.

HONES, E. W., Jr , ASBRIDGE, J. R., BAME, S. J. and SINGER, S. (1973) Substorm variations of the magnetotail plasma sheet from $X_{SM} \approx -6 R_E$ to $X_{SM} \approx -60 R_E$. J. Geophys. Res., **78**, 109–132.

HONES, E. W., Jr , AKASOFU, S.-I., WOLCOTT, J. H., BAME, S. J., FAIRFIELD, D H. and MENG, C -I (1976)· Correlated observations of several auroral substorms. J. Geophys. Res ,

81, 1725–1736

HORNING, B L, MCPHERRON, R L and JACKSON, D D (1974) Application of linear inverse theory to a line current model of substorm current systems. J Geophys Res, **79**, 5202–5210.

HORWITZ, J L and AKASOFU, S.-I (1977) The response of the dayside aurora to sharp northward and southward transitions of the interplanetary magnetic field and to magnetospheric substorms. J. Geophys Res, **82**, 2723–2732

HORWITZ, J L, DOUPNIK, J R and BANKS, P M (1978a) Chatanika radar observations of the latitudinal distributions of auroral zone electric fields, conductivities and currents J. Geophys Res, **83**, 1463–1481.

HORWITZ, J L, DOUPNIK, J R., BANKS, P M, KAMIDE, Y and AKASOFU, S-I (1978b) The latitudinal distributions of auroral zone electric fields and ground magnetic perturbations, and their response to variations in the interplanetary magnetic field J Geophys Res, **83**, 2071–2084

HRUSKA, A (1973) Structure of high-latitude irregular electron fluxes and acceleration of particles in the magnetotail J. Geophys Res, **78**, 7509–7514.

HUGHES, T. J and ROSTOKER, G (1977) Current flow in the magnetosphere and ionosphere during periods of moderate activity J. Geophys. Res, **82**, 2271–2282

HULTQVIST, B (1972) Auroral particles. Geofys Publ, **29**, 27–40.

HULTQVIST, B (1974) Rocket and satellite observations of energetic particle precipitation in relation to optical aurora Ann Geophys, **30**, 233–250.

HULTQVIST, B (1975) The aurora The Magnetosphere of the Earth and Jupiter, ed by V. FORMISANO Dordrecht, D. Reidel, 77–111 (Astrophys Space Sci. Lib, Vol 52)

HULTQVIST, B, BORG, H, CHRISTOPHERSEN, P., RIELDER, W and BERNSTEIN, W. (1974) Energetic protons in the keV energy range and associated keV electrons observed at various local times and disturbance levels in the upper ionosphere. NOAA Tech Rep 305—SEL 29, Boulder, Colorado, U S A, 30 p

HUNSUCKER, R D, ROMICK, G. R, ECKLUND, W L., GREENWALD, R A, BALSLEY, B B and TSUNODA, R T. (1975) Structure and dynamics of ionization and auroral luminosity during the auroral events of March 16, 1972 near Chatanika, Alaska Radio Sci, **10**, 813–822

IGLESIAS, G E and ANDERSON, H R (1975) Neutral hydrogen flux measured at 100- to 200-km altitude in an electron aurora J Geophys Res, **80**, 2169–2171

IIJIMA, T (1973a) Interplanetary and ground magnetic conditions preceding SSC-triggered substorms Rep Ionos Space Res. Jpn, **27**, 205–208

IIJIMA, T. (1973b) Enhancement of the S_q^p field as the basic component of polar magnetic disturbances Rep Ionos Space Res Jpn, **27**, 199–203

IIJIMA, T (1974a) Signatures of field-aligned currents at geostationary satellite ATS 1 and a refined three-dimensional substorm current system Rep Ionos Space Res Jpn, **28**, 173–178

IIJIMA, T (1974b) Development of polar magnetic substorms Rep Ionos Space Res Jpn, **28**, 69–76

IIJIMA, T and KOKUBUN, S (1973)· Geomagnetic S_q^p variation on an extremely quiet day. Rep Ionos Space Res Jpn, **27**, 195–198

IIJIMA, T. and NAGATA, T. (1972): Signatures for substorm development of the growth phase and expansion phase. Planet. Space Sci., **20**, 1095–1112.

IIJIMA, T. and POTEMRA, T. A. (1976a): The amplitude distribution of field-aligned currents at northern high latitudes observed by Triad. J. Geophys Res, **81**, 2165–2174.

IIJIMA, T. and POTEMRA, T. A. (1976b): Field-aligned currents in the dayside cusp observed by Triad J Geophys. Res., **81**, 5971–5979.

IIJIMA, T and POTEMRA, T. A. (1978): Large-scale characteristics of field-aligned currents associated with substorms. J. Geophys. Res., **83**, 599–612.

IMHOF, W. L., NAKANO, G. H., GAINES, E. E. and REAGAN, J. B. (1975a): A coordinated two-satellite study of energetic electron precipitation events. J. Geophys. Res., **80**, 3622–3628.

IMHOF, W. L, NAKANO, G. H. and REAGAN, J. B. (1975b): Satellite observations of X rays associated with energetic electron precipitation near the trapping boundary. J. Geophys. Res, **80**, 3629–3634.

ISMAIL, S, WALLIS, D. D. and COGGER, L. L. (1977): Characteristics of polar cap sun-aligned arcs. J. Geophys. Res., **82**, 4741–4749.

IVANOV, K G. and MIKERINA, N. V. (1973): Southern component of the interplanetary magnetic field and magnetospheric substorms. Geomagn. Aeron., **13**, 412–414.

IYEMORI, T, MAEDA, H. and KAMEI, T. (1978): Impulse response of geomagnetic indices to interplanetary magnetic field. To be published in J. Geomagn. Geoelectr., **30**.

JAGGI, R. K. and WOLF, R. A. (1973): Self-consistent calculation of the motion of a sheet of ions in the magnetosphere. J. Geophys. Res., **78**, 2852–2866.

JEFFRIES, R. A., ROACH, W. H., HONES, E.W., Jr., WESCOTT, E. M., STENBAEK-NIELSEN, H. C., DAVIS, T. N. and WINNINGHAM, J. D. (1975): Two barium plasma injections into the northern magnetospheric cleft. Geophys. Res. Lett., **2**, 285–287.

JOHNSON, R. E. (1976): The multiplicity of auroral infrasonic wave forms. J. Geophys Res, **81**, 6077–6082.

JOHNSON, R. H., SHARP, R. D. and SHELLEY, E. H. (1974): The discovery of energetic He^+ ions in the magnetosphere. J Geophys. Res., **79**, 3135–3139.

JOHNSTONE, A. D. and DAVIS, T. N. (1974): Low-altitude acceleration of auroral electrons during breakup observed by a mother-daughter rocket. J. Geophys. Res., **79**, 1416–1425.

JOHNSTONE, A. D., BOYD, J. S. and DAVIS, T. N. (1974): Study of a small magnetospheric substorm. J. Geophys. Res., **79**, 1403–1415.

JONES, R. A. and REES, M. H. (1973): Time dependent studies of the aurora, 1. Ion density and composition. Planet. Space Sci., **21**, 537–557.

JONES, A. V. (1974): Aurora. Dordrecht, D. Raidel, 301 p. (Geophys. Astrophys. Monogr., Vol 9).

KAMIDE, Y. (1974) Association of DP and DR fields with the interplanetary magnetic field variation. J. Geophys. Res., **79**, 49–55.

KAMIDE, Y. (1978): On current continuity at the Harang discontinuity. Planet. Space Sci, **26**, 237–244.

KAMIDE, Y. and AKASOFU, S.-I. (1974): Latitudinal cross section of the auroral electrojet and its relation to the interplanetary magnetic field polarity. J. Geophys. Res., **79**, 3755–3771.

KAMIDE, Y. and AKASOFU, S.-I. (1975): The auroral electrojet and global auroral features. J. Geophys. Res, **80**, 3585–3602.

KAMIDE, Y and AKASOFU, S-I. (1976a). The location of the field-aligned currents with respect to discrete auroral arcs. J Geophys Res, **81**, 3999–4003

KAMIDE, Y. and AKASOFU, S-I (1976b) The auroral electrojet and field-aligned current. Planet. Space Sci, **24**, 203–213

KAMIDE, Y. and BREKKE, A (1975). Auroral electrojet current density deduced from the Chatanika radar and from the Alaska meridian chain of magnetic observatories J. Geophys. Res, **80**, 587–594

KAMIDE, Y and BREKKE, A (1977) Altitude of the eastward and westward auroral electrojets J Geophys Res, **82**, 2851–2853

KAMIDE, Y and FUKUNISHI, H. (1973) Simultaneous growth of high-latitude positive bay and DR-field in the course of proton aurora substorm J. Atmos Terr Phys, **35**, 2085–2090.

KAMIDE, Y. and FUKUSHIMA. N (1972): Positive geomagnetic bays in evening high-latitudes and their possible connection with partial ring current Rep. Ionos Space Res Jpn, **26**, 79–101

KAMIDE, Y and HORWITZ, J L (1978) Chatanika radar observations of ionospheric and field-aligned currents. J Geophys. Res, **83**, 1063–1070

KAMIDE, Y. and MATSUSHITA, S (1978a) A unified view of substorm sequences J Geophys. Res, **83**, 2103–2108

KAMIDE, Y. and MATSUSHITA, S (1978b) Simulation studies of ionospheric electric fields and currents in relation to field-aligned currents, 1 Quiet periods. To be published in J Geophys Res, **83**

KAMIDE, Y and MATSUSHITA, S (1978c) Simulation studies of ionospheric electric fields and currents in relation to field-aligned currents, 2 Substorms To be published in J Geophys Res

KAMIDE, Y and MCILWAIN, C E. (1974) The onset time of magnetospheric substorms determined from ground and synchronous satellite records J Geophys Res, **79**, 4787–4790.

KAMIDE, Y and ROSTOKER, G (1977) The spatial relationship of field-aligned currents and auroral electrojets to the distribution of nightside auroras J Geophys Res, **82**, 5589–5608.

KAMIDE, Y and WINNINGHAM, J D. (1977) A statistical study of the 'instantaneous' nightside auroral oval The equatorward boundary of electron precipitation as observed by the Isis 1 and 2 satellites J. Geophys. Res., **82**, 5573–5588.

KAMIDE, Y, YASUHARA, F and AKASOFU, S-I (1974) On the cause of northward magnetic field along the negative X axis during magnetospheric substorms Planet Space Sci, **22**, 1219–1229

KAMIDE, Y, AKASOFU, S-I, DEFOREST, S. E and KISABETH, J L (1975) Weak and intense substorms Planet Space Sci., **23**, 579–587

KAMIDE, Y, AKASOFU, S-I and BREKKE, A (1976a) Ionospheric currents obtained from the Chatanika radar and ground magnetic perturbations at the auroral latitude Planet Space Sci, **24**, 193–201

KAMIDE, Y, YASUHARA, F and AKASOFU, S-I (1976b) A model current system for the magnetospheric substorm Planet. Space Sci, **24**, 215–222.

KAMIDE, Y., AKASOFU, S.-I. and ROSTOKER, G (1976c) Field-aligned currents and the auroral electrojet in the morning sector. J Geophys Res, **81**, 6141–6147

KAMIDE, Y, KANAMITSU and AKASOFU, S-I. (1976d) A new method of mapping worldwide

potential contours for ground magnetic perturbations Equivalent ionospheric current representation. J. Geophys. Res., **81**, 3810–3820.

KAMIDE, Y., KROEHL, H. W., KANAMITSU, M., ALLEN, J. H. and AKASOFU, S.-I. (1976e): Equivalent ionospheric current representations by a new method illustrated for 8–9 Nov. 1969 magnetic disturbance. Rep. UAG-55, WDC-A, NOAA, Boulder, Colorado, U S A , 189 p.

KAMIDE, Y., BURCH, J. L., WINNINGHAM, J. D. and AKASOFU, S.-I. (1976f): Dependence of the latitude of the cleft on the interplanetary magnetic field and substorm activity. J. Geophys. Res., **81**, 698–704.

KAMIDE, Y., PERREAULT, P. D., AKASOFU, S.-I. and WINNINGHAM, J. D. (1977a) Dependence of substorm occurrence probability on the interplanetary magnetic field and on the size of the auroral oval. J. Geophys. Res., **82**, 5521–5528.

KAMIDE, Y , AKASOFU, S.-I. and RIEGER, E. P. (1977b) Coexistence of two substorms in the midnight sector. J. Geophys. Res., **82**, 1620–1624.

KAMIDE, Y., MURPHREE, J. S., ANGER, C. D., BERKEY, F. T. and POTEMRA, T. A. (1978)· Simultaneous observations of field-aligned currents and visible auroral by the Triad and Isis 2 satellites. To be published in J. Geophys Res , **83**.

KAN, J. R. and AKASOFU, S.-I. (1978): A mechanism for current interruption in a collisionless plasma. J. Geophys Res., **83**, 735–740.

KANE, R. P. (1974) Relationship between interplanetary plasma parameters and geomagnetic D_{st}. J. Geophys. Res., **79**, 64–72.

KANE, R P. (1976) Geomagnetic field variations. Space Sci. Rev., **18**, 413–540.

KANGAS, J., LUKKARI, L. and HEACOCK, R. R. (1974): On the westward expansion of substorm-correlated particle phenomena. J. Geophys. Res., **79**, 3207–3210.

KANGAS, J , LUKKARI, L., TANSKANEN, P., TREFALL, H., STADNES, J., KREMSER, G. and RIEDLER, W. (1975): On the morphology of auroral-zone X-ray events—IV. Substorm related electron precipitation in the local morning sector. J. Atmos. Terr. Phys , **37**, 1289–1299

KASTING, J. F. and HAYS, P. B. (1977): A comparison between N_2^+ 4278-Å emission and electron flux in the auroral zone. J. Geophys. Res., **82**, 3319–3323.

KAUFMANN, R L., DUSENBERY, P. B., THOMAS, B. J. and ARNOLDY, R. L. (1978) Auroral electron distribution function. J. Geophys. Res., **83**, 586–598.

KAWASAKI, K. and AKASOFU, S.-I. (1973): A possible current system associated with the S_q^p variation. Planet. Space Sci., **21**, 329–337.

KAWASAKI, K. and FUKUSHIMA, N. (1974): Equivalent current pattern of ionospheric and field-aligned currents generated by geomagnetic S_q^p field with closed equatorward auroral boundary. Rep. Ionos Space Res. Jpn., **28**, 187–190.

KAWASAKI, K., FUKUSHIMA, N. and KAMIDE, Y. (1974) Time variation of low latitude geomagnetic bay with three-dimensional substorm current development. Rep Ionos Space Res. Jpn , **28**, 77–82.

KAWASAKI, K , MENG, C.-I and KAMIDE, Y (1974)· The development of the three-dimensional current system during a magnetospheric substorm. Planet. Space Sci , **22**, 1471–1484.

KAWASAKI, K , YASUHARA, F. and AKASOFU, S.-I. (1973). Short-period interplanetary and polar magnetic field variations. Planet. Space Sci., **21**, 1743–1755.

KELLEY, M. C. and MOZER, F. S. (1975) Simultaneous measurement of the horizontal components of the earth's electric field in the atmosphere and in the ionosphere. J. Geophys. Res.,

80, 3275–3276.

KELLEY, M C., STARR, J. A. and MOZER, F. S. (1971) Relationship between magnetospheric electric fields and the motion of auroral forms. J. Geophys. Res., **76**, 5269–5277.

KELLEY, M C, HAERENDEL, G., KAPPLER, H., MOZER, F. S. and FAHLESON, U. V. (1975): Electric field measurements in a major magnetospheric substorm. J. Geophys. Res, **80**, 3181–3195

KELLEY, M. C, PEDERSEM, A, FAHLESON, U. V., JONES, D. and KOHN, D. (1974). Active experiments simulating waves and particle precipitation with small ionospheric barium releases J. Geophys. Res., **79**, 2859–2867.

KINTNER, P M., CAHILL, L. J., Jr. and ARNOLDY, R L. (1974) Current system in an auroral substorm. J. Geophys. Res, **79**, 4326–4330.

KINTNER, P. M., ACKERSON, K. L., GURNETT, D. A. and FRANK, L. A (1978). Correlated electric field and low-energy measurements in the low-altitude polar cusp. J. Geophys Res, **83**, 163–168.

KIRCHHOFF, V. W. and CARPENTER, L. A. (1976): The day-to-day variability in ionospheric electric fields and currents. J. Geophys. Res, **81**, 2737–2742

KISABETH, J. L. (1972) The dynamical development of the polar electrojets. Ph D Thesis, University of Alberta, Canada, 233 p.

KISABETH, J. L. (1978) Interpretation of magnetic perturbations observed over the auroral oval by high altitude polar orbitry satellites. To be submitted to J. Geophys

KISABETH, J. L and ROSTOKER, G. (1971). Development of the polar electrojet during polar magnetic substorms. J. Geophys. Res, **76**, 6815–6828.

KISABETH, J. L. and ROSTOKER, G. (1973)· Current flow in auroral loops and surges infered from ground-based magnetic observations. J. Geophys. Res, **78**, 5573–5584.

KISABETH, J. L. and ROSTOKER, G. (1974): The expansive phase of magnetospheric substorms, 1. Development of the auroral electrojets and auroral arc configuration during a substorm J Geophys Res, **79**, 972–984.

KISABETH, J. L and ROSTOKER, G (1977) Modelling of three-dimensional current systems associated with magnetospheric substorms. Geophys. J. R. Astron Soc, **49**, 655–683.

KIVELSON, M. G. (1976) Magnetospheric electric fields and their variation with geomagnetic activity Rev. Geophys. Space Phys, **14**, 189–197.

KIVELSON, M G, RUSSELL, C. T, NEUGEBAUER, M., SCARF, F. L and FREDRICKS, R W. (1973) Dependence of the polar cusp on the north-south component of the interplanetary magnetic field. J. Geophys. Res, **78**, 3761–3772.

KLUMPAR, D M. (1976) Field-aligned currents in the evening MLT sector and their association with primary and secondary auroral particle fluxes (Abstract). EOS, Trans, Am. Geophys. Union, **57**, 988

KLUMPAR, D. M, BURROWS, J. R and WILSON, M. D (1976). Simultaneous observations of field-aligned currents and particle fluxes in the post-midnight sector. Geophys. Res Lett., **3**, 395–397

KOKUBUN, S (1972) Relationship of interplanetary field structure with development of substorm and storm main phase. Planet. Space Sci., **20**, 1033–1049.

KOKUBUN, S (1979). Jikiken-nai no ULF hadô (ULF waves in the magnetosphere A topical review). To be published in Nankyoku Shiryo (Antarct. Rec), **64**.

KOKUBUN, S. and IIJIMA, T. (1975): Time-sequence of polar magnetic substorms. Planet. Space Sci., **23**, 1483–1494.

KOKUBUN, S., MCPHERRON, R. L. and RUSSELL, C. T. (1977): Triggering of substorms by solar wind discontinuities. J. Geophys. Res., **82**, 74–84.

KONRADI, A., SEMAR, C. L. and FRITZ, T. A. (1975): Substorm-injected protons and electrons and the injection boundary model. J. Geophys. Res., **80**, 543–552.

KONRADI, A., SEMAR, C. L. and FRITZ, T. A. (1976): Injection boundary dynamics during a geomagnetic storm. J. Geophys. Res., **81**, 3851–3865.

KUPPERS, F., UNTIEDT, J. and BAUMJOHANN, W. (1978): A two-dimensional array for ground-based observations of auroral zone electric currents during the IMS. To be published in J. Geophys., **44**.

KUZNETSOV, B. M. and TROSHICHV, O. A. (1977): On the nature of polar cap magnetic activity during undisturbed periods. Planet. Space Sci., **25**, 15–21.

LANGEL, R A. (1973): Average high latitude magnetic field: variation with interplanetary sector and with season. 1, Disturbed conditions. Planet. Space Sci., **21**, 839–855.

LANGEL, R. A. (1974a): Near-earth magnetic disturbance in total field at high latitudes. 1, Summary of data from OGO 2, 4, and 6. J. Geophys. Res., **79**, 2363–2371.

LANGEL, R. A. (1974b): Near-earth magnetic disturbance in total field at high latitudes. 2, Interpretation of data from OGO 2, 4, and 6. J. Geophys. Res., **79**, 2373–2392.

LANGEL, R. A. (1974c): Variation with interplanetary sector of the total magnetic field measured at the OGO-2, 4, and 6 satellites. Planet. Space Sci., **22**, 1413–1425.

LANGEL, R. A. (1975): Relation of variations in total magnetic field at high latitude with the parameters of the interplanetary magnetic field and with DP2 fluctuations. J. Geophys. Res., **80**, 1261–1270.

LASSEN, K. (1972): On the classification of high-latitude auroras. Geofys. Publ., **29**, 87–97.

LASSEN, K. (1974): Relation of the plasma sheet to the nighttime auroral oval. J. Geophys. Res., **79**, 3857–3858.

LASSEN, K. and WEILL, G. (1976). Precipitation of auroral particles in the central polar cap during a sudden commencement magnetic storm. Planet. Space Sci., **24**, 487–498.

LEADABRAND, R. L , BARON, M. J., PETRICEKS, J. and BATES, H. F. (1972): Chatanika, Alaska, auroral zone incoherent scatter facility. Radio Sci., **7**, 747–757.

LEDLEY, B. G. and FARTHING, W. H. (1974): Field-aligned current observations in the polar cusp ionosphere. J. Geophys. Res., **79**, 3124–3128.

LENNARTSSON, O. W. (1973): Ionospheric electric field and current distribution associated with high altitude electric field inhomogeneities. Planet. Space Sci., **21**, 2089–2112.

LEZNIAK, T. W. and WINCKLER, J. R. (1970): Experimental study of magnetospheric motions and the acceleration of energetic electrons during substorms. J. Geophys. Res., **75**, 7075–7098.

LUI, A. T. Y. and ANGER, C. D. (1973). A uniform belt of diffuse auroral emission seen by the Isis-2 scanning auroral photometer. Planet. Space Sci , **21**, 799–809.

LUI, A. T. Y. and BURROWS, J. R. (1978): On the location of auroral arcs near substorm onsets. J. Geophys. Res., **83**, 3342–3348.

LUI, A. T. Y., ANGER, C. D. and AKASOFU, S.-I. (1975): The equatorward boundary of the diffuse aurora and auroral substorms as seen by the Isis-2 auroral scanning photometer.

J. Geophys Res , **80**, 3603–3614.

LUI, A T Y., PERREAULT, P. D., AKASOFU, S -I and ANGER, C D. (1973) The diffuse aurora. Planet Space Sci , **21**, 857–861

LUI, A. T. Y., AKASOFU, S -I , HONES, E. W., Jr , BAME, S J. and MCILWAIN, C. E. (1976) Observation of the plasma sheet during a contracted oval substorm in a prolonged quiet period. J Geophys. Res., **81**, 1415–1419.

LUI, A T. Y., VENKATESAN, D., ANGER, C. D , AKASOFU, S.-I., HEIKKILA, W J., WINNINGHAN, J. D and BURROWS, J. R. (1977). Simultaneous observations of particle precipitations and auroral emissions by the Isis-2 satellite J. Geophys Res , **82**, 2210–2226

LUNDIN, R (1976) Rocket observations of electron spectral and angular characteristics in an "inverted V" event. Planet. Space Sci , **24**, 499–514

LYNCH, J., LEACH, R., PULLIAM, D. and SCHERB, F. (1977) Composition and energy spectrum variations of auroral ions J. Geophys Res , **82**, 1951–1955.

LYNCH, J , PULLIAM, D , LEACH, R and SCHERB, F (1976) The charge spectrum of positive ions in a hydrogen aurora J Geophys. Res , **81**, 1264–1268

MADSEN, M M , IVERSEN, I. B. and D'ANGELO, N. (1976). Measurements of high-latitude ionospheric electric fields by means of balloon-borne sensors J Geophys Res , **81**, 3821–3824

MAEHLUM, B N and MOESTUE, H. (1973). High temporal and spatial resolution observations of low energy electrons by a mother-daughter rocket in the vicinity of two quiescent auroral arcs Planet. Space Sci., **21**, 1957–1967.

MAEZAWA, K. (1976) Magnetospheric convection induced by the positive and negative Z components of the interplanetary magnetic field Quantitative analysis using polar cap magnetic records J Geophys. Res , **81**, 2289–2303.

MAHON, H P , SMIDDY, M and SAGALYN, R. C (1977) Electric fields in diffuse aurora Planet. Space Sci., **25**, 859–868.

MALTSEV, Y P (1974) The effect of ionospheric conductivity on the convection system in the magnetosphere. Geomagn. Aeron , **14**, 128–129

MATSUSHITA, S (1975) Morphology of slowly-varying geomagnetic external fields—A review Phys Earth Planet Inter , **10**, 299–312

MATSUSHITA, S. (1978) IMF and lower thermospheric currents and motions—A review To be published in J. Geomagn. Geoelectr., **30**.

MATSUSHITA, S , TARPLEY, J D and CAMPBELL, W H (1973) IMF sector structure effects on the quiet geomagnetic field. Radio Sci , **8**, 963–975.

MAUK, B H and MCILWAIN, C E (1974) Correlation of K_p with substorm—injected plasma boundary J. Geophys Res , **79**, 3193–3196

MAYNARD, N C (1974a) Electric field measurements across the Harang discontinuity J Geophys Res , **79**, 4620–4631

MAYNARD, N C (1974b) The Harang discontinuity as defined by electric fields (Abstract). EOS, Trans , Am Geophys Union, **55**, 1003

MAYNARD, N C and JOHNSTONE, A D (1974) High-latitude dayside electric field and particle measurements J Geophys Res , **79**, 3111–3123.

MAYNARD, N. C., EVANS, D. S , MAEHLUM, B and EGELUND, E. (1977) Auroral vector electric field and particle comparisons, 1 Premidroy convection. J Geophys Res , **82**, 2227–2236.

MAYNARD, N C., BAHNSEN, A., CHRISTOPHERSEN, P , EGELAND, A. and LUNDIN, R. (1973)· An example of anticorrelation of auroral particles and electric fields J Geophys Res., **78**, 3976–3980

MCDIARMID, D. R. (1976): On errors in the measurement of the aspect sensitivity of radio aurora. J Geophys. Res., **81**, 4007–4009.

MCDIARMID, D. R. and HARRIS, F. R (1976) The structure of a connected sequence of magnetospheric substorms. Planet Space Sci., **24**, 269–280.

MCDIARMID, D. R., HARRIS, F. R. and MCNAMARA, A. G. (1976). Relationships between radio aurora, visual aurora and ionospheric currents during a sequence of magnetospheric substorms Planet. Space Sci , **24**, 717–725.

MCDIARMID, I. B , BURROWS, J. R. and BUDZINSKI, E. E. (1975) Average characteristics of magnetospheric electrons (150 eV to 200 keV) at 1400 km. J. Geophys. Res , **80**, 73–79.

MCDIARMID, I. B , BURROWS, J. R. and BUDZINSKI, E. E. (1976): Particle properties in the dayside cleft. J. Geophys. Res., **81**, 221–226.

MCDIARMID, I. B., BURROWS, J. R. and WILSON, M. D. (1978): Comparison of magnetic field perturbations at high latitudes with charged particle and IMF measurements J. Geophys. Res., **83**, 681–690.

MCDIARMID, I. B., BUDZINSKI, E. E., WILSON, M. D. and BURROWS, J. R (1977): Reverse polarity field-aligned currents at high latitudes. J. Geophys. Res., **82**, 1513–1518.

MCEWEN, D J. (1977): Electron precipitation observations from a rocket flight through the dayside auroral oval. Planet. Space Sci., **25**, 1166–1175.

MCILWAIN, C. E. (1974). Substorm injection boundaries. Magnetospheric Physics, ed. by B. M. MCCORMAC. Dordrecht, D. Reidel, 143–154 (Astrophys. Space Sci. Lib., Vol. 44).

MCILWAIN, C. E. (1975): Auroral electron beans near the magnetic equator. Physics of the Hot Plasma in the Magnetosphere, ed. by B. HULTQVIST and L. STENFLO. New York, Plenum Press, 91–112.

MCPHERRON, R. L. (1974) Critical problems in establishing the morphology of substorms in space Magnetospheric Physics, ed. by B. M. MCCORMAC. Dordrecht, D Reidel, 335–349 (Astrophys. Space Sci Lib., Vol. 44).

MCPHERRON, R. L. and BARFIELD, J. N. (1978): A seasonal change in the effect of field-aligned currents at synchronous orbit. To be published in J. Geophys. Res., **83**

MCPHERRON, R. L , RUSSELL, C. T. and AUBRY, M. P. (1973a): Satellite studies of magnetospheric substorms, 9, Phenomenological model for substorms. J. Geophys. Res., **78**, 3131–3149.

MCPHERRON, R L , RUSSELL, C T., KIVELSON, M G. and COLEMAN, P. J., Jr. (1973b) Substorms in space: The correlation between ground and satellite observations of the magnetic field. Radio Sci , **8**, 1059–1070.

MEAD, G D. and FAIRFIELD, D. H. (1975). A quantitative magnetosphere model derived from spacecraft magnetometer data J. Geophys. Res., **80**, 523–534.

MENDE, S B and EATHER, R. H. (1975) Spectroscopic determination of the characteristics of precipitating auroral particles. J. Geophys. Res , **80**, 3211–3216.

MENDE, S. B. and SHELLEY, E. G (1976): Coordinated ATS 5 electron flux and simultaneous auroral observations. J Geophys Res., **81**, 97–110.

MENG, C -I. (1976) Simultaneous observations of low energy electron precipitation and

optical auroral arcs in the evening sector by the DMSP 32 satellite. J. Geophys. Res., **81**, 2771–2785.

MENG, C.-I. and AKASOFU, S.-I. (1969) A study of polar magnetic substorms, 2. Three-dimensional current system. J. Geophys. Res., **74**, 4035–4053.

MENG, C.-I. and AKASOFU, S.-I. (1976) The relation between the polar cap auroral arc and the auroral oval arc. J. Geophys. Res., **81**, 4004–4006.

MENG, C.-I. and KROEHL, H. W. (1977) Intense uniform precipitation of low-energy electrons over the polar cap. J. Geophys. Res., **82**, 2305–2310.

MENG, C.-I., AKASOFU, S.-I. and ANDERSON, K. A. (1977). Dawn-dusk gradient of the precipitation of low-energy elections over the polar cap and its relation to the interplanetary magnetic field. J. Geophys. Res., **82**, 5271–5273.

MENG, C.-I., HOLZWORTH, R. H. and AKASOFU, S.-I. (1977) Auroral circle-delineating the poleward boundary of the quiet auroral belt. J. Geophys. Res., **82**, 164–172.

MENG, C.-I., SNYDER, A. L., Jr., and KROEHL, H. W. (1978). Observations of auroral westward traveling surges and electron precipitations. J. Geophys. Res., **83**, 575–579.

MENG, C.-I., TSURUTANI, B., KAWASAKI, K. and AKASOFU, S.-I. (1973) Cross-correlation analysis of the *AE* index and the interplanetary magnetic field B_z component. J. Geophys. Res., **78**, 617–629.

MIKKELSEN, I. S., JORGENSEN, T. S. and KELLEY, M. C. (1975) Observation and interpretation of plasma motions in the polar cap ionosphere during magnetic substorms. J. Geophys. Res., **80**, 3197–3204

MILLER, J. R. and WHALEN, B. A. (1976). Characteristics of auroral proton precipitation observed from sounding rockets. J. Geophys. Res., **81**, 147–154.

MISHIN, V. M. (1977). High-latitude geomagnetic variations and substorms. Space Sci. Rev., **19**, 621–690.

MIZERA, P. F. (1974) Observations of precipitating protons with ring current energies. J. Geophys. Res., **79**, 581–588.

MIZERA, P. F. and FENNELL, J. F. (1978): Satellite observations of polar, magnetotail lobe, and interplanetary electrons at low energies. Rev. Geophys. Space Phys., **16**, 147–180.

MIZERA, P. F., CROLEY, D. R., Jr., MORSE, F. A. and VAMPOLA, A. L. (1975) Electron fluxes and correlations with quiet time auroral arcs. J. Geophys. Res., **80**, 2129–2136.

MOE, K., MOE, M. M., CARTER, V. L. and RUGGERA, M. B., Jr. (1977) The correlation of thermospheric densities with charged particle precipitation through the magnetospheric cleft. J. Geophys. Res., **82**, 3304–3308

MONTBRIAND, L. E. (1971) The proton aurora and auroral substorms. The Radiating Atmosphere, ed. by B. M. McCORMAC. Dordrecht, D. Reidel, 336–372 (Astrophys. Space Sci. Lib., Vol. 24).

MOORCROFT, D. R. and TSUNODA, R. T. (1978) Rapid-scan Doppler-velocity maps of the UHF diffuse radar aurora. To be published in J. Geophys. Res., **83**.

MOREELS, G., CHAHROKHI, D. and BLAMONT, J. E. (1976). OH emission intensity measurements during the 1969 NASA airborne auroral expedition. J. Geophys. Res., **81**, 5467–5478.

MORGAN, B. G. and ARNOLDY, R. L. (1978) A determination of *F* region convective electric fields from rocket measurements of ionospheric thermal ion spectra. J. Geophys. Res., **83**, 1055–1058.

MOZER, F. S. (1973a). Electric fields and plasma convection in the plasmasphere Rev. Geophys. Space Phys., **11**, 755–790.

MOZER, F. S. (1973b): Analysis of techniques for measuring DC and AC electric fields in the magnetosphere. Space Sci. Rev., **14**, 272.

MOZER, F. S. (1973c) On the relationship between the growth and expansion phases of substorms and magnetospheric convection. J. Geophys Res., **78**, 1719–1722.

MOZER, F. S. and FAHLESON, U. V. (1970): Parallel and perpendicular electric fields in an aurora. Planet Space Sci., **18**, 1563–1571.

MOZER, F. S. and LUCHT, P. (1974): The average auroral zone electric field. J. Geophys. Res., **79**, 1001–1006.

MOZER, F. S., BOGOTT, F. H. and TSURUTANI, B. (1973) Relations between ionospheric electric fields and energetic trapped and precipitated electrons. J. Geophys. Res., **78**, 630–639.

MOZER, F S, SERLIN, R, CASPENTER, D. L. and SIREN, J. (1974): Simultaneous electric field measurements near $L=4$ from conjugate balloons and whistlers. J Geophys. Res., **79**, 3215–3217.

MOZER, F S, CARLSON, C. W., HUDSON, M. K., TORBERT, R. B., PARADY, B., YATTEAU, J and KELLEY, M. C. (1977): Observations of paired electrostatic shocks in the polar magnetosphere. Phys. Rev. Lett., **38**, 292–295.

MURAYAMA, T and HAKAMADA, K. (1975): Effects of solar wind parameters on the development of magnetospheric substorms. Planet. Space Sci., **23**, 75–91.

MURPHREE, J. S. and ANGER, C. D. (1978)· An observation of the instantaneous optical auroral distribution by ISIS-2. To be published in J. Geophys. Res., **83**.

NAGATA, T. (1975): Auroral flares and solar flares. Space Sci. Rev., **17**, 205–220.

NAGATA, T and FUKUSHIMA, N. (1971): Morphology of magnetic disturbance. Encyclopedia of Physics, **49**, New York, Springer Verlag, 5–130.

NAGATA, T, HIRASAWA, T., TAKIZAWA, M. and TOHMATSU, T. (1975): Antarctic substorm events observed by sounding rockets, ionization of the D- and E-regions by auroral electrons. Planet. Space Sci., **23**, 1321–1327.

NISHIDA, A. (1975): Interplanetary field effect on the magnetosphere. Space Sci Rev., **17**, 353–389.

NISHIDA, A. and HONES, E W., Jr. (1974): Association of plasma sheet thinning with neutral line formation in the magnetotail. J. Geophys. Res., **79**, 535–547.

NISHIDA, A. and NAGAYAMA, N. (1975): Magnetic-field observations in the low-latitude magnetotail during substorms. Planet. Space Sci., **23**, 1119–1125.

NOPPER, R. W, Jr. and HERMANCE, J. F. (1974): Phase relations between polar magnetic substorm fields at the surface of a finite conducting earth. J. Geophys. Res., **79**, 4799–4801.

OBAYASHI, T. (1975): Energy build-up and release mechanisms in solar and auroral flares. Space Sci Rev, **17**, 195–203.

OGAWA, T. (1973): Analyses of measurement techniques of electric fields and currents in the atmosphere. Contrib. Geophys. Inst. Kyoto Univ., **13**, 111–139.

OGAWA, T. (1976) Possibility of measuring the large scale electric field at ground level Planet. Space Sci, **24**, 801–802.

OGUTI, T. (1973)· Hydrogen emission and electron aurora at the onset of the auroral breakup. J. Geophys Res, **78**, 7543–7547.

OGUTI, T (1974a)· Rotational deformations and related drift motions of auroral arcs. J. Geophys Res, **79**, 3861–3865.

OGUTI, T (1974b) Dynamics of auroras during substorms (Extended abstract). EOS, Trans, Am Geophys. Union, **55**, 1008–1009

OGUTI, T (1975a) Metamorphoses of aurora Mem Natl Inst. Polar Res, Ser A, **12**, 101 p

OGUTI, T (1975b) Similarity between global auroral deformations in DAPP photographs and small scale deformations observed by a TV camera. J Atmos. Terr. Phys, **37**, 1413–1420

OGUTI, T (1975c) Two-tiered auroral band. J Atmos. Terr Phys, **37**, 1501–1507

OGUTI, T (1976) Recurrent auroral patterns J Geophys Res, **81**, 1782–1786.

OGUTI, T and WATANABE, T. (1976) Quasi-periodic poleward propagation of dawn aurorae and associated geomagnetic pulsations. J. Atmos. Terr. Phys., **38**, 543–549

OLDENBURG, D W. (1976): Ionospheric current structure as determined from ground-based magnetometer data. Geophys. J. R. Astron. Soc., **46**, 41–66

OLDENBURG, D W (1978)· A quantitative technique for modeling ionospheric and magnetospheric current distributions J Geophys. Res, **83**, 3320–3326

OLESEN, J K, PRIMDAHL, F., SPANGSLEV, F., UNGSTRUP, E, BAHNSEN, A, FAHLESON, U. V., FALTHAMMER, C-G. and PETERSEN, A. (1976). Rocket-borne wave, field and plasma observations in unstable polar cap *E* region. Geophys Res. Lett, **3**, 399–403.

OLSON, J. V and ROSTOKER, G (1975) Pi 2 pulsations and the auroral electrojet Planet Space Sci, **23**, 1129–1139.

OLSON, J. V and ROSTOKER, G. (1977) Latitude variation of the spectral components of auroral zone Pi 2. Planet. Space Sci., **25**, 663–672.

PARK, C G. (1976)· Downward mapping of high-latitude ionospheric electric fields to the ground J Geophys Res, **81**, 168–174.

PARK, C. G. and MENG, C-I (1973): Distortions of the nightside ionosphere during magnetospheric substorms. J. Geophys Res., **78**, 3828–3840.

PARK, D. (1974) Magnetic field at the earth's surface produced by a horizontal line current J. Geophys Res, **79**, 4802–4804.

PARK, R. J. (1974). Comparison of field-aligned currents with ionospheric currents and electric fields at Chatanika, Alaska (Abstract). EOS, Trans., Am Geophys Union, **55**, 1175

PASCHMANN, G, HAERENDEL, G., SCKOPKE, N., ROSENBAUER, H. and HEDGECOCK, P. C. (1976): Plasma and magnetic field characteristics of the distant polar cusp near local noon The entry layer. J Geophys Res, **81**, 2883–2899.

PATEL, V L and DESAI, U D. (1973) Interplanetary magnetic field and geomagnetic D_{st} variations Astrophys Space Sci, **20**, 431–438.

PAZICH, P M and ANDERSON, H. R. (1975) Rocket measurement of auroral electron fluxes associated with field-aligned currents J. Geophys. Res, **80**, 2152–2160.

PELLAT, R and LAVAL, G. (1972) Magnetospheric substorm phenomena Critical Problems of Magnetospheric Physics, ed. by E. R DYER. Washington, IUCSTP, 237 p.

PELLINEN, R J and HEIKKILA, W J (1977). Observations of auroral breakup, Paper GA 463, presented at IAGA Seattle Meeting, August 1977 (Abstract). EOS, Trans, Am Geophys Union, **58**, 757.

PEMBERTON, E. V. and SHEPHERD, G. G (1975) Spatial characteristics of auroral brightness fluctuation spectra Can J Phys, **53**, 504–515.

PERREAULT, P. D (1974). On the relationship between interplanetary magnetic fields and magnetospheric storms and substorms. Ph. D. Thesis, University of Alaska, Fairbanks, 205 p.

PERREAULT, P. D. and AKASOFU, S.-I. (1978): A study of geomagnetic storms. To be published in Geophys. J.

PERREAULT, P. D, BARON, M. J. and STENBAEK-NIELSEN, H. C. (1977): Comparison of Chatanika radar optical measurements of *E*-region neutral winds. Geophys. Res Lett., **4**, 573–577.

PETERSON, W. K., DOERING, J. P., POTEMRA, T. A., MCENTIRE, R. W., BOSTROM, C O., HOFFMAN, R. A., JANETZKE, R. W. and BURCH, J. L. (1977): Observations of 10-eV to 25-keV electrons in steady diffuse aurora from Atmospheric Explorer C and D. J. Geophys Res., **82**, 43–47.

PFOTZER, G. (1976): Review of important problems in physics of the auroral zone. Eur Space Agency Sci. Tech. Rev., **2**, 181–197.

PIKE, C. I and WHALEN, J. A. (1974)· Satellite observations of auroral substorms. J. Geophys. Res, **79**, 985–1000.

PIKE, C P., WHALEN, J. A. and BUCHAU, J. (1977): A 12-hour case study of auroral phenomena in the midnight sector: F layer and 6300-Å measurements. J. Geophys. Res., **82**, 3547–3559.

PIKE, C. P, MENG, C.-I, AKASOFU, S.-I and WHALEN, J. A. (1974) Observed correlations between interplanetary magnetic field variations and the dynamics of the auroral oval and the high-latitude ionosphere. J. Geophys. Res., **79**, 5129–5142.

POTEMRA, T. A. (1977): Large-scale characteristics of field-aligned currents determined from the TRIAD magnetometer experiment. Dynamical and Chemical Coupling between the Neutral and Ionized Atmosphere, ed by B. GRANDAL and J. A. HOLTET Dordrecht, D. Reidel, 337–352.

POTEMRA, T. A., DOERING, J. P., PETERSON, W K., BOSTROM, C. O., HOFFMAN, R. A. and BRACE, L H. (1978) AE-C observations of low energy particle and ionospheric temperatures in the turbulent polar cusp: Evidence for the Kelvin-Helmholtz instability. J. Geophys. Res., **83**, 3877–3882.

POTEMRA, T. A., PETERSON, W. K., DOERING, J. P., BOSTROM, C. O., MCENTIRE, R. W. and HOFFMAN, R. A. (1977): Low-energy paritcle observations in the quiet dayside cusp from AE-C and AE-D. J. Geophys. Res., **82**, 4765–4774.

POTTER, W. E (1970)· Rocket measurements of auroral electric and magnetic fields. J. Geophys. Res., **75**, 5415–5431.

PRIMDAHL, F. and SPANGSLEV, F. (1977): Cross-polar cap horizontal *E* region currents related to magnetic disturbances and to measured electric fields. J. Geophys. Res, **82**, 1137–1143.

PRIMDAHL, F., OLESEN, J. K. and SPANGSLEV, F. (1974): Backscatter from a postulated plasma instability in the polar cap ionosphere and the direct measurement of a horizontal *E* region current. J. Geophys. Res., **79**, 4262–4268.

PUDOVKIN, M. I. (1974): Electric fields and currents in the ionosphere. Space Sci. Rev, **16**, 727–770

PYTTE, T. and WEST, H. I, Jr. (1978b): Ground-satellite correlations during pre-substorm magnetic field configuration changes and plasma sheet thinning in the near-earth magnetotail J. Geophys Res., **83**, 3791–3804.

PYTTE, T., MCPHERRON, R L. and KOKUBUN, S (1976b)· The ground signatures of the expansion phase during multiple onset substorms Planet. Space Sci., **24**, 1115–1132

PYTTE, T , MCPHERRON, R. L , KIVELSON, M. G., WEST, H I , Jr. and HONES, E. W , Jr. (1976c) Multiple-satellite studies of magnetospheric substorms· Radial dynamics of the plasma sheet J Geophys. Res., **81**, 5921–5933

PYTTE, T , MCPHERRON, R L , KIVELSON, M. G., WEST, H I , Jr. and HONES, E. W (1978a) Multiple-satellite studies of magnetospheric substorms· Plasma sheet recovery and the poleward leap of auroral-zone activity J. Geophys. Res , **83**, 663–678.

PYTTE, T , TREFALL, H , KREMSER, G , JALONEN, L. and RIEDLER, W (1976a) On the morphology of energetic ($\geq$30 keV) electron precipitation during the growth phase of magnetospheric substorms J. Atmos. Terr. Phys , **38**, 739–752

RAITT, W. J and SOJKA, J. J. (1977) Field-aligned suprathermal electron fluxes below 270 km in the auroral zone Planet. Space Sci , **25**, 5–13

REARWIN, S and HONES, E W , Jr (1974) Near-simultaneous measurement of low-energy electrons by sounding rocket and satellite. J. Geophys. Res., **79**, 4322–4325.

REASONER, D L. and CHAPPELL, C. R. (1973) Twin payload observations of incident and backscattered auroral electrons J. Geophys. Res , **78**, 2176–2186.

REES, M H (1963) Auroral ionization and excitation by incident energetic electrons Planet. Space Sci , **11**, 1209–1220.

REES, M H (1975): Magnetospheric substorm energy dissipation in the atmosphere Planet Space Sci , **23**, 1589–1596.

REES, M. H. (1975) Processes and emissions associated with electron precipitation. Atmospheres of Earth and the Planets, ed. by B. M MCCORMAC Dordrecht, D Reidel, 323–332 (Astrophys. Space Sci Lib , Vol. 51).

REES, M H and JONES, R A. (1973) Time dependent studies of the aurora—II Spectroscopic morphology. Planet. Space Sci., **21**, 1213–1235

REES, M. H., ROMICK, G. J , ANDERSON, H. R. and CASSERLY, R. T., Jr (1976): Calculation of auroral emissions from measured electron precipitation Comparison with observation. J. Geophys Res , **81**, 5091–5096.

REES, M H , STEWART, A. I., SHARP, W. E , HAYS, P. B., HOFFMAN, R. A , BRACE, L H., DOERING, J P and PETERSON, W. K. (1977): Coordinated rocket and satellite measurements of an auroral event, 1. Satellite observations and analysis. J Geophys. Res , **82**, 2250–2265.

REIFF, P. H , HILL, T. W and BURCH, J. L. (1977) Solar wind plasma injection at the dayside magnetospheric cusp J Geophys. Res , **82**, 479–491.

RÉME, H and BOSQUED, J M (1971) Evidence near the auroral ionosphere of a parallel electric field deduced from energy and angular distributions of low-energy particles J Geophys. Res , **76**, 7683–7693

RICHMOND, A D (1976) Electric field in the ionosphere and plasmasphere on quiet days J Geophys. Res , **81**, 1447–1450

RIEDLER, W (1972) Auroral particle precipitations Earth's Magnetospheric Processes, ed by B. M. MCCORMAC. Dordrecht, D. Reidel, 133–148 (Astrophys Space Sci Lib , Vol 32).

RIEDLER, W and BORG, H. (1972). High latitude precipitation of low-energy particles as observed by ESROIA. Space Res , **12**, 1397–1410

RINO, C L , BREKKE, A and BARON, M J (1977) High-resolution auroral zone *E* region

neutral wind and current measurements by incoherent scatter radar. J. Geophys. Res., **82**, 2295–2306.

RINO, C. L., WICKWAR, V. B., BANKS, P. M., AKASOFU, S.-I. and RIEGER, E. (1974): Incoherent scatter radar observations of westward electric fields, 2. J. Geophys. Res., **79**, 4669–4678.

ROBLE, R. G. and REES, M. H. (1977): Time-dependent studies of the aurora: Effects of particle precipitation on the dynamic morphology of ionospheric and atmospheric properties. Planet. Space Sci., **25**, 991–1003.

ROEDERER, J. G. (1977): Global problems in magnetospheric plasma physics and prospects for their solution. Space Sci. Rev., **21**, 23–71.

ROGERS, E., NELSON, D. and SAVAGE, R. (1974): Auroral photography from a satellite. Science, **183**, 951–953.

ROMICK, G. J., BELON, A. E. and STRINGER, W. J. (1974): Photometric measurements of H-beta in the aurora. Planet. Space Sci., **22**, 725–733.

ROMICK, G. J., ECKLUND, W. L., GREENWALD, R. A., BALSLEY, B. B. and IMHOF, W. L. (1974): The interrelationship between the >130-keV electron trapping boundary, the VHF radar backscatter, and the visual aurora. J. Geophys. Res., **79**, 2439–2443.

ROSENBAUER, H., GRÜNWALDT, H., MONTGOMERY, M. D., PASCHMANN, G. and SCKOPKE, N. (1975): HEOS-2 plasma observations in the distant polar magnetosphere: The plasma mantle. J. Geophys. Res., **80**, 2723–2737.

ROSENBERG, T. J., FOSTER, J. C., MATTHEWS, D. L., SHELDON, W. R. and BENBROOK, J. R. (1977): Microburst electron precipitation at L≈4. J. Geophys. Res., **82**, 177–180.

ROSSBERG, L. (1976): Prebay electron precipitation as seen by balloons and satellites. J. Geophys. Res., **81**, 3437–3440.

ROSTOKER, G. (1972): Geomagnetic indices. Rev. Geophys. Space Phys., **10**, 935–950.

ROSTOKER, G. (1974a): Current flow in the magnetosphere during magnetospheric substorms. J. Geophys. Res., **79**, 1994–1998.

ROSTOKER, G. (1974b): Ground based magnetic signatures of the phases of magnetospheric substorms. Magnetospheric Physics, ed. by B. M. MCCORMAC. Dordrecht, D. Reidel, 325–337 (Astrophys. Space Sci. Lib., Vol. 44).

ROSTOKER, G. (1977): Recent developments in the area of electric fields, magnetic fields including ground based observations. Preprint, Inst. Earth. Planet. Phys., Univ. Alberta, Edmonton, Canada, 75 p.

ROSTOKER, G. and BOSTROM, R. (1976): A mechanism for driving the gross Birkeland current configuration in the auroral oval. J. Geophys. Res., **81**, 235–244.

ROSTOKER, G. and HRON, M. (1975): The eastward electrojet in the dawn sector. Planet. Space Sci., **23**, 1377–1389.

ROSTOKER, G. and KISABETH, J. L. (1973): Responses of the polar electrojets in the evening sector to polar magnetic substorms. J. Geophys. Res., **78**, 5559–5571.

ROSTOKER, G , ARMSTRONG, J. C. and ZMUDA, A. J. (1975): Field-aligned current flow associated with the intrusion of the substorm intensified westward electrojet into the evening sector J. Geophys. Res., **80**, 3571–3579.

ROSTOKER, G., SHARMA, R. P. and HRON, M. P. (1976): Thermal plasma enhancements in the topside ionosphere and their relationship to the auroral electrojets. Planet. Space Sci , **24**, 1081–1091.

ROSTOKER, G., KISABETH, J. L., SHARP, R. D. and SHELLEY, E. G. (1975): The expansive phase of magnetospheric substorms, 2. The response at synchronous altitude of particles of different energy range. J. Geophys. Res., **80**, 3557–3570.

ROSTOKER, G , CHEN, A. J , YASUHARA, F., AKASOFU, S.-I. and KAWASAKI, K. (1974)· High latitude equivalent current systems during extremely quiet times. Planet. Space Sci., **22**, 427–437.

ROSTOKER, G , WINNINGHAM, J. D., KAWASAKI, K., BURROWS, J. R., and HUGHES, T. J. (1978): Energetic particle precipitation into the high latitude ionosphere and the auroral electrojet and field-aligned current flow at the dusk meridian. To be published in J. Geophys. Res , **83**.

ROYRVIK, O (1976): Pulsating aurora Local and global morphology. Ph. D. Thesis, University of Alaska, Fairbanks, 120 p.

ROYRVIK, O and DAVIS, T. N. (1977)· Pulsating aurora Local and global morphology. J. Geophys. Res., **82**, 4720–4728.

RUSSELL, C. T. (1977)· High altitude observations of Birkeland currents Ann Geophys., **33**, 435–448

RUSSELL, C. T. and ATKINSON, G. (1973): Comments on a paper by J. P. HEPPNER, "Polar cap electric field distributions related to interplanetary magnetic field direction". J. Geophys. Res , **78**, 4001–4002.

RUSSELL, C. T and MCPHERRON, R. L. (1973): The magnetotail and substorms. Space Sci. Rev , **15**, 205–235.

RUSSELL, C. T., NEUGEBAUER, M. and KIVELSON, M. G (1974a) OGO 5 observations of the magnetopause. Correlated Interplanetary and Magnetospheric Observations, ed by D. E. PAGE. Dordrecht, D. Reidel, 139–150 (Astrophys. Space Sci. Lib., Vol. 42).

RUSSELL, C. T., MCPHERRON, R. L and BURTON, R. K. (1974b)· On the cause of geomagnetic storms. J. Geophys. Res., **79**, 1105–1109.

SAFLEKOS, N. A , POTEMRA, T. A. and IIJIMA, T. (1978). Small-scale transverse magnetic disturbances in the polar regions observed by Triad. J. Geophys. Res., **83**, 1493–1503.

SAITO, T. (1974): Examination of the models for the substorm-associated magnetic pulsations, Ps 6. Sci. Rep. Tôhoku Univ., Ser. 5 (Geophys.), **22**, 35–59.

SAITO, T., SAKURAI, T. and KOYAMA, Y. (1976a): Mechanism of association between Pi 2 pulsation and magnetospheric substorm. J. Atmos. Terr. Phys., **38**, 1265–1269.

SAITO, T., YUMOTO, K. and KOYAMA, Y. (1976b): Magnetic pulsation Pi 2 as a sensitive indicator of magnetospheric substorm. Planet. Space Sci., **24**, 1025–1029.

SAITO, T , TAKAHASHI, F., MORIOKA, A. and KUWASHIMA, M. (1974): Fluctuations of electron precipitation to the dayside auroral zone modulated by compression and expansion of the magnetosphere. Planet. Space Sci., **22**, 939–953.

SAKURAI, T. and SAITO, T. (1976)· Magnetic pulsation Pi 2 and substorm onset Planet. Space Sci , **24**, 573–575.

SANDFORD, P. B. (1968)· Variations of auroral emissions with time, magnetic activity and the solar cycle. J. Atmos. Terr. Phys., **30**, 1921–1935.

SATO, T. (1974): Possible sources of field-aligned currents. Rep Ionos Space Res Jpn., **28**, 179–184

SATO, T. (1976) Field-aligned currents and polar cap electric fields J Geophys. Res , **81**, 263–264.

SERGEEV, V. A. (1974): On the longitudinal localization of the substorm active region and its changes during the substorm. Planet. Space Sci., **22**, 1341–1343.

SERGEEV, V. A. and SHUMILOV, O. I. (1974a): Mechanism of electron precipitation in the morning and afternoon magnetosphere. Geomagn. Aeron., **14**, 150–152.

SERGEEV, V. A. and SHUMILOV, O. I. (1974b): Dynamics and mechanism of formation of the morning auroral absorption maximum. Geomagn. Aeron., **14**, 381–383.

SESIANO, J. and CLOUTIER, P. A. (1976): Measurements of field-aligned currents in a multiple auroral arc system. J. Geophys. Res., **81**, 116–122.

SHAFTAN, V. A. and VOSHCHINA, L. K. (1974): Irregular geomagnetic pulsations and radar auroras as a result of the turbulence of the polar electrojet. Geomagn. Aeron., **14**, 262–265.

SHARP, W. E. and HAYS, P. B. (1974): Low-energy auroral electrons. J. Geophys. Res., **79**, 4319–4325.

SHAWHAN, S. D., FALTHAMMER, C.-G. and BLOCK, L. P. (1978): On the nature of large auroral zone electric fields at 1-R_E altitude. J. Geophys. Res., **83**, 1049–1052.

SHEPHERD, G. G. and THIRKETTLE, F. W. (1973): Magnetospheric dayside cusp: A topside view of its 6300 Å atomic emission. Science, **180**, 737–738.

SHEPHERD, G. G., ANGER, C. D., BRACE, L. H., BURROWS, J. R., HEIKKILA, W. J., HOFFMAN, J., MAIER, E. J. and WHITTEKER, J. H. (1973): An observation of polar aurora and airglow from the ISIS-2 spacecraft. Planet. Space Sci., **21**, 819–829.

SHEPHERD, M. M. and EATHER, R. H. (1976): On the determination of auroral electron energies and fluxes from optical spectral measurements. J. Geophys. Res., **81**, 1407–1410.

SIREN, J. C. (1975): Pulsating aurora in high-latitude satellite photographs. Geophys. Res. Lett., **2**, 557–559.

SIREN, J. C., DOUPNIK, J. R. and ECKLUND, W. L. (1977) A comparison of auroral currents measured by the Chatanika radar with 50-MHz backscatter observed from Anchorage. J. Geophys. Res., **82**, 3577–3579.

SIVJEE, G G and MCEWEN, D. J. (1976): Rocket observations of the interaction of auroral electrons with the atmosphere. Planet. Space Sci., **24**, 131–138.

SMIDDY, M., KELLEY, M. C., BURKE, W., RICH, F., SAGALYN, R., SHUMAN, S., HOYS, R. and LAI, S. (1977): Intense poleward-directed electric fields near the ionospheric projection of the plasmapause. Geophys. Res. Lett., **4**, 543–549.

SNYDER, A. L., Jr. and AKASOFU, S.-I. (1974): Major auroral substorm features in the dark sector by a USAF DMSP satellite. Planet. Space Sci., **22**, 1511–1517.

SNYDER, A. L., Jr. and AKASOFU, S.-I. (1976): Auroral oval photographs from the DMSP-8531 and 10533 satellites. J. Geophys. Res., **81**, 1799–1804.

SNYDER, A. L, Jr., AKASOFU, S.-I. and DAVIS, T. N. (1974): Auroral substorms observed from above the north polar region by a satellite. J. Geophys. Res, **79**, 1393–1402.

SNYDER, A. L., Jr., AKASOFU, S.-I. and KIMBALL, D. S. (1975): The continuity of the auroral oval in the afternoon sector. Planet. Space Sci., **23**, 225–227.

SOLVANG, G., BREKKE, A. and HAUG, A. (1977): Auroral zone *E*-region motions deduced from spaced receiver observations. J. Atmos. Terr. Phys., **39**, 823–829.

SORAAS, F, LINDALEN, H. R., MASEIDE, K., EGELAND, A., STEN, T. A. and EVANS, D. S (1974): Proton precipitation and the H_β emission in a post-breakup auroral glow. J. Geophys. Res., 961–979.

SØRENSEN, J., BJORDAL, J., TREFALL, H., KVIFTE, G. J. and PETTERSEN, H. (1973)· Correlation between pulsations in auroral luminosity variations and X-rays. J. Atmos. Terr. Phys., **35**, 961–979.

SONNERUP, B. U. Ö (1974). Magnetopause reconnection rate. J. Geophys. Res., **79**, 1546–1549.

SPIGER, R. J. and ANDERSON, H. R. (1975): Electron currents associated with an auroral band. J. Geophys. Res., **80**, 2161–2164.

STARKOV, G. V., FELDSTEIN, Y. I. and SHEVNINA, N. F. (1973): Auroras on the dayside of the oval during substorms. Geomagn. Aeron, **13**, 72–75.

STENBAEK-NIELSEN, H. C. (1974): Indications of a longitudinal component in auroral phenomena. J. Geophys. Res, **79**, 2521–2523.

STENBAEK-NIELSEN, H. C., WESCOTT, E. M., DAVIS, T. N. and PETERSON, R. W. (1973): Differences in auroral intensity at conjugate points. J. Geophys. Res., **78**, 659–671.

STERN, D. P. (1977) Large-scale electric fields in the earth's magnetosphere. Rev Geophys. Space Phys, **15**, 156–194.

SU, S.-Y. and KONRADI, A. (1974) On correlation analysis of the Explorer 12 substorm protons with some geophysical parameters. J. Geophys Res., **79**, 301–304.

SUGIURA, M (1975) Identification of the polar cap boundary and the auroral belt in the high-latitude magnetosphere: A model for field-aligned currents. J. Geophys Res., **80**, 2057–2068.

SUGIURA, M. (1976). Field-aligned currents observed by the Ogo 5 and Triad satellites. Ann. Geophys, **32**, 267–279.

SUGIURA, M and POROS, D. J. (1971) Hourly values of equatorial D_{st} for the years 1957 to 1970 GSFC Rep X-645-71-278, NASA Goddard Space Flight Center, Greenbelt, Maryland.

SUGIURA, M and POTEMRA, T A (1976): A net field-aligned current observed by Triad J. Geophys Res., **81**, 2155–2164

SUZUKI, A (1978)· Geomagnetic σ_η fields at successive universal times. To be published in J Atmos Terr Phys., **40**.

SVALGAARD, L. (1973) Polar cap magnetic variations and their relationship with the interplanetary sector structure. J Geophys. Res., **78**, 2064–2078.

SVALGAARD, L (1975) On the use of Godhavn H component as an indicator of the interplanetary sector polarity. J. Geophys. Res, **80**, 2717–2722.

SWIFT, D. W. (1971) Possible mechanism for formation of the ring current belt. J Geophys Res., **76**, 2276–2297.

SWIFT, D. W. and GURNETT, D A (1973) Direct comparison between satellite electric field measurements and visual auroras J. Geophys. Res., **78**, 7306–7313.

TANAKA, Y., OGAWA, T. and KODAMA, M (1977a)· Stratospheric electric fields and currents measured at Syowa Station, Antarctica—1. The vertical component. J Atmos. Terr Phys., **39**, 523–533

TANAKA, Y, OGAWA, T. and KODAMA, M. (1977b)· Stratospheric electric fields and currents measured at Syowa Station, Antarctica—2. The horizontal component J Atmos Terr Phys, **39**, 921–931.

TERASAWA, T. (1979) Ôrora ryûshi no kasoku kikô (review) (Accerelation mechanisms of auroral particles, A review). Nankyoku Shiryo (Antarct. Rec), **63**, 1–16.

TESTUD, J., AMAYENC, P. and BLANC, M. (1975): Middle and low latitude effects of auroral disturbances from incoherent-scatter. J. Atmos. Terr. Phys., **37**, 989–996.

THEILE, B. and PRAETORIUS, H. M. (1973): Field-aligned currents between 400 and 3000 km in auroral and polar latitudes. Planet. Space Sci., **21**, 179–187.

THOMAS, I. L., SCOURFIELD, M. W. J. and PARSONS, N. R. (1973): Classification of optical auroral pulsations. Can. J. Phys., **51**, 2209–2215.

TITHERIDGE, J. E. (1976): Ionospheric heating beneath the magnetospheric cleft. J. Geophys. Res , **81**, 3221–3226.

TROSHICHEV, O. A., KUZNETSOV, B. M. and PUDOVKIN, M. I. (1974): The current systems of the magnetic substorm growth and explosive phases. Planet. Space Sci., **22**, 1403–1412.

TSUNODA, R. T. (1975): Electric field measurements above a radar scattering volume producing 'diffuse' auroral echoes. J. Geophys. Res., **80**, 4297–4306.

TSUNODA, R. T. (1976): Doppler-velocity maps of the diffuse radar aurora. J. Geophys. Res., **81**, 425–435.

TSUNODA, R. T. and FREMOUW, E. J. (1976a): Radar auroral substorm signatures, 1. Expansive and recovery phases. J. Geophys. Res., **81**, 6148–6158.

TSUNODA, R. T. and FREMOUW, E. J. (1976b): Radar auroral substorm signatures, 2. East-west motions. J. Geophys. Res., **81**, 6159–6168.

TSUNODA, R. T. and PRESNALL, R. I. (1976): On a threshold electric field associated with the 398-MHz diffuse radar aurora. J. Geophys. Res., **81**, 88–96.

TSUNODA, R. T., PRESNELL, R. I. and LEADABRAND, R. L. (1974): Radar auroral echo characteristics as seen by a 398-MHz phased array radar operated at Homer, Alaska. J. Geophys. Res , **79**, 4709–4724.

TSUNODA, R. T., PRESNELL, R. I. and POTEMRA, T. A. (1976a): The spatial relationship between the evening radar aurora and field-aligned currents. J. Geophys. Res., **81**, 3791–3802.

TSUNODA, R. T., PRESNELL, R. I., KAMIDE, Y. and AKASOFU, S.-I. (1976b). Relationship of radar auroral, visual aurora and auroral electrojets in the evening sector. J. Geophys. Res., **81**, 6005–6015.

TVERSKAYA, L. V. and KHOROSHEVA, O. V. (1974): Some characteristics of the development of gigantic DP-2 variations during magnetic storms. Geomagn. Aeron., **14**, 86–89.

UNGSTRUP, E., BAHNSEN, A., OLESEN, J. K., PRIMDAHL, F., SPANGSLEV, F., HEIKKILA, W. J., KLUMPAR, D. M., WINNINGHAM, J. D., FAHLESON, U. V., FALTHAMMER, C.-G. and PETERSEN, A. (1975) Rocket-borne particle, field and plasma observations in the cleft region. Geophys. Res. Lett., **2**, 345–347.

UNWIN, R. S. and KEYS, J. G. (1975): Characteristics of the radio aurora during the expansive phase of polar substorms. J. Atmos. Terr. Phys., **37**, 55–59.

VASYLIUNAS, V. M. (1972): The interrelationship of magnetospheric process. Earth's Magnetospheric Processes, ed. by B. M. MCCORMAC. Dordrecht, D. Reidel, 29–38 (Astrophys. Space Sci. Lib., Vol. 32).

VASYLIUNAS, V. M. (1976): An overview of magnetospheric dynamics. Magnetospheric Particles and Fields, ed. by B. M. MCCORMAC. Dordrecht, D. Reidel, 99–105 (Astrophys. Space Sci. Lib., Vol. 58).

VASYLIUNAS, V. M. and WOLF, R. A. (1973): Magnetospheric substorms: Some problems and controversies. Rev. Geophys. Space Phys., **11**, 181–195.

VENKATARANGAN, P., BURROWS, J. R. and MCDIARMID, I. B. (1975): On the angular distributions of electrons in 'inverted V' substructure J. Geophys. Res., **80**, 66–72.

VIJ, K. K, VENKATESAN, D. and ANGER, C. D. (1975) Investigation of electron precipitation during an auroral substorm by rocket-borne detectors. J. Geophys. Res, **80**, 3205–3210.

VOLLAND, H. (1973) A semiempirical model of large-scale magnetospheric electric fields. J. Geophys. Res., **78**, 171–180.

VONDRAK, R. R (1975): Model of Birkeland currents associated with an auroral arc. J. Geophys Res, **80**, 4011–4014.

VONDRAK, R R and SEARS, R. D (1978) Comparison of incoherent-scatter radar and photometric measurements of the energy distribution of auroral electrons J Geophys Res, **83**, 1665–1674.

VOROBJEV, V. G. and REZHENOV, B. V. (1973): Progressive westward displacements of the region of the auroral substorm localization in conjunction with impulsive variations of the magnetic field Inst. Ass. Geomag Aeron. Bull, **34**, 441–449.

VOROBJEV, G. V, GUSTAFSSON, G., STARKOV, G. V., FELDSTEIN, Y. I and SHEVNIN, N. F (1975)· Dynamics of day and night aurora during substorms. Planet. Space Sci., **23**, 269–278.

VOROBJEV, V. G, STARKOV, G. V. and FELDSTEIN, Y. I. (1976). The auroral oval during the substorm development. Planet. Space Sci., **24**, 955–965.

WALLIS, D. D. (1976). Comparison of auroral electrojets and the visible aurora Magnetospheric Particles and Fields, ed. by B. M. MCCORMAC. Dordrecht, D. Reidel, 247–255 (Astrophys. Space Sci. Lib., Vol. 58).

WALLIS, D. D., ANGER, C. D. and ROSTOKER, G. (1976). The spatial relationship of auroral electrojets and visible aurora in the evening sector. J. Geophys. Res., **81**, 2857–2869

WANG, T. N C. and TSUNODA, R. T. (1975) On a crossed field two-stream plasma instability in the auroral plasma. J Geophys Res, **80**, 2172–2182.

WEBER, E. J., WHALEN, J. A., WAGNER, R A. and BUCHAU, J. (1977)· A 12-hour case study of auroral phenomena in the midnight sector: Electrojet and precipitating particle characteristics. J Geophys. Res., **82**, 3557–3566.

WEDDE, T, DOUPNIK, J. R. and BANKS, P. M. (1977): Chatanika observations of the latitudinal structure of electric fields and particle precipitation on November 21, 1975. J Geophys. Res., **82**, 2743–2753.

WELCOTT, J. H, PONGRATZ, M B, HONES, E. W., Jr. and PETERSON, R W. (1976). Correlated observations of two auroral substorms from an aircraft and from a Vela satellite. J. Geophys. Res, **81**, 2709–2718.

WESCOTT, E M, STOLARIK, J. D. and HEPPNER, J P (1969) Electric fields in the vicinity of auroral forms from motions of barium vapor releases. J Geophys. Res, **74**, 3469–3487.

WESCOTT, E M, STOLARIK, J D. and HEPPNER, J. P. (1970). Auroral and polar cap electric fields from barium releases Particles and Fields in the Magnetosphere, ed. by B. M. MCCORMAC Dordrecht, D. Reidel, 230–238 (Astrophys. Space Sci Lib., Vol 17)

WESCOTT, E M., RIEGER, E. P., STENBAEK-NIELSEN, H C, DAVIS, T N, PEEK, H M. and BOTTOMS, P. J. (1975)· The $L=6.7$ quiet time barium shaped charge injection experiment "Chachalaca" J. Geophys. Res, **80**, 2738–2744.

WESCOTT, E. M., STENBAEK-NIELSEN, H C., DAVIS, T. N. and PEEK, H. M. (1976) The Skylab barium plasma injection experiments, 1. Convection observations. J. Geophys Res., **81**,

4487–4494.

WESCOTT, E. M., STENBAEK-NIELSEN, H. C., HALLINEN, T., DAVIS, T. N. and PEEK, H. M. (1976): The Skylab barium plasma injection experiments, 2. Evidence for a double layer. J. Geophys. Res., **81**, 4495–4502.

WESCOTT, E. M., STENBAEK-NIELSEN, H. C., DAVIS, T. N., JEFFRIES, R. A. and ROACH, W. H. (1978). The TORDO I polar cusp barium plasma injection experiment. J. Geophys. Res, **83**, 1565–1575.

WESCOTT, E. M., RIEGER, E. P., STENBAEK-NIELSEN, H. C., DAVIS, T. N., PEEK, H. M. and BOTTOMS, P. J. (1974): $L=1.24$ conjugate magnetic field line tracing experiments with barium shaped charges. J. Geophys. Res., **79**, 159–168.

WHALEN, B. A. and MCDIARMID, I. B. (1972): Observations of magnetic-field-aligned auroral-electron precipitation. J. Geophys. Res., **77**, 191–202.

WHALEN, B. A. and MCDIARMID, I. B. (1973): Pitch angle diffusion of low-energy auroral electrons. J. Geophys. Res., **78**, 1608–1614.

WHALEN, B. A, BERNSTEIN, W. and DALY, P. W. (1978): Low altitude acceleration of ionospheric ions Geophys. Res. Lett., **5**, 55–58.

WHALEN, B. A, GREEN, D. W. and MCDIARMID, I. B. (1974): Observations of ionospheric ion flow and related convective electric fields in and near an auroral arc. J. Geophys. Res., **79**, 2835–2842.

WHALEN, B. A., VERSCHELL, H. J. and MCDIARMID, I. B. (1975): Correlations of ionospheric electric fields and energetic particle precipitation. J. Geophys Res., **80**, 2137–2145.

WHALEN, J. A. and PIKE, C. P. (1973): F-layer and 6300 Å measurements in the day sector of the auroral oval. J. Geophys. Res., **78**, 3848–3856.

WHALEN, J. A., WAGNER, R. A. and BUCHAU, J. (1977): A 12-hour case study of auroral phenomena in the midnight sector: Oval, polar cap, and continuous auroras. J. Geophys. Res, **82**, 3529–3535.

WHITTEKER, J. H. (1976): The magnetospheric cleft-ionospheric effects. J. Geophys. Res., **81**, 1279–1288.

WICKWAR, V. B., BARON, M. J. and SEARS, R. D. (1975): Auroral energy input from energetic electrons and Joule heating at Chatanika. J. Geophys. Res., **80**, 4364–4367.

WIENS, R. G. and ROSTOKER, G. (1975): Characteristics of the development of the westward electrojet during the expansive phase of magnetospheric substorms. J. Geophys. Res., **80**, 2109–2128.

WILHJELM, J., FRIIS-CHRISTENSEN, E. and POTEMRA, T. A. (1978): Relation between ionospheric- and field-aligned currents in the dayside cusp. J. Geophys. Res, **83**, 5586–5594.

WILLIAMS, D. J. and TREFALL, H. (1976): Field-aligned precipitation of >30-keV electrons. J. Geophys. Res, **81**, 2927–2930.

WILSON, C R. (1973): Seasonal variation of auroral infrasonic wave activity. J. Geophys. Res., **78**, 4801–4802.

WILSON, C. R. (1974) Trans-auroral zone auroral infrasonic wave observations Planet. Space Sci, **22**, 151–173.

WILSON, C. R. (1975)· Infrasonic wave generation by aurora. J. Atmos. Terr. Phys., **37**, 973–978.

WILSON, C. R. and HARGREAVES, J. K. (1974): The motions of peaks in ionospheric auroral

absorption and auroral infrasonic waves. J. Atmos. Terr. Phys., **36**, 1555–1565.

WINCKLER, J. R., ARNOLDY, R. L. and HENDRICKSON, R. A. (1975): Echo 2: A study of electron beams injected into the high-latitude ionosphere from a large sounding rocket. J. Geophys. Res., **80**, 2083–2088.

WINNINGHAM, J. D. and HEIKKILA, W. J. (1974). Polar cap auroral electron fluxes observed with Isis 1. J. Geophys. Res., **79**, 949–957.

WINNINGHAM, J. D., KAWASAKI, K. and ROSTOKER, G. (1978) Energetic particle precipitation into the high latitude ionosphere and the auroral electrojets, 1. Definition of electrojet boundaries using energetic electron spectra and ground-based magnetometer data To be published in J. Geophys. Res., **83**.

WINNINGHAN, J D., AKASOFU, S.-I., YASUHARA, F. and HEIKKILA, W. J. (1973): Simultaneous observations of auroras from the South Pole Station and of precipitating electron by Isis 1. J. Geophys. Res., **78**, 6579–6594.

WINNINGHAM, J. D , YASUHARA, F., AKASOFU, S.-I. and HEIKKILA, W. J. (1975). The latitudinal morphology of 10-eV to 10-keV electron fluxes during magnetically quiet and disturbed times in the 2100–0300 MLT sector. J. Geophys. Res., **80**, 3148–3171.

WINNINGHAM, J. D., SPEISER, T. W., HONES, E. W., Jr., JEFFRIES, R. A., ROACH, W. H , EVANS, D. S and STENBAEK-NIELSEN, H. C. (1977): Rocket-borne measurements of the dayside cleft plasma The Tordo experiment. J. Geophys. Res., **82**, 1876–1884.

WOLF, R. A. (1974): Calculations of magnetospheric electric fields. Magnetospheric Physics, ed. by B. M. MCCORMAC Dordrecht, D. Reidel, 167–177 (Astrophys. Space Sci. Lib., Vol. 44).

WOLF, R. A. (1975) Ionosphere-magnetosphere coupling. Space Sci. Rev , **17**, 537–562.

YASUHARA, F (1975) Field-aligned and ionospheric currents. Ph. D Thesis, University of Alaska, Fairbanks, 258 p.

YASUHARA, F. and AKASOFU, S.-I. (1977)· Field-aligned currents and ionospheric electric field. J. Geophys. Res., **82**, 1279–1284.

YASUHARA, F., KAMIDE, Y. and AKASOFU, S.-I. (1975). A modeling of the magnetospheric substorms. Planet. Space Sci , **23**, 575–578

YASUHARA, F., KAMIDE, Y. and AKASOFU, S -I. (1975). Field-aligned and ionospheric currents Planet. Space Sci., **23**, 1355–1368.

YASUHARA, F., AKASOFU, S.-I., WINNINGHAM, J. D. and HEIKKILA, W. J. (1973). Equatorward shift of the cleft during magnetospheric substorms as observed by ISIS 1 J. Geophys Res., **78**, 7286–7291.

YEAGER, D M. and FRANK, L. A (1976) Low-energy electron intensities at large distances over the earth's polar cap. J. Geophys. Res., **81**, 3966–3976

ZAITZEVA, S. A. and PUDOVKIN, M. I. (1976) On the longitudinal extent of the polar cusp. Planet Space Sci., **24**, 518–519.

ZMUDA, A J. and ARMSTRONG, J. C. (1974a): The diurnal variation of the region with vector magnetic field changes associated with field-aligned currents J. Geophys. Res , **79**, 2501–2502.

ZMUDA, A. J. and ARMSTRONG, J. C. (1974b): The diurnal flow pattern of field-aligned currents. J. Geophys. Res., **79**, 4611–4619.

ZMUDA, A. J., ARMSTRONG, J. C. and HEURING, F. T. (1970): Characteristics of transverse

magnetic disturbances observed at 1100 km in the auroral oval. J. Geophys. Res., **75**, 4757–4762.

ZMUDA, A. J., POTEMRA, T. A. and ARMSTRONG, J. C. (1974): Transient parallel electric fields from electromagnetic induction associated with motion of field-aligned currents. J. Geophys. Res., **79**, 4222–4226.

ZWICK, H. H. and SHEPHERD, G. G. (1973): Upper atmospheric temperatures from Doppler line widths, V. Auroral electron energy spectra and fluxes deduced from the 5577 and 6300 Å atomic oxygen emissions. Planet. Space Sci., **21**, 605–621.

(*Received June 10, 1978*)